Multi-Tracer Study of Karst Waters and Lake Sediments in Croatia and Bosnia-Herzegovina: Plitvice Lakes National Park and Bihać area

Dissertation
zur
Erlangung des Doktorgrades (Dr. rer. nat.)
der
Mathematisch-Naturwissenschaftlichen Fakultät
der
Rheinischen Friedrich-Wilhelms-Universität Bonn

vorgelegt von
SLAVICA BABINKA
aus Vinkovci
Kroatien

BONN, 2007

Ich versichere an Eides statt, dass ich diese Arbeit selbständig ausgeführt habe und keine außer den angegebenen Hilfsmitteln verwendet habe.

Referent:	Prof. Dr. Barbara Reichert
Korreferent:	Prof. Dr. Hans-Joachim Kümpel
Tag der mündlichen Prüfung:	28.06.2007
Erscheinungsjahr:	2007

Diese Dissertation ist auf dem Hochschulschriftenserver der ULB Bonn http://hss.ulb.uni-bonn.de/diss_online elektronisch publiziert.

Abstract

Karst aquifers in Croatia and Bosnia-Herzegovina represent an important freshwater resource for the Plitvice Lakes National Park and the Bihać area. In the present study an integrative approach was applied to investigate karst water and lake sediments with isotope-hydrological, geochemical and geochronological methods. The thesis focuses on the determination of groundwater flow dynamics, the water balance of the Plitvice Lakes National Park and the estimation of aquifer storage capacity using mean residence times (MRTs) of spring water. Sediment dating with $^{137}\mathrm{Cs}$ and $^{210}\mathrm{Pb}$ methods was performed on five cores of the Plitvice Lakes to establish a chronology of anthropogenic input into the lakes, since some of the lakes became biologically more productive (eutrophication) in the last decades and human influence cannot be excluded.

Stable isotopes (^{2}H and ^{18}O) give evidence for a predominantly continental (80%) and less the Mediterranean (20%) influence in precipitation of the Plitvice Lakes. Infiltrated water flows through hydraulically connected aquifers from two different recharge areas in Croatia towards Bosnia-Herzegovina and emerges in springs used for drinking water supply.

For calculations of water balance pumping rates, water mixing, evaporative ^{2}H enrichment and lake stratification were considered. From the Plitvice Lakes area variable water loss from the Korana River bed flowing towards springs near Bihać could be quantified, yielding e.g. 65% in September 2004.

A multi-tracer lumped parameter approach was applied to model MRTs of the karst springs using stable isotopes (^{2}H and ^{18}O), tritium (^{3}H), chlorofluorocarbons (CFC-11, CFC-12, CFC-113), sulfur hexafluorid (SF_6) and noble gases (^{3}He, ^{4}He, ^{20}Ne, ^{22}Ne). Two groundwater flow components in karst aquifer could be distinguished: a) a quick

flow component in the conduit network of a low storage capacity with a MRT up to 0.5 years, and b) a slow flow component in the fissured-porous aquifer of a high storage capacity with a MRT up to 28 years. Considering MRTs and discharge of each spring, a water storage capacity in the catchment area of springs could be obtained: up to 40 Mio. m^3 in the conduit network and up to 670 Mio. m^3 in the fissured-porous aquifer.

Sedimentation rates obtained by $^{137}\mathrm{Cs}$ range between 0.5 and 1.8 kg/(m^2 yr) and between 0.8 and 4.4 kg/(m^2 yr) for $^{210}\mathrm{Pb}$. The great lakes Prošće (PR) and Kozjak (K1) are characterized by slower sedimentation rates than the small lakes Gradinsko (GR) and Kaludjerovac (KA). The most reliable dating model in this study is the ^{210}Pb CF (constant flux) model. The dating results and chemical analysis have shown in Kozjak Lake a recent pollution through detergent-derived chemicals linear alkylbenzene sulphonates (LAS) with an increasing trend since the year 2000 (max. 4600 ng/g). It is most probably caused by the defects in the sewerage system. So an anthropogenic influence on eutrophication processes of the Plitvice Lakes cannot be excluded.

This work can be used by National Park administration and local water authorities for issues of sustainable water management and protection of groundwater resources in the transboundary karst aquifer. It also shows how the multi-tracer approach can give deeper insight into the karst system and points to the limitations on lumped parameter models applied to karst. Groundwater dating with ^{3}H/^{3}He using only the ^{3}He/^{4}He and helium and neon concentrations gives no unique results in this study due to the variable infiltration temperatures. With helium and neon concentrations only it is not possible to deduce any fractionation of excess air and possible gas loss. For this reason in karst studies also the heavy noble gases argon, krypton and xenon should be measured.

Zusammenfassung

Karstaquifere im Grenzgebiet zwischen Kroatien und Bosnien-Herzegowina sind wichtige Trinkwasserresourcen für den Nationalpark Plitwitzer Seen und die Region um die Stadt Bihać. In der vorliegenden Arbeit wird ein integrativer Ansatz verwendet, der isotopen-hydrologische, geochemische und geochronologische Methoden kombiniert. Diese Arbeit beschäftigt sich mit der Bestimmung der Grundwasser-Fließdynamik im Aquifer, der Wasserbilanz der Plitwitzer Seen, sowie mit der Bestimmung der mittleren Verweilzeiten (MVZ) des Quellwassers im Aquifer, welche bei der Abschätzung der Trinkwasserreserven berücksichtigt werden. Dazu wurden fünf Seesedimentkerne in den Plitwitzer Seen gamma-spektrometrisch datiert ($^{137}\mathrm{Cs}$ and $^{210}\mathrm{Pb}$), um die Chronologie des anthropogenen Eintrags in die Seen zu bestimmen, da eine anthropogene Verschmutzung als Ursache für die Eutrophierung nicht ausgeschlossen werden kann.

Stabile Isotope (^{2}H and ^{18}O) im Niederschlag der Plitwitzer Seen sind zu 80% kontinentalen und zu 20% mediterranen Ursprungs. Die Karstaquifere sind hydraulisch miteinander verbunden, wobei das Grundwasser von zwei Infiltrationsgebieten in Kroatien Richtung Bosnien-Herzegowina fließt und Trinkwasserquellen speist.

Für die Wasserbilanz-Berechnung der Plitwitzer Seen wurden Pumpraten, Mischung verschiedener Wasserkomponenten, evaporative ^{2}H-Anreicherung im Seewasser und Seestratifizierung berücksichtigt. Von den Plitwitzer Seen konnte eine stark variierende Wassermenge quantifiziert werden, die vom Korana-Flussbett Richtung Trinkwasserquellen in der Nähe von Bihać fließt: z.B. 65% in September 2004.

Für die Bestimmung der mittleren Verweilzeiten des Quellwassers wurde eine Multi-Tracer-Studie mit stabilen Isotopen (^{2}H und ^{18}O), Tritium (^{3}H), Fluorchlorkohlenwasserstoffen (CFC-11, CFC-12, CFC-113), Schwefelhexafluorid (SF_6) und Edelgasen (^{3}He,

^{4}He, ^{20}Ne, ^{22}Ne) durchgeführt. Zwei Grundwasserkomponenten konnten unterschieden werden: a) eine schnelle, die sich durch Karstkanäle ausbreitet mit MVZ bis zu 0.5 Jahren und b) eine langsame im klüftig-porösen Aquifer mit MVZ bis zu 28 Jahren. Aus MVZ und Abflüssen der Quellen ergaben sich Wasser-Speicherkapazitäten im Einzugsgebiet einer Quelle: bis zu 40 Mio. m^3 im Karstkanalnetz und bis zu 670 Mio. m^3 im klüftig-porösen Aquifer.

Sedimentationsraten für die ^{137}Cs-Methode liegen zwischen 0.5 und 1.8 kg/(m^2 yr), während sie bei der ^{210}Pb-Methode zwischen 0.8 und 4.4 kg/(m^2 yr) variieren. Die großen Seen Prošće und Kozjak weisen eine kleinere Sedimentationsrate als die kleinen Seen Gradinsko and Kaludjerovac auf. Das CF (constant flux) Model der ^{210}Pb-Methode ist das zuverlässigste Datierungsmodel in dieser Studie. Die Ergebnisse der Sedimentdatierung und chemischer Analysen zeigen eine rezente Verschmutzung der Plitwitzer Seen, da seit 2000 ein Anstieg der aus Waschmitteln stammenden linearen Alkylbenzolsulfonaten im See Kozjak zu beobachten ist (max. 4600 ng/g). Das ist möglicherweise auf Defekte im Abwassersystem zurückzuführen. Daher kann ein menschlicher Beitrag zu Eutrophierung der Plitwitzer Seen nicht ausgeschlossen werden.

Diese Arbeit kann zu effektivem Grundwassermanagement in einem grenzüberschreitenden Aquifer genutzt werden. Die vorliegende Arbeit zeigt auch die Anwendungsgrenzen der lumped parameter Modelle: Die Grundwasser-Datierung mit ^{3}H/^{3}He ergibt mit nur ^{3}He/^{4}He, Helium und Neon Konzentrationen keine einheitlichen Ergebnisse wegen der variablen Infiltrationstemperaturen. Mit He und Ne allein ist es nicht möglich, eine Fraktionierung des Luftüberschusses und einen möglichen Gasverlust aus dem Aquifer zu bestimmen. Aus diesem Grund sollten neben den leichten Edelgasen auch die schweren Edelgase Argon, Krypton und Xenon gemessen werden.

Preface

This PhD thesis was realized at the Leibniz Institute for Applied Geosciences (GGA-Institut) in Hannover in cooperation with the Hydrogeology Group (Geological Institute) of Bonn University, Germany. It was kindly supervised by Prof. Dr. Barbara Reichert (University of Bonn), Prof. Dr. Hans-Joachim Kümpel (GGA-Institut/University of Hannover) and Dr. Axel Suckow (GGA-Institut/presently at the International Atomic Energy Agency, Vienna, Austria).

The presented study forms part of the multilateral research project of the European Union "Study of anthropogenic pollution after the war and establishing of measures for protection of the Plitvice National Park and Bihać region at the border area of Croatia and Bosnia-Herzegovina" (acronym: ANTHROPOL.PROT). It was a cooperation between scientific organizations from Bosnia-Herzegovina[1], Croatia[2], Germany[3] and Spain[4]. The project was funded by the European Union (INCO: International Scientific Cooperation Projects, contract number ICA2-CT-2002-10009 - ANTHROPOL.PROT).

[1] Biotechnical Faculty, University of Bihać, Geological Institute of Bosnia-Herzegovina, Sarajevo

[2] Rudjer Bošković Institute, Laboratory for Measurements of Low-level Radioactivity; Institute of Geology, Department of Hydrogeology and Engineering Geology, Zagreb

[3] Leibniz Institute for Applied Geosciences - GGA-Institut, Hannover

[4] Universitat Autónoma de Barcelona, Department of Geology, Barcelona Bellaterra

The objective of the project was the assessment of anthropogenic pollution after the war events (1991-1995) and its impacts on the karst ecosystem in a border zone between Croatia and Bosnia-Herzegovina. Data collected by partners within the project, as well as physico-chemical and isotopic analysis of samples collected during three years of the project served as a background for elaborating a hydrogeological model and further modeling of intrinsic vulnerability, hazard and risk assessment of surface and groundwater resources of transboundary aquifers (ANTHROPOL.PROT, 2006).

Fig. 1: Sampling of karst water and lake sediments in Bosnia-Herzegovina and Croatia (from a leaflet of Babinka & Herrmann, 2005 for the EU project ANTHROPOL.PROT)

Since my childhood, I'm impressed by the beauty of the Plitvice Lakes and Una River. Unfortunately, this area was the place of destruction of nature and human relationships through the war events, which started during my grammar school time in Vinkovci and continued during my study time in Zagreb (Croatia). After my change to the University of Bonn I was looking for a way to apply my geoscientific background in this area and to contribute in this manner to "repair" at least some parts of these senseless destructions. My work by the GGA-Institut in Hannover and the PhD at the University of Bonn gave me this opportunity.

Contents

List of Figures

List of Tables

Symbols and Abbreviations

Frequently used symbols

C	concentration	
t	time unit	
A	initial ratio of excess air	[Nml/g]
E	evaporation	[mm]
F	fractionation parameter as defined in Eq. 2.19 and 2.20	[-]
f	residual fraction of water	[%]
g	weighted function	
h	humidity	[%]
Pe	Péclet number	[1]
R	ratio of heavy to light isotope	[-]
R_0	initial ratio of heavy to light isotope	[-]
Q	discharge	[m^3/s]
V	volume	[m^3]
z	atmospheric volume fraction of noble gas i in dry air	[%]
α	isotope fractionation factor as defined in Eq. 2.11	[-]
δ	stable isotope ratio as defined in Eq. 2.8	[‰]
$\Delta\epsilon$	kinetic enrichment factor as defined in Eq. 2.12	[-]
ϵ	equilibrium enrichment factor in Eq. 2.12	[-]
λ	radioactive decay term	

Subscripts

a	atmospheric vapour
c	conduit network of karst aquifer
ce	closed system equilibrium
in	input
out	output
p	fissured-porous karst aquifer
pr	partial diffusive re-equilibration

Abbreviations

ANTHROPOL.PROT	acronym for the EU project (ANTHROPOL.PROT, 2006)
CFCs	chlorofluorocarbons CFC-11, CFC-12, CFC-113
DHMZ	Meteorological and Hydrological Service of Croatia
DM	dispersion model
EM	exponential model
EMDM	exponential-dispersion model
EPM	exponential-piston flow model
GGA-Institut	Leibniz Institute for Applied Geosciences (Institut für Geowissenschaftliche Gemeinschaftsaufgaben), Hannover, Germany
GMWL	global meteoric water line
GR	sediment core from Gradinsko Lake
KA	sediment core from Kaludjerovac Lake
K1	sediment core 1 from Kozjak Lake
K2	sediment core 2 from Kozjak Lake
KWI	Karst Water Institute
LAS	linear alkylbenzene sulphonates
LMWL	local meteoric water line
LPM	lumped parameter model
m a.s.l.	meter above sea level
Mio.	Million
MRT	mean residence time
MVZ	mittlere Verweilzeit
PMEM	piston flow-exponential model
PMDM	piston flow-dispersion model
PR	sediment core from Prošće Lake
STP	standard temperature: 0°C, and pressure: 1.023 atm (cm^3 STP/g of dry air per g of water)
TU	tritium unit, 1 TU = 0.12 Bq/l,

Chapter 1

Introduction

Background and Scope

Karst aquifers represent an important freshwater resource world-wide. Although only some 12% of the Earth's land surface is underlain by karst rocks, up to a quarter of the world's population is supplied by karst groundwaters (Ford & Williams, 1989). The transboundary aquifers between Croatia and Bosnia-Herzegovina contain several springs, which are used for the drinking water supply of the Plitvice Lakes National Park and the municipalities Bihać and Kulen Vakuf. In this area many potential contaminant sources for the karst water do exist. Examples are an abandoned military airport Željava with land mines positioned during the last war events in this region (1991-1995), industrial and domestic wastes or waste waters from tourist accommodations and a former saw mill in the National Park (Džankić et al., 2006; Kapelj et al., 2006; Miošić et al., 2006). In the sensitive aquatic system of the Plitvice Lakes calcium carbonate precipitates in water, forming biodynamic tufa barrier dams thus creating 15 lakes that are interlinked by cascades and waterfalls. In the last decades some of the lakes became biologically more productive (eutrophication) as a result of natural processes or by anthropogenic pollution of the lakes (Obelić et al., 2006).

The knowledge of *groundwater flow dynamics*, *lake water balance*, *mean residence time of water (MRT)* as well as the *aquifer storage capacity* plays a key role for effective management of water resources and for their protection. However, their quantification poses a challenge due to the karst heterogeneities in porosity and permeability,

variations of discharge, structural complexity as well as lack of quantitative data for hydrogeological and chemical characteristics of springs.

Numerical models are a classical approach characterizing groundwater flow in non-karst porous media since the 1960s. In the karst aquifers they still represent a particular challenge due to their strong heterogeneity and erratic hydraulic behaviour (Kovács, 2003). Karst studies use a wide variety of tracers of **natural** or **anthropogenic** origin as a tool to determine those parameters. Water soluble tracers, like fluorescent dyes and salts form the main group. Another group of tracers includes drift bodies such as spores, bacteria or phages (Käss et al., 1998). In karst terrains, they are usually injected into sinkholes (Hötzl, 1998). The use of certain tracers is often restricted by the hydrogeological conditions or the aquifer properties. Also mechanical effects, chemical reactions between tracer and rock, and biological degradation can be limiting factors in getting reliable tracing results (Drew, 1999). Another disadvantage of those tracer tests is that they usually supply information only on preferential flow paths, which do not represent the whole karst aquifer (Hötzl, 1998; Maloszewski et al., 2002). However, a distribution of **environmental isotope tracers** represent the whole system and not only the preferential flow paths (Maloszewski et al., 2002). In combination with conventional hydrological and geochemical methods, environmental tracers can provide deeper insights into the dynamics of groundwater flow, the relation between surface and groundwater, mean residence times (MRTs) of groundwater, recharge rates, or the storage properties of aquifers (e.g. Gat & Gonfiantini, 1981; Nativ et al., 1999; Cook & Herczeg, 2000; Plummer et al., 2001; Maloszewski, 2006).

This thesis evaluates methods of system analysis with the combined use of several environmental tracers measured in spring, lake and surface water. The environmental tracers applied are stable isotopes (^{18}O and ^{2}H), chlorofluorocarbons (CFC-11, CFC-12, CFC-113), sulphur hexafluoride (SF_6), tritium (^{3}H), helium (He) and neon (Ne) as well as the isotope ratio of helium (^{3}He/^{4}He). Tritium and stable isotopes are particularly suitable for tracing the water cycle. As constituents of the water molecule they are ideally transported in the hydrological cycle. Noble gases helium and neon and inert gases CFCs and SF_6 are nearly ideal tracers, but can be affected by several processes

that may significantly change their concentration. Examples are loss of gas through the water table or microbial degradation of CFCs in anaerobic environments or retarded transport (e.g. Cook & Solomon, 1997; Bauer et al., 2001). All these disturbing factors have to be considered, and if possible corrected, prior to modeling the MRT of water in the catchment area of springs.

Several detailed studies have compared the age information obtained when a series of environmental tracers was measured in the recharge area of aquifers (e.g. Ekwurzel et al., 1994; Cook & Solomon, 1995; Solomon & Cook, 1999). Only in a few studies this method has been applied in discharge areas, such as springs (Rank et al., 1992; Maloszewski et al., 2002). In this work a multi-tracer approach is used to calculate a MRT of spring water and to assess water storage capacities of karst aquifers, which are important drinking water resources.

The previous investigations of lake water balance for the Plitvice Lakes with classical hydrological methods (Beraković, 2005; Zwicker et al., 2006) do not consider different factors such as evaporation from the lake water body, lake stratification, mixing of lake waters and their tributaries, and pumping from Kozjak Lake for drinking water supply of the National Park.

The current amount of pumped water of 0.06 m^3/s from Kozjak Lake will not be high enough to satisfy the expected future demand for tourism at the Plitvice Lakes National Park. Therefore, the opening of new pumping capacities is planned. Due to the sensibility of tufa growth on changes of hydrological circumstances (Zwicker et al., 2006) the subsidence of the water level in Kozjak Lake was investigated.

Besides the investigation of water, this work also includes the investigation of recent lake sediments (<150 years) of the Plitvice Lakes. Sediments are very suitable media to record the history of contamination input. Once the pollutant attains the water, it will be subsequently accumulated in the sediment (Schell & Barnes, 1986; Gäbler & Suckow, 2003). The knowledge of the sediment accumulation rate and thus the age of specific sediment layers is of fundamental importance to understand the fluxes into the sediment and to establish a chronology of environmental changes, including a possible anthropogenic input into the sediment. Possible pollutants are trace elements

(heavy metals) and detergent-derived linear alkylbenzene sulphonates (LAS). To determine sedimentation rates, activities of anthropogenic (^{134}Cs, ^{137}Cs) and natural (^{210}Pb, ^{214}Pb, ^{214}Bi) radionuclides were measured.

Thesis Structure

This study uses a combined approach of isotope-hydrological, geochemical and geochronological methods to investigate karst waters and lake sediments. A short outline of this thesis is given in the following:

- Chapter 1 introduces the scope and outline of the project.
- Chapter 2 provides the basic theoretical background about karst aquifers, dating groundwater, lumped parameter models and environmental isotope tracers.
- Chapter 3 gives insight into the specific features of the study area, including climate, geological setting and the hydrogeology of the investigated aquifer.
- Chapter 4 addresses sampling and measurement techniques for spring, lake and stream waters.
- Chapter 5 traces the origin of precipitation and flow paths of groundwater in the hydrological connected aquifers.
- Chapter 6 provides an evaluation of the lake water balance inferred from water mixing, evaporative enrichment of deuterium along the lake chain, lake stratification, pumping rate, precipitation and discharge data.
- Chapter 7 is dedicated to the modeling of mean residence times of springs using the multi-tracer approach and to estimate the storage capacity of the karst aquifer.
- Chapter 8 investigates lake sediments of the Plitvice Lakes and establishes the chronology of anthropogenic input into the sediments.
- Chapter 9 synthesizes all chapters, draws conclusions and gives an outlook which suggests further research strategies.

Chapter 2

Theoretical Background

2.1 Karst Aquifer

The term **karst aquifer** is generally used instead of carbonate aquifer, which is limited to limestone and dolomite rocks (Drew, 1999). The main hydrological characteristic that distinguishes karst systems from non-karstic systems is the existence of enlarged underground spaces generated by the dissolving action of water. Water infiltrates through pre-existent fissures[1] and enlarges them, generating a complex conduit network[2] (KWI, 1999). Several conceptual models describe the karst systems (e.g. Mangin, 1975; Doerfliger et al., 1999; Gunn, 2004) that generally distinguish three main zones or sub-systems: soil and epikarst, unsaturated and saturated zone (Fig. 2.1). The **soil and the epikarst (or subcutaneous)** zone is described as the uppermost part of exposed karstified rocks, which is characterized by high permeability. This zone is assumed to absorbe and temporarily store rainfall water. Moreover, it can rapidly drain infiltrating water towards enlarged vertical shafts, thus enhancing concentrated infiltration. The remaining stored water constitutes a perched saturated zone, and may contribute to diffuse recharge. Thus, by its storage capacity, epikarst contributes to the base flow to shafts and to an overall base flow[3] of the karst aquifer through quite prolonged periods of drought (Klimchouk, 2000). The **unsaturated (or infiltration**

[1] Voids with average dimensions from 10 to 100 mm.
[2] Includes all voids from 100 mm to 10 m in diameter.
[3] The part of stream discharge that is not attributable to rapid infiltration, and generally sustained by groundwater storage.

or vadose) zone connects the upper sub-system to the saturated zone by drainage through a vertical network of fissures and conduits. The **saturated (or phreatic) zone** splits into a network of high permeability conduits and low permeability volumes with a high storage capacity.

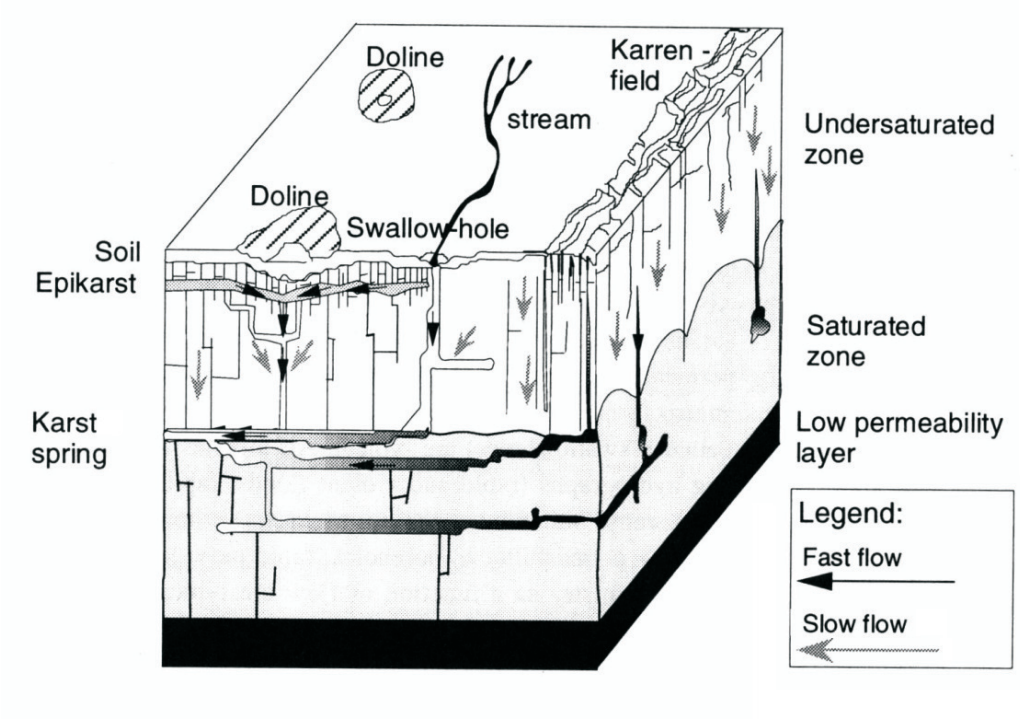

Fig. 2.1: Conceptual model of a karst aquifer with three sub-systems (epikarst, unsaturated and saturated zone) and typical karst landforms like swallow-holes, karrenfields and dolines (Doerfliger et al., 1999). **Swallow hole or ponor (Slavic.)**: Hole or opening in the bottom or side of a depression where a surface stream or lake flows either partially or completely underground into the karst ground-water system. **Doline or sinkhole**: A basin- or funnel-shaped hollow in limestone, ranging in diameter from a few meters up to a kilometer and in depth from a few to several hundred meters. **Karren (German.)**: Channels or furrows, caused by solution on massive bare limestone surfaces; they vary in depth from a few millimeters to more than a meter and are separated by ridges. In modern usage, the terms are general, describing the total complex of superficial solution forms found on compact pure limestone, KWI (1999).

In general, the hydrogeology of karst aquifers is characterized by great heterogeneity, conduit[4] and diffuse[5] flow, and variations in amount of recharge[6] and discharge[7]. There is often little or no soil cover, resulting in poor filtration and prepurification, and rapid infiltration, making the karst aquifer vulnerable in respect to pollution.

Karst Springs

Karst springs are those places where karst groundwater emerges at the surface (Gunn, 2004). In the study area freshwater from the springs is exploited for drinking water supply. Karst springs occur most frequently in places of a contact between permeable carbonate masses and impermeable layers like flysch or dolomite. The latter act as barriers to groundwater flow, and karst springs tend to develop as "contact" springs, where the boundary between the karst and impermeable rock is exposed at the surface (Gunn, 2004). Karst springs have been classified in many different ways, whereby ten different attributes can be distinguished: flow duration, reversing flow, conduit type at spring, geology, topographic position, relationship to bodies of surface water, distributaries, discharge, chemistry, and exploitation. Bögli (1980) presents three types of spring classification according to the following features:

- outflow hydrograph
- geologic and tectonic conditions
- water origin

According to the **outflow hydrograph**, Bögli (1980) distinguishes: (1) perennial (permanent), (2) periodic (intermittent), (3) rhythmically following (or ebb and flow springs), and (4) episodical springs. For the drinking water supply, the **permanent springs** play the most important role. As the name suggests, the groundwater in the spring is existent over the whole year. Intermittent springs are typical in karst areas of Croatia and Bosnia-Herzegovina, but they are only rarely exploited (Bonacci, 1987).

[4] Conduit flow is generally turbulent, but can also be laminar. It is also called concentrated or quick flow.

[5] The diffuse flow is generally slow-moving, may be laminar, and have a uniform discharge and slow response to storm events. It is also called slow or seepage flow.

[6] Recharge (autogenic) is derived from precipitation directly onto the karst landscape. **Diffuse** recharge is used to describe the slow percolation of recharge through a myriad of small openings while **concentrated** recharge occurs by flow into large fractures, sinkholes, and sinking streams.

[7] The volumetric flow of water through a given cross-section, unit: [m^3/s].

Those springs are mostly situated in the zone of vertical circulation and the groundwater appears in the spring only in the periods following heavy precipitation. According to the **geologic and tectonic conditions** springs are divided into: (1) bedding springs (Fig. 2.2A, B); (2) springs emerging from fractures (Fig. 2.2C); (3) overflow types of springs (Fig. 2.2D); (4) ascending springs (Fig. 2.2E).

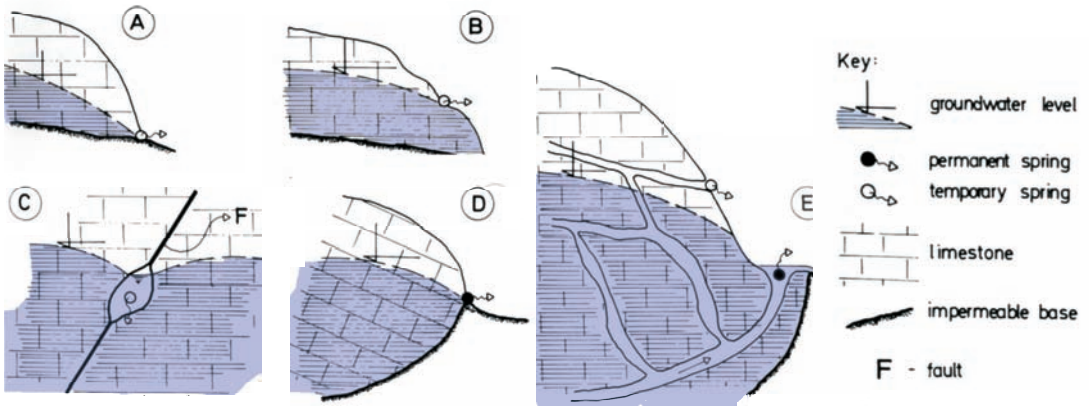

Fig. 2.2: Classification of karst springs according to their geologic and tectonic conditions: bedding springs (A) and (B); spring emerging from fractures (C); overflow types of springs (D); ascending spring (E); modified after Bonacci (1987).

Taking into account the **origin of water**, Bögli (1980) suggests the following classification: (1) emergence[8]; (2) resurgence[9]; and (3) exsurgence[10]springs. For drinking water supply, the first type is of the greatest importance. By large permanent karst springs this is the most frequent way of water appearing in the spring.

[8]A general term for the outflowing water, for the opening or for the area of outflow of a karst spring: includes exsurgence and resurgence, KWI (1999).

[9]Resurgence is the re-emergence of karst ground water. A part or all of the water is derived from surface inflow into ponors at higher levels, KWI (1999).

[10]Exsurgence springs are fed only by percolating water, KWI (1999).

2.2 Dating Groundwater

Several substances, called "tracers", sampled at a well or spring allow dating of young and old groundwaters, covering a certain age-range (Fig. 2.3). For the dating of groundwater younger than 50 years the following tracers can be applied and were used in this study:

- stable isotopes deuterium (δ^2H or D) and oxygen-18 (δ^{18}O)
- chlorofluorocarbons (CFCs) and sulfur hexafluoride (SF_6)
- tritium (^{3}H or T)
- tritium/helium-3 (^{3}H/^{3}He) and helium-4 (^{4}He).

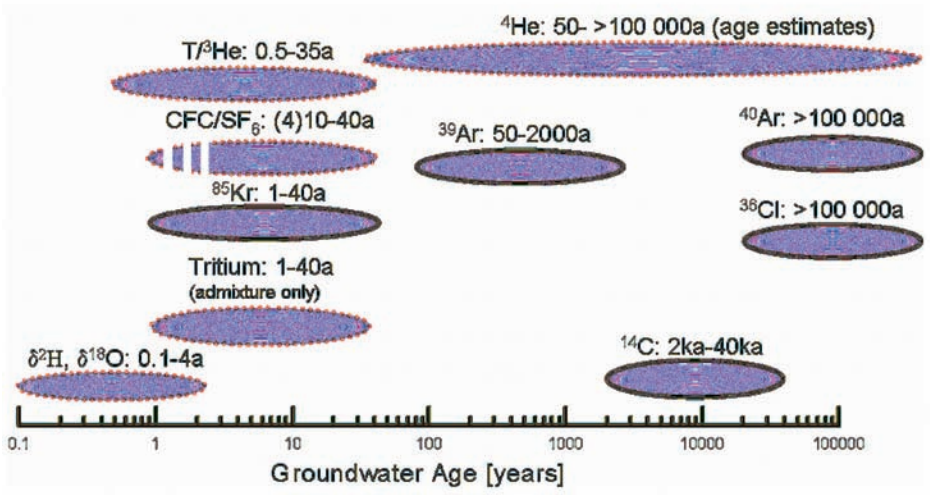

Fig. 2.3: Approximate range (in years) of dating applications with environmental tracers. Substances used for dating groundwater in this study are marked with a red dotted line, modified after Kendall & McDonnell (1998) and Suckow (2004), Lectures on Isotope Hydrology, pers. comm..

Difference Between Age and Mean Residence Time (MRT) of Groundwater

The term "**age**" of groundwater describes the time the water spent in underground from the point of recharge to the point of collection at a well or spring. An "age" assumes a strong assumption on the water sample (Suckow, 2006):

- the water parcel is regarded as being a well defined entity and

- no mixture between groundwater parcels took place or their mixing is negligible.

Also the chosen substance for dating has to be able to deliver the age. Whereas stable isotopes and tritium are not able to determine the age of water, since the input functions are not unique, CFCs, SF_6, and $^3H/^3He$ are able to deliver this information, if the assumptions described above are fulfilled (Suckow, 2006). However, such idealized cases are very rare in nature, and instead of age, the expression "**mean residence time**" (MRT) is used in the literature (e.g. Kendall & McDonnell, 1998; Plummer et al., 2001; Ozyurt & Bayari, 2005). Determination of MRT assumes:

- mixing took place between water parcels with different age
- the mixture is well defined (Suckow, 2006).

A well known mixture can be mathematically described and the MRT is derived using convolution integral. The mathematical description using the MRT as the main unknown parameter is called a lumped parameter model (LPM).

2.3 Lumped Parameter Models (LPM) in Isotope Hydrology

For the dating purposes in isotope hydrology lumped parameter models (LPM, often called black-box models) were developed to describe groundwater systems with small amount of parameters (Maloszewski & Zuber, 1996). LPM treat the whole groundwater system as one system and assumes constant and stable flow through the system. Furthermore, they assume that the relative contribution of water parcels of certain age (flow pattern) can be mathematically described by the convolution integral

$$C_{out}(t) = \int_{-\infty}^{t} C_{in}(t') \cdot g(t - t') \cdot e^{-\lambda(t-t')}\, dt' \tag{2.1}$$

$C_{out}(t)$	output concentration of a certain tracer sampled at a well or spring
$C_{in}(t^{'})$	input concentration of a certain tracer
$t^{'}$	time of entry
$g(t-t^{'})$	weighting function describing the relative contribution of water with a certain age $(t-t^{'})$ within the mixed sample
$e^{-\lambda(t-t^{'})}$	radioactive decay term

The integration from or to infinity means that the whole input curve (C_{in}) has to be included to get a correct output concentration (C_{out}). Figure 2.4 describes the principle of a LPM with the convolution integral using the input function for tritium in precipitation. The relationship between the input concentration of tritium, $C_{in}(t)$ and the concentration measured in the output at spring $C_{out}(t)$ after leaving the "black-box" is resolved by the convolution integral and its weighting function $g(t-t^{'})$. The weighting function is a function of age, i.e. of the time difference between the infiltration and the output time. The kind of the lumped parameter models differ from each other obviously with respect to the weighting function. Maloszewski & Zuber (1996) developed weighting functions for mathematical description of tracer transport in aquifers: for the piston flow model (PM or PFM), the exponential model (EM), the exponential-piston flow model (EPM), the dispersion model (DM), the linear model (LM) etc.

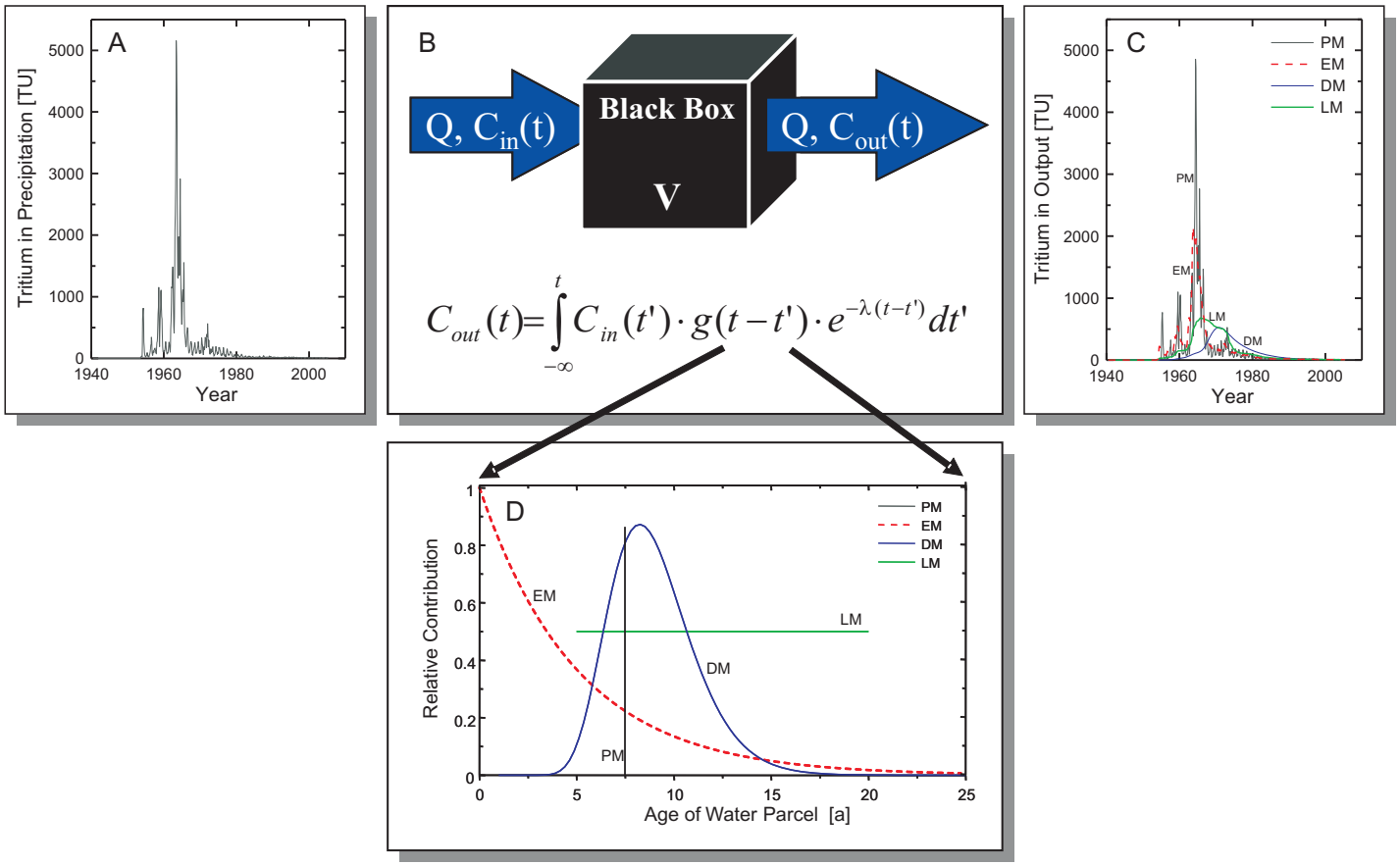

Fig. 2.4: The principle of lumped parameter models (LPM): Input function for tritium in precipitation (IAEA/WMO, 2006): Ottawa before 1966, Lüttich 1966-1969, Groningen 1970-1975, Zagreb 1975-2003, Plitvice Lakes 2003-2005 (A); black-box model with the convolution integral, MRT of water is also defined as the ratio of water volume V to the volumetric flow rate Q through the system (Maloszewski & Zuber, 1996) (B); tritium output curves for piston flow model (PM or PFM), exponential model (EM), dispersion model (DM), and linear model (LM) (C); curves obtained by the weighting function for PM, EM, DM, and LM (D), modified after Suckow (2004), Lectures on Isotope Hydrology, pers. comm..

The **piston flow model (PM or PFM)** assumes that no mixing at all takes place in the aquifer system and the hydrodynamic dispersion and diffusion are negligible. All water masses that have entered the aquifer at different times in the past flow to the sampling point without any mixing in between. Furthermore, the PM assumes that the water sample from spring or well is represented only by water of one age. Mathematically this is described by the weighting function $g(t^{'})$ as the Dirac delta distribution:

$$g(t - t^{'}) = \delta(t^{'} - t_c) \tag{2.2}$$

$\delta(t^{'})$ Dirac function

t_c mean residence time of water in the conduit network.

In this work the PM is used to describe the water flow along a karst conduit network.

Contrary to the PM, where the water sample from a spring or well is represented only by water of one age, the **exponential model (EM)** considers the water sample as an ideal mixture. The water mixture contains an exponential distribution of different water ages, i.e. the youngest water component has an age of zero and the eldest has an age equal to infinity. The condition for the EM approach is a presence of a recent component with age zero in the mixture (Maloszewski & Zuber, 1996). The weighting function for the EM is given by Maloszewski & Zuber (1996) as

$$g(t - t^{'}) = t_p^{-1}\, exp\, (t^{'}/t_p) \tag{2.3}$$

t_p MRT in the fissured-porous karst aquifer.

The EM is used in this work to describe a tracer transport in the fissured-porous aquifer.

The **dispersion model (DM)** can be described as the most applicable lumped parameter model in the karst system studies (e.g. Maloszewski et al., 2002; Suckow, 2006). The model idea is that the transport, which the piston flow model describes like a sharp particle movement of a well defined water parcel, is "smeared" by a dispersion-like process around the first moment of transport. Here it is of no importance whether this mixing process is a real hydrodynamic dispersion during water movement, or takes

place during sampling or is the result of recharge taking place in an area with different origins of flow lines representing the sample instead of one flow line only. For the mathematical solution the DM needs a second parameter besides the MRT, namely the Péclet number. This number describes the relative importance of advective and dispersive flow within the system as a whole. It is defined as

$$Pe = l \cdot v/d \tag{2.4}$$

Pe Péclet number

l characteristic length of the system

v advective velocity

d dispersion.

It can be shown that for very large Péclet numbers the DM mathematically approximates the PM, while for small Péclet numbers it approximates the EM (Maloszewski & Zuber, 1996; Suckow, 2006). The DM is used in this work to describe the MRT in the fissured-porous karst aquifer, where stagnant zones are present and even an ideal tracer may be delayed in respect to the water flow due to diffusion exchange between mobile water in the conduit network and stagnant water in the matrix. The weighting function for the DM is

$$g\left(t - t^{'}\right) = \frac{1}{t^{'}\sqrt{4\,\pi\,Pe\,t^{'}/t_p}} \cdot exp\left[\frac{\left(1 - t^{'}/t_p\right)^2}{4\,Pe\,t^{'}/t_p}\right] \tag{2.5}$$

t_p MRT of water in the fissured-porous karst aquifer

Pe Péclet number.

By calculation of the MRT for one spring applying the lumped parameter models the selection of the "right" LPM is very important. The same measured tracer values lead to different MRTs, if different models are used. Furthermore, the determination of MRT with one lumped parameter model is nearly always not unique (Suckow, 2006).

2.3.1 Conceptual Models of Groundwater Flow in Karst Aquifers

Dating groundwater by means of environmental tracers and LPMs require a conceptual model of groundwater flow. Usually, the groundwater flow in such conceptual models is described as a single flow system. However, for the complex karst system such approximation is not sufficient. A good description of the groundwater flow would be to use many different flow systems, but this approach can be neither mathematically solved nor sufficiently parameterized with measurements. In this work the karst groundwater flow is regarded as a two component system as proposed by Maloszewski et al. (2002).

In this conceptual model the karst reservoir is approximated by two interconnected parallel flow systems of a **fissured-porous aquifer** (karst massif) and a **conduit network** (Fig. 2.5). The first system has a high storage capacity and contains mobile water in the fissures and fractures and quasi-stagnant or stagnant water in the microporous matrix (V_p). The infiltrating water at the surface of the catchment area enters this system with a certain volumetric flow rate $Q_p(t)$ and flow through it to conduit network with a low storage capacity. This network is regarded as a separate flow system, mainly supplied from swallow holes having a different volume of water $V_c(t)$ with the volumetric flow rate $Q_c(t)$. Water entering the fissured-porous aquifer from the conduit network is regarded as a part of $Q_p(t)$. The conduits are finally drained by springs. The discharge $Q(t)$ at the spring is the sum of the volumetric flow rate through the fissured-porous aquifer, $Q_p(t)$, and of the direct component $Q_c(t)$ entering the conduit network through swallow holes:

$$Q(t) = Q_p(t) + Q_c(t). \tag{2.6}$$

The water infiltrating the karst system is marked by a specific trace substance, for instance with CFC or tritium. This input concentration $C_{in}(t)$ is transported through the karst system to the springs. The tracer concentration in each spring, $C_{out}(t)$, results from the weighted mixing of both water fluxes:

$$Q(t)C_{out}(t) = Q_p(t)C_p(t) + Q_c(t)C_c(t). \tag{2.7}$$

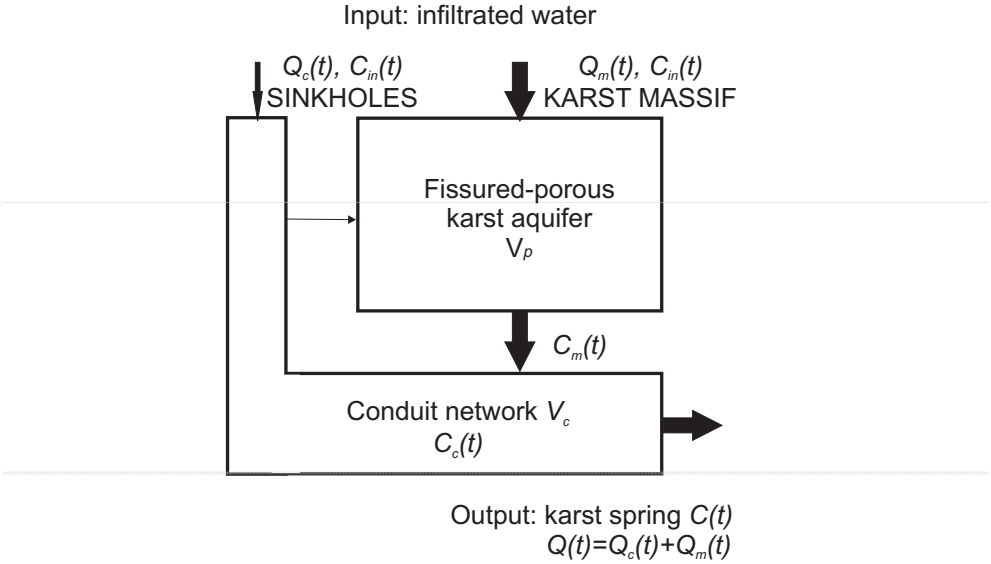

Fig. 2.5: Conceptual model of water flow in the karst aquifer. The thin arrow indicates a possible contribution from a conduit network flow to the fissured-porous system, which is regarded as a part of the flow through that system, modified after Maloszewski et al. (2002).

2.3.2 Data Storage and Processing

Data storage and processing were performed using the LabData Database and Laboratory management system (Suckow & Dumke, 2001). This software also contains a module "**Lumpy**" dealing with the computation of MRTs of water according to the PM, EM, EPM, LM, and DM. A combination of two such models in parallel is also possible. Therefore, "Lumpy" allows also to model pure binary mixtures (two PM in parallel), bypass flow (a model with MRT = 0 parallel to any other model) or admixtures of tracer-free water to any of the above models (a model with MRT > 100 years in parallel). "Lumpy" seems to be the only lumped parameter code available which is able to fit time series of several tracers at one site simultaneously (Suckow, 2006).

2.4 Environmental Isotope Tracers

A distribution of **environmental tracers** in the karst system does not just represent the preferential flow paths but the whole system. The **natural isotope tracers** of hydrogen, carbon, oxygen, nitrogen, sulphur (H, C, N, O, S) are the naturally occurring isotopes of elements found in abundance in environment and are principal elements of hydrological, geological and biological systems. The isotopic composition of water for instance, is modified by meteoric processes, and thus the recharge water in a particular environment will have a characteristic isotopic signature that serves as a natural tracer for the provenance of groundwater, for the determination of both pathways and time scales of environmental processes (Clark & Fritz, 1997). In this study the natural isotopes of hydrogen ($^{1}H/^{2}H$) and oxygen ($^{16}O/^{18}O$) were used. The second category of environmental tracers used in this work belong to the group of **anthropogenic isotope tracers**. The release of those tracers into the atmosphere includes events such as nuclear bomb tests that released tritium (^{3}H) and caesium (^{134}Cs, ^{137}Cs) in the 1950s and early 1960s. Another example is the release of chemical substances like the chlorofluorocarbons (CFCs) from refrigeration and other sources starting in the 1930s. These substances entered in the Earth's atmospheric and hydrologic cycle, and can be found in groundwater that has been recharged within the past 50 years. Another common name for these tracers is **transient tracers**. They are like 'dyes' with known delivery rates to the environment and available over a certain period of time, and their concentrations in air have changed over time. In this study the transient tracers ^{3}H, ^{3}He, CFCs, and SF_6 were considered.

2.4.1 Stable Isotopes (^{2}H, ^{18}O)

Tracing groundwater by means of the environmental isotopes deuterium (^{2}H or D) and oxygen-18 (^{18}O) offers information on groundwater flowpaths, recharge area, and the mean residence time of water. It also allows a quantitative evaluation of mixing and other physical processes such as evaporation. As constituents of the water molecule $^{2}H/^{18}O$ carry a fingerprint of the meteorological processes they were produced in, thus providing the information on the origin of precipitation or groundwater (Cook & Her-

czeg, 2000; Mook, 2001). The isotopic composition of precipitation is influenced by a number of factors, such as seasonal, latitude, altitude, continental, and amount effects, as is well documented in the literature (e.g. Rozanski et al., 1993; Clark & Fritz, 1997; Kendall & McDonnell, 1998; Cook & Herczeg, 2000). Stable isotopes are measured as the ratio of the two most abundant isotopes of a given element (^{18}O/^{16}O, ^{2}H/^{1}H). Their ratios are conventionally reported as δ-values in parts per thousand (‰):

$$\delta(‰ VSMOW) = (R_x/R_s - 1) \cdot 1000 \tag{2.8}$$

VSMOW	the name of the standard used (Vienna Standard Mean Ocean Water)
R	the ratio of the heavy to the light isotope (^{2}H/^{1}H or ^{18}O/^{16}O) in compounds of the sample (R_x) and the standard (R_s).

Negative δ-values indicate that the sample is depleted in heavy isotopes relative to a standard, positive means that it is enriched.

Isotopic Fractionation Processes

Investigation with stable isotopes is based on the concept of isotopic fractionation. Isotopes are partitioned or fractionated by thermodynamic reactions due to differences in the rates of reaction for different molecular species (e.g. Clark & Fritz, 1997; Kendall & McDonnell, 1998; Cook & Herczeg, 2000). By such physical or chemical reactions, the stable isotopes can be fractionated under

- equilibrium conditions
- nonequilibrium (kinetic) conditions.

At **isotopic equilibrium**, the forward and backward reaction rates of any particular isotope are identical (i.e. no net forward or backward reaction). Isotopic equilibrium between two phases does not mean that the two phases have identical proportions of heavy and light isotopes, only that the ratio at a given temperature of these proportion is constant. A process typically viewed as an equilibrium process is condensation of water in rain clouds (Kendall & McDonnell, 1998). The heavier water isotopes (δ^2H

and $\delta^{18}\mathrm{O}$) become enriched in the liquid (rain) phases while the lighter isotopes ($\delta^{1}\mathrm{H}$ and $\delta^{16}\mathrm{O}$) remain in the vapour (cloud) phase:

$$\alpha^{2}\mathrm{H}_{\mathrm{water-vapour}} = \frac{(^{2}\mathrm{H}/^{1}\mathrm{H})_{\mathrm{water}}}{(^{2}\mathrm{H}/^{1}\mathrm{H})_{\mathrm{vapour}}} \tag{2.9}$$

or generally expressed:

$$\alpha = \frac{R_{\mathrm{reactant}}}{R_{\mathrm{product}}} \tag{2.10}$$

- α equilibrium fractionation factor
- R the ratio of the heavy to the light isotope for the reactant and product.

In most systems, complete physicochemical equilibrium is seldom, and a net transfer of reactant and product occurs. At such **nonequilibrium (kinetic) conditions**, forward and backward reaction rates are not identical due to rapid freezing of water to ice, the addition or removal of a reactant by biological reactions etc. (Cook & Herczeg, 2000). In the hydrological cycle such a nonequilibrium process occurs during *evaporation* from surface water bodies (Gonfiantini, 1986). In this work the evaporation processes from the surface of the lakes in the Plitvice Lakes National Park are of interest.

Evaporation in Lakes

During evaporation lake water becomes progressively enriched in $^{2}\mathrm{H}$ and $^{18}\mathrm{O}$. This enrichment is affected by humidity h. If h remains close to 0%, there is no exchange of the lake water with the vapour phase. In this case, the enrichment follows a **Rayleigh distillation**. This is an exponential function that describes the progressive partitioning of heavy isotopes ($^{2}\mathrm{H}$ or $^{18}\mathrm{O}$) into the lake water reservoir as it dimnishes in size (Clark & Fritz, 1997):

$$R = R_{0}\, f^{(1/\alpha - 1)} \tag{2.11}$$

R the isotope ratio when only a residual fraction f remains in the lake water

R_0 the initial ratio in the lake water

α fractionation factor.

However, the mean annual air humidity in the area of the Plitvice Lakes is not less than 77%[11]. Therefore, the evaporation from the lake water body does not follow the Rayleigh distillation, because the exchange of the lake water with the vapour phase reduces the exponential enrichment. For this case Gonfiantini (1986) gives an equation that describes the variation of the evaporation conditions of an evaporating water body as the residual liquid fraction decreases:

$$\frac{d\delta}{dlnf} = \frac{h(\delta - \delta_a) - (\delta + 1)(\Delta\epsilon + \epsilon/\alpha)}{1 - h + \Delta\epsilon} \tag{2.12}$$

h humidity [%]

δ isotopic composition of the lake water [‰]

δ_a isotopic composition of the atmospheric vapour [‰]

$\Delta\epsilon$ kinetic enrichment factor representing the additional isotopic enrichment introduced by the transport of vapour across the molecular diffusion layer of the atmosphere, $\Delta\epsilon^2\mathrm{H}‰ = 12.5(1 - \mathrm{h})$.

α equilibrium fractionation factor

ϵ equilibrium enrichment factor ($\epsilon = \alpha - 1$)

f residual fraction of water in the lake [%].

Global Meteoric Water Line

The partitioning of ^{2}H and ^{18}O through the hydrological cycle is an important phenomenon for investigations in isotope hydrology. It is essentially driven by the Rayleigh distillation of isotopes from vapour water masses as they cool and rain-out over the continents. In this process ^{2}H and ^{18}O are being selectively removed from the vapour phase in such a way that rain becomes progressively depleted in ^{2}H and ^{18}O. Isotope fractionation is strongly dependent on the temperature of the reaction. The fractionation of

[11] According to data from the DHMZ between 2000 and 2005.

deuterium ^{2}H between water and vapour, for example, decreases from about 106‰ at 0°C to 27‰ at 100°C (Clark & Fritz, 1997). The strong correlation between temperature and δ^2H and δ^{18}O controls the position of precipitation signature on Craig's (1961) **Global Meteoric Water Line (GMWL)** (Eq. 2.13). From this correlation isotope effect due to seasons, altitude, latitude, continentality and paleoclimates can be derived (Clark & Fritz, 1997):

$$\delta^2\mathrm{H} = 8\,\delta^{18}\mathrm{O} + d \tag{2.13}$$

In this equation the slope is 8 and so-called "deuterium excess" d equals 10 on a global basis. The value of d may differ significantly from area to area owing to various origins and conditions (Froehlich et al., 2002). It is primarily a function of the mean relative humidity of the atmosphere above the oceans. Stable isotope ratios may locally represent different meteoric conditions and are described by a **Local Meteoric Water Line (LMWL)**.

Mixing of Water with Distinct Stable Isotope Signature

In respect to the lake waters of the Plitvice Lakes and their tributaries, mixing processes have to be elucidated. ^{2}H and ^{18}O are conservative in mixing relationships and so the mixture will preserve the mixing ratio of two distinct waters (a and b in Fig. 2.6). The proportion of mixing for a given sample will then relate directly to its position on the mixing line, according to

$$\delta_{sample} = f\delta_a + (1-f)\delta_b \tag{2.14}$$

f	the fraction of groundwater "a" in the "a,b" mixture, expressed in %
δ_a, δ_b	isotopic composition of the mixing components a and b.

Only when the mixing components a and b have a distinct isotopic signature, they can be considered for the mixing calculation. The difference in the end members has to be large compared to the analytical uncertainty of the measurements. Any difference in the end members smaller than twice this analytical uncertainty has to be treated as if the waters are of identical isotopic composition (Clark & Fritz, 1997).

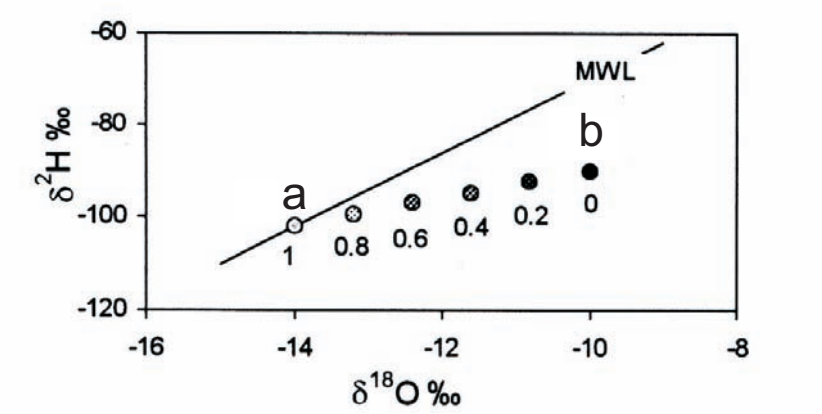

Fig. 2.6: The fractional mixing of two groundwaters quantified on the basis of their stable isotope contents, shown as the fraction of groundwater "a" in the "a,b" mixture of the sample, modified after Clark & Fritz (1997).

Dating Groundwater with Stable Isotopes

The seasonal variations in the stable isotope composition of spring discharge can be used to estimate the mean residence time (Maloszewski et al., 1983). It is based on differences between heights of two amplitudes, namely a) the amplitude of the precipitation ^{2}H (or ^{18}O) variation and b) the amplitude of the groundwater ^{2}H (or ^{18}O) variation. The seasonal variation of stable isotope values in most of the spring waters is a strong indication that these springs contain a component with mean residence times smaller than 5 years. For exponential mixing Maloszewski et al. (1983) gave an equation to compute the mean residence time from the amplitude ratio a of a signal in the input and output:

$$MRT = \omega^{-1}(a^2 - 1)^{\frac{1}{2}} \tag{2.15}$$

- ω equals to 2π per year for seasonal signals
- a amplitude ratio of ^{2}H (or ^{18}O) variations in precipitation and groundwater.

2.4.2 Tritium (^{3}H or T)

Tritium is a short-lived isotope of hydrogen with a half-life of 12.32 years (Lucas & Unterweger, 2000). Tritium activities are measured in tritium units [TU], where 1 tritium unit equals 1 tritium atom in 10^{18} hydrogen atoms. In SI units, one tritium unit is about 0.118 bequerels per liter [Bq/l], where the bequerel is one decay per second. Tritium in precipitation is influenced by seasonal and continental effects (e.g. Kendall & McDonnell, 1998; Cook & Herczeg, 2000). Naturally, tritium results in the upper atmosphere from the bombardment of nitrogen by the flux of neutrons in cosmic radiation (Clark & Fritz, 1997):

$$^{14}\mathrm{N} + {}^{1}\mathrm{n} \rightarrow {}^{12}\mathrm{C} + {}^{3}\mathrm{H}. \tag{2.16}$$

The natural level of tritium in precipitation is only a few TU and thus would have a limited applicability. However, large quantities of tritium (>2000 TU) were introduced into the hydrological cycle by the nuclear weapon testing in the 1950s and 1960s, producing a huge peak in 1963, which became a marker used in many hydrological studies (e.g. Schlosser et al., 1988; Solomon & Cook, 1999). However, the concentrations of tritium in precipitation and groundwater is now largely back to the natural, cosmogenic levels.

Dating Groundwater with Tritium

Tritium is like deuterium directly incorporated into the water molecule as HTO and thus suitable for dating groundwater. Tritium is one of the eldest and common methods for dating young groundwater. Clark & Fritz (1997) describe five different methods for dating with tritium and here an overview of these is given. In the performed karst groundwater study only two of these dating methods are applicable (time series analysis and qualitative interpretation).

The calculation of groundwater age by **radioactive decay** assumes a known tritium input concentration and piston flow (i.e. without significant mixing or dispersion along the flow path), according to the decay equation

$$^{3}H_t = {}^{3}H_0\, e^{-\lambda t} \tag{2.17}$$

$^{3}\mathrm{H}_0$ the initial tritium activity [TU]

$^{3}\mathrm{H}_\mathrm{t}$ the residual activity measured in sample after decay over time t

$e^{-\lambda t}$ radioactive decay term.

Equation 2.17 can be rewritten using the decay term λ, which is equal to ln2 divided by a half-life ($t/2$) for the radioactive isotope (tritium's $t/2$ = 12.32 years):

$$t = -17.77 \ln \frac{^{3}\mathrm{H_t}}{^{3}\mathrm{H_0}} \tag{2.18}$$

In this study Equation 2.18 cannot be applied for dating, since the radioactive decay of tritium is undiscernible from the tritium input curve since 1975.

A **multi-year ^{3}H input function** can be determinated from (1) a weighted contribution of ^{3}H from each year, with (2) a correction for the decay of each year's contribution of precipitation during storage in the recharge area (Clark & Fritz, 1997) (Fig. 2.7). This method too cannot be applied for the dating, because the mathematical solution of MRT calculations is not unique.

Time series analysis is the third method for dating waters with tritium. Repeated sampling from specific points (e.g. springs) over several years allows the monitoring of seasonal variations and long-term variations in the aquifer, thus giving an indication of the mean residence time. This dating method is applied for the investigated area. The time series of tritium in spring waters contain data from monthly sampling of data over a time period of two years (2003-2005).

Qualitative interpretation of tritium for the groundwater age determination can also be applied. For example, the tritium activity in continental regions <0.8 TU means the presence of submodern waters, recharged prior to 1952 and tritium activity >50 TU means a recharge dominantly in the 1960s.

The bomb spike in precipitation from 1963 can be preserved in hydrogeological systems where advective mixing is minimal, when the recharge water transits thick non-saturated zones. Here, new water displaces older water downward along the profile.

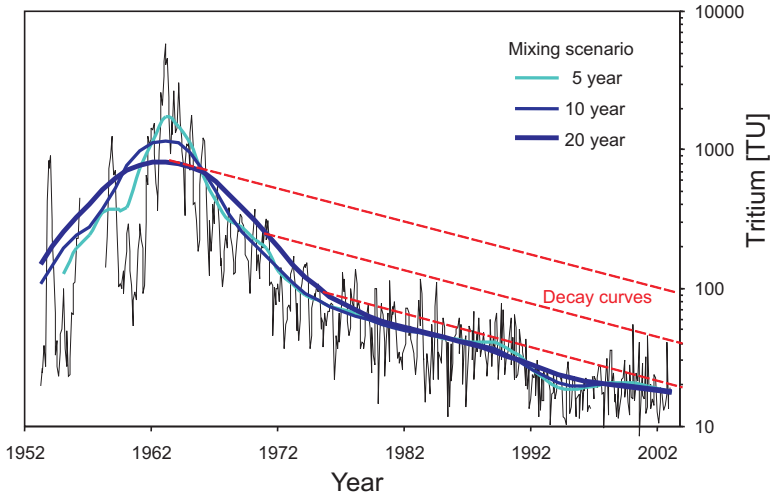

Fig. 2.7: Composite monthly tritium concentration in precipitation from Ottawa (black line). Multi-year mixing scenarios are shown for 5, 10 and 20 year cases, using a normal distribution function to weight the annual tritium contributions (Clark & Fritz, 1997).

In such a profile the **movement of the 1963 ^{3}H-peak** can be observed and thus the groundwater age can be determined. However, this method cannot be applied in the investigated karst aquifer since it assumes piston flow along the depth profile without water mixing and requires high-resolution multi-level sampling at one site.

2.4.3 Noble Gases (He, Ne)

Noble gases in groundwaters originate from three major sources: i) dissolution of atmospheric air at solubility equilibrium, ii) injection of additional or "excess air" bubbles entrapped during infiltration and dissolved in groundwater, and iii) radiogenic noble gases produced by radioactive decay and terrigenic noble gases from different geochemical compartments of the Earth (Andrews, 1991; Kipfer et al., 2002).

i) Solubility Equilibrium

The dissolved concentrations of the noble gases in equilibrium with the atmosphere depend upon the **salinity**, **temperature**, and **atmospheric pressure** during infiltration of the water (Kipfer et al., 2002). In Figure 2.8 the grey and black solubility lines present the dissolved noble gas concentrations for temperatures between 0°C and 50°C and the atmospheric pressures at altitudes 700 m a.s.l. and 3000 m a.s.l., respectively. Decreasing temperatures cause increasing dissolved helium and neon concentrations in groundwater. At atmospheric pressures at 700 m a.s.l. more helium and neon is dissolved than at the higher altitude.

The temperature at which air-equilibration of groundwater occurs in the unsaturated zone is close to the mean annual air temperature of the geographical region of recharge (Andrews, 1991). For the Plitvice Lakes and Una River area a recharge temperature of 8.9°C and an altitude of 700 m a.s.l. is assumed. However, these values present only an approximation of the infiltration conditions and may vary from sample to sample.

ii) Excess Air

In most groundwaters noble gas concentrations are higher than the concentrations expected at atmospheric solubility equilibrium. This gas excess is commonly called "excess air" (Heaton & Vogel, 1981). The authors explain the phenomenon of excess air through the complete dissolution of small air bubbles trapped in soil pores, introducing excess gases into the groundwater in the same ratio as in the atmosphere. The driving force for dissolution of trapped air bubbles is pressure; for example the hydro-

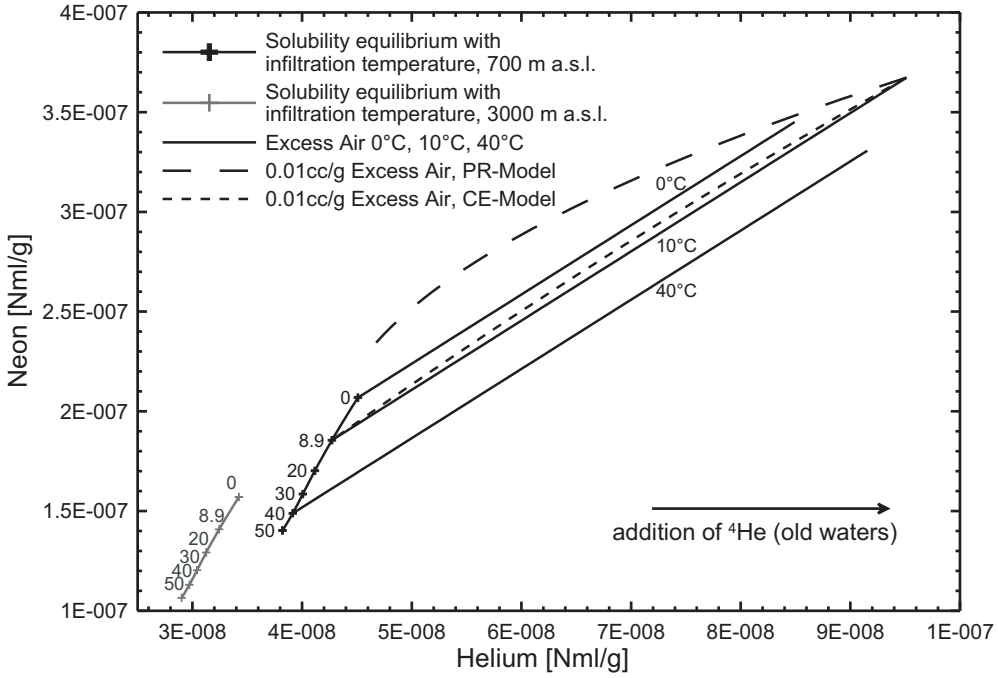

Fig. 2.8: Concentrations of helium and neon in groundwater. Equilibrium concentrations were calculated for infiltration altitudes of 700 m a.s.l. and 3000 m a.s.l. and the temperatures indicated (grey and black solid line). The excess air-line corresponds to an altitude of 700 m a.s.l. and infiltration temperatures of 0°C, 10°C and 40°C and admixtures of up to 0.01 cc/g. Dashed lines correspond to the closed system equilibrium (CE) and partial diffusive re-equilibration (PR) models starting from an initial concentration corresponding to the maximum concentration of the excess air line (temperature=10°C, altitude=700 m a.s.l., excess air=0.01 cc/g or 10 cc/kg).

static pressure may be enhanced through the water table fluctuation during or after a strong rainfall. The quantification of the amount of excess air is crucial for reliable groundwater age calculations. To quantify excess air in groundwater, neon is used, because atmospheric concentrations are constant over time, and the atmosphere is the only source of neon in shallow groundwater. The equilibrium concentration of neon in groundwater samples can be calculated using the known solubility and the infiltration temperature. The amount of excess air can then be determined from the difference between the calculated equilibrium concentration and the actually measured neon concentration (Kipfer et al., 2002).

Fractionated Excess Air

Heaton & Vogel (1981) have assumed that the excess air is pure atmospheric air due to complete dissolution of trapped air bubbles in the ground. However, recent studies have shown that the excess air tends to be fractionated relative to the atmospheric air, with an enrichment of the heavy gases compared to the light gases (e.g. Holocher et al., 2002). Two models have been developed to describe this phenomenon: the partial re-equilibration model **(PR-model)** introduced by Stute et al. (1995) and the closed system equilibration model (**CE-model)** by Aeschbach-Hertig et al. (2000).

The **PR-model** assumes that initially trapped air bubbles dissolve completely, but later a part of the resulting excess is lost by molecular diffusion through the water table. Because the molecular diffusivities of the noble gases decrease with atomic mass, the light noble gas helium is lost much faster than neon that is the heavier one. This process leads thus to a typical fractionation pattern of the noble gas composition in the gas excess of groundwater and results in the curved shape of the green dashed line in Figure 2.8. It may be written as

$$C_i(T, S, P, A_{pr}, F_{pr}) = C_i^*(T, S, P) + A_{pr} \cdot z_i \cdot exp(-F_{pr}\frac{D_i}{D_{Ne}}) \qquad (2.19)$$

C_i^* the equilibrium concentration between atmosphere and water at atmospheric pressure P, water temperature T and salinity S during air-water partitioning

A_{pr} the amount of initial excess air

F_{pr} the fractionation parameter describing the degree of diffusive re-equilibration

z_i the atmospheric volume fraction of noble gas *i* in dry air

D_i molecular diffusivity of noble gas *i*

D_{Ne} the molecular diffusivity of Ne

The **CE-model** does not postulate a complete dissolution of bubbles, but assumes that a reservoir of entrapped gas remains in the quasi-saturated zone. Water and entrapped gas are thought to form a closed system which equilibrates at the hydrostatic

pressure and surrounding soil temperature. This process changes the concentrations and the relative composition of noble gases in the groundwater and in the entrapped gas. The CE-model is described by

$$C_i(T,S,P,A_{ce},F_{ce}) = C_i^*(T,S,P) + \frac{(1-F_{ce})A_{ce}z_i}{1+F_{ce}A_{ce}z_i/C_i^*(T,S,P)} \tag{2.20}$$

C_i^* same as in Eq. 2.19

A_{ce} the initial STP-volume of dry air in the trapped gas per unit mass of water

F_{ce} the fractionation parameter, which is restricted to the interval between 0 and 1, whereby $F_{ce} = 0$ implies unfractionated excess air and $F_{ce} = 1$ implies no gas excess

z_i the atmospheric volume fraction of noble gas *i* in dry air

The dissolved helium and neon concentrations in the groundwater resulting from the closed-system equilibration are represented in Figure 2.8.

iii) Radiogenic and Terrigenic Noble Gases

Radiogenic noble gases are produced either directly by radioactive decay or indirectly by subsequent nuclear reactions triggered by the initial radioactive disintegration. For dating purposes of young groundwater having residence times up to 50 years the radioactive decay of atmospheric tritium ^{3}H to tritiugenic helium $^3\mathrm{He}_{\mathrm{trit}}$ is of importance. For dating of old groundwaters, recharged on time scales of thousands of years, the $^4\mathrm{He}$ concentration as the decay product of uranium is used (Kipfer et al., 2002). **Terrigenic noble gases** in meteoric waters originate either from the Earth's mantle or the continental crust. The ratio of $^3\mathrm{He}/^4\mathrm{He}$ is the defining feature of the respective terrigenic component (Kipfer et al., 2002).

Considering the components described in sections i) to iii) the total amount of helium measured in groundwater in [TU] can be expressed as

$$^3\mathrm{He}_{\mathrm{meas}} = {}^3\mathrm{He}_{\mathrm{trit}} + {}^3\mathrm{He}_{\mathrm{eq}} + {}^3\mathrm{He}_{\mathrm{ex}} + {}^3\mathrm{He}_{\mathrm{terr}} + {}^3\mathrm{He}_{\mathrm{rad}} \tag{2.21}$$

$$^4\mathrm{He}_{\mathrm{meas}} = {}^4\mathrm{He}_{\mathrm{eq}} + {}^4\mathrm{He}_{\mathrm{ex}} + {}^4\mathrm{He}_{\mathrm{terr}} + {}^4\mathrm{He}_{\mathrm{rad}} \tag{2.22}$$

He subscripts indicate the helium components; meas: measured (total), trit: tritiugenic, eq: atmospheric solubility equilibrium, ex: excess air, terr: terrigenic, rad: radiogenic

However, prior to dating groundwater with ^{3}H/^{3}He, it is necessary to separate the $^3\mathrm{He}_{\mathrm{trit}}$ component from the other helium components. A detailed description of the separation method can be found in e.g. Kipfer et al. (2002).

Dating Groundwater with ^{3}H/^{3}He

The ^{3}H/^{3}He dating method allows precise dating of water in the range of months up to ca. 40 years. The use of the ^{3}H/^{3}He tracer to study groundwater flow and recharge was first proposed in 1969 by Tolstikhin and Kamensky. However, it took nearly two decades until actual groundwater studies based on this method were published (Poreda et al., 1988; Schlosser et al., 1988). As ^{3}H enters groundwater systems and begins to radioactively decay, the noble gas ^{3}He is produced. Once isolated from the atmosphere below the water table, dissolved ^{3}He concentrations will increase as groundwater becomes older. The primary advantage of this approach is that an estimate of age can be made independent from the tritium input function and that the method is also applicable with tritium contamination (Cook & Herczeg, 2000). The ^{3}H/^{3}He age is defined as

$$t = \lambda^{-1} \ln\left(\frac{^3\mathrm{He}_{\mathrm{trit}}}{^3\mathrm{H}} + 1\right) \tag{2.23}$$

t estimated groundwater age

$^3\mathrm{He}_{\mathrm{trit}}$ tritiugenic helium concentration derived from tritium (^{3}H) decay

A difficulty of the $^3H/^3He$ dating method, especially in the karst system, lies in the occurrence of the varying and probably fractionated "excess air" in groundwater, which has to be taken into account in the calculation of noble gas infiltration temperatures.

Advantages of Measuring the Heavy Noble Gas Species Ar, Kr, Xe

The heavy noble gases argon, krypton and xenon are very helpful to determine the infiltration temperature of recent and paleogroundwaters (e.g. Aeschbach-Hertig et al., 2000). The solubilities of Ar, Kr, Xe in water depend strongly on temperature, much more than those of helium and neon. The measurement of heavy noble gas concentrations in groundwater allows therefore the determination of the temperature at the time of infiltration. Another advantage is that the dating based on these radioactive noble gases can be applied even if the water is affected by strong elemental fractionation (Kipfer et al., 2002).

2.4.4 Chlorofluorocarbons (CFCs) and Sulfur Hexafluoride (SF_6)

CFCs and SF_6 are anthropogenic tracers with a relatively well-known global input-function. CFCs are stable, synthetic, halogenated alkanes, which have a wide range of industrial and refrigerant applications (Rowland, 1990) and were developed in the early 1930s. Their production was followed by a release into the atmosphere and incorporation into the hydrologic cycle (Fig. 2.9).

Trichlorofluoromethane CFC-11 (CCl_3F) and dichlorodifluoromethane CFC-12 (CCl_2F_2) were emitted early, whereas trichlorofluoroethane CFC-113 ($C_2Cl_3F_3$) has only been emitted since about thirty years. Current estimates of the atmospheric lifetimes of CFC-11, CFC-12, and CFC-113 are 45$\pm$7, 87$\pm$17, and 100$\pm$32 years (Volk et al., 1997). The only known sinks in the atmosphere are photocatalytic processes in the stratosphere. A slight concentration decrease can occur under anaerobic conditions in the groundwater (Oster, 1994). Sulfur hexafluoride (SF_6) is extremely stable and predominantly used as isolation gas in high voltage engineering. The atmospheric concentration of this gas increases since the 1970s and its atmospheric life-span is larger than 3000 yr (Cook & Herczeg, 2000).

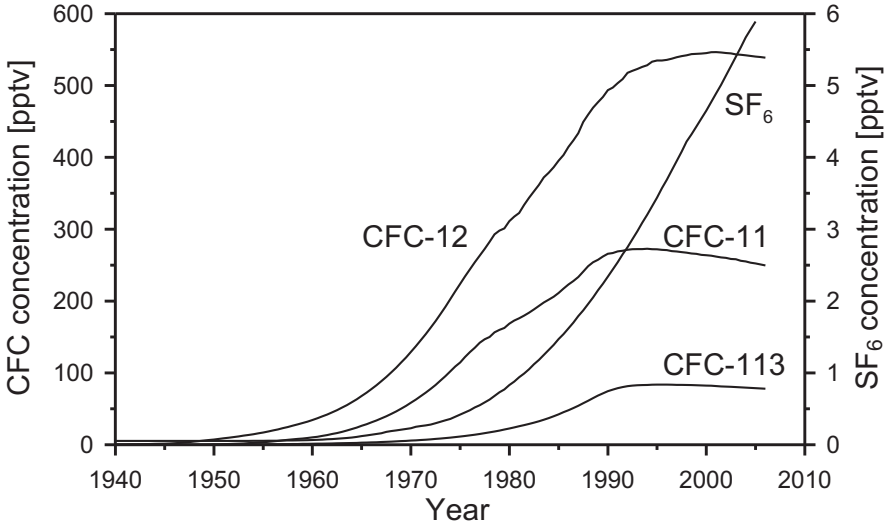

Fig. 2.9: Development of atmospheric concentrations of chlorofluorocarbons (CFCs) and sulfur hexafluoride (SF_6), as compiled from data available at NOAA (2006).

CFCs and SF_6 move fast through the unsaturated zone to the water table by gas diffusion. The concentration of soluted gases in groundwater varies as a function of the atmospheric partial pressures of the CFCs/SF_6 (respectively elevation a.s.l.) and the temperature at the water table during recharge, according to Henry's law.

Dating Groundwater with CFCs/SF_6

The known atmospheric input functions and the known solubilities of CFCs/SF_6 make the dating of young groundwater (less than 50 years) possible. The age refers to the time since the recharge water was isolated from air. The CFCs/SF_6 age is determined by comparing calculated concentration of CFCs/SF_6 that would be in air in equilibrium with the concentration in groundwater to CFCs/SF_6 concentrations measured in air for that particular location.

The simplest and most common transport assumption in CFC-based dating is to assume piston flow. However, many processes occur during recharge and in the groundwater environment that can affect CFC/SF_6 concentrations beyond those set by air-water equilibrium, and that consequently affect interpretation of apparent age. They

are: not exactly known recharge temperature, addition of air trapped and dissolved during recharge (excess air), microbial degradation in anaerobic environments, CFCs and SF_6 contamination through adding both gases to water from local anthropogenic sources, in addition to that of air-water equilibrium. Whereas the addition of typical excess air has negligible effect on CFC ages, SF_6 is particulary sensitive in respect to excess air due to the low solubility in water.

Chapter 3

Study Area

3.1 Location

The study area is situated in the border zone between Croatia and Bosnia-Herzegovina. One part of the investigated area is located in the Plitvice Lakes National Park, a plateau at 700-800 m a.s.l. between the slopes of mountains Lička Plješivica (1640 m), Mala Kapela (1280 m) and Medvedjak (884 m), covering an area of approximately 260 km^2. Typical karst areas in the adjacent south of the Plitvice Lakes are the karst fields Koreničko polje, Lapačko polje and Krbavsko polje (Fig. 3.1).

The other part lies in the NW of Bosnia-Herzegovina, including the area of the Bihać and Kulen Vakuf municipalities. Between both regions Una River meanders along the boarder of Croatia and Bosnia-Herzegovina. It emerges in Croatia (520 m a.s.l.) from the northeastern slopes of the Stražbenica mountain and flows through Kulen Vakuf and Bihać (231 m a.s.l.). Besides from the primary spring, Una River is fed by additional springs, which are resources for the water supply of both cities.

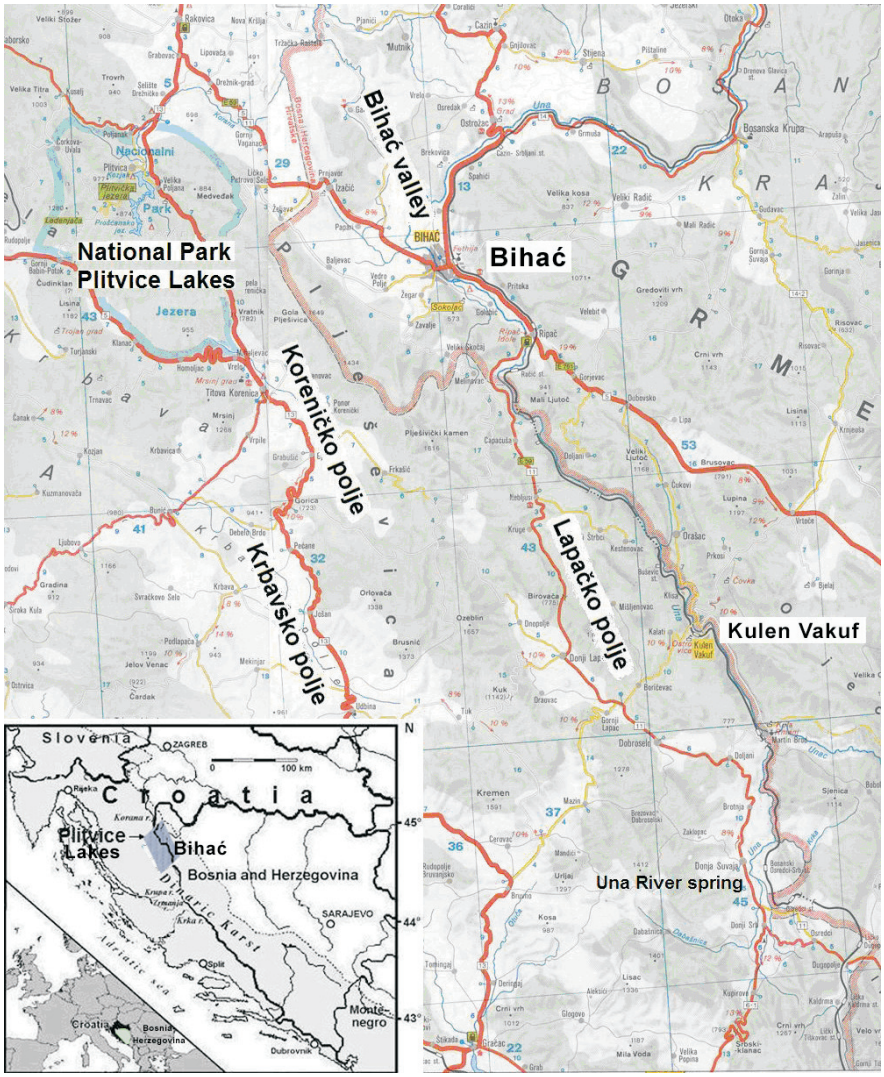

Fig. 3.1: Location of the study area in the boarder area of Croatia and Bosnia-Herzegovina, modified after Kapelj et al. (2006).

3.2 Climate

The climatic characteristics of the Plitvice Lakes are influenced by the location of the lakes at the mountain pass and the Adriatic Sea at about 50 km distance. The transitional type of Mediterranean and continental climate is prevailing. The average annual air temperature in the Plitvice Lakes ranges from 8 to 10°C, while average annual precipitation is in the order of 1200-1500 mm (Kapelj et al., 2006). During the cold winter

months January-March the lakes are mostly covered by surface ice. The spring time is characterized by snow melting and an average temperature up to 8°C. In the dry summer months the mean midday temperature is 24°, the autumn is rich in rain and has an average temperature of 5°C (Penzar, 2006). The mean potential evapotranspiration during one year is 490 mm (Beraković, 2005). The Bihać area is situated at around 231 m a.s.l. and has a moderate continental type of climate. The average annual rainfall is 1245 mm and average annual temperature is 10.8°C.

3.3 Hydrogeological Setting

Hydrogeologically, the investigated karst aquifers belong to the Black Sea catchment (Fig. 3.2). Geologically, they are situated in the unit Dinaric Karst, which forms a mountain chain from the NW to the SE, spanning areas of Slovenia, Croatia, Bosnia and Herzegovina, Montenegro and Albania (light grey colored area in the small map in Fig. 3.2). It forms a part of the Dinaric carbonate platform, which consists predominantly of karstified carbonate sediments such as Cretaceous, Jurassic and Triassic limestones and dolomites (Tari, 2002; Schmid et al., 2006). Dinaric karst has formed in response to Adria underthrusting the Dinaric carbonate platform domain in the late Jurassic stage until recent (Tari, 2002). This structural pre-disposition is reflected in the Dinaric strike (NW-SE) of tectonic structures (Fig. 3.2). The hydrology of the entire area is strongly controlled by these structural features. The general groundwater flow direction is SW to NE. However, the area is dominated by a large number of NE-SW trending faults strongly hydraulically influencing the groundwater flow direction.

According to the hydrogeological function of rocks and sediments, four main types can be distinguished (Kapelj et al., 2006; Miošić et al., 2006):

- high permeable carbonate rocks (deeply karstified and fractured limestones)
- medium permeable carbonate rocks (limestone with dolomite)
- low permeable carbonate rocks (dolomite)
- impermeable clastic rocks (silt, shale, clastic flysch).

The karst aquifers in the study area are hydraulically connected, as was shown by tracing experiments performed between 1973 and 1989 (Kapelj et al., 2006; Miošić

et al., 2006). The infiltration takes place in Croatia through the mostly high permeable carbonate rocks of the upper part of the aquifer (epikarst). This water flows towards Una River through a complex karst conduit network and emerges at the springs in Bosnia-Herzegovina. The groundwater infiltrated in the south of the Plitvice Lakes by Krbavsko polje, Koreničko polje and Prijeboj discharges in the springs Klokot and Privilica near Bihać. More in the south, the infiltrated waters around Lapačko polje and Mazin in Croatia discharge in the springs Una, Toplica and Ostrovica (Fig. 3.2).

Most of investigated springs are exploited for public supply purposes of the region. Table 3.1 gives an overview of the discharge data, municipalities using the spring water, and the spring type according to outflow hydrograph, origin of water, geologic and tectonic conditions, as outlined in Chapter 2.1. The lack of many discharge data, especially for the springs in Bosnia-Herzegovina, is due to the war in this region.

Table 3.1: Minimum, maximum and mean annual discharge (Q), spring type shown in Fig. 2.2: overflow (o), permanent (p), emerging (em), ascending spring (a), spring emerging from fractures (f), overflow spring (b), unknown (u); data source for the springs 1, 2, 3: Meteorological and Hydrological Service of Croatia; 4, 5, 10: Kapelj et al. (2006); 6, 7, 8, 9: Miošić et al. (2006).

Nr.	**Spring Name**	**Q [m^3/s]**			**User**	**Spring Type**	**Data**
		Q_{min}	Q_{max}	Q_{mean}			
1	Plitvica	0.03	16.4	0.7	Plitvice Lakes	p, em, o	1981-1990, 2003-2004
2	Bijela Rijeka	0.02	1.9	0.44	Plitvice Lakes	p, em, o	1982-1990, 2003-2004
3	Crna Rijeka	0.02	6.9	1.4	Plitvice Lakes	p, em, f	1980-1990, 2003-2004
4	Stipinovac	0.001	0.01	-	-	p, em, u	1980-1990
5	Vrelo	0.01	0.1	-	Korenica	p, em, u	1980-1990
6	Klokot	3	21.8	9.5	Bihać	p, em, a	1982-1983, 2000
7	Privilica	0.03	2	-	Bihać	p, em, u	u
8	Ostrovica	0.7	16	-	Donji Lapac	p, em, f	u
9	Toplica	0.06	1	-	Kulen Vakuf	p, em, f	u
10	Una	0.1	1	-	-	p, em, u	u

The Plitvice Lakes

Since 1979 the National Park is in the UNESCO's List of World Natural Heritage with ca. one millon visitors per year. The Plitvice Lakes basin is a geomorphological formation of biological origin, formed during the warm and humid interglacial period 6000-8000 years before present (Horvatinčić et al., 2000). It is a complex aquatic system, where calcium carbonate precipitates intensively in water forming tufa[1] barriers in the presence of moss, algae and aquatic bacteria between 15 smaller and larger lakes (Fig. 3.3). Additionally, calcium carbonate precipitates as the sediment on the bottom of the lakes (e.g. Obelić et al., 2005, 2006).

Recharge of the Plitvice Lakes occurs predominantly through runoff of the northern side of the carbonate massif Mala Kapela (Božičević & Biondić, 1999). Groundwater emerges in the south of the Plitvice Lakes at the springs Bijela and Crna Rijeka. A hydrogeological section A-B through the Plitvice Lakes shows that Crna Rijeka is a "contact" spring, where the groundwater emerges along a fault at the boundary between high permeable limestones and low permeable layered dolomites (Fig. 3.3).

[1]Tufa deposites are formed by calcite precipitation from freshwater supersaturated with calcium carbonate. This process is largely controlled by the outgasing of CO_2 or its consumption by plants (Horvatinčić et al., 2000).

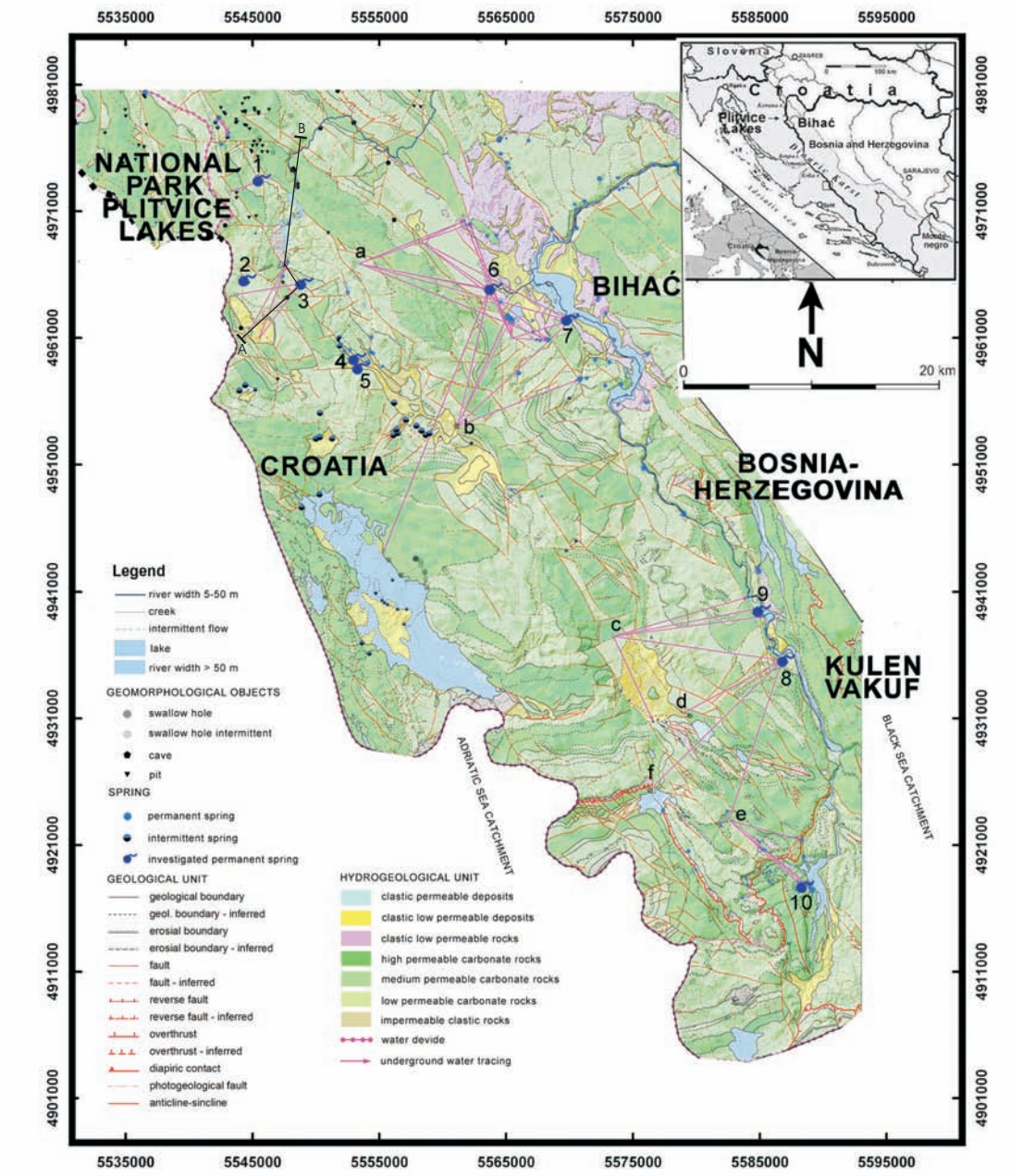

Fig. 3.2: Hydrogeological map, structural patterns and typical karst geomorphological features within the study area. Note swallow holes as injection points for tracing experiment between 1973 and 1989: a Prijeboj, b River Korenica inside of Koreničko polje, c, d Donji and Gornji Lapac inside of Lapačko polje, e Ponor Brezovac, f Mazin. Investigated springs: 1 Plitvica, 2 Bijela Rijeka, 3 Crna Rijeka, 4 Stipinovac, 5 Vrelo, 6 Klokot, 7 Privilica, 8 Ostrovica, 9 Toplica, 10 Una, A-B cross-section through the Plitvice Lakes (see Fig. 3.3), modified after Kapelj et al. (2006).

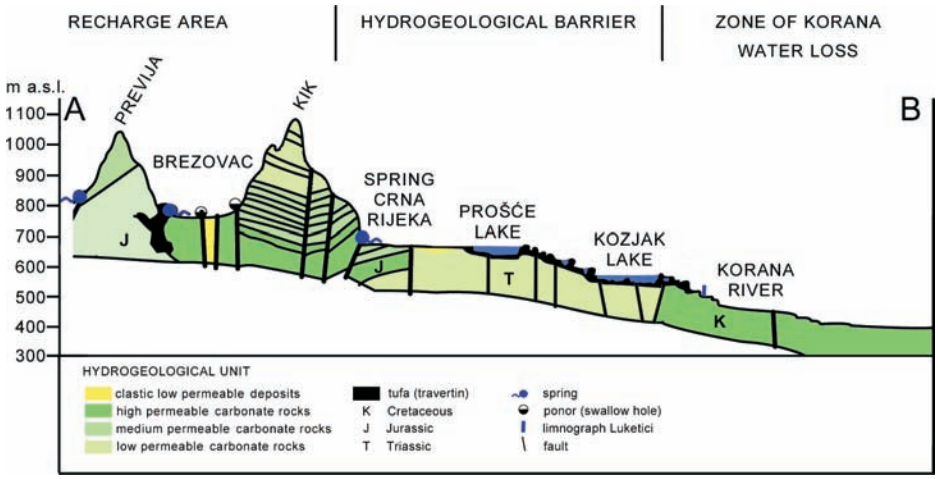

Fig. 3.3: Hydrogeological cross-section through the recharge area (mountain Mala Kapela) of the Plitvice Lakes, the zone of the hydrological barrier and the zone of the water loss in Korana River. See Fig. 3.2 for the position of the cross-section A-B, modified after Božičević & Biondić (1999).

The confluence of Bijela and Crna Rijeka builds Matica River flowing into the lakes, cascading over approximately 9 km through the lakes basin towards the Korana River canyon from 639 m a.s.l. to 481 m a.s.l.. The lakes between Prošće and Kozjak Lake[2] are mostly built on the Triassic low permeable dolomite base forming a hydrogeological barrier, whereas the lakes downstream of Kozjak[3] and the canyon of Korana River are located in a high permeable upper Cretaceous limestone bedrock.

Except for the water coming from the springs Bijela and Crna Rijeka, the lower lakes get water of the spring Plitvica feeding Plitvica Brook, seeping down over the 78 m high Veliki Slap Waterfall into Korana River. In its canyon various karst landforms like caverns and swallow holes developed (Fig. 3.2). In that part the Korana River flow is characterized by significant water loss; especially during the dry summer months the river bed dries up completely along several kilometers downstream the lakes and reappears after the beginning of the rainy period in autumn (DHMZ, 1989; Beraković, 2005; Zwicker et al., 2006).

[2]Upper lakes: Prošće, Ciginovac, Okrugljak, Batinovac, Veliko Jezero, Malo Jezero, Vir, Galovac, Gradinsko, Burgetići, Kozjak

[3]Lower Lakes: Milinovac, Gavanovac, Kaludjerovac, Novakovića Brod.

Chapter 4

Field and Laboratory Techniques

4.1 Water Sampling

Sampling sites of springs and surface waters in the area of the Plitvice Lakes and Una River catchment are depicted in Figure 4.1. A more detailed map of the Plitvice Lakes (Figure 4.2) shows the sampling sites along the lake chain and their tributaries.

Sampling for the investigation of **stable isotopes (^{2}H/^{18}O)** was performed at 15 sampling points at the Plitvice Lakes area and at 8 sites along Una River, including springs, rivers, lakes and their tributaries. Besides the sampling of surface and groundwater also atmospheric water (precipitation) from the Meteorological station at the Plitvice Lakes were collected. The sampling was performed on a monthly basis between April 2003 and June 2005. The water was collected in 100 ml plastic bottles. In the two largest lakes, Prošće and Kozjak, sampling was also done once in September 2004 for vertical water profiles down to 25 m and 45 m, respectively.

Water samples for **tritium** measurements were collected in 1000 ml plastic bottles from the precipitation of the Plitvice Lakes and from 10 karst springs also on the monthly basis between April 2003 and June 2005, but sampling was performed only from springs the springs Klokot, Privilica, Ostrovica and Toplica. Measurements were performed at the Rudjer Bošković Institute, Zagreb, Croatia. Tritium measurements for all 10 springs for the sampling campaigns in November 2003 and July 2004 were performed at the Institute of Environmental Physics/Oceanography, University of Bremen,

Germany. The stable isotopes and tritium data for sampling periods before 2003 were obtained from previous research conducted at the Rudjer Bošković Institute, Zagreb, Croatia or from the GNIP database (IAEA/WMO, 2006).

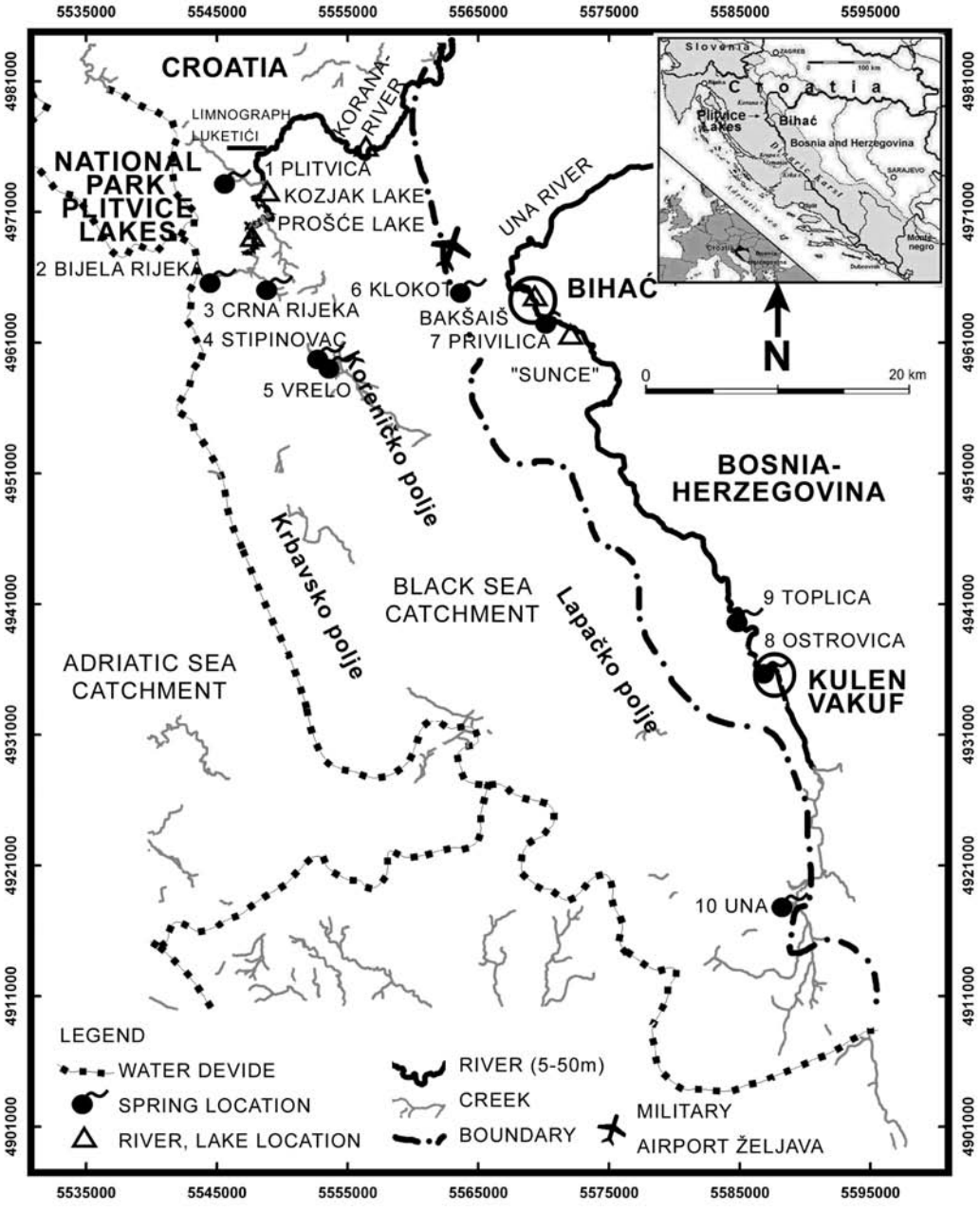

Fig. 4.1: Sampling sites numbered for spring, lake and river waters at the Plitvice Lakes and Una River. Note the position of the abandoned military airport Željava NW from Bihać, which is mined, modified after Kapelj et al. (2006).

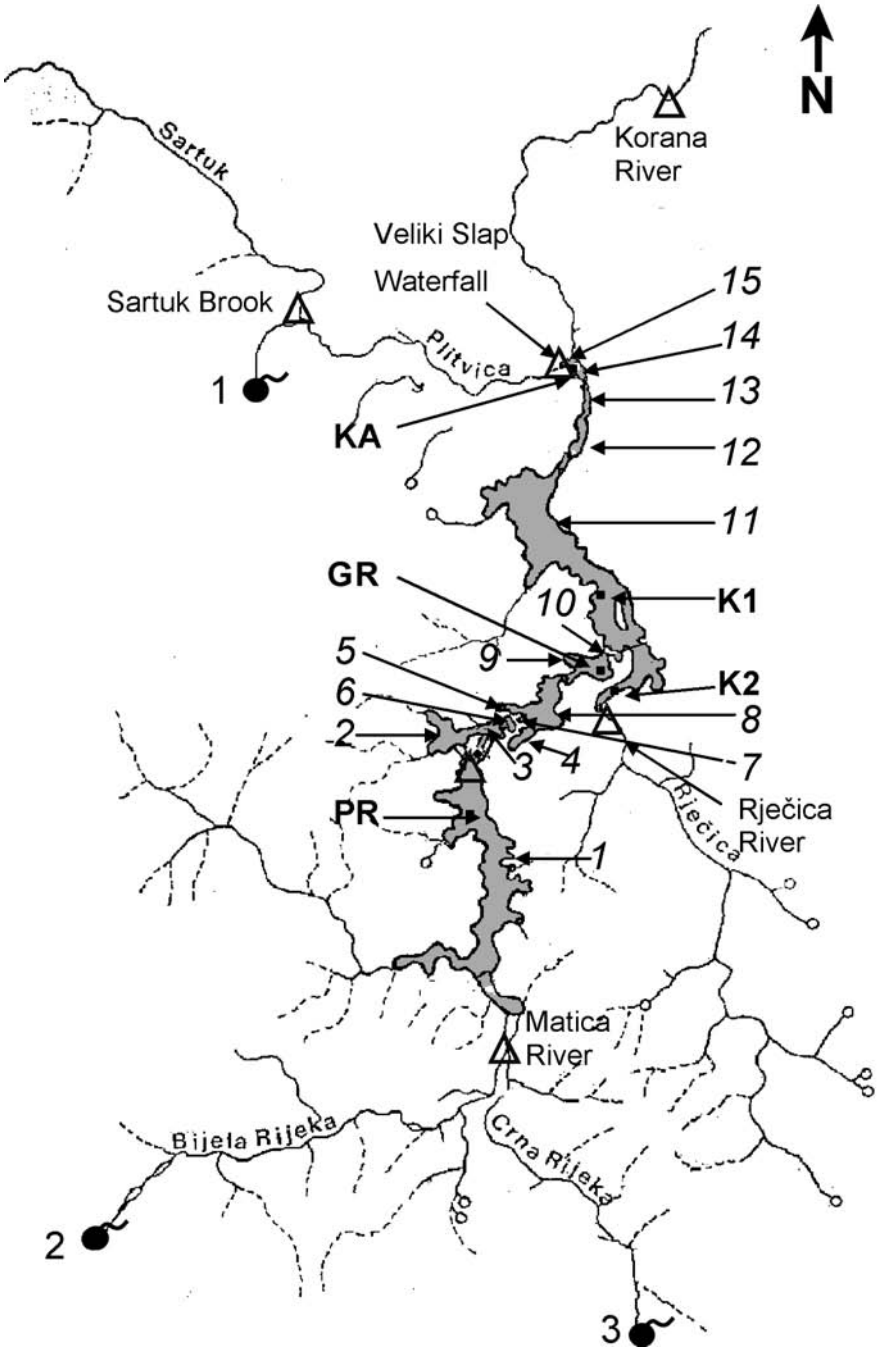

Fig. 4.2: Sampling sites at the Plitvice Lakes: Upper lakes: *1* Prošće, *2* Ciginovac, *3* Okrugljak, *4* Batinovac, *5* Veliko Jezero, *6* Malo Jezero, *7* Vir, *8* Galovac, *9* Gradinsko, *10* Burgetići, *11* Kozjak, Lower Lakes: *12* Milinovac, *13* Gavanovac, *14* Kaludjerovac, *15* Novakovića Brod. Triangles mark sampling points from river waters used in this study (Matica, Rječica, Sartuk, Korana). Numbers 1, 2, 3 mark the springs Plitvica, Bijela Rijeka and Crna Rijeka. Squares mark the position of the five sites for sediment sampling: Prošće Lake (PR), Gradinsko Lake (GR), Kozjak Lake (K1, K2), and Kaludjerovac Lake (KA), modified after Srdoč et al. (1985).

The sampling for tritium and stable isotopes was performed by the partners of the EU project (ANTHROPOL.PROT, 2006). The sampling of CFCs/SF_6 and $^3H/^3He$ was part of this study. A first campaign including special sampling techniques (s. below) was performed in November 2003 during the wet season, when springs had high discharge, and a second campaign for the same set of springs during the dry season and low discharge state (base flow) in July 2004. Additionally four samples were taken from surface water for CFCs and SF_6. Two of these surface samples were taken from Prošće and Kozjak Lake of the Plitvice Lakes, two are from locations along Una River, upstream ("Sunce") and downstream (Bakšaiš) of Bihać.

CFCs and SF_6 water samples were collected using 500 ml glass bottles in a metal tin. For this sampling technique a glass bottle is placed into a metal tin (1.5 l) which itself is placed in a bucket (10 l). The outflow of the tubing coming from the pump is placed at the bottom of the sample bottle and the whole system is thoroughly flushed with at least 10 l sample water (20 times the sample amount) until the water fills the bucket completely. Then bottle and tin are closed under water to avoid any contamination with air (Fig. 4.3).

$^3H/^3He$ samples were collected in 40 ml copper tubes connected directly to the pump outlet using a transparent tygon tubing of less than 3 m length. At the outlet end of the copper tube a clear plastic tube and regulator valve were attached. The copper tubes were sealed at each end with stainless steel pinch-off clamps after thoroughly flushing until no gas bubbles were detected in the inlet and outlet tubes (Fig. 4.4).

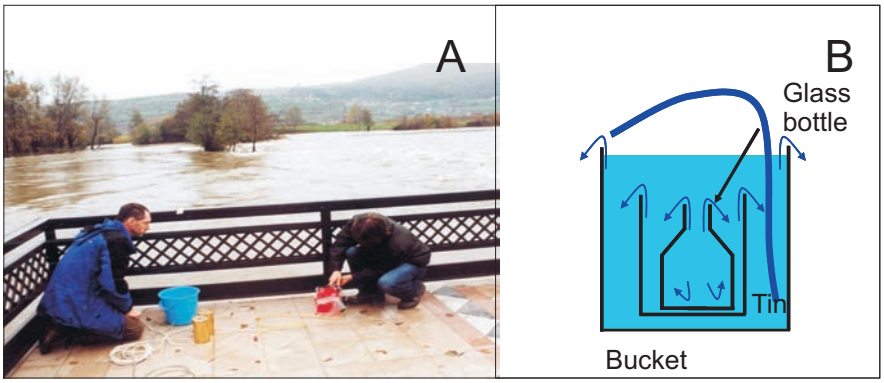

Fig. 4.3: Water sampling for CFCs/SF_6 measurements at the sampling site "Sunce", Una River, 2003-11-02 (A); sampling with 50 ml glass bottle and metal tin (B).

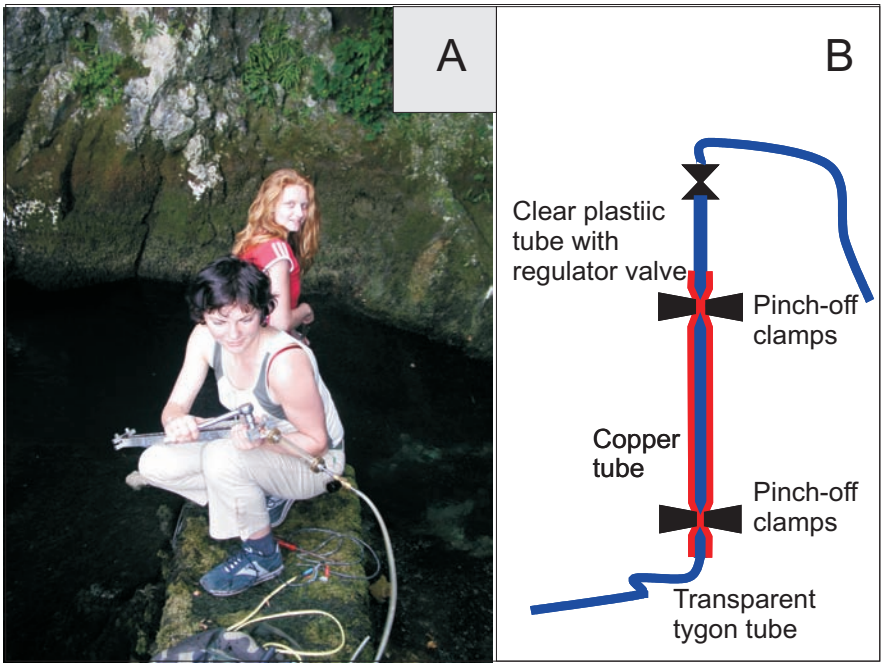

Fig. 4.4: Water sampling for $^3H/^3He$ measurements at the spring Klokot, Una River, 2003-11-02 (A); sampling of noble gases with 40 ml copper tube (B).

4.2 Measurement Techniques

At the Leibniz Institute for Applied Geosciences (GGA-Institut) in Hannover, Germany, a chromium reactor was used to reduce 1 μl water to hydrogen (Finnigan H/Device). The **stable isotope deuterium (^{2}H)** in the hydrogen gas was analyzed using a dual inlet mass spectrometer (Finnigan Delta-S). A subset of the samples was measured in the laboratories of Umweltforschungszentrum Leipzig-Halle (UFZ) and the International Atomic Energy Agency (IAEA) to cross-check stable isotope analytical precision.

Tritium from karst springs and precipitation was measured by the Rudjer Bošković Institute, Zagreb, Croatia, using Gas Proportional Counter (GPC) with a detection limit of 1 TU. The samples from the two sampling campaigns were measured by the ^{3}He ingrowth technique at the Institute of Environmental Physics/Oceanography, University of Bremen, Germany, where also the noble gas samples from springs were measured.

Noble gas concentrations for ^{3}He and ^{4}He were determined with a MAP 215-50 noble gas mass spectrometer using the methods outlined in Bayer et al. (1989). ^{20}Ne and ^{22}Ne were measured in a quadrupole mass spectrometer (Balzers QMG112). The system was calibrated using defined quantities of air. Absolute concentrations of the noble gases were determined with a precision of $\pm$1%, ^{3}He/^{4}He ratios to better than 0.5%.

Measurements of **CFCs and SF$_6$** from the two sampling campaigns were performed at the Spurenstofflabor Dr. Harald Oster, Wachenheim, Germany, using purge and trap gas chromatography with electron capture detection (Bullister & Weiss, 1988; Oster, 1994). The reproducibility of the whole procedure consisting of sampling and measurement is about 1% in air and 3% in water (Oster et al., 1996).

Chapter 5

Tracing Precipitation and Flow Paths of Groundwater

5.1 Precipitation in the Study Area

This chapter discusses the origin of precipitation as the main source for groundwater recharge. The investigated area is situated in the continental part of Croatia and Bosnia-Herzegovina adjacent the Adriatic Sea. Accordingly, the precipitation in the area may have both the continental and Mediterranean influence. Using the amount of precipitation and data for the wind direction from the Meteorological station Plitvice Lakes for the years 2003 and 2004, it was possible to calculate for each month the percentage of the entire precipitation originating from a certain direction. Winds from the northeast transport the largest single contribution of precipitation amounting to 44.8% and 32.8% of the total in 2003 and 2004, respectively (Fig. 5.1). In the total balance, clouds transported with N, NE, E, SE, NW winds account for approximately 80% of the precipitation to the Plitvice Lakes and contribute the continental influence. Winds blowing from S, SW, and W direction transport 20% of the precipitation and contribute the Mediterranean influence.

Besides the analysis of moisture origin and wind directions described above, also the isotopic pattern in precipitation allows to deduce the origin of moisture. Therefore, the stable isotope data from the Una River and Plitvice Lakes were compared with the

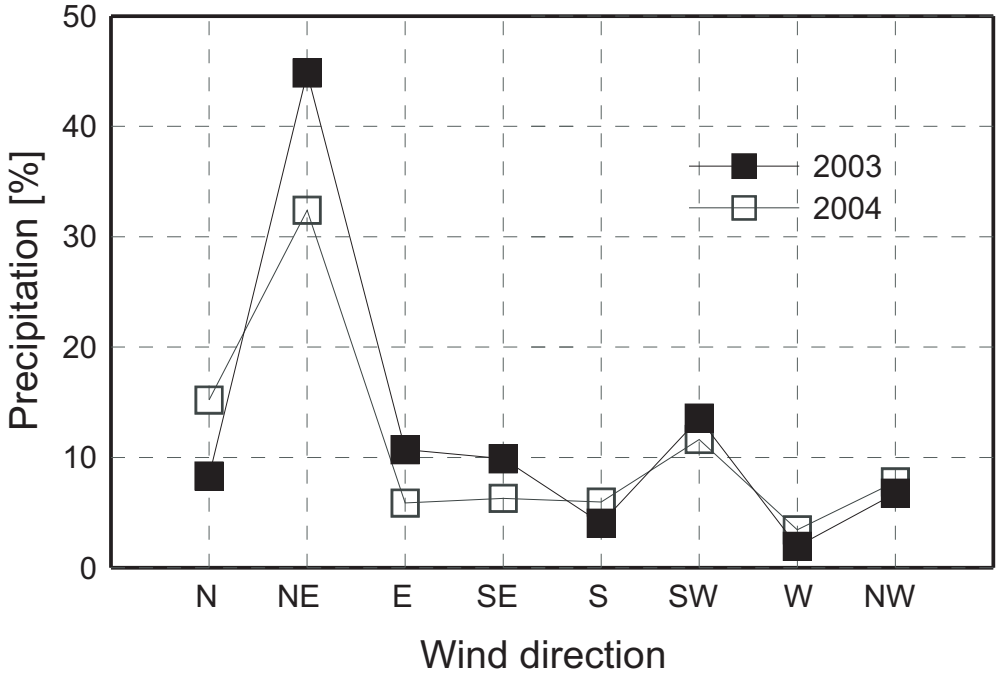

Fig. 5.1: Percentage of precipitation in relation to the wind direction for 2003 and 2004 at the meteorological station at the Plitvice Lakes. The data owner is the Meteorological and Hydrological Service of Croatia (DHMZ).

data from the IAEA/WMO GNIP database for the stations nearby: Ljubljana and Zagreb from the continental part of Slovenia and Croatia, and Zavižan, Zadar, and Dubrovnik, which are situated in the Adriatic region of Croatia (Fig. 5.2). The comparison of data shows a very good agreement of the Plitvice Lakes data with those from Ljubljana and Zagreb. This fact justifies considering the Zagreb data as the input function for the modeling with stable isotopes, which is helpful, because the time series of data for the Plitvice Lakes is too short to serve as an input function for the models.

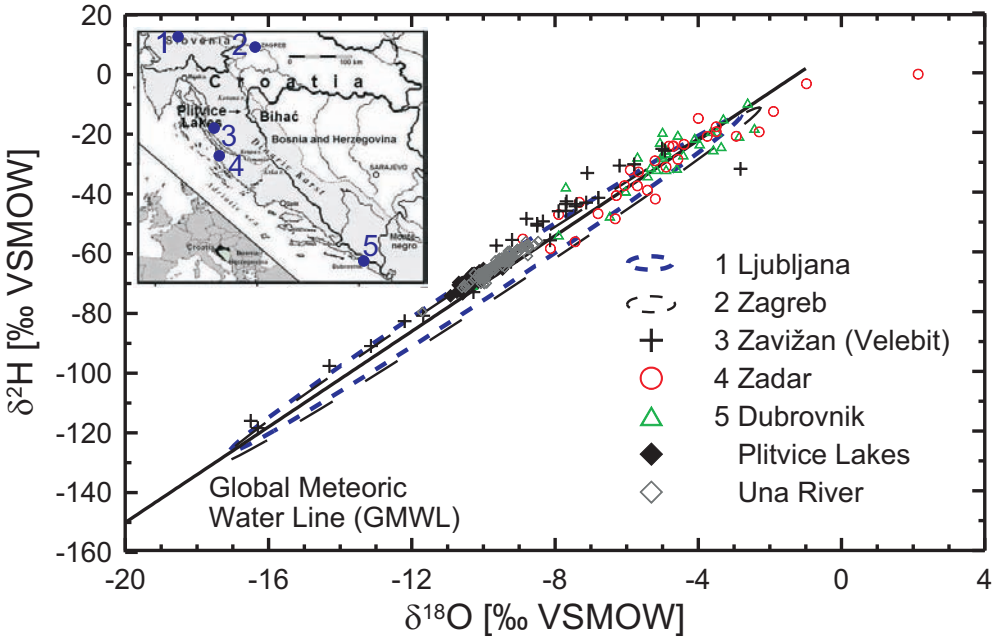

Fig. 5.2: Stable isotope plot with GWML of the sites nearby the Plitvice Lakes and Bihać on the basis of the IAEA/WMO GNIP Database: 1 Ljubljana (1984-2002), 2 Zagreb (1975-2003), 3 Zavižan, 4 Zadar, 5 Dubrovnik (2000-2003), Plitvice Lakes, Una River (2003-2005).

5.2 Hydrological Connection Between Aquifers

The continental and Mediterranean influence in precipitation and different meteoric conditions is reflected in the specific isotopic signature of the investigated water. It is shown in the Global Meteoric Water Line-plot (Fig. 5.3). The stable isotopes (^{2}H and ^{18}O) of the Plitvice Lake and Una River plot above the GMWL and their ratio is described by the Local Meteoric Water Line (LMWL). Most samples seem to have some influence from the Mediterranean area, where deuterium excess higher than 10‰ prevails (mean 13.5‰). As it was concluded in the previous chapter, this isotopic signature originates from the precipitation transported from clouds by S, SW and W winds to the study area. Two clusters of surface and spring water can be discerned in the δ^2H/δ^{18}O plot, with values lower and higher than δ^{18}O = -9.7‰: more positive values are from Una River, more negative values are from the Plitvice Lakes catchment. Some springs

feeding Una River (Klokot, Privilica) have the stable isotope signature of the Plitvice catchment, which suggests a hydrologic connection of these two systems and the same infiltration area in Croatia. The more positive deuterium values of the Una River catchment suggest another infiltration area more in the south and closer to the moisture source from the Adriatic Sea and indicate lower mean altitude of recharge area of Una River (average altitude 230 m a.s.l.) than that of the Plitvice Lakes catchment (average altitude 700 m a.s.l.). Figures 5.2 and 5.3 show that stable isotopes in precipitation sampled at stations Zadar and Dubrovnik are positioned close to the values of Una River.

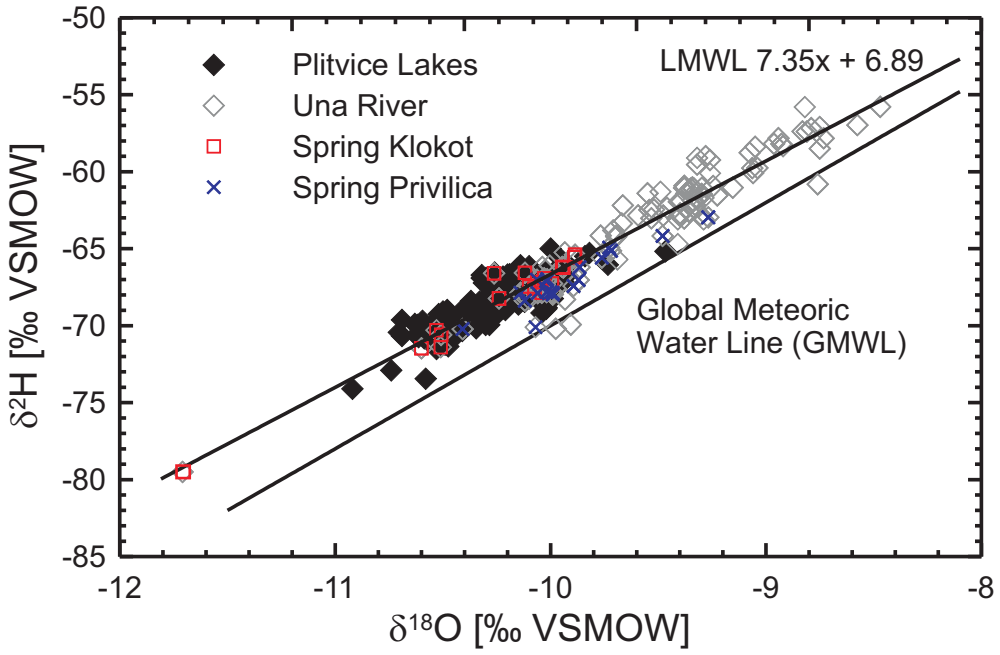

Fig. 5.3: $\delta^{18}O/\delta^{2}H$ plot with GMWL and LMWL from the Plitvice Lakes and Una River with data obtained between 2003 and 2005. "Plitvice Lakes" catchment includes all sampling points in Croatia, whereas "Una River" includes all sampling points in Bosnia-Herzegovina.)

Besides the groundwater flow from the karst fields in the south of the Plitvice Lakes to Una River, which have been proven with dye and isotopic methods, the stable isotope pattern also suggests a groundwater flow from the north side of the Plitvice Lakes towards Una River. This hypothesis is emphasized by a very similar isotopic signature of

Korana River (Plitvice Lakes) and the springs Klokot and Privilica near Bihać (Fig. 5.4). The time series of deuterium values at Klokot follows the one at Korana River with a lag of approximately 2-3 months. In the plot a distinctive deuterium value of -81‰ from the sample collected in April 2005 in the spring Klokot can be observed. Deuterium in precipitation of the Plitvice Lakes also shows a very negative value of -133‰, but one month earlier than in the spring Klokot (Fig. 5.4). Such negative values are a result of the isotope fractionation owing to temperatures down to -20°C in February 2005. A comparison of deuterium values in the spring water and the precipitation shows that the precipitation reaches the spring in rather short time as the quick flow component. On the other hand the deuterium value of Korana River in April 2005 does not show such a distinctive negative signature. This behaviour could be expected, because the water sample is a mixture of the snow melt and the great volume of the lake water.

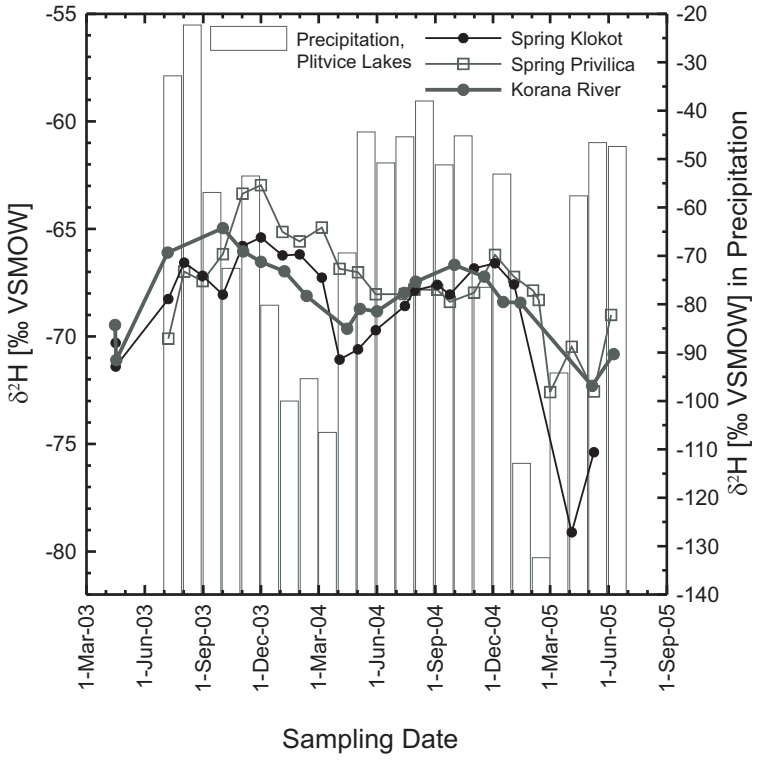

Fig. 5.4: Comparison of deuterium variations in precipitation of the Plitvice Lakes with deuterium variations in water sampled at Korana River (outflow of the Plitvice Lakes), spring Klokot, and spring Privilica. See Figure 4.1 for the position of the sampling points.

Chapter 6

Water Balance of the Plitvice Lakes

As described in Chapter 5.2 the water balance of the Plitvice Lakes is strongly influenced by the hydrological connection between Korana River at the outflow of the Plitvice Lakes and the springs Klokot and Privilica in Bosnia-Herzegovina. Another factor influencing the water balance is the pumping of water from Kozjak Lake. A current extraction rate (0.06 m^3/s) will not be high enough to satisfy the future demand of the tourist infrastructure at the Plitvice Lakes National Park. Therefore, the opening of new pumping capacities is planned. Zwicker et al. (2006) and Zwicker & Rubinić (2005) have shown that the depleting in the mean annual discharge of Kozjak Lake (0.04 m^3/s per year) and elevated water levels for the period between 1953 and 2005 have caused the slowing-down of tufa growth rates in the lakes. Due to the sensibility of tufa growth on changes in hydrological circumstances the change of the Kozjak water level by enhanced water exploitation is investigated in this study.

The previous investigations of water balance for the Plitvice Lakes (Beraković, 2005; Zwicker et al., 2006; Zwicker & Rubinić, 2005) do not consider factors such as evaporation from the lake water body, water mixing mechanism within the lakes (thermocline), mixing of lakes waters and their tributaries, and pumping from Kozjak Lake for drinking water supply of the National Park. Analysis of all these factors will be an issue of the following chapters. First, the lake volume is newly determined, due to obvious mistake made earlier in literature (Petrik, 1958).

6.1 Lake Volume

In the literature often cited number for the lake volume of the Plitvice Lakes is 400 000 m^3, as determined by Petrik (1958) in a first complex limnological research determining altitude, depth and surface of 15 lakes (Tab. 6.1). The results of the depth measurements for all lakes were depicted in isobate maps (Fig. 6.1 for the two biggest lakes). However, a first glance to the maps shows that this value is too small: volume of 400 000 m^3 corresponds to a lake of 2 000 m length, 200 m width and 1 m depth and all these values are already exceeded by Kozjak Lake. The lake volume here is newly calculated using the isobate maps from Petrik's work (1958), assuming that they were reliable, whereas a volume number is false[1]. Accordingly, the total lake volume is 22.95 Mio. m^3. Lakes Prošće and Kozjak contribute 89% to this volume. The newly calculated lake volumes are summarized in Table 6.1.

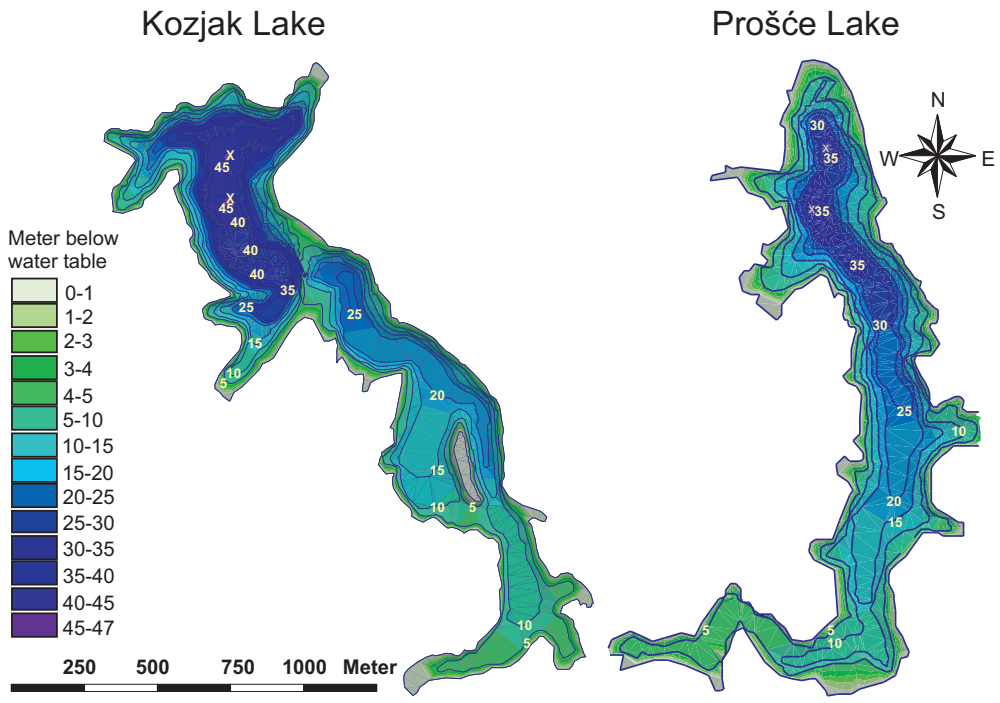

Fig. 6.1: Isobate maps for Kozjak Lake and Prošće Lake, after Petrik (1958).

[1]The isobate maps were digitized and the lake volume was calculated with the software ArcView GIS and its extensions Spatial and 3D Analyst.

Table 6.1: Calculated lake water volume of the Plitvice Lakes (V_{lake}). Lake surface (S_{lake}), maximum depth (d_{lake}) and altitude (h_{lake}) of particular lakes as given in the work of Petrik (1958). Malo Jezero* is the recent name for lake Jovinovac used in the work of Petrik (1958).

Lake Number	**Lake Name**	**V_{lake}** [**Mio. m^3**]	**S_{lake}** [**ha**]	**d_{lake}** [**m**]	**h_{lake}** [**m a.s.l**]
	Upper Lakes				
1	Prošće	7.67	68.20	37.40	636.60
2	Ciginovac	0.47	7.50	11.10	625.60
3	Okrugljak	0.19	4.10	15.30	613.60
4	Batinovac	0.04	1.50	5.50	610.10
5	Veliko Jezero	0.05	2.00	8.10	607.50
6	Malo Jezero*	0.03	2.00	9.00	605.60
7	Vir	0.007	0.60	5.00	598.70
8	Galovac	1.08	12.50	24.40	584.60
9	Gradinsko	0.26	8.10	10.00	553.00
10	Burgetići		-	-	-
11	Kozjak	12.71	82.00	46.40	535.00
	Lower Lakes				
12	Milinovac	0.31	3.20	18.40	523.30
13	Gavanovac	0.03	0.70	10.00	519.00
14	Kaludjerovac	0.11	2.10	13.40	505.20
15	Novakovića Brod	0.004	0.40	4.50	503.00
	Σ	**22.95**	**194.90**		

6.2 Mixing of Water

The waters of the Plitvice Lakes present mixture of different mixing components (springs, lakes, tributaries and river water), which have distinct δ^2H signatures. Deuterium is a conservative tracer and the mixing components will contribute their mixing ratio in the δ^2H value to the mixture according to Equation 2.14. Four cases were chosen to calculate mixing ratios of components a and b in the mixture c (Fig. 6.2):

- Case A: spring Bijela Rijeka (a) + spring Crna Rijeka (b) = Matica River (c)
- Case B: Rječica River (a) + Burgetići Lake (b) = Kozjak Lake (c)

- Case C: Sartuk Brook (a) + spring Plitvica (b) = Veliki Slap Waterfall (c)
- Case D: Veliki Slap Waterfall (a) + Kaludjerovac Lake (b) at the end of the lake chain = Korana River (c).

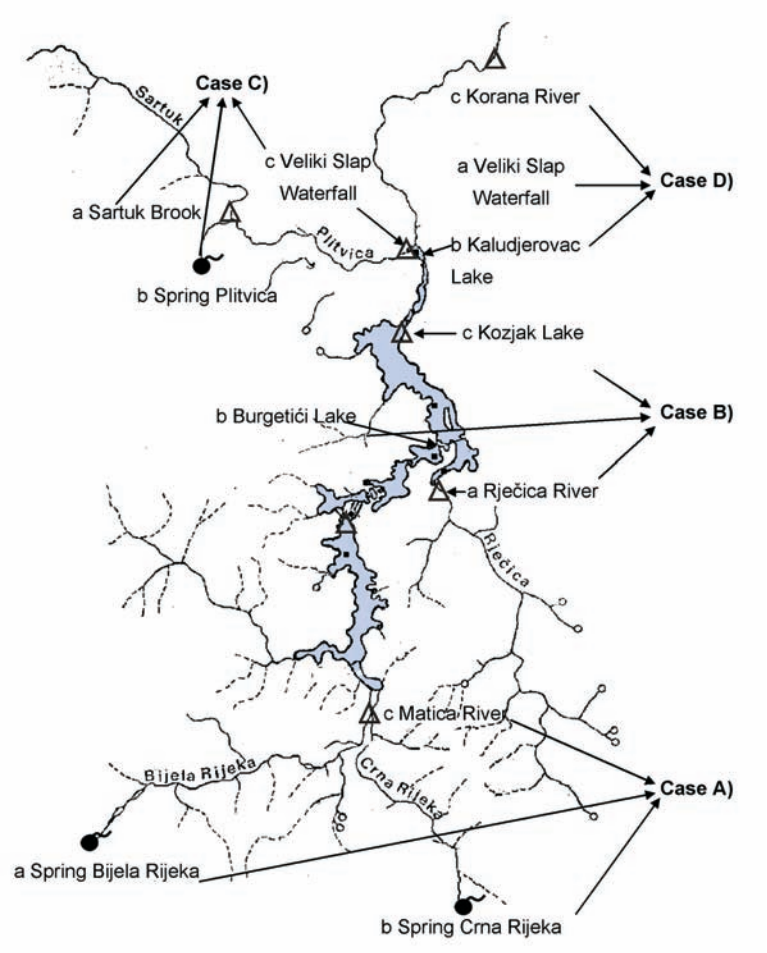

Fig. 6.2: Map of the Plitvice Lakes with locations for δ^2H sampling in water for determination of mixing ratios of waters with different origin. Four mixing cases (A, B, C, D) were investigated to determinate mixing ratios of particular mixing components (a, b) in mixture (c).

Deuterium measurements used for case studies are shown in Figure 6.3. Some assumptions concerning deuterium have to be fulfilled if Equation 2.14 is used. The difference in the end members has to be large compared to the analytical uncertainty of the measurements, which is $\pm 0.7‰$ for δ^2H in the Hannover laboratory. Any difference

in the end members smaller than twice this analytical uncertainty has to be treated as if the waters are of identical isotopic composition. In practice this means that the difference in δ^2H between two waters used for these mixing calculations has to be at least 2.8‰.

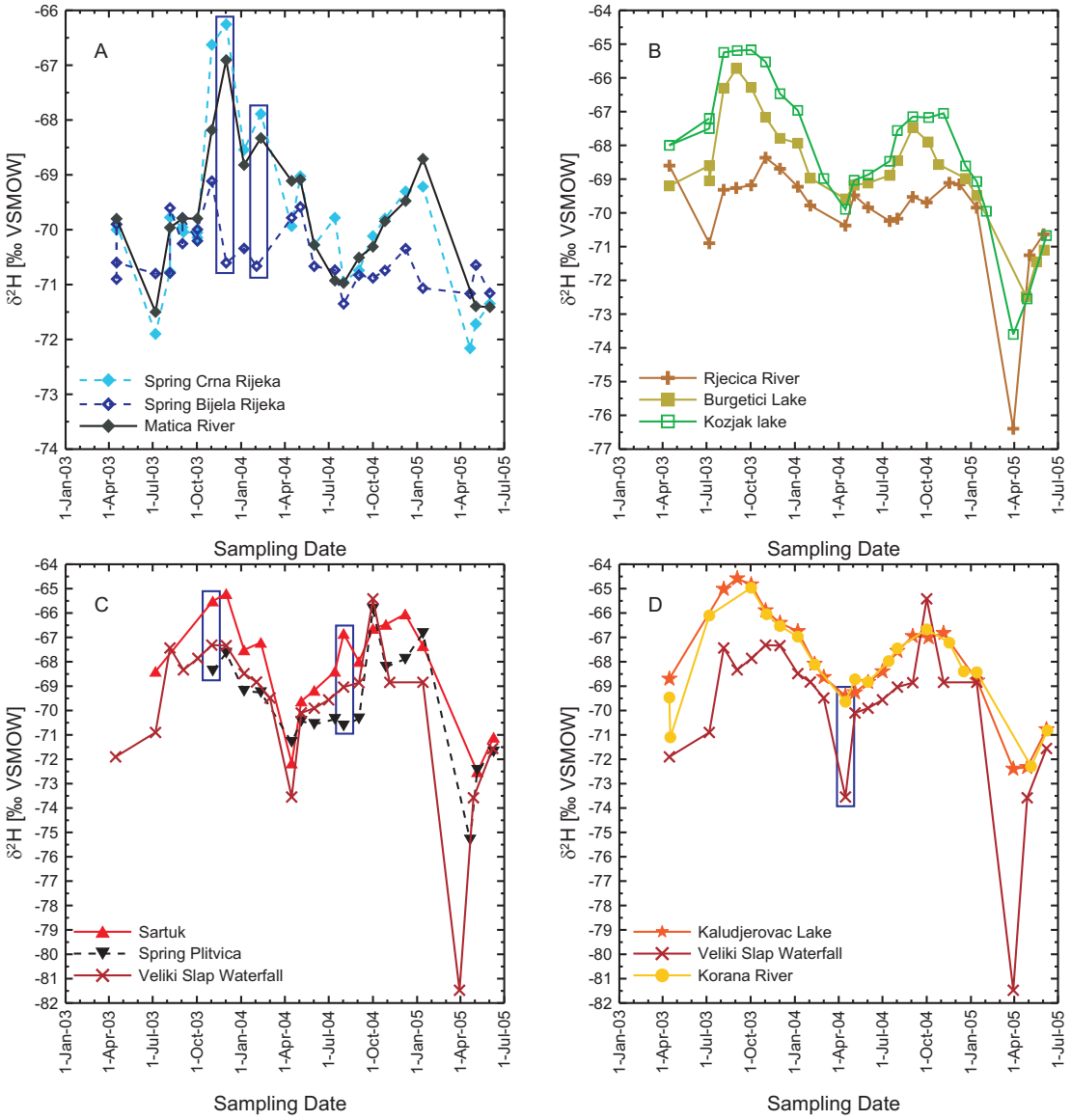

Fig. 6.3: Time series of deuterium used for determination of mixing ratios of spring waters, lake waters and their tributaries for four case studies (A, B, C, D) Blue rectangles in δ^2H-plots mark the time, where the assumption of a minimum isotopic difference between the end members is fulfilled.

Case A: Spring Bijela Rijeka, Spring Crna Rijeka, Matica River

The spring Bijela Rijeka contributed in December 2003 and February 2004 with ca. 15% and the spring Crna Rijeka with ca. 85% to their confluence Matica River. However, discharge [2] measurements for December, 2003 showed the springs Crna and Bijela Rijeka are not the only sources feeding Matica River, but 0.72 m^3/s originates from an unknown source, which might be smaller surface tributaries or underground water (Table 6.2).

Table 6.2: Isotopic and discharge values for case A for December 2003 and three mixing components (a, b, x) of Matica River (c). $\delta_{\mathrm{a,b,c,x}}$ mark deuterium values for each of the mixing components, $\Delta\delta_{\mathrm{a,b,c,x}}$ is the absolute analytical error for deuterium, $\mathrm{Q}_{\mathrm{a,b,c,x}}$ marks discharge measurements and $\Delta\mathrm{Q}_{\mathrm{a,b,c,x}}$ is their absolute error of 10%.

Case A	**Comp.**	δ^2**H [‰VSMOW]**				**Q [m^3/ s]**			
Spring Bijela Rijeka	a	δ_{a}	-69.10	$\Delta\delta_{\mathrm{a}}$	0.70	$\mathrm{Q_a}$	0.31	$\Delta\mathrm{Q_a}$	0.03
Spring Crna Rijeka	b	δ_{b}	-66.60	$\Delta\delta_{\mathrm{b}}$	0.70	$\mathrm{Q_b}$	1.81	$\Delta\mathrm{Q_b}$	0.18
Matica River	c	δ_{c}	-68.20	$\Delta\delta_{\mathrm{c}}$	0.70	$\mathrm{Q_c}$	2.84	$\Delta\mathrm{Q_c}$	0.28
Unknown Component	x	δ_{x}	-71.68	$\Delta\delta_{\mathrm{x}}$	4.71	$\mathrm{Q_x}$	0.72	$\Delta\mathrm{Q_x}$	0.07

If one assumes there is only one unknown component x feeding the Matica River, its isotopic composition and error can be calculated by Equations 6.1 and 6.2 describing a three component mixing relation

$$\delta_{\mathrm{x}} = \frac{\mathrm{Q_c}\delta_{\mathrm{c}} - \mathrm{Q_a}\delta_{\mathrm{a}} - \mathrm{Q_b}\delta_{\mathrm{b}}}{\mathrm{Q_x}} \tag{6.1}$$

$$\Delta\delta_{\mathrm{x}} = \frac{\sqrt{{\delta_{\mathrm{a}}}^2 * {\Delta\mathrm{Q_a}}^2 + {\delta_{\mathrm{b}}}^2 * {\Delta\mathrm{Q_b}}^2 + {\delta_{\mathrm{c}}}^2 * {\Delta\mathrm{Q_c}}^2 + {\mathrm{Q_a}}^2 * {\Delta\delta_{\mathrm{a}}}^2 + {\mathrm{Q_b}}^2 * {\Delta\delta_{\mathrm{b}}}^2 + {\mathrm{Q_c}}^2 * {\Delta\delta_{\mathrm{c}}}^2}}{\mathrm{Q_x}} \tag{6.2}$$

The unknown δ_x is found to be -71.68‰. However, its error $\Delta\delta_x$ with 4.71‰ is too huge to discern this isotopic value from those of the springs Bijela and Crna Rijeka and

[2] The data owner for discharge measurements in the area of the Plitvice Lakes is the Meteorological and Hydrological Service of Croatia (DHMZ).

Matica River. The reason for the seemingly large error is not the insufficient analytical precision of deuterium measurements, but the small difference in isotopic values between the mixing components and the analytical error in discharge measurements. Only if the uncertainty of $\Delta Q_{a,b,c,x}$ would be smaller than 1%, then $\Delta\delta_x$ would be 0.67‰ and small enough to look for the origin of this contribution.

Case B: Rječica River, Burgetići Lake, Kozjak Lake

The isotopic signature of the water mixture in Kozjak Lake does not fall between the end members Rječica River and Burgetići Lake. For this reason these isotope values cannot be used for such a mixing calculation. This is not unexpected since the contribution of Rječica River is small and evaporative enrichment of the Kozjak Lake will shift its isotopic composition towards more positive values.

Case C: Sartuk Brook, Spring Plitvica, Veliki Slap Waterfall

The spring Plitvica and Sartuk Brook feed Plitvica Brook, seeping down over the 78 m high Veliki Slap Waterfall into Korana River (Fig. 6.4). The spring Plitvica contributed to Veliki Slap Waterfall much more water than Sartuk Brook: in November 2003 63% of total amount of water flowing over the waterfall, in February 2004 84%.

Case D: Veliki Slap Waterfall, Kaludjerovac Lake, Korana River

94% of the water sampled at Korana River on 2004-04-11 originates from Kaludjerovac Lake and only 6% water is contributed from Veliki Slap Waterfall (Fig. 6.4). Between Kaludjerovac Lake, Veliki Slap Waterfall and the sampling point at Korana River there is a limnograph called Luketići, which noted a discharge value of 6.24 m^3/s for this date. However, the whole discharge from the Plitvice Lakes including springs, lakes and their tributaries yield 7.03 m^3/s. This means that approximately 12% of the water does not reach the sampling point at Korana River and is lost, probably to swallow holes in the riverbed. Such sinks are evident since Korana River dries out from time to time during the summer months. In the opposite hydrologic situation - the rainy months in autumn - a part of water oozes slowly out into the river bed. This means that the swallow holes

during this time are a source of water to the river bed. The origin of this additional groundwater is not yet known. The isotopic signature of water at the sampling point Korana River is nearly identical to the isotopic signature of Kaludjerovac Lake at the end of the lake chain. So, the water flowing from the swallow holes to the river bed has either the same origin as the lake water (hidden connection with Kozjak and the Lower lakes?) or its isotopic signature is by chance similar enough to be not distinguishable.

The results of all mixing ratio calculations are summarized in Table 6.3.

Table 6.3: Mixing ratios of the lake, river and spring waters of the Plitvice Lakes.

Case	**Mixing Component**		**Mixture**	**Sampling Date**	**Mixture**	
	a	**b**	**c = a+b**		**a in c [%]**	**b in c [%]**
A	Spring	Spring	Matica	01.12.2003	15	85
	Bijela Rijeka	Crna Rijeka	River	11.02.2004	16	84
B	Rječica	Burgetići	Kozjak	-	determination	determination
	River	Lake	Lake		not possible	not possible
C	Sartuk	Spring	Veliki Slap	03.11.2003	37	63
	Brook	Plitvica	Waterfall	11.02.2004	16	84
D	Veliki Slap	Kaludjerovac	Korana	15.04.2004	6	94
	Waterfall	Lake	River			

Fig. 6.4: Kaludjerovac Lake, Veliki Slap Waterfall and Plitvica Brook at the outflow of the Plitvice Lakes and the beginning of the limestone canyon of Korana River.

6.3 Lake Depth Profiles

For the determination of a lake water balance the mixing mechanism inside the lake is also important. In the temperate region of the Plitvice Lakes, lakes exhibit a dimictic thermal pattern caused by seasonal differences in temperature and the mixing effects of wind (Kapelj et al., 2006). A typical dimictic lake undergoes stratification in the summer and mixes completely twice a year in the spring and in the autumn. In the winter, surface ice prevents further mixing by wind. During the winter months, there is no great variation in density and temperature in the lake water column. Whereas the cooler water (0°C) stays near the surface, the warmer and more dense water (4°C) extends to the bottom (Wetzel & Likens, 1991). In the summer the dimictic lakes stratify into three layers: the upper portion (*epilimnion*) is heated by the sun, and the heat is distributed by wind and waves that circulate the water. Below the well mixed epilimnion is the *metalimnion* or *thermocline* region, a layer of water in which the temperature declines rapidly with depth. *Hypolimnion* is the bottom layer with a nearly uniform temperature distribution. With the onset of autumn, the temperatures decrease and the surface waters become more dense than the bottom waters and sink. This happens until a uniform temperature and density is shared by the entire lake. The energy required to mix the two layers is provided by wind. In winter, as temperature drops further, ice forms at the lake surface, and stops any further mixing (Wetzel & Likens, 1991).

Only the lake water above the thermocline is able to have exchange with the atmosphere, i.e to evaporate. The evaporation rates will be given in Chapter 6.4. In Chapter 6.5 these values will be considered in the water balance calculations of the Plitvice Lakes. For the determination of the thermocline position in two largest lakes Prošće and Kozjak Lake deuterium (δ^2H), temperature (T), conductivity (C), and oxygen concentration (O_2) were measured along the vertical profiles. A water sampling of a vertical profile of each lake was performed on 2004-09-22 at the Institute of Geology of Zagreb, Croatia. While the temperature (T), conductivity (C), and oxygen concentration (O_2) were measured directly at site at the Rudjer Bošković Institute, Zagreb, Croatia, the stable isotope deuterium (δ^2H) was measured afterwards at the GGA-Institut in

Hannover. The combination of physico-chemical and isotopic measurements in Prošće Lake suggests the existence of the thermocline layer at a depth between 10 and 15 m. The thermocline in Kozjak Lake is approximately 15-18 m deep (Fig. 6.5).

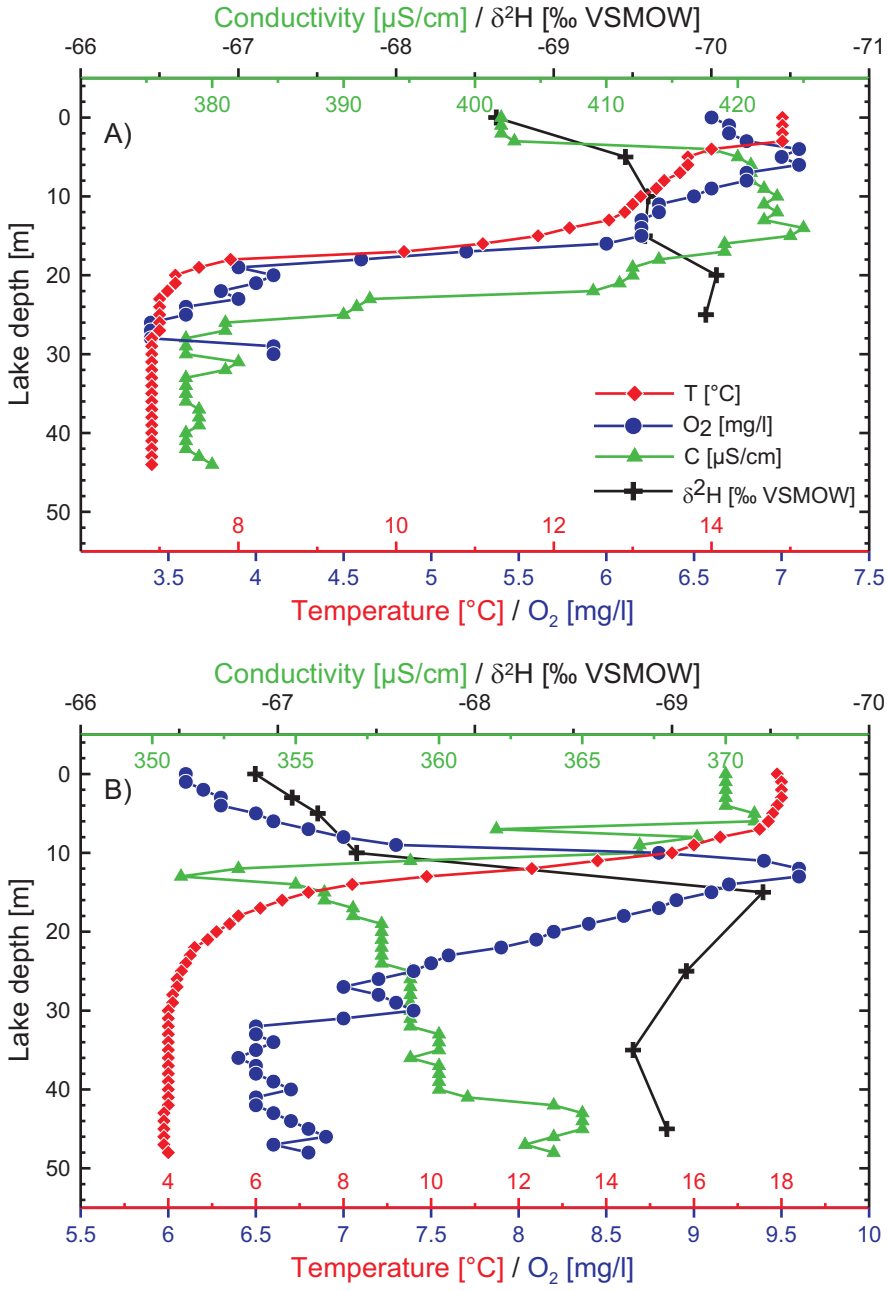

Fig. 6.5: Temperature (T), conductivity (C), oxygen concentration (O_2), and deuterium (δ^2H) abundance along the vertical profile of Prošće Lake (A) and Kozjak Lake (B). T, C, O_2 values were measured at the Rudjer Bošković Institute, Zagreb, Croatia.

6.4 Evaporation

6.4.1 Deuterium Enrichment Along the Lake Chain

Time series of deuterium (2003-2005) show evaporative enrichment along the lake chain from the inflow at Matica River towards the outflow at Korana River (Fig. 6.6). In this S-N direction the δ^2H values of lake water become more and more "positive". This means that that the lake water is becoming more and more enriched in deuterium (^{2}H), whereas the lighter hydrogen (^{1}H) escapes to the atmosphere. The enrichment takes place only during the summer months, whereas during the winter months January-March the isotopic values of the different sampling sites along the lake chain vary within the analytic uncertainty. During the winter months, the lakes were mostly covered by surface ice, preventing mixing of the lake water by the wind and also evaporation of surface water. Between the outflow of the Plitvice Lakes at Kaludjerovac Lake and the sampling point at Korana River there are no more lakes. Between both sites, there is no evaporation discernible, because the deuterium values of the both sampling sites are almost identical (Fig. 6.6).

6.4.2 Evaporation Rate of the Lake Water Body

Deuterium variations in the lake water enable the calculation of its evaporation rate according to Eq. 2.12. Taking the necessary assumptions for this Equation into account, the difference in isotopic composition between Matica River and Kaludjerovac Lake is with 1.4 ‰ VSMOW big enough at the same sampling date, and the mean monthly air temperatures and humidity data are available. Therefore, the percentage of evaporated water for eight sampling dates can be obtained (symbol E in Table 6.4). The lowest evaporation rate during the observed period was in April 2003 (0.080% of lake water) and the highest in August 2003 (0.458% of lake water).

In the following, two different cases were chosen to calculate the evaporation rate and the evaporated water volume. The first one is for April 2003 with a high spring discharge after snow melt and without lake stratification. The other example is for September 2004 with low discharge after the dry summer months and stratified lakes.

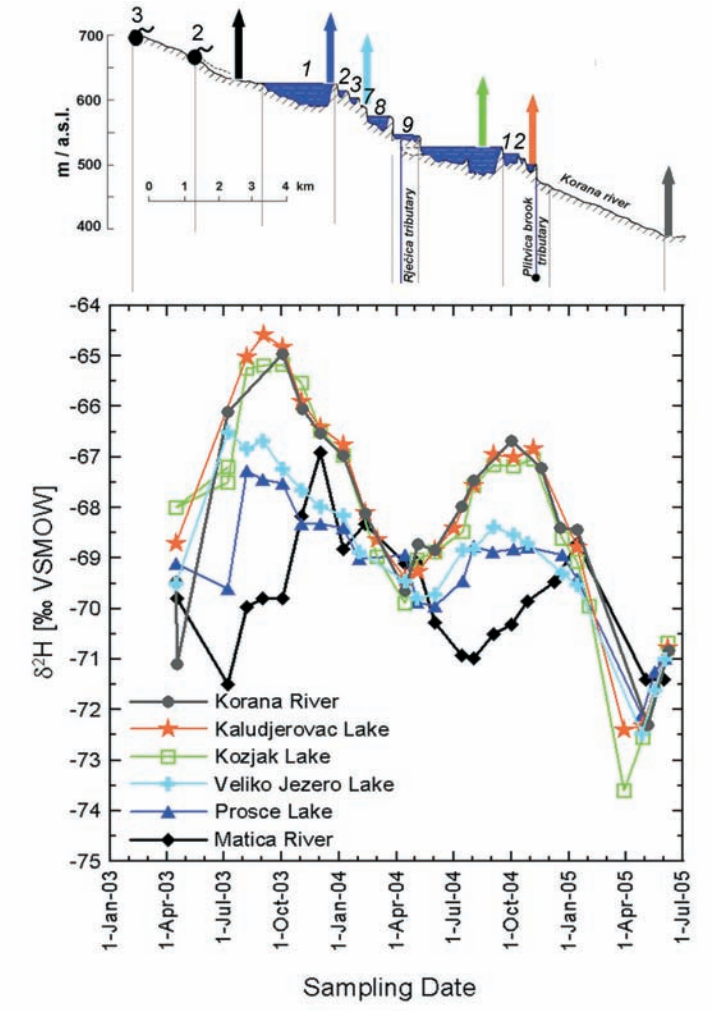

Fig. 6.6: Evaporative deuterium enrichment along the lake chain of the Plitvice Lakes. Arrows in the cross-section mark the sampling sites for deuterium depicted in this figure. Numbers mark the position of particular lakes as given in Fig. 4.2.

September was chosen, because the thermocline position in this month is well known (Chapter 6.3). The lake water level in September 2004 was 40 cm lower than in April 2003, resulting in a reduction of the water volume from 22.95 Mio. m^3 in April to 22.37 Mio. m^3 in September[3]. In April 18 000 m^3 (25.9 mm) of water evaporated. In September 27 000 m^3 (39.4 mm) above the thermocline evaporated from the lakes Prošće, Kozjak and all other lakes. The results are presented in Table 6.5.

[3]Obtained by digitized isobate maps of the Plitvice Lakes and the software ArcView GIS and its extensions Spatial and 3D Analyst.

Table 6.4: Lake water evaporation calculated by means of deuterium enrichment along the lake chain of the Plitvice Lakes. δ^2H MR and δ^2H KL are the measured deuterium values in Matica River and Kaludjerovac Lake, dδ is the isotopic difference of MR and KL, T is the mean monthly air temperature measured at the Plitvice Lakes, h is the mean monthly air humidity, δ_a is isotopic composition of the atmospheric vapour, α is equilibrium fractionation factor, ϵ is the equilibrium enrichment factor, $\Delta\epsilon$ is kinetic isotopic fractionation, f is residual fraction of water in the lake, and E is the percentage of evaporated water from the lake above the thermocline.

Sampling Date	δ^2**H MR** [‰]	δ^2**H KL** [‰]	**d**δ	**T** [°C]	**h** [%]	δ_a [‰]	α	ϵ	$\Delta\epsilon$	**f**	**E** [%]
17.04.2003	-69.80	-68.70	1.10	8.10	68	-137.80	1.100303	-100.30	4.00	0.999202	0.080
07.07.2003	-71.50	-67.10	4.40	20.10	67	-138.50	1.084914	-84.91	4.13	0.996225	0.378
06.08.2003	-69.96	-65.01	4.95	21.70	66	-135.96	1.083054	-83.05	4.25	0.995424	0.458
01.09.2003	-69.80	-64.58	5.21	12.20	79	-148.80	1.094743	-94.74	2.63	0.997416	0.258
02.10.2003	-69.80	-64.83	4.97	7.80	81	-150.80	1.100723	-100.72	2.38	0.997903	0.210
01.06.2004	-70.27	-68.84	1.44	15.70	79	-149.27	1.090251	-90.25	2.63	0.999257	0.074
01.08.2004	-70.97	-67.56	3.41	18.20	76	-146.97	1.087178	-87.18	3.00	0.997935	0.207
02.09.2004	-70.51	-66.95	3.56	12.90	81	-151.51	1.093827	-93.83	2.38	0.998409	0.159

Table 6.5: Evaporation from the Plitvice Lakes. Lake water volume (V_{lake}), depth of thermocline (d_{therm}), lake water volume above thermocline able to evaporate ($V_{above\ therm}$), percentage of evaporation obtained by isotope-hydrologic means (E), V_E evaporated lake water volume above thermocline, lake surface S_{lake}, E* evaporation calculated in mm.

Lake Name	**V_{lake} [Mio. m^3]**	**d_{therm} [m]**	**$V_{above\ therm}$ [Mio. m^3]**	**E [%]**	**V_E [m^3]**	**S_{lake} [ha]**	**E* [mm]**
April 2003							
Prošće Lake	7.67	-	7.67	0.08	6 140	68.2	9.0
Kozjak Lake	12.71	-	12.71	0.08	10 100	82.0	12.3
Other Lakes	2.57	-	2.57	0.08	2 060	44.7	4.6
Σ	**22.95**	-	**22.95**		**18 300**		**25.9**
September 2004							
Prošće Lake	7.42	15-18	6.27	0.159	9 900	68.2	14.5
Kozjak Lake	12.38	10-15	8.24	0.159	13 100	82.0	16.0
Other Lakes	2.57	-	2.57	0.159	4 000	44.7	8.9
Σ	**22.37**		**17.08**		**27 000**		**39.4**

6.5 Water Balance

This chapter synthesizes previous observations of water balance components like evaporation and lake stratification. Based on these information and quantification of inflow and outflow components (Fig. 6.7), a calculation of water balance can be performed. The main inflow sources of the Plitvice Lakes are the springs Bijela and Crna Rijeka, building Matica River flowing into Prošće Lake and cascading over fifteen lakes. Together with different smaller tributaries lake water flows into Korana River canyon, which is the only surface water outflow (Fig. 4.2 and 6.7). During the dry summer months the water disappears partly or completely from the Korana river bed. A water loss occurs also through evaporation, as shown in Chapter 6.4. Additionally, the pumping of water (60 l/s or 0.06 m^3/s) from Kozjak Lake for drinking water supply has to be considered. In Chapter 6.2 a possible water loss from Kozjak Lake flowing towards Korana River bed is suggested, but it could not be proven by isotopic measurements.

Equation 6.3 summarizes all water balance components:

$$I_{MR,RJ,PL} + I_{pr} + I_u - O_{pump} - O_E - O_u \rightarrow O_K \tag{6.3}$$

$I_{MR,RJ,PL}$	inflow: Matica River (MR) downstream the confluence of the springs Bijela and Crna Rijeka, tributaries Rječica River (RJ) and Plitvica Brook (PL)
I_{pr}	inflow: mean monthly precipitation
I_u	unknown underground inflow
O_{pump}	outflow through pumping of water from Kozjak Lake
O_E	outflow through evaporation
O_u	outflow through underground water loss from lakes
O_K	outflow at the limnograph Luketići at Korana River, characterized by surface flow (O_{Ks}) or water loss from the river bed (O_{Ku})

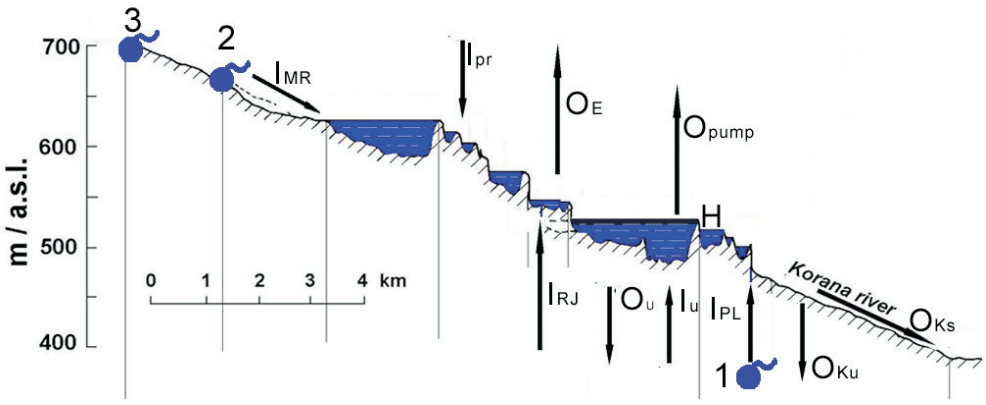

Fig. 6.7: Components for the water balance calculation of the Plitvice Lakes.

The water balance is calculated for the same months as the evaporation rates (in Chapter 6.4: April 2003 and September 2004), particular components are summarized in Table 6.6 and shown in Figures 6.7 and 6.8. In April 2003 8.48 Mio. m^3 reached the outflow of the Plitvice Lakes flowing into Korana River canyon. The comparison with the discharge data at the limnograph at Korana River shows only the surface flow

at that time and no water loss from the river bed. However, in September 2004 65% from 3.71 Mio. m^3 coming from the lakes were lost through the swallow-holes in the river bed flowing towards springs Klokot and Privilica near Bihać. This hydrologic connection was suggested by time series of deuterium (Fig. 5.4 in Chapter 5.2).

Table 6.6: Water balance components with inflow abbreviations (I) for Matica River (MR), Rječica River (RJ), Plitvica Brook (PL), precipitation (pr) and with outflow abbreviations (O): pumping (pump), evaporation (E), surface and underground flow of Korana River (Ks, Ku) .

	April 2003		**September 2004**	
		[Mio. m^3]		[Mio. m^3]
$I_{MR,RJ,PL}$	3.47 m^3/s	9.00	1.37 m^3/s	3.57
I_{pr}	90.3 mm	0.18	170 mm	0.33
O_{pump}	0.06 m^3/s	0.16	0.06 m^3/s	0.16
O_E	0.08%	0.018	0.159%	0.027
Σ		8.48		3.71
O_{Ks}	3.32 m^3/s	8.61	0.49 m^3/s	1.29
O_{Ku}	0%	0	65%	2.42

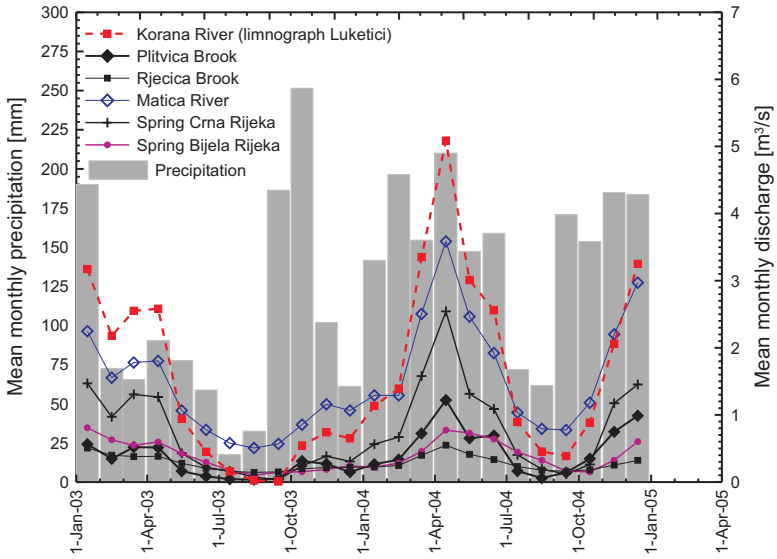

Fig. 6.8: Mean monthly precipitation and mean monthly discharge of the Plitvice Lakes (2003-2005).

A current extraction rate of 0.06 m^3/s will not be high enough to satisfy the future demand of the tourist infrastructure at the Plitvice Lakes National Park. Due to the sensibility of tufa growth on changes in hydrological circumstances the change of the Kozjak water level by enhanced water exploitation is investigated.

Water level and discharge of Kozjak Lake for April and September for 2003 and 2004, respectively were compared to see how the increased pumping rate of 0.5 m^3/s instead of 0.06 m^3/s would influence the water level change (Fig. 6.9). For comparison, the increased pumping rate of 0.5 m^3/s in September 2004 would lower the water level of Kozjak Lake by less then 10 cm. Even great discharge oscillations between 1 and 9 m^3/s cause differences in the water level at a maximum of 70 cm. Therefore, an increasing extraction rate from Kozjak Lake will not result in a great lowering of the water table, endangering so the tufa growth of the UNESCO heritage.

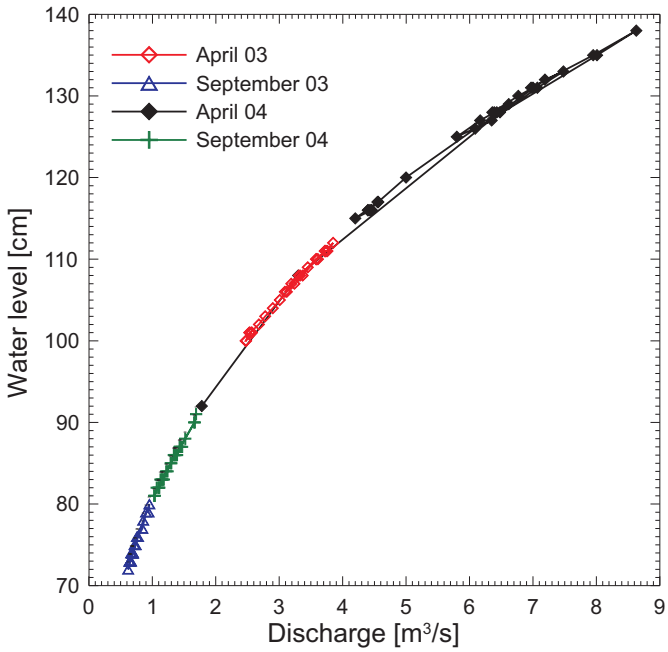

Fig. 6.9: Daily discharge and water level values for Kozjak Lake for 30 days during April and September 2003 and 2004, data of the Meteorological and Hydrological Service of Croatia.

Chapter 7

Storage Capacity of the Karst Aquifers

In the first part of this chapter the results of isotopic measurements for the stable isotope deuterium and for tritium, chlorofluorocarbons and sulfur hexafluoride will be presented. In the second part the results of lumped parameter modeling are shown with mean residence time calculations for ten springs. These are the basis for estimating karst aquifer storage capacities, which are necessary for a sustainable management of drinking water supply in the Plitvice Lakes National Park (Croatia), Bihać and Kulen Vakuf municipalities (Bosnia-Herzegovina).

7.1 Results of Isotopic Measurements

7.1.1 Deuterium and Tritium (^{2}H, ^{3}H)

The seasonal variation of deuterium values in most of the springs that were sampled on a monthly basis between April 2003 and June 2005 is a strong indication that these springs contain a component with MRT $<$ 5 years (Fig. 7.1). Exceptions with no seasonality within a detection limit of 0.8‰ are the springs Bijela Rijeka, Stipinovac and Vrelo indicating MRT of spring water $>$ 5 years (2, 4, 5 in Fig. 7.1A). Equation 2.15 allows to compute the MRT from the ratio a of the amplitude in the input and output signals, where ω is equal to 2π per year for seasonal signals. The amplitude

of a sinus curve fitted to deuterium in Zagreb and Plitvice Lakes precipitation is 25‰. The amplitude of the deuterium signal is largest for the springs Toplica and Ostrovica (4‰) and smallest for the spring Bijela Rijeka, where it is not visible with an analytical precision of 0.8‰ for deuterium. On the other hand, any system showing a seasonality in stable isotopes can also be described as a mixture of at least two components, one having a seasonality and the other a constant output value. This would only decrease the amplitude of the seasonality of the young component due to dilution.

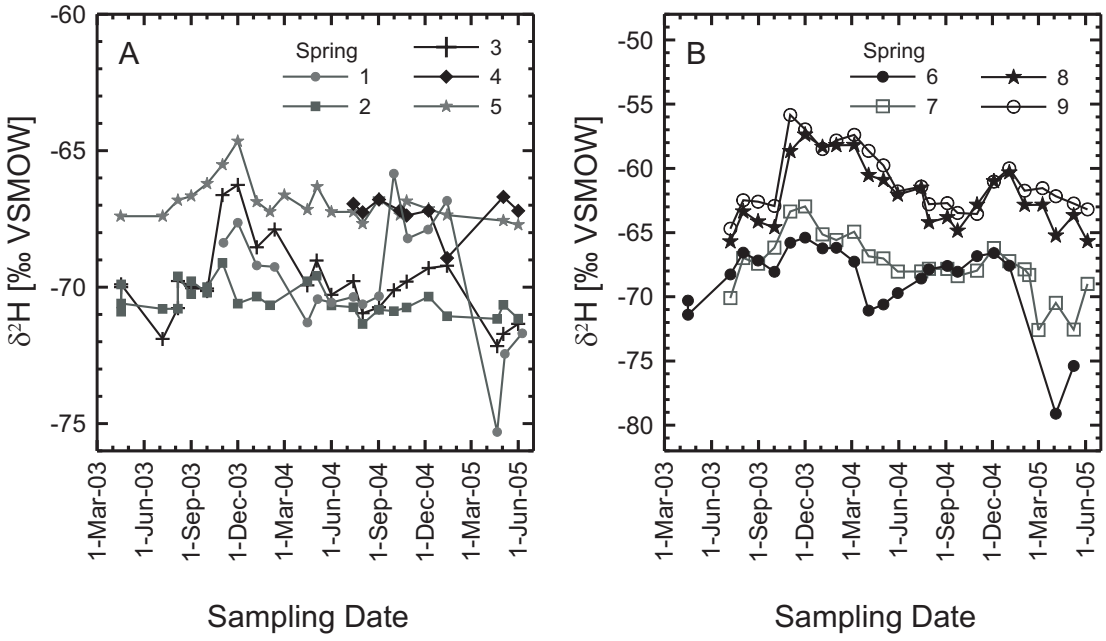

Fig. 7.1: Seasonal variations of deuterium in springs: 1 Plitvica, 2 Bijela Rijeka, 3 Crna Rijeka, 4 Stipinovac, 5 Vrelo (A); 6 Klokot, 7 Privilica, 8 Ostrovica, 9 Toplica (B). Sampling mostly one value per month.

Unlike for deuterium, time series of tritium activity have been gathered only for the Bosnian springs 6, 7, 8, and 9, which are used for water supply of the Bihać and Kulen Vakuf municipality. For springs 1, 2, 3, 4, 5 and 10 there are no time series, but single measurements for November 2003 and July 2004 (Fig. 7.2).

The seasonal variation in tritium activity in the spring Privilica (2.3-9.5 TU) is the smallest compared with the other three springs (1.7-12.2 TU), indicating the longest MRT for the spring water mixture. On the other hand, the stronger tritium fluctuations

in the springs Toplica, Ostrovica and Klokot indicate the greater influence of the short-term component (Fig. 7.2). In the same plot the time series of mean tritium activity in precipitation of the Plitvice Lakes is shown. The comparison of this values with the mean tritium values from four Bosnian springs shows a better agreement of tritium values in the springs Klokot and Privilica near Bihać than in the springs Ostrovica and Toplica near Kulen Vakuf (Table 7.1)[1]. Deuterium measurements have already shown that the springs Klokot and Privilica have the stable isotope signature of the Plitvice catchment, suggesting a hydrologic connection of these two systems and the same infiltration area (Chapter 5.2).

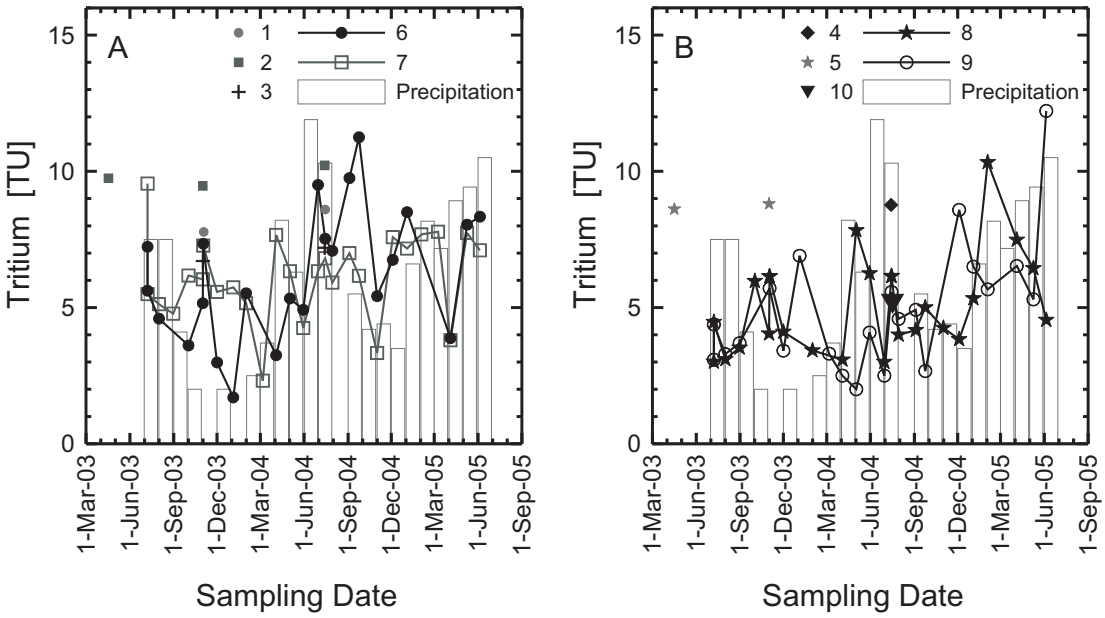

Fig. 7.2: Comparison of tritium activity in precipitation of the Plitvice Lakes and springs: 1 Plitvica, 2 Bijela Rijeka, 3 Crna Rijeka, 6 Klokot, 7 Privilica (A); 4 Stipinovac, 5 Vrelo, 8 Ostrovica, 9 Toplica, 10 Una (B); Sampling mostly one value per month for 6, 7, 8, 9; individual measurements for other sites .

[1]The comparison of both was carried out at the Rudjer Bošković Institute, Zagreb (Obelić et al., 2006).

Table 7.1: Comparison of tritium activity in precipitation of the Plitvice Lakes and four Bosnian springs. The mean tritium activities are expressed in Bq/l and TU.

Spring Number	Sampling Location	Mean Tritium Activity	
		[Bq/l]	[TU]
6	Klokot	0.67 ± 0.34	5.6 ± 2.9
7	Privilica	0.75 ± 0.17	6.3 ± 1.4
8	Ostrovica	0.55 ± 0.25	4.6 ± 2.1
9	Toplica	0.50 ± 0.33	4.2 ± 2.8
	Plitvice Lakes (Precipitation)	0.77 ± 0.47	6.5 ± 3.9

7.1.2 Chlorofluorocarbons and Sulfur Hexafluoride (CFCs and SF_6)

Two sampling campaigns of spring waters were performed for the geochemical tracers CFCs and SF_6: a first one in November 2003 during the wet season when springs had high discharge and a second campaign for the same set of springs during the dry and low-discharge period in July 2004. The two sampling campaigns for gas tracers show systematic differences in the CFC and SF_6 concentrations (Fig. 7.3). All sampling locations with exception of the Spring Privilica contain higher concentrations of CFCs and SF_6 in November 2003 than in July 2004. The systematic differences in the CFCs and SF_6 concentrations can be explained by different mixing ratios of young and old water components during high and low discharge conditions, namely, the spring water collected in July 2004 contains elder MRT-components than the spring water sampled in November 2003. This situation can be expected from the hydrological point of view. During the dry summer months the base flow component prevails in the spring water. On the other hand, the rain-rich autumn contributes to the spring water composition with the younger water component.

Some of the springs are located within uninhabited areas with virtually no possibility for anthropogenic contamination besides that of locally enriched air (e.g. spring Una). Other springs, e.g. Privilica or Klokot, might be contaminated from anthropogenic point sources like industrial or domestic waste waters in the surrounding of the municipality Bihać or the former military airport Željava north-east of Bihać. The

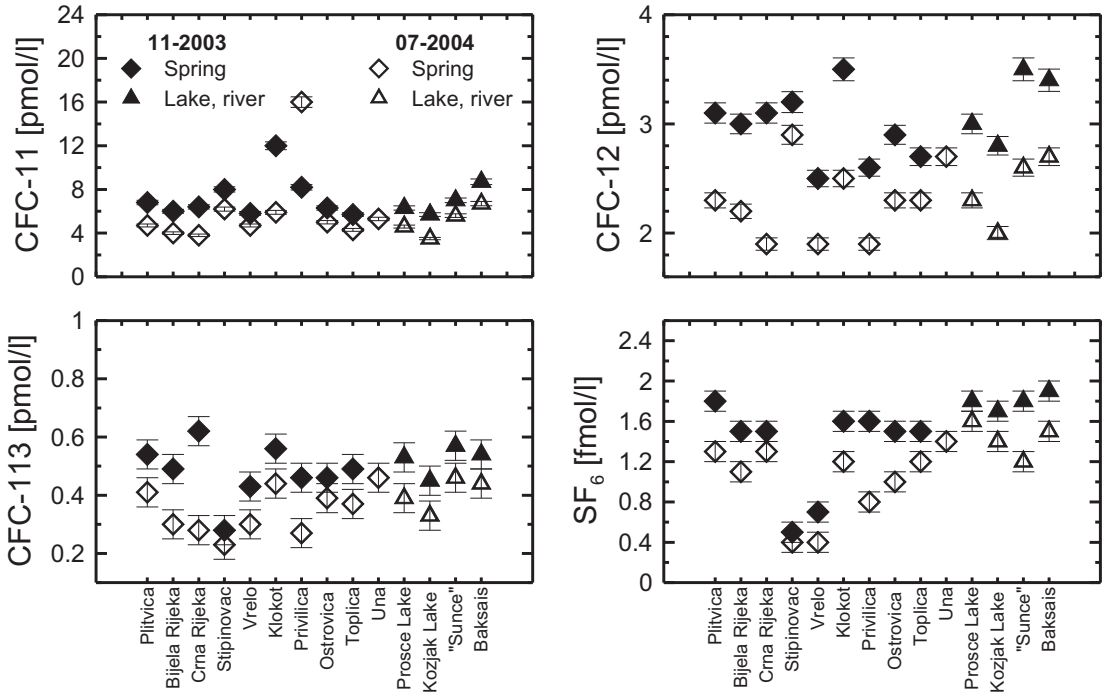

Fig. 7.3: Concentrations of CFC-11, CFC-12, CFC-113 and SF_6 from the springs and surface waters collected during sampling campaigns in November 2003 and July 2004 from the sampling sites of the Plitvice Lakes and Una River. Spring water for the sampling campaign in November 2003 is marked with black and for July 2004 with white rhombs. Surface water from the Plitvice Lakes (Prošće and Kozjak Lake) and Una River ("Sunce" upstream and Bakšaiš downstream of Bihać) is marked with black, respectively white triangles.

comparison of CFCs and SF_6 values upstream ("Sunce") and downstream (Bakšaiš) of Bihać indicate an input of CFCs and SF_6 into Una River through the municipality. In November 2003 CFC-11 values for Bakšaiš are 20% higher than for "Sunce" and 5% for SF_6. CFC-12 and CFC-113 do not show such an increase of values downstream of the municipality. In July 2004 the same tendency like in November 2003 can be observed: CFC-11 increased by 16%, SF_6 increased by 20%. CFC-12 and CFC-113 did not differ upstream and downstream of the municipality. The elevated gas tracer values through the anthropogenic input in the springs Privilica and Klokot were not used for dating purposes.

The CFCs and SF_6 values in surface waters of the Plitvice Lakes (Prošće and Koz-

jak Lake) reflect the values in the springs Bijela and Crna Rijeka feeding the lakes, indicating no additional anthropogenic input along the lake chain of the Plitvice Lakes.

7.1.3 Noble Gases (Helium, Neon)

Two sampling campaigns of spring waters were performed for noble gases: a first one in November 2003 and a second campaign in July 2004. As described in Chapter 2.4.3, the measured helium concentrations (^{3}He and ^{4}He) consist of several components: helium at atmospheric solubility equilibrium ($^{3,4}\mathrm{He}_{\mathrm{eq}}$), helium originating from radioactive decay of tritium ($^3\mathrm{He}_{\mathrm{trit}}$), excess air ($^{3,4}\mathrm{He}_{\mathrm{ex}}$), terrigenic ($^{3,4}\mathrm{He}_{\mathrm{terr}}$), and radiogenic helium ($^{3,4}\mathrm{He}_{\mathrm{rad}}$). However, prior to the dating of groundwater with the tritium/^{3}He method, it is necessary to separate $^3\mathrm{He}_{\mathrm{trit}}$ component from the other helium components (Kipfer et al., 2002). Since deuterium, tritium, CFCs, and SF_6 are directly measured on the water samples, the determination of tritiugenic helium ($^3\mathrm{He}_{\mathrm{trit}}$) requires "model" calculations including some assumptions concerning the recharge conditions like altitude, infiltration temperature and excess air. Moreover, ^{3}He is the most volatile of the gas tracers used in this study. Therefore it is important to discuss the possibility of loss of $^3\mathrm{He}_{\mathrm{trit}}$ in the karst aquifer. Also a possible fractionation of excess air has to be taken into account.

Consistency Check I for ^{3}H/^{3}He Dating: He - Ne Plot

The first consistency check for tritium/^{3}He dating can be done by plotting helium versus neon (Fig. 7.4). The plot compares the noble gas data with the line of solubility equilibrium calculated for an infiltration altitude of 700 m a.s.l. and temperatures from 0°C to 20°C. Since all samples are above this equilibrium line there is no evidence for helium or neon loss due to gas stripping from this plot, neither in the aquifer nor during sampling. Only one sample contains a noticeable terrigenic helium component (spring Una, sampled only in July 2004), but several samples contain a noticeable component of excess air. As described by Kipfer et al. (2002), the measured noble gas concentrations have to be corrected for this excess air component. The lines for excess air correspond to 700 m a.s.l. and infiltration temperatures of 0°C, 8.9°C and 20°C, with

amounts of excess air between 0 up to 10 cc/kg, respectively. The mean annual air temperature in the region is 8.9°C, but most of the precipitation occurs during autumn to spring, therefore lower infiltration temperatures than 8.9°C are expected for most samples. Yet in a karst system higher infiltration temperatures are also possible, e.g. caused by a heavy summer rain. Most points of measured helium and neon concentrations can be reached by parallels to the excess air lines, and therefore can be explained by infiltration at different temperatures and different amounts of unfractionated excess air.

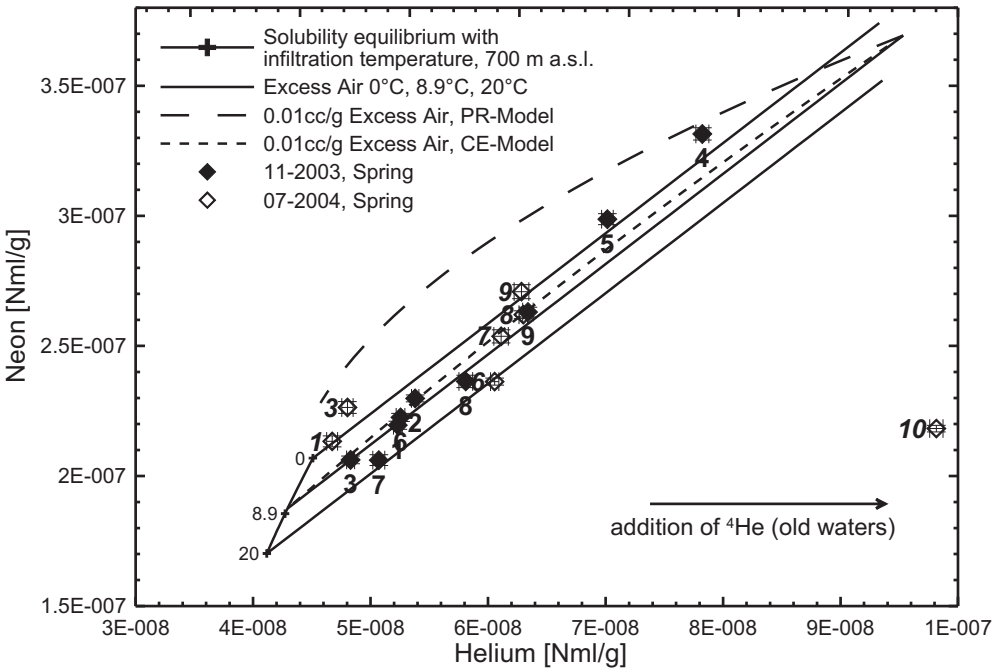

Fig. 7.4: Concentrations of helium and neon in springs (1 Plitvica, 2 Bijela Rijeka, 3 Crna Rijeka, 4 Stipinovac, 5 Vrelo, 6 Klokot, 7 Privilica, 8 Ostrovica, 9 Toplica, 10 Una) and calculated lines of solubility equilibrium and excess air. Black rhombs display noble gas data for sampling campaigns in November 2003, vs. white rhombs for July 2004.

However, He and Ne values from 2003 for the springs Stipinovac and Vrelo (4 and 5) and from 2004 for the springs Bijela Rijeka, Crna Rijeka and Toplica (1, 3, 9) indicate that the water infiltrated at a temperature below 0°C, which is not possible. At least for these springs it is necessary to apply fractionation models: the partial re-equilibration

model (PR-model) and the closed system equilibration model (CE-model), which could correct this fractionated values of excess air (dashed lines). PR and CE lines originate from a point corresponding to 10 cc/kg excess air added to He and Ne in solubility equilibrium at 20°C and 700 m a.s.l. With exception of the spring Una all measurement points lie within the region between the excess air line and the curve of the PR model.

It can be concluded that all data but the sample from the spring Una can be explained by infiltration at temperatures between 0°C and 20°C and varying amounts of excess air, where in some cases excess air was fractionated by conditions of the partial re-equilibration or closed system equilibration. Since especially the PR fractionation can occur in air-filled karst voids, possible losses of $^{3}\mathrm{He}_{\mathrm{trit}}$ cannot be excluded and will be discussed in the following chapter.

Consistency Check II: ^{3}H/^{3}He Infiltration Year vs. Tritium in Precipitation

Computation of apparent tritium-helium ages assumes that a piston flow model can describe the water movement. This is an assumption that generally is not accepted for karst systems from the hydrogeological point of view, where at least the base flow of karst springs is normally described using an exponential mixing model. Figure 7.5A compares the measured values of tritium and computed values for $^{3}\mathrm{He}_{\mathrm{trit}}$ (together) with the apparent $^{3}\mathrm{H}/^{3}\mathrm{He}$ age and the observed input function. In case the data points are situated within the range of the input function, the piston flow model can be a valid description of the tritium, helium, neon and $^{3}\mathrm{He}/^{4}\mathrm{He}$ data. But as it was pointed out by Aeschbach-Hertig et al. (1998) this plot is not very sensitive for the assumption of a piston flow model. An exponential mixing model or a 10-years running mean will also result in data points falling within the seasonal variation of the tritium input curve, and very near to the mean annual input curve. Only admixtures of several percent of old water being free of tritium can shift the data points towards smaller stable tritium values. Nevertheless this plot can constrain possible losses of $^{3}\mathrm{He}_{\mathrm{trit}}$. Figure 7.5B compares the measurements with several model curves that correspond to the exponential and piston flow models. The lines describe the output for these models for a sampling date of 2005-01-01. They are computed in a synoptic way for mean

residence times from zero up to more than 100 years. From this model output, stable tritium, the $^3H/^3He$ age and the infiltration year are computed. The varying parameter for the different model runs is the loss of $^3He_{trit}$, which is simulated to be between 0 and 90%. It is obvious from these curves that a bad confinement of ^3He leads to values above the local input curve. This is due to the fact that a loss of $^3He_{trit}$ shifts the $^3H/^3He$ age in a non-linear way towards younger ages. The loss of $^3He_{trit}$ in the sum tritium and ^3He on the other hand is not large enough to shift the "stable tritium" to values below the input curve - the not yet decayed tritium content from the vicinity of the peak is high enough to keep the values above the input curve. In order to explain the values below the input curve an admixtures of old, tritium-free waters has to be taken into account. On the other hand some of the samples can also be described by exponential mixing. And finally these plots show that the loss of a large amount of $^3He_{trit}$ on the flow path cannot be neglected.

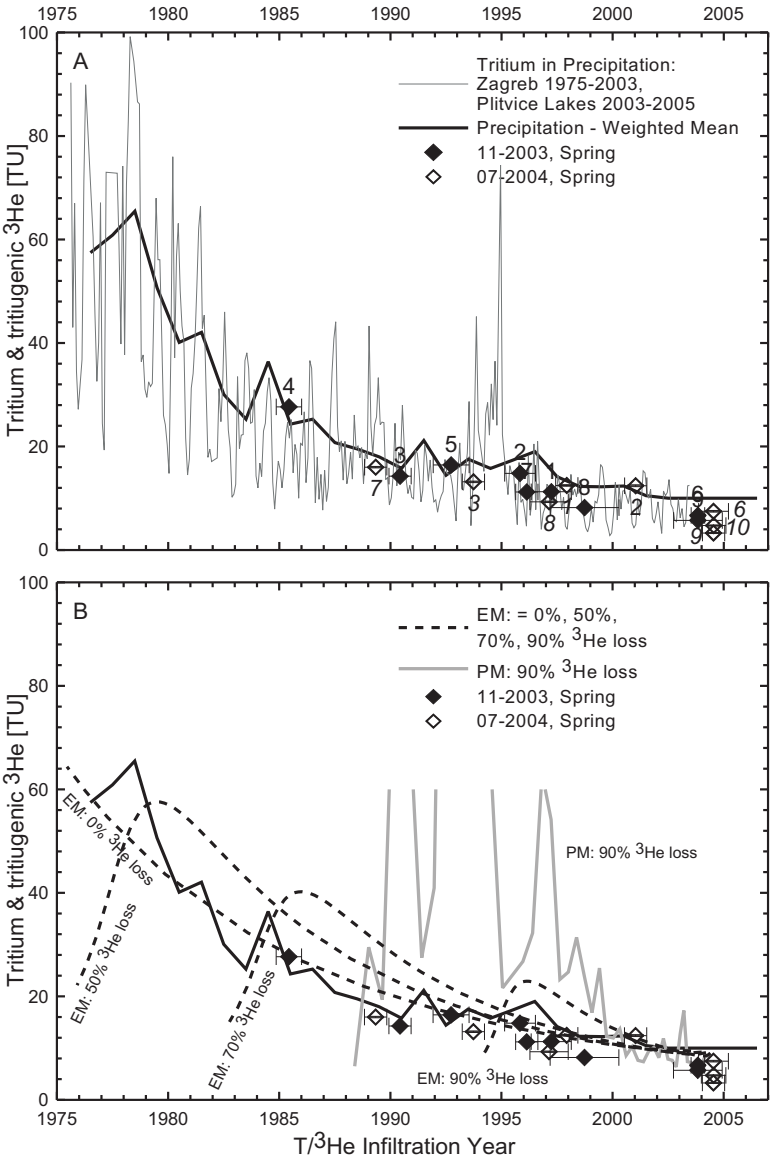

Fig. 7.5: Sum of tritium and $^3\mathrm{He}_{\mathrm{trit}}$ as a function of the apparent $^3\mathrm{H}/^3\mathrm{He}$ age. Values from springs are compared with monthly mean values for tritium in precipitation for Zagreb and the Plitvice Lakes, 1 Plitvica, 2 Bijela Rijeka, 3 Crna Rijeka, 4 Stipinovac, 5 Vrelo, 6 Klokot, 7 Privilica, 8 Ostrovica, 9 Toplica, 10 Una (A); exponential and piston flow model output taking into account variable degrees of confinement of $^3\mathrm{He}_{\mathrm{trit}}$ (B).

Conclusion

For the dating with the tritium/$^3\mathrm{He}_{\mathrm{trit}}$ method recharge conditions of infiltrating water including altitude, infiltration temperature, amount of excess air and its fractionating have to be known. These are not sufficiently known for the present study and show great variations. Furthermore, the loss of $^3\mathrm{He}_{\mathrm{trit}}$ cannot be excluded. For this reason, it is not possible to use the tritium/$^3\mathrm{He}_{\mathrm{trit}}$ method based on only He and Ne concentration and the $^3\mathrm{He}/^4\mathrm{He}$ ratio, to get reliable mean residence time of karst spring water. In case that the heavy noble gases Ar, Kr, Xe would be also measured on the same samples, most of these unknowns could be assessed. As Kipfer et al. (2002) have shown, these additional data can quantify the infiltration temperature, excess air, and possible fractionation during infiltration.

7.2 Lumped Parameter Models (LPM) for the Determination of Mean Residence Time (MRT) of Spring Water

Data processing was performed using the LabData Database and Laboratory management system. This includes a module called "Lumpy" for MRT calculations (Suckow & Dumke, 2001). For computation of the MRT for ten springs either an **one-component model** (exponential model: EM, dispersion model: DM) or a **two-component model** (piston flow-dispersion model: PMDM, piston flow-exponential model: PMEM) is used. The two component-model describes a mixture between two water contributions of different mean residence times. For the PMDM it means the combination of a piston flow model for the "young" component in the karst conduit network and a dispersion model for the "old" component in the fissured-porous aquifer.

The tracer values for one spring can be mathematically described with different LPM and MRTs. A comparison of one transient tracer (e.g. CFC-12) versus other tracers is a useful tool for finding out which LPM is able to describe the measured tracer values in the spring (Plummer et al., 2001). Figure 7.6 compares the transient tracers CFC-11 (A), CFC-113 (B), SF_6 (C), tritium (D), and tritiugenic helium (E) in the spring waters versus CFC-12, with calculations for three hypothetical models - the piston flow (PM),

the exponential model (EM), and the dispersion model (DM) with Péclet numbers 1, 2, and 7[2]. The thick solid line describes the PM case without any mixture, the dashed line for the EM describes a well-mixed system, and thin solid lines for the DM describe a tracer transport influenced by advection and dispersion. All models are computed for an output at 2005-01-01, using a recharge temperature of 8.9°C and an altitude of 700 m. It is evident from this figure, that from the CFC species alone it is only possible to distinguish young waters from old ones, but not to decide which model is the better approximation to the natural system, since the analytic uncertainties are too large. More possibilities to distinguish different model approaches are in principal given by plotting the tritiugenic helium vs. CFC-12 (Fig. 7.6E). One of the great advantages of using ^{3}He as a tracer on its own for this purpose is that the input curve of ^{3}He has a shape different from both the tritium input curve which is peak-shaped and the CFCs and SF_6 input curves which increase later than the ^{3}He input. However, in this study, this is not very reliable due to constraints concerning ^{3}He, as described in Chapter 6.1. For this reason, for each spring and tracer, all lumped parameter model possibilities were tested to find the best model describing the MRT of spring water.

Figure 7.6 also gives information about a possible contamination of the springs. It seems that the springs Privilica, Klokot, and Stipinovac are contaminated with respect to CFC-11, and Crna Rijeka, Klokot, and Stipinovac with CFC-12. These measurements were not used for the MRT calculations.

[2]The data are presented as water concentrations and not as recompiled concentrations in air (Plummer et al., 2001), since this would already need precise assumptions concerning the infiltration conditions (recharge temperature, altitude, excess air etc.), which is not available on a sample to sample basis.

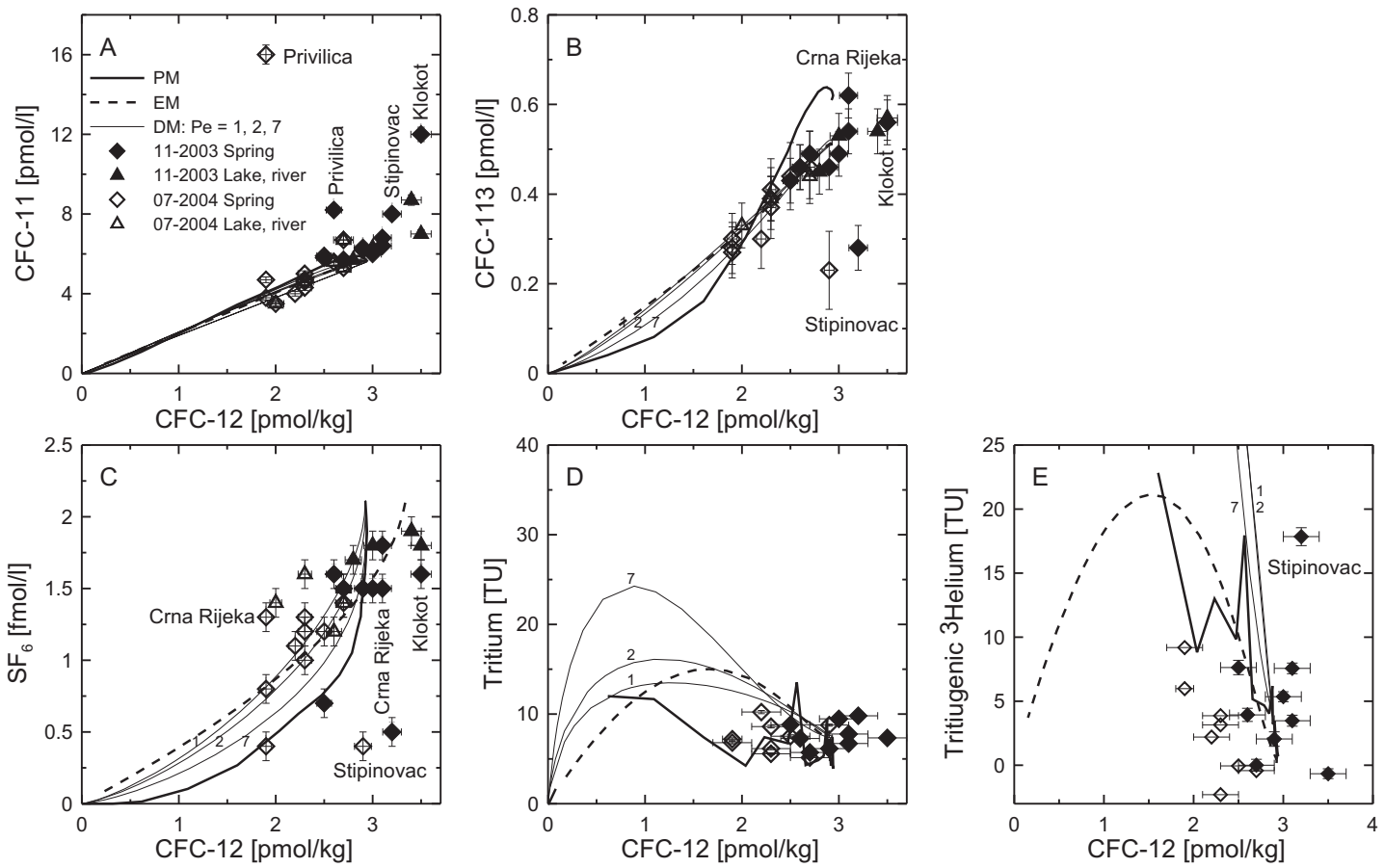

Fig. 7.6: Comparison of the mixing ratios of CFC-11 and CFC-12 (A); CFC-113 and CFC-12 (B); SF_6 and CFC-12 (C); tritium and CFC-12 (D); and tritiugenic helium (^{3}He) and CFC-12 (E) for water sampled in springs and surface waters in November 2003 and July 2004. The data are compared to three hypothetical mixing models. The thick solid lines correspond to the piston flow model (PM), the dashed lines to the exponential model (EM), and the thin solid lines to the dispersion model (DM) with Péclet numbers 1, 2, 7.

The LPM results and the measured tracer values in ten springs of the Plitvice Lakes and Una River are depicted in seven plots in the following way (e.g. Fig. 7.7):

- In plots A and B the time series of deuterium (^{2}H) and tritium (^{3}H) are compared with model output. Both tracers were used to calibrate the model, or more specific: to minimize the quadratic difference between measured and modeled values.

- Plot C shows how tritiugenic helium ($^3\mathrm{He}_{\mathrm{trit}}$) compares to this model. Although the model output for $^3\mathrm{He}_{\mathrm{trit}}$ is compared with the measured results, it is not used as a fit parameter in the LPM calculations.

- Since discharge varies during the two sampling campaigns, and since the CFC-11, CFC-12, CFC-113, and SF_6 results show different concentrations during two sampling campaigns, these two different discharge states were modeled separately. The results are depicted in the plots D, F, E, and G. **State I** describes the wet season and high spring discharge. The data used for LPM are time series of ^{2}H and ^{3}H as well as CFCs and SF_6 sampled in November 2003. **State II** describes the dry season and low spring discharge. The data used for LPM are the time series of ^{2}H and ^{3}H as well as CFCs and SF_6 sampled in July 2004.

To be able to distinguish different models at first glance, red color is used for the EM, blue for the DM, green for the PMDM, and dark red for the PMEM (e.g. Fig. 7.7). Subsequently, the multi-tracer approach will be discussed in detail for the spring Ostrovica. The plots for the other nine springs are shown in Appendix (A.1 - A.9) and their modeling results are summarized in Table 7.2.

LPM for Spring Ostrovica, State I

The time series of **deuterium** and **tritium** in the spring Ostrovica can be described by four different model approaches (Fig. 7.7A,B):

- The first model **(EM)** curve is created with the exponential model and a MRT of 2 years (red solid curve).
- The second model **(PMDM)** curve is created using the piston flow model with a MRT of 0.2 years together with an admixture of 90% of an "old" component, having the eight-year mean δ^2H value of -62‰. This second component is obtained by the dispersion model and Péclet number 3 (green curve).
- The third model **(DM)** curve is created using the dispersion model with a MRT of 2.5 years and Péclet number 3 (blue solid curve).
- The fourth model **(PMEM)** curve is created using the piston flow model with a MRT of 0.2 years together with admixture of 90% of an 300 years "old" component, obtained by the exponential model (dark red dash-dotted curve).

In the case of the PMDM, the DM, and the PMEM the MRT needed to obtain a good match between model and measured data can be interpreted directly as the flow time between rain and outflow at the spring. On the other hand, the EM needs an additional delay of 0.3 years. The physical interpretation of this delay can be the time the water spends in the unsaturated zone. These two descriptions of the data assume that the variation within the δ^2H signal is a seasonal one. Unfortunately, this is not the only possible explanation, within the precision of the deuterium measurements. There was a strong increase in the amount of precipitation in October and November 2003 and so a strong increase in discharge of the springs. From a strict point of view this finding is a contradiction to the application of most lumped parameter models, since their convolution integral is based on the assumption of constant flow conditions. A quantitative numerical description of variable hydrological conditions would need an unsteady lumped parameter approach as discussed in Ozyurt & Bayari (2005), but this needs discharge values for the springs with at least monthly resolution, which are not

quantified for springs in this region. But nevertheless these possibilities for different interpretation of the same data set demonstrate the weakness of a single tracer in a karst system: even with a two-year long monthly time series no unique solution is obtained.

Whereas the deuterium data are well described by all four LPM curves, the tritium time series data shows that the PMEM with the 300-old water component match the tritium data best (Fig. 7.7B). However, the modeling with **CFCs** and **SF**$_6$ shows that such an old component does not describe the MRT of the spring Ostrovica at all (Fig. 7.7D-G). It means that PMEM is not a good LPM description for the MRT of the spring Ostrovica. $^3\mathrm{He}_{\mathrm{trit}}$ in Fig. 7.7C also supports this finding, but this tracer is here considered to be constrained due to possibly He loss through the water table. The LPM matches best all measured tracers with the DM and a MRT of 2.5 years and a Péclet number 3.

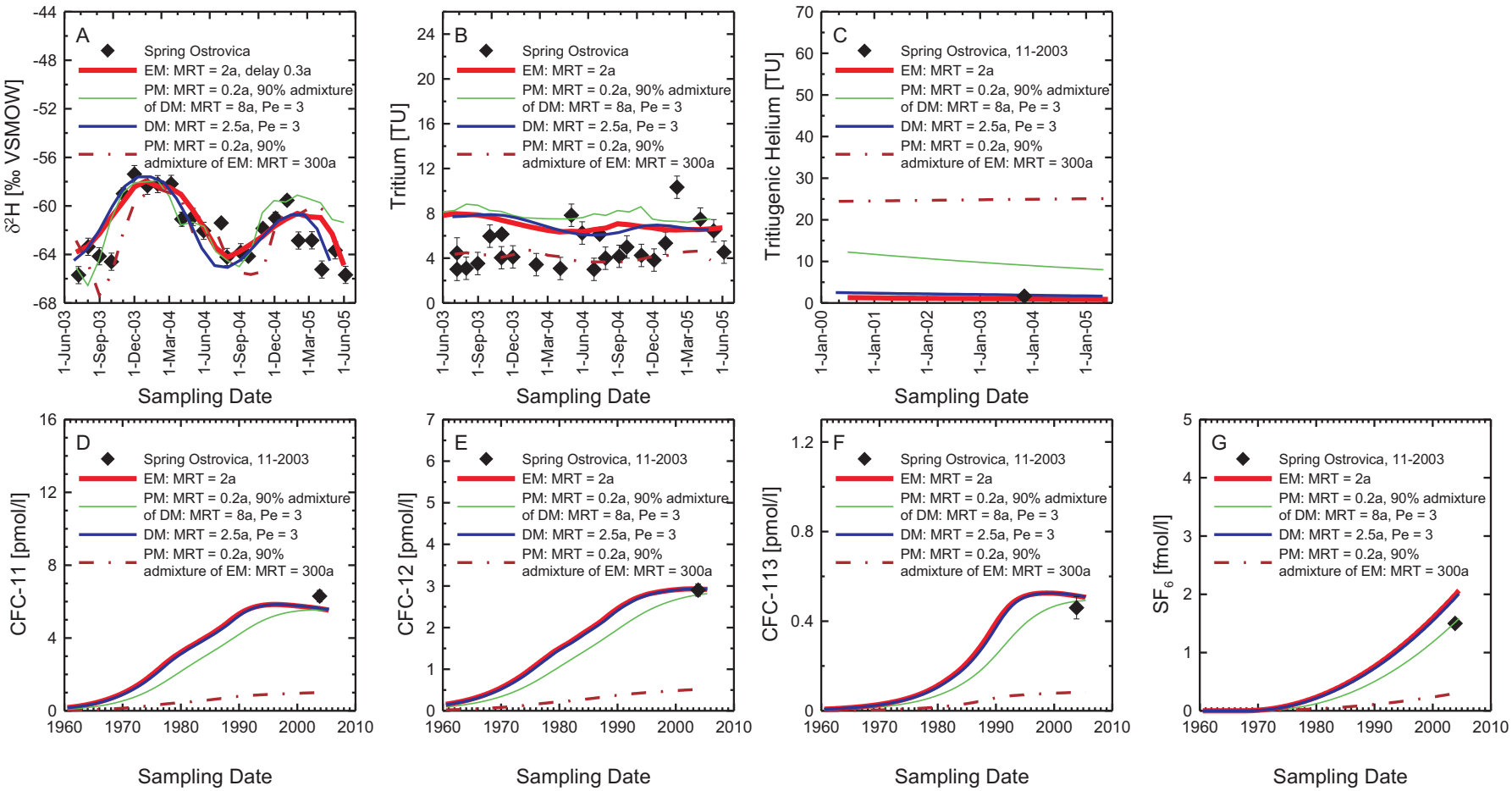

Fig. 7.7: Results of lumped parameter models for the spring Ostrovica for deuterium (A); tritium (B); noble gases (C); CFC-11 (D); CFC-12 (E); CFC-113 (F); and SF_6 (G). CFCs, SF_6 and noble gas data are from the sampling campaign in November 2003.

LPM for Spring Ostrovica, State II

Since the high discharge state in November 2003 is best described with the DM and MRT of 2.5 of years, it may be expected that the spring water sampled in July consists of older base flow water:

- The first model **(EM)** curve is created with the exponential model and a MRT of 15 years (red dashed curve).
- The second model **(PMDM)** curve is created using the two-component model: the "young" component in the karst conduit network is described by the piston flow model with a MRT of 0.2 years. The "old" component in the karst fissured-porous aquifer, obtained by the dispersion model with Péclet number 3, contributes to the spring water admixture with 90%, having the 17-year mean δ^2H value of -62‰ (green dashed curve).
- The third model **(DM)** curve is created using the dispersion model with a MRT of 17 years and Péclet number 3 (blue dashed curve).

All three models deliver similar results for the MRT, where the DM, from the hydrological point of view, is the best approximation describing the MRT of spring water in a karst system. Whereas for July 2004 the three model outputs exactly match each of the single measurement values for CFC-11, CFC-12, CFC-113 and SF_6, deuterium and tritium time series do not match so well. This is not too surprising, because the time series includes values for the period of two years and the geochemical tracers CFCs and SF_6 present the water age composition only from a single sampling. On the other hand, the model outputs for the single measurement values for CFC-11, CFC-12, CFC-113 and SF_6 for November 2003 and the time series of deuterium and tritium are congruent. Accordingly, the spring water contains components with MRTs of 2.5 and 17 years, but in this mixture the 2.5 years old component with 90% of volume is the dominant one.

Thus, for the quantification of storage capacity of the karst aquifers used for the drinking water supply of the Plitvice Lakes National Park and the Bihać and Kulen Vakuf municipalities, only the results from tritium, deuterium, CFCs and SF_6 from "State I" were considered. More detailed information on this issue can be found in Chapter 7.4.

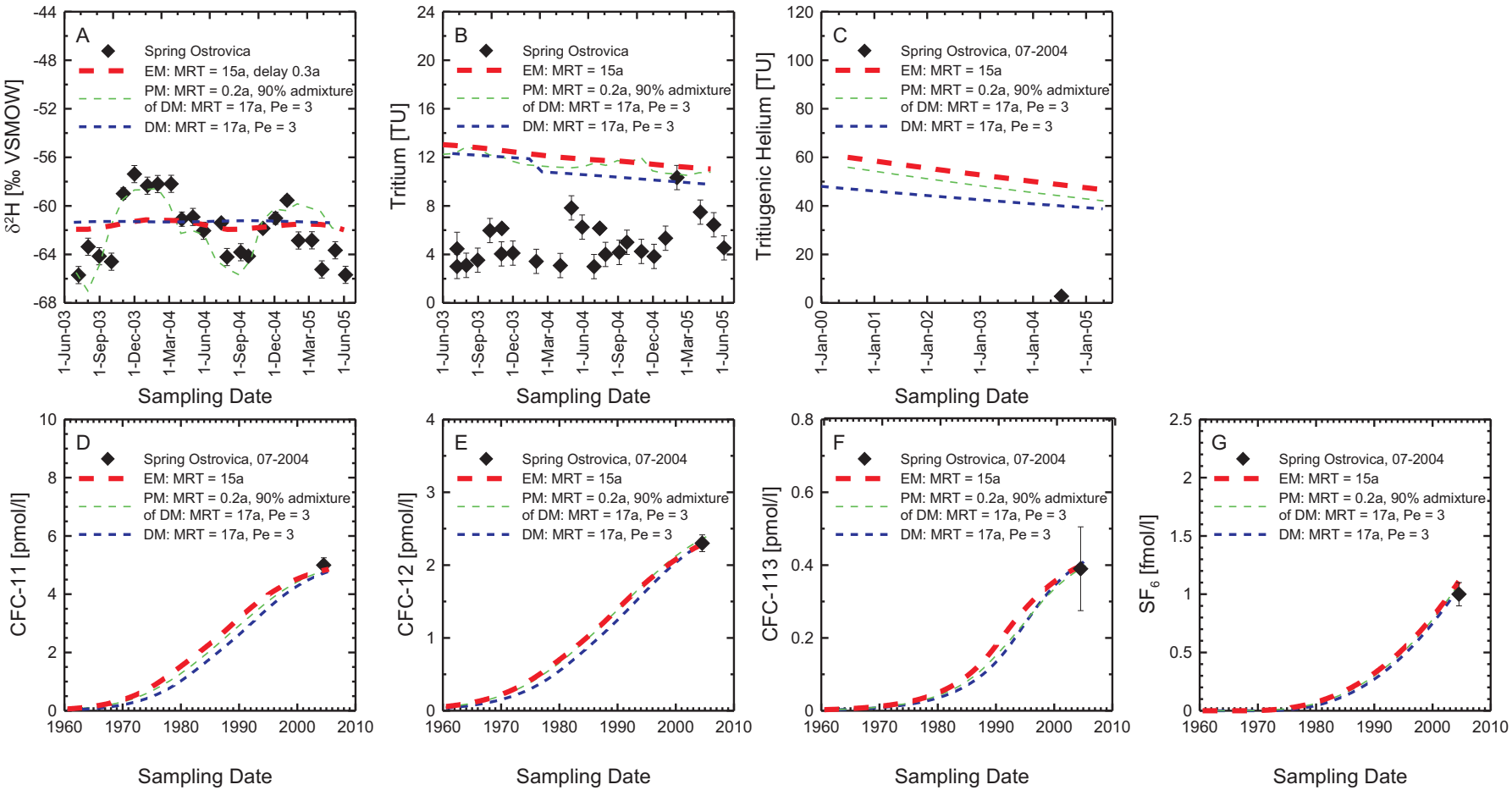

Fig. 7.8: Results of LPM for the spring Ostrovica for deuterium (A); tritium (B); noble gases (C); CFC-11 (D); CFC-12 (E); CFC-113 (F); and SF_6 (G). CFCs, SF_6 and noble gas data are from the sampling campaign in July 2004.

Table 7.2: Results of lumped parameter models (LPM) for ten springs in Croatia and Bosnia-Herzegovina, obtained with the LPM module "Lumpy" of the LabData database system (Suckow & Dumke, 2001). For computation of the MRT either an one-component model (exponential model: EM; dispersion model: DM) or a two-component model (piston flow-dispersion model: PMDM) is used. PMDM describes a mixture between two water components with different MRTs. The PM describes the "young" component in the karst conduit network (t_c) and the DM describes the "old" component in the fissured-porous aquifer (t_p). Due to systematic differences in the CFCs and SF_6 concentrations during the sampling campaign in November 2003 and July 2004, these both states were computed separately (State I and II). Pe is the Péclet number, as one modeling parameter of the DM. δ^2H shift describes the difference between mean values of the input functions for Zagreb and the Plitvice Lakes. In the last two columns of the table the ratio of the "young" water component in the conduit network (r_c) and the "old" water component in the karst fissured-porous aquifer (r_p) is presented. The MRT of the springs marked with * was determined in the work of Horvatinčić et al. (1986) by measuring monthly tritium activity in the springs Plitvica and Bijela Rijeka (1983-1985), and Crna Rijeka (1979-1982, 1983-1985). The MRT was obtained by the exponential model, ranging between 1 and 4 years on average.

Spring Number	**Spring Name**	**LPM**	δ^2**H Shift [‰]**	**Pe**	**MRT [yr] State I**		**MRT [yr] State II**		**Admixture [%]**	
					t_c	t_p	t_c	t_p	r_c	r_p
1	Plitvica*	EM	-7.8	-	0	4	0	13.5	0	100
2	Bijela Rijeka*	DM	-9.5	3	0	6	0	20	0	100
3	Crna Rijeka*	PMDM	-7.9	2.5	0.4	3	0.4	28	10	90
4	Stipinovac	DM	-5.2	6.5	0	13	-	-	0	100
5	Vrelo	DM	-5.2	7	0	11	0	17	0	100
6	Klokot	PMDM	-5.6	1	0.1	2.5	0.1	12	10	90
7	Privilica	PMDM	-5.3	3	0.2	1.5	0.2	27	10	90
8	Ostrovica	DM	0	2.5	0	2.5	0	17	0	100
9	Toplica	DM	1	1	0	3	0	20	0	100
10	Una	PMDM	-	10	-	-	0.5	15	50	50

7.3 Estimation of Water Storage Capacity Considering MRTs

The investigated springs are the main sources for the drinking water supply in the region. The volume of water in the catchment area of the springs can be estimated using the discharge data and the MRTs of water (Maloszewski et al., 2002). The lumped parameter modeling of the MRTs was performed according to the conceptual model of the karst aquifer. As mentioned before, one may distinguish the MRT of water in the conduit network (t_c) from the MRT in a fissured-porous karst aquifer (t_p). The water storage capacity in the conduit network (V_c) and the fissured-porus aquifer (V_p) is calculated as follows:

$$V_c = Q_c \cdot t_c \ , \ V_p = Q_p \cdot t_p \ , \ V_{total} = V_c + V_p \tag{7.1}$$

$$Q_c = r_c \cdot Q \ , \ Q_p = r_p \cdot Q \tag{7.2}$$

V_c, V_p water volume in conduit network and fissured-porous aquifer in the catchment area of the spring

Q_c, Q_p calculated mean annual discharge in the conduit network and the fissured-porous aquifer in Table 7.3 using the discharge data from Table 3.1

t_c, t_p MRT of water in the conduit network and the fissured-porous aquifer obtained by LPM with time series of deuterium and tritium, as well as with CFCs/SF_6 data for November 2003 (Table 7.2)

r_c, r_p ratio of the water component in conduit network and fissured-porous aquifer obtained by LPM (Table 7.2)

Q mean annual discharge of springs (Table 3.1).

The total volume of water in the catchment area of the springs is shown in Table 7.4. The karst aquifers in the area contain great water resources; for example, the calculated mean storage capacity for the spring Klokot is 677 Mio. m^3. This water reservoir hosts

Table 7.3: Calculated minimum, maximum and mean annual discharge in conduit network (Q_c) and fissured-porous aquifer (Q_p).

Spring Number	Spring Name	r_c [%]	r_p [%]	Q_c [m^3/s]			Q_p [m^3/s]		
				Q_{min}	Q_{max}	Q_{mean}	Q_{min}	Q_{max}	Q_{mean}
1	Plitvica	0	100	0	0	0	0.03	16.4	0.7
2	Bijela Rijeka	0	100	0	0	0	0.02	1.9	0.4
3	Crna Rijeka	10	90	0.002	0.7	0.1	0.02	6.3	1.3
4	Stipinovac	0	100	0	0	-	0.001	0.01	-
5	Vrelo	0	100	0	0	-	0.01	0.1	-
6	Klokot	10	90	0.3	2.2	1	2.7	9.7	8.6
7	Privilica	10	90	0.003	0.2	-	0.03	1.8	-
8	Ostrovica	0	100	0	0	-	0.8	16	-
9	Toplica	0	100	0	0	-	0.06	1	-
10	Una	50	50	0.05	0.5	-	0.05	0.5	-

a mixture of water with different ages. The lumped parameter models have shown that the groundwaters of the spring Klokot contain water components that are 0.1, 2.5 and 12 years old. The fraction of total discharge (or absolute volume) of water younger than one year is of special interest for the drinking water supply: this ratio is a measure of vulnerability because any "mean annual recharge contamination" will be diluted by this value in the discharge. It also can be regarded as the maximum amount of water that can be exploited per year without drastically changing the system behaviour. It also can serve as a measure of possible discharge fluctuations in dry years. LPMs enabled the calculation of the percentage of this young water component in the whole mixture from the weighted functions. The groundwater mixture of the springs Plitvica, Klokot, Privilica, and Ostrovica contains up to 48% of this young water component. The ratio of this young water is however, in the springs Stipinovac, Vrelo, and Una less then 1%. The last three columns in Table 7.4 contain the calculated volume of groundwater in the karst aquifer younger than one year.

Table 7.4: Minimum, maximum and mean annual volume of water in the catchment area of the springs in the conduit network (V_c) and the fissured-porous aquifer (V_p), $V_{total}=V_c+V_p$, percentage of volume of groundwater younger than one year ($V_{total\ <1\ year}$) in V_{total}.

Spring Number	**Spring Name**	$\mathbf{V_c}$ **[Mio. m^3]**			$\mathbf{V_p}$ **[Mio. m^3]**			$\mathbf{V_{total}}$ **[Mio. m^3]**			$\mathbf{r_{total\ <1\ year}}$ **[%]**	$\mathbf{r_{total\ <1\ year}}$ **[Mio. m^3]**		
		$\mathbf{V_{min}}$	$\mathbf{V_{max}}$	$\mathbf{V_{mean}}$	$\mathbf{V_{min}}$	$\mathbf{V_{max}}$	$\mathbf{V_{mean}}$	$\mathbf{V_{min}}$	$\mathbf{V_{max}}$	$\mathbf{V_{mean}}$		$\mathbf{V_{min}}$	$\mathbf{V_{max}}$	$\mathbf{V_{mean}}$
1	Plitvica	0	0	-	3.5	2068.8	88.3	3.5	2068.8	88.3	36.3	1.3	751	32.1
2	Bijela Rijeka	0	0	-	3.4	370.9	83.3	3.4	370.9	83.3	9.9	0.3	36.7	8.2
3	Crna Rijeka	0.03	44.2	8.8	1.8	593.5	119.2	1.8	602.3	163.4	18.6	0.3	112	30.4
4	Stipinovac	0	0	-	0.4	4.1	-	0.4	4.1	-	0.9	0.004	0.04	-
5	Vrelo	0	0	-	3.5	34.7	-	3.5	34.7	-	0.6	0.02	0.2	-
6	Klokot	1	6.9	3	212.9	1549	674.1	213.8	1555.9	677.1	41.5	88.7	645.7	281
7	Privilica	0.02	1.3	-	1.3	85.2	-	1.3	86.4	-	44.4	0.6	38.4	-
8	Ostrovica	0	0	-	59.1	1261.4	-	59.1	1261.4	-	48.8	28.9	615.6	-
9	Toplica	0	0	-	5.7	94.6	-	5.7	94.6	-	47.6	2.7	45.1	-
10	Una*	0.8	7.9	-	23.7	236.5	-	24.4	244.4	-	0.1	0.002	0.24	-

7.4 Discussion of Age Models

Whereas older studies using well-established model codes like FlowPC from Maloszewski & Zuber (1996) mainly focused on one transient tracer in a single box model, the data set in this study can rely on monthly records of deuterium and tritium for at least two years together with two single sampling campaigns applying CFCs, SF_6 and the isotopes of helium and neon.

A detailed analysis based on multi-tracer lumped parameter modeling shows, that most karst springs present a more complicated behaviour than can be described by a simple exponential model, often used in the karst studies, and that several components can be resolved by the multi-tracer approach. The application of the module "Lumpy" shows how the combination of time series of several tracers during different hydrological conditions can give deeper insight into the system and sheds new light on the strengths and limitations on LPM applied to karst systems.

It can be concluded:

- For the karst spring water study in Croatia and Bosnia-Herzegovina there is no alternative to the lumped parameter modeling.
- Although "Lumpy" enables simultaneous fit of several tracers, shift ^{2}H input functions, delay ^{2}H and ^{3}H input functions, and simulates loss of daughter gas tracers ($^3\mathrm{He}_{\mathrm{trit}}$), some of the practical problems of the studies are external to modeling (CFCs contamination and degradation, gas loss or re-equilibration etc).
- The basic LPM assumptions as stationary flow, closed system etc. are not fulfilled.
- Loss of $^3\mathrm{He}_{\mathrm{trit}}$ is a special problem in karst aquifers and very difficult to detect.
- The ^{3}H/^{3}He approach with only ^{3}He/^{4}He ratio and helium and neon concentrations does not render reliable ($^3\mathrm{He}_{\mathrm{trit}}$) results due to fractionation of excess air and possible ($^3\mathrm{He}_{\mathrm{trit}}$) loss. For this reason heavy noble gases argon, krypton, xenon should be taken.

- In multi-parameter studies, two-component mixing models are often not able to describe all measurements consistently.
- For more sophisticated time dependent lumped parameter modeling the necessary calibration data (time series of discharge and gas tracers etc.) are not available.

Chapter 8

Chronology of Anthropogenic Input in Lake Sediments

In the complex aquatic system of the Plitvice Lakes calcium carbonate precipitates intensively in water forming tufa barriers between 15 smaller and larger lakes in the presence of moss, algae and aquatic bacteria. It also precipitates as a fine-grained sediment on the bottom of the lakes (e.g. Obelić et al., 2005, 2006). In the last decades the process of eutrophication[1] in some of the lakes was developed and is in progress.

The possible anthropogenic sources of pollution in the past were logging and sawmill industry recorded since 1800. Those were phased out entirely by the early 1960s (e.g. Srdoč et al., 1992; Ahel & Terzić, 2006). Up to the 1960s, the area of the National Park was used as a traffic connection between interior Croatia and its littoral regions. More recently, the area was affected by the war destructions (1991-1995). In the last decades the area was threatened by sparsely populated neighbouring settlements and untreated wastewaters from tourists accommodations. More recently, (ca. 2000) the sewerage system was repaired.

The anthropogenic input on lacustrine environments over the past 50-100 years is recorded in lake sediments in the form of significant changes in chemical and isotopic constituents (e.g. Schell & Barnes, 1986). Lake sediments store information about

[1]The process by which the lakes gradually age and become biologically more productive. It can be the result of natural processes and then takes thousands of years to develop. However, the process can be accelerated by anthropogenic influence: e.g. by increased runoff of plant nutrients derived from human activities, mainly from sewerage, agricultural and livestock holdings (Obelić et al., 2005).

environmental contaminants, such as heavy metals, detergents and cleaning agents, which settled to the lake bottom while adsorbed to particulate matter. These chemicals can be used as tracers to document the history of their release into the environment, which, in turn, allows to assess the success of measures taken to reduce their use.

In this study, the recent lake sediments were dated with ^{210}Pb and ^{137}Cs method, in order to establish a chronology of possible anthropogenic input into the lakes. Whereas chemical analysis of trace elements were performed on each core, detergent-derived linear alkylbenzene sulphonates (LAS) were measured in Prošće and Kozjak Lake only, as the largest lakes of the Plitvice Lakes system. The positions of the ca. 40 cm long cores obtained in particular lakes are shown in Figure 4.2.

8.1 Isotopic Analysis Performed on Lake Sediments

Sedimentation rates of lake sediments were obtained by gamma-spectrometric measurements of the nuclides ^{210}Pb and ^{137}Cs produced by radioactive decay processes. Radioactive decay is affected by two alternative types of particle emission: either the moderately heavy *alpha particle* or the light *beta particle*. The particles are released with great energy and are often accompanied by the emission of electromagnetic radiation called *gamma radiation* (Ivanovich, 1992). Gamma rays vary in energy between 10 keV[2] and 7 MeV. A nuclide in an excited state decays by alpha or beta decay and in a number of instances gamma ray are emitted. Most of the long-lived, heavy radioactive elements, such as ^{238}U, decay into daughter products that are themselves radioactive (Fig. 8.1), such as ^{210}Pb used for the dating purposes of lake sediments. These decay in turn and thus form a decay series (or chain) which end in a stable daughter nuclide like ^{206}Pb in case of ^{238}U. A decay series is in *radioactive equilibrium* when, on average, for each decaying parent atom one of each intermediate daughter atom also decays. The number of atoms of each intermediate daughter will be in direct proportion to its half-life, or in inverse proportion to the respective decay constant.

[2] An electron-volt (eV) is the kinetic energy acquired by an electron falling through a potential difference of 1 V and is equal to $1.6{\cdot}10^{-19}$ J (Ivanovich, 1992).

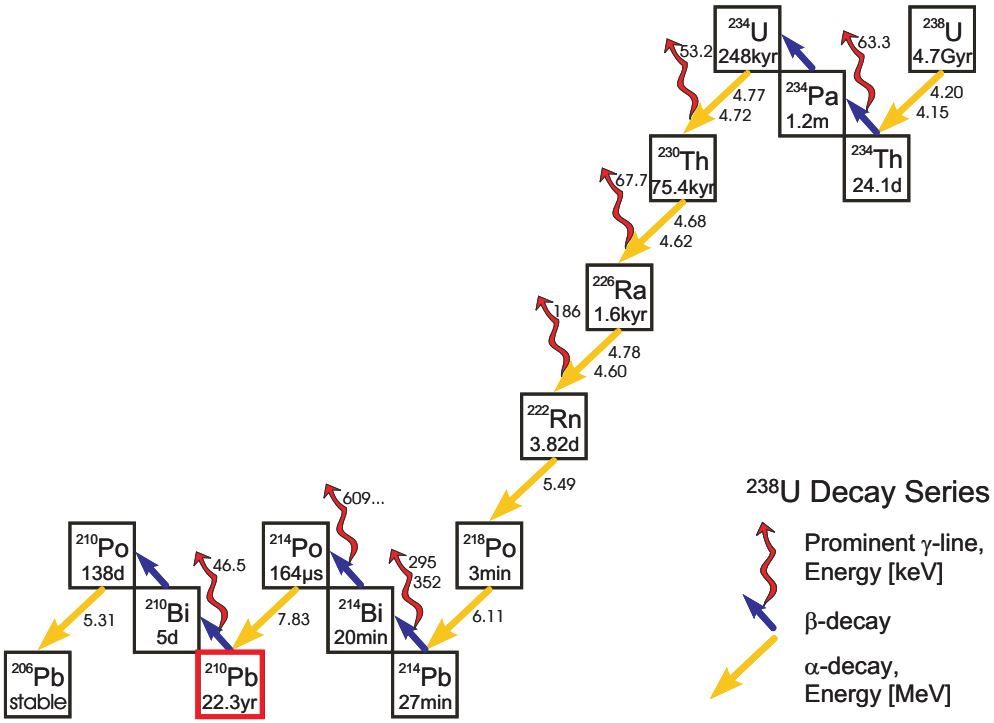

Fig. 8.1: The uranium decay series with a ^{210}Pb radionuclide, modified after Ivanovich (1992).

The Principle of ^{210}Pb Dating

Sediment and ice geochronology using ^{210}Pb was first suggested in 1963 by Goldberg and first applied to lake sediments by Krishnaswamy et al. (1971). ^{210}Pb with a half-life of 22.3 years occurs naturally as one of the radioisotopes in the ^{238}U decay series (Fig. 8.1). One of the precursor products of ^{210}Pb within the radioactive decay chain is the noble gas ^{222}Rn, which diffuses from the earth crust to the atmosphere and decays there with a half-life of 3.82 days via a series of short-lived intermediate nuclides to ^{210}Pb (Fig. 8.1 and 8.2; Appleby & Oldfield (1992)).

Therefore, ^{210}Pb in sediments has two origins (Appleby & Oldfield, 1992):

- "Supported" ^{210}Pb, which is produced in the sediment *in situ* from its parent isotope ^{226}Ra, where the precursor ^{222}Rn did not reach the atmosphere. Using gamma-spectrometry it is measured as the activity of ^{214}Bi and ^{214}Pb from the gamma lines at 609 keV and 295 keV, respectively (Fig. 8.1 and 8.2)

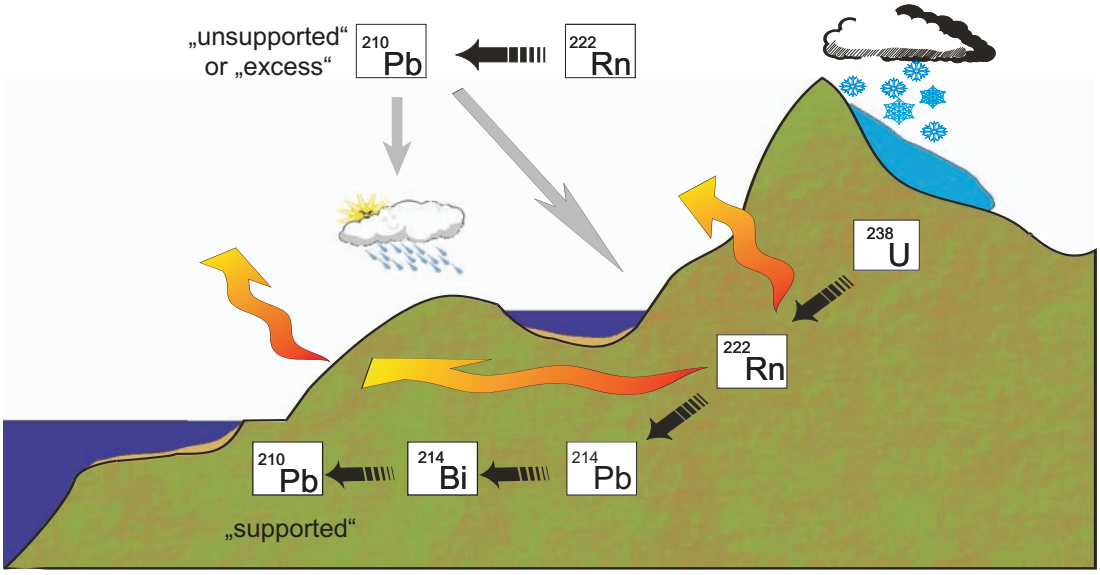

Fig. 8.2: The principle of ^{210}Pb dating of sediments, modified after Suckow (2004), Lectures on Geochronology, pers. comm.

- "Unsupported" or "excess" ^{210}Pb (in the following $^{210}\mathrm{Pb}_{\mathrm{exc}}$), which originates from radioactive decay of ^{222}Rn in the atmosphere. $^{210}\mathrm{Pb}_{\mathrm{exc}}$ is removed from the atmosphere by precipitation or dry deposition. A part of it is adsorbed on to sedimentary particles in lake water and subsequently incorporated in the lake sediment. $^{210}\mathrm{Pb}_{\mathrm{exc}}$ in a given layer decays exponentially with time in accordance to the law of radioactive decay. $^{210}\mathrm{Pb}_{\mathrm{exc}}$ can be used for dating after subtracting the supported ^{210}Pb (measured as ^{214}Pb) from the total measured ^{210}Pb (gamma line at 46.5 keV in Fig. Fig. 8.1 and 8.2).

Interpretation of $^{210}\mathrm{Pb}_{\mathrm{exc}}$ depth profiles has to take sediment compaction into account (Suckow & Gäbler, 1997). Therefore all age models do not use the depth in the core directly but the "mass depth", describing the dry sediment mass (in kg/m^2) above a certain depth in the core. Sedimentation rates are obtained as the accumulated dry mass per area unit and per time unit [kg/(m^2 yr)]. For the calculation of sedimentation rates, the following models were used (Appleby & Oldfield, 1992):

- The CSR model (constant sedimentation rate) is the most common and most sim-

ple approach. It assumes constant sedimentation rates and constant concentration of $^{210}Pb_{exc}$ at the sediment-water interface. This results in a straight line of ln($^{210}Pb_{exc}$) versus mass depth which is only due to radioactive decay of $^{210}Pb_{exc}$.

- The CIC model (constant initial concentration of $^{210}Pb_{exc}$) assumes a constant concentration of $^{210}Pb_{exc}$ at the sediment-water interface over the period of time for which the $^{210}Pb_{exc}$ is measurable, but allows a variable sedimentation rate. This means that $^{210}Pb_{exc}$ decreases monotonic with (mass) depth due to radioactive decay.

- The CF or CRS model (constant flux or constant rate of supply of $^{210}Pb_{exc}$) also allows a variable sedimentation rate, but assumes a constant rate of supply of $^{210}Pb_{exc}$ to the sediment-water interface. During age computation this flux is computed from the total $^{210}Pb_{exc}$ inventory, which is expressed in kBq/m^2. As a consequence also depth profiles that do not show a monotonic decrease with depth can be interpreted: these "minima" in the depth profile are explained in this model as a stronger dilution of the $^{210}Pb_{exc}$ signal by a higher rate of $^{210}Pb_{exc}$-free sediment.

Obviously, when the sedimentation rate is constant all three models should yield dating results that are identical within the measurement uncertainty (Suckow & Gäbler, 1997).

The Principle of ^{137}Cs Dating

^{137}Cs with a half-life of 30.2 years is an anthropogenic isotope first introduced into the atmosphere as a result of nuclear weapon testings beginning 1954 (Pennington et al., 1973). Fallout of ^{137}Cs is peak-shaped in time and reached the highest values in 1963. Since 1980 bomb fallout has been negligible (Walling & Quine, 1992), but the 1986 reactor accident of Chernobyl introduced a spatially very variable component of this nuclide. ^{137}Cs is used as an event-marker, which implies that dating with ^{137}Cs allows only interpretations using constant sedimentation rates. These rates are obtained attributing either 1954 to the deepest sample in the core containing ^{137}Cs or attributing

the peaks of the ^{137}Cs depth profile to the years 1963 (maximum bomb fallout) and/or 1986 (Chernobyl fallout). The mass depth for these sample positions is then divided by the time between the years 1954, 1963, 1986 and the year 2003 as the year of sediment sampling, giving 49 yr, 40 yr or 17.5 yr respectively. After dividing, the sedimentation rate is obtained, expressed in kg/(m^2 yr).

In earlier studies it was sometimes possible to distinguish between the Chernobyl and bomb-fallout peaks using the radionuclide ^{134}Cs with a half-life of 754 days as the marker for the Chernobyl fallout (Suckow & Gäbler, 1997). This is no longer possible, since the activity of ^{134}Cs meanwhile decayed to 1/350 of its initial value, therefore interpretation of ^{137}Cs peaks is not completely free of ambiguity.

8.2 Sampling and Measurement Techniques

Undisturbed lake sediment cores were obtained in November 2003 by two scuba divers (Fig. 8.3A) from the bottom of 4 different lakes at 5 different locations. The position of the sediment cores in Prošće (PR, 19 m water depth), Gradinsko (GR, 5 m), Kozjak (K1, 21 m), Kozjak (K2, 2 m), and Kaludjerovac Lake (KA, 3 m) are given in Figure 4.2. Immediately after sampling, the approximately 50 cm long cores were frozen in a chest freezer by -20°C. In the laboratory of the Rudjer Bošković Institute, Zagreb, Croatia the cores were cut into 1-2 cm thick samples and the obtained aliquots were oven dried and milled using a mortar (Fig. 8.3B, C, D).

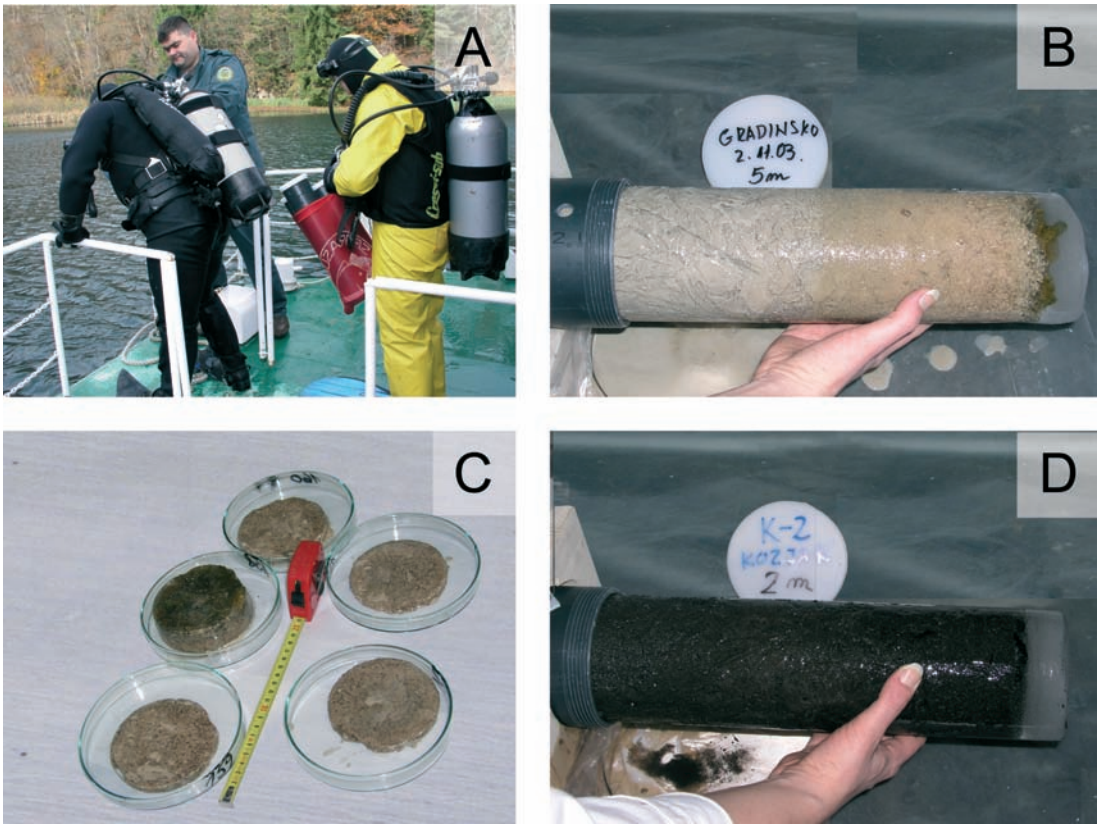

Fig. 8.3: Scuba divers just before sampling sediments from the bottom of Kozjak Lake in November 2003 (A), frozen core of Gradinsko Lake (GR) just before cutting in 1-2 cm thick aliquots (B), aliquots of the GR core (C), frozen core of Kozjak Lake (K2) (D).

Radionuclide analysis of sediment samples was performed in the GGA-Institut, Hannover by gamma-spectrometry using a low-background, well-type, high-purity germanium (HPGe) detector of 240 cm^3 active volume and 40 mm active well depth. Spectra were taken with standard electronics (EG&G 92X) and evaluated with commercial software (GammaVision). Sample vials were filled with sediment to a constant height of 38 mm, sealed air tight and stored for at least four weeks to establish radioactive equilibrium between ^{226}Ra, ^{222}Rn and ^{214}Pb/^{214}Bi. After this time, activities of the anthropogenic (^{137}Cs, ^{134}Cs, ^{241}Am) and natural (^{210}Pb, ^{214}Pb, ^{214}Bi) radionuclides were determined. The accuracy of ^{210}Pb activity measurements is in the range of 5-7% (Gäbler & Suckow, 2003).

8.3 Results and Interpretation of Sediment Dating

Prošće Lake (PR)

The anthropogenic fallout nuclide ^{137}Cs was found in the core Prošće Lake down to a sediment depth of 14 cm (Fig. 8.4A), which corresponds to a mass depth of 45 kg/m^2. So a sedimentation rate of 0.92 kg/(m^2 yr) from the fallout of atmospheric nuclear weapon tests beginning in 1954 is calculated. The ^{137}Cs activity versus depth profile has a well-resolved peak at 8.5 cm, which is interpreted as Chernobyl fallout. Taking it as the time marker, a mean sedimentation rate of 0.54 kg/(m^2 yr) is obtained. Below 20 cm all ^{137}Cs activities are at or below the detection limit, the lowest sample being above detection limit is at 18-20 cm depth.

Figure 8.4B shows three measured values for each depth. Values on the left side of the graph (connected by a line) are the activities of ^{214}Pb and ^{214}Bi and correspond to supported ^{210}Pb produced in the sediment in situ. On the right side the measured total ^{210}Pb is depicted (unconnected points), which corresponds to supported ^{210}Pb + $^{210}\mathrm{Pb}_{\mathrm{exc}}$. Accordingly, $^{210}\mathrm{Pb}_{\mathrm{exc}}$ is the difference between these curves, which decreases due to radioactive decay and is used for age-dating. Supported ^{210}Pb is comparably constant throughout the core and total ^{210}Pb shows a nearly exponential decrease. Unsupported ^{210}Pb concentrations decline more or less exponentially with depth but

some of values do not follow a declining trend ^{210}Pb, so that CIC model (constant sedimentation rate) cannot be applied. The CSR model (constant sedimentation rate) assumes that both the initial concentration and the sedimentation rate measured as dry mass supply to a unit area per time remained constant (the latter being an implicit assumption in ^{137}Cs dating too). So the CSR model can be excluded for the same reason as the CIC. In consequence, ^{210}Pb dates calculated using the dating models CF is unequivocal (Fig. 8.4C). The dating results with the CF method indicate sedimentation rates with a mean value of 1.3 $\mathrm{kg/m^2yr}$.

Results of sediment dating with $^{210}\mathrm{Pb}$ and $^{137}\mathrm{Cs}$ show a remarkable good agreement with a mean value of 1.3 $\mathrm{kg/m^2yr}$ for the CF model. This model places 1986 at 8.5 cm depth where the $^{137}\mathrm{Cs}$ activity versus depth has a very well-resolved peak so suggesting the fallout from the Chernobyl accident in 1986. The $^{137}\mathrm{Cs}$ activities (around 8 Bq/kg) can be attributed to bomb fallout. The onset of fallout in 1954 is within the numerical uncertainty of the CF model in agreement with the deepest measured $^{137}\mathrm{Cs}$ activity at 18-20 cm depth. Figure 8.4C reveals that the CF, CSR ($^{137}\mathrm{Cs}$) and CSR ($^{137}\mathrm{Cs}$) agree with their uncertainty, so the choice of any of these models leads to the same interpretation. The dating results for the core PR are summarized in Tables 8.1 and 8.2.

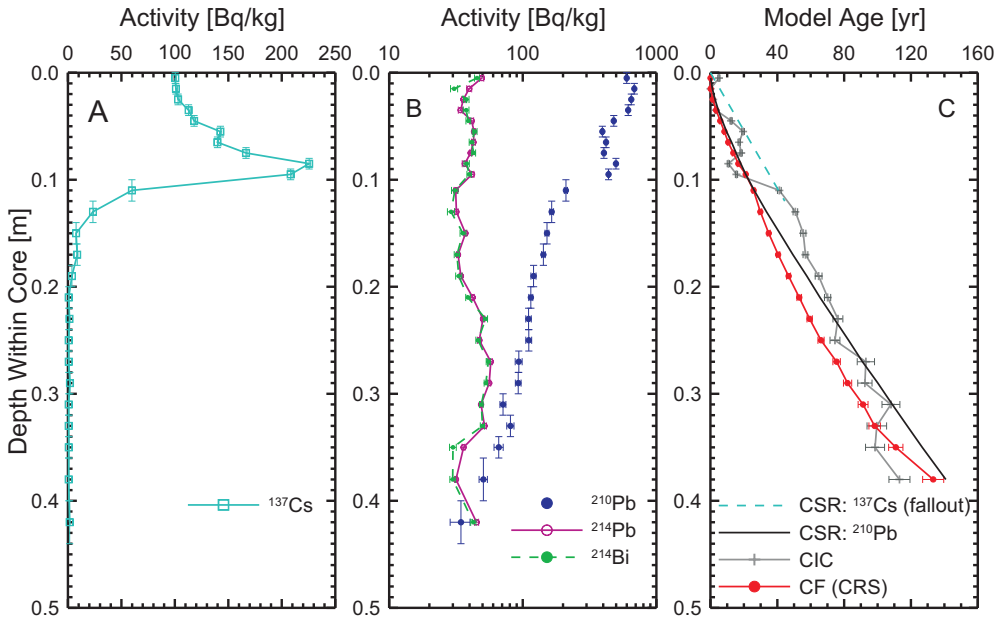

Fig. 8.4: Radionuclide depth profile for the core from Prošće Lake, ^{137}Cs-peak at 8.5 cm depth is interpreted as Chernobyl fallout in 1986 (A); supported ^{210}Pb from ^{214}Pb (violet) and ^{214}Bi (green) and total ^{210}Pb (blue) from supported + unsupported ^{210}Pb (B); sediment age obtained by dating models CSR (constant sedimentation rate) from ^{137}Cs fallout (cyan) and ^{210}Pb (black), CIC (constant initial concentration of $^{210}\mathrm{Pb}_{\mathrm{exc}}$, grey), CF (CRS) (constant flux or constant rate of supply of $^{210}\mathrm{Pb}_{\mathrm{exc}}$, red) (C).

Gradinsko Lake (GR)

In the core from Gradinsko Lake two ^{137}Cs peaks were found. The upper peak at a sediment depth of 7 cm corresponds to Chernobyl fallout. Beneath this peak ^{137}Cs activity drops, but rises again slightly in samples at a sediment depth of 14 cm. This lower peak corresponds to the bomb fallout in 1963 (Fig. 8.5A). The lowest ^{137}Cs activity is being 2.1 Bq/kg, i.e. none of the samples measured in this core is below the detection limit. Both supported $^{210}\mathrm{Pb}$ and $^{210}\mathrm{Pb}_{\mathrm{exc}}$ show stronger variations with depth and non-monotonic features, so the CIC and CSR model cannot be used but the CF model. If the ^{137}Cs peaks at 7 cm and 14 cm are interpreted as Chernobyl and bomb fallout, respectively, no agreement with the CF model for $^{210}\mathrm{Pb}$ is obtained. $^{210}\mathrm{Pb}$ dates calculated using the CF model place 1986 at a depth of 16 cm and 1963

at a depth between 22 and 24 cm. The CF model indicates non-uniform sedimentation rates since ca 1909, with a mean value of 3.3 $\mathrm{kg/(m^2 yr)}$. The dating results for the core GR are summarized in Tables 8.1 and 8.2.

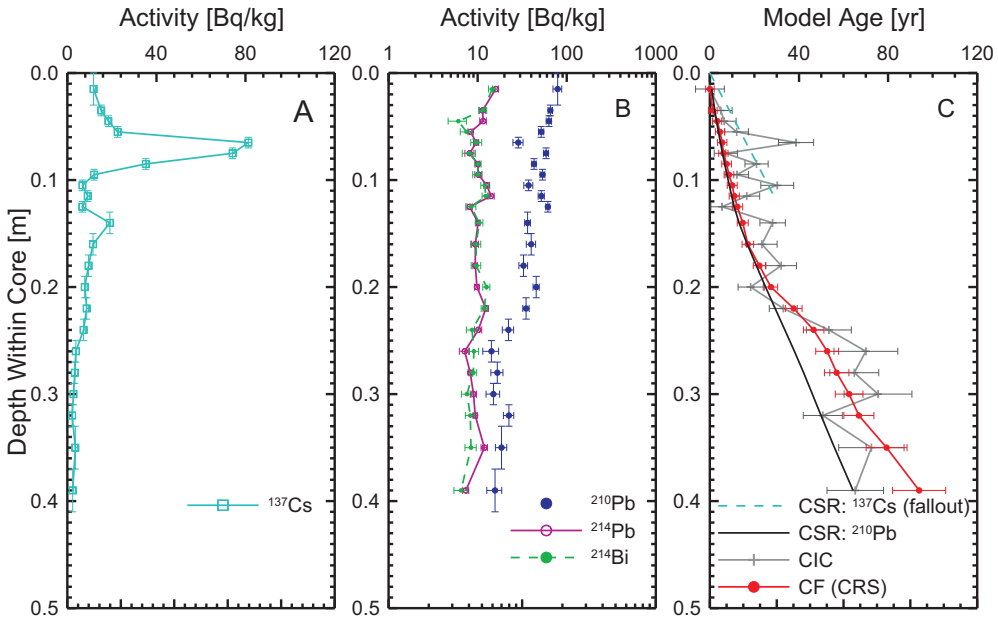

Fig. 8.5: Radionuclide depth profile for the core from Gradinsko Lake, ^{137}Cs-peaks at 7 cm and 14 cm depth are interpreted as Chernobyl fallout and 1963-bomb fallout, respectively (A); supported ^{210}Pb from ^{214}Pb (violet) and ^{214}Bi (green) and total ^{210}Pb (blue) from supported + unsupported ^{210}Pb (B); sediment age obtained by dating models CSR (constant sedimentation rate) from ^{137}Cs fallout (cyan) and ^{210}Pb (black), CIC (constant initial concentration of $^{210}\mathrm{Pb_{exc}}$, grey), CF (CRS) (constant flux or constant rate of supply of $^{210}\mathrm{Pb_{exc}}$, red) (C).

Kozjak Lake (K1)

^{137}Cs was found in the core from Kozjak Lake (K1) down to a sediment depth of 14 cm, corresponding to a mass depth of 37 kg/m^2 and a sedimentation rate of 0.76 kg/(m^2 yr) (Fig. 8.6A). No peaks were observed in the ^{137}Cs depth profile. Both the ^{137}Cs and the ^{210}Pb values are more or less constant down to a depth of 8 cm within the core. This points towards either a very fast sedimentation process or a slump that reworked some of the sediments at the slope of the lake and deposited it at greater water depth (instantaneous deposition of reworked sediment with a "mean"

activity). The fact that there is no ^{137}Cs at depth greater than 14 cm points towards negligible bioturbation below this depth, so maybe this holds also for the shallowest part of the sediment. It is also possible that the first 8 cm were mixed during the sampling procedure. If one assumes that this slump filling the sediment column down to 8 cm occurred "yesterday", one could calculate a mean sedimentation rate for the section 8-12 cm, yielding 1.3 mm/yr from adaption of the ^{210}Pb profile and roughly 1 mm/yr from ^{137}Cs. This assumes that the sediment column of 8 cm to 14 cm was deposited during the last 49 years, i.e. since the onset of ^{137}Cs fallout in 1954. No peaks are discernible in the ^{137}Cs depth profile, and similar to the findings in Prošće Lake, all samples from more than 15 cm depth are below the detection limit for ^{137}Cs.

For the same reason as for the core of Prošće Lake, the CIC model does not deliver the reliable dating results (Table 8.1). CF and CSR models show very good agreement with the ^{137}Cs results. Because there is no ^{137}Cs peak discernible in this core, the beginning of nuclear weapon tests in 1954 is used as a time marker. 1954 is placed by ^{137}Cs method at a depth of 14 cm and for ^{210}Pb methods at a depth between 13.5 and 14.5 cm. Both ^{210}Pb dating methods indicate uniform sedimentation rates since ca 1895, with a mean value of 0.8 kg/(m^2 yr) for the CF model. Figure 8.4C reveals that the CF, CSR (^{137}Cs) and CSR (^{137}Cs) agree with their uncertainty, so the choice of any of these models leads to the same interpretation.

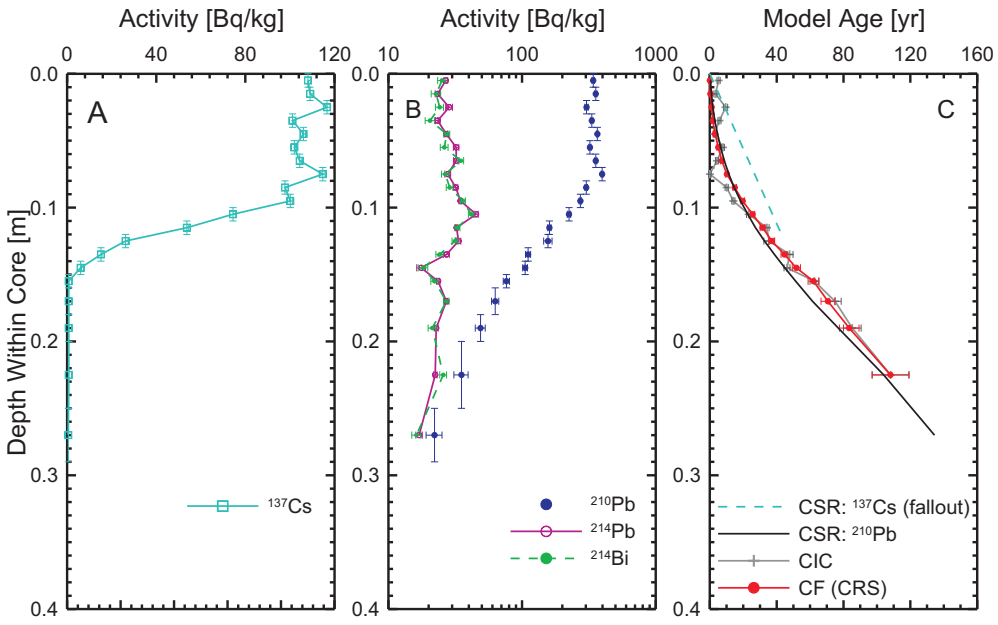

Fig. 8.6: Radionuclide depth profile for the core from Kozjak Lake (K1), ^{137}Cs activity (A); supported ^{210}Pb from ^{214}Pb (violet) and ^{214}Bi (green) and total ^{210}Pb (blue) from supported + unsupported ^{210}Pb (B); sediment age obtained by dating models CSR (constant sedimentation rate) from ^{137}Cs fallout (cyan) and ^{210}Pb (black), CIC (constant initial concentration of $^{210}\mathrm{Pb}_{\mathrm{exc}}$, grey), CF (CRS) (constant flux or constant rate of supply of $^{210}\mathrm{Pb}_{\mathrm{exc}}$, red) (C).

Kozjak Lake (K2)

The second core from Kozjak Lake (K2) cannot be used for assessing of sedimentation rates, since ^{210}Pb shows radioactive disequilibrium with ^{214}Pb and ^{214}Bi along the whole core (Fig. 8.7B). Measurable ^{137}Cs below 20 cm depth points towards bioturbation that transports some of the bomb fallout down to this depth (Fig. 8.7A). Supported ^{210}Pb shows high absolute values and strong internal variations along the core, indicating a strong detritic source. Together with ^{137}Cs this indicates that the whole sediment column of 40 cm length is younger than 1963, probably even younger than 1986. So besides bioturbation, another possible explanation for this behaviour is rapid transport of land material into the lake at a rate greater than 2.5 kg/(m^2 yr). This is a probable explanation, since this core was taken near the estuary of Rječica River.

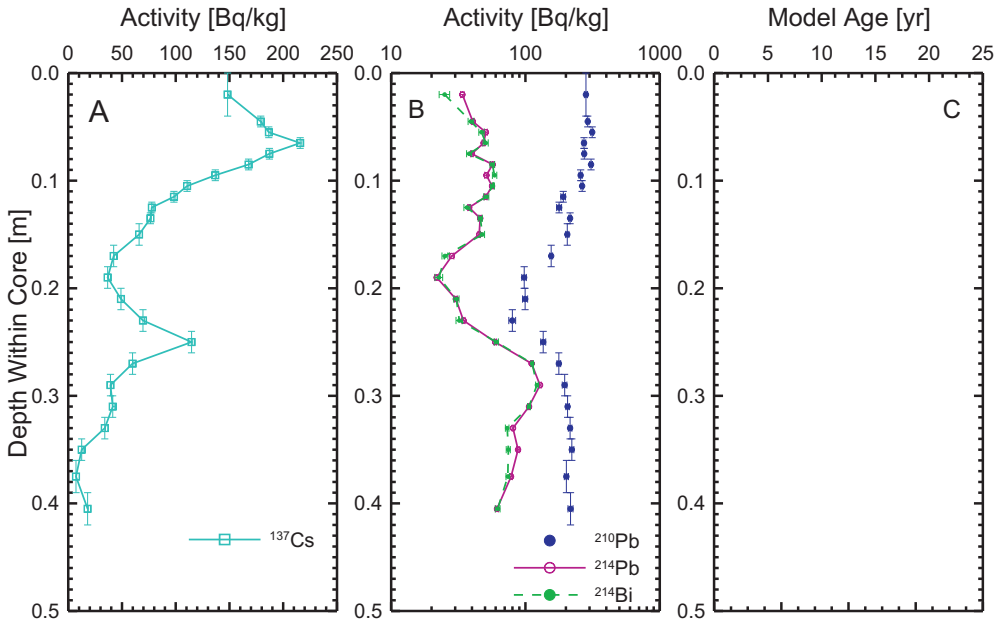

Fig. 8.7: Radionuclide depth profile for the core from Kozjak Lake (K2), ^{137}Cs activity (A); supported ^{210}Pb from ^{214}Pb (violet) and ^{214}Bi (green) and total ^{210}Pb (blue) from supported + unsupported ^{210}Pb (B).

Kaludjerovac Lake (KA)

Similar to Gradinsko Lake the core of Kaludjerovac Lake shows a ^{137}Cs peak around 100 Bq/kg at 5.5 cm depth, and a second weaker peak around 25 Bq/kg at 14 cm depth. The first ^{137}Cs peak is interpreted as Chernobyl fallout and the subsidiary peak as the 1963-fallout peak. Only the deepest three samples at 34-40 cm depth have values near or at the detection limit. Both the supported and total ^{210}Pb show some scatter but the depth profile in total shows the expected decrease in $^{210}\mathrm{Pb}_{\mathrm{exc}}$. ^{210}Pb dates calculated using the CF model places 1986 at a depth between 8.5 and 9.5 cm and 1963 at a depth between 17 and 19 cm. A mean sedimentation rate of 2.6 kg/(m^2 yr) is obtained. The agrement between the different ^{210}Pb age models and ^{137}Cs dating results (interpreting the both ^{137}Cs peaks) is reasonable.

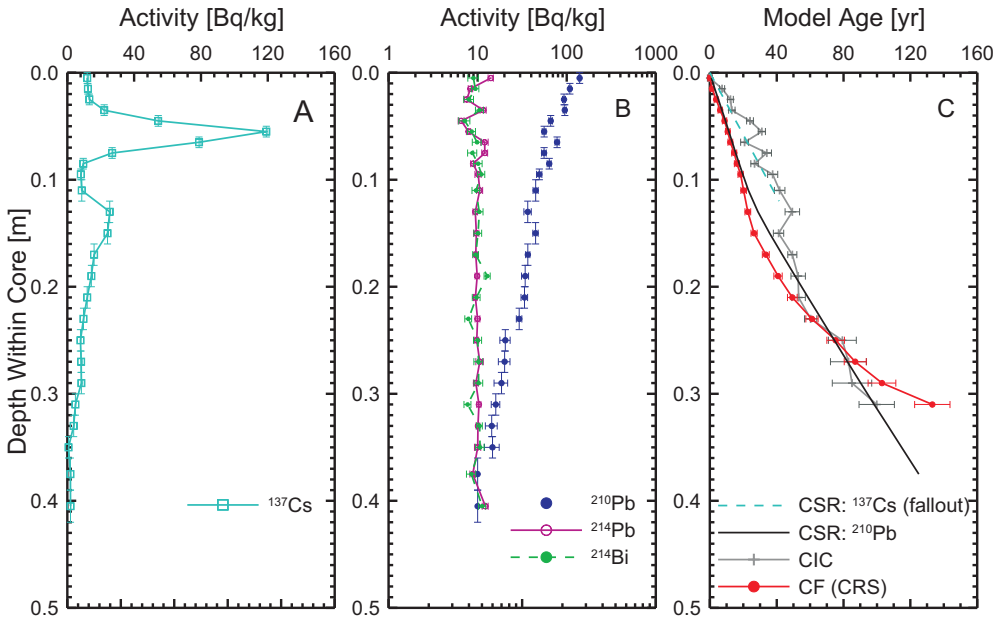

Fig. 8.8: Radionuclide depth profile for the core from Kaludjerovac Lake, ^{137}Cs-peak at 7 cm depth is interpreted as Chernobyl fallout in 1986 and the lower peak at 14 cm depth as 1963-fallout (A); supported ^{210}Pb from ^{214}Pb (violet) and ^{214}Bi (green) and total ^{210}Pb (blue) from supported + unsupported ^{210}Pb (B); sediment age obtained by dating models CSR (constant sedimentation rate) from ^{137}Cs fall-out (cyan) and ^{210}Pb (black), CIC (constant initial concentration of $^{210}\mathrm{Pb}_{\mathrm{exc}}$, grey), CF (CSR) (constant flux or constant rate of supply of $^{210}\mathrm{Pb}_{\mathrm{exc}}$, red) (C).

The dating results with ^{137}Cs and ^{210}Pb methods on five cores are summarized in Table 8.1. Results of gamma-spectrometric dating with ^{210}Pb and the CF (constant flux) model are shown in Table 8.2.

Table 8.1: Summary of the gamma-spectrometric investigations on five sediment cores of the Plitvice Lakes.

	Radionuclide	**PR**	**GR**	**K1**	**K2**	**KA**
Inventory	^{137}Cs	4.76	2.60	2.63	-	4.80
[kBq/m^2]	^{210}Pb	20.40	5.62	9.53	13.58	7.73
Sedimentation Rate	^{137}Cs	0.54-0.92	1.40	0.76	-	1.80
[kg/m^{2}yr] (CF model)	^{210}Pb	1.30	3.40	0.80	-	2.60
Lake Area [ha]		68.20	8.10	82.00	82.00	2.10

Table 8.2: Results of gamma-spectrometric dating with ^{210}Pb and the CF (constant flux) model for Prošće Lake (PR), Gradinsko Lake (GR), Kozjak Lake (K1), Kaludjerovac Lake (KA). MD: mean depth, SR: sedimentation rate.

Prošće Lake (PR)			**Gradinsko Lake (GR)**			**Kozjak Lake (K1)**			**Kaludjerovac Lake (KA)**		
MD [m]	**CF Model [yr]**	**SR [kg/m^{2}yr]**	**MD [m]**	**CF Model [yr]**	**SR [kg/m^{2}yr]**	**MD [m]**	**CF Model [yr]**	**SR [kg/m^{2}yr]**	**MD [m]**	**CF Model [yr]**	**SR [kg/m^{2}yr]**
0.005	2003 ± 0	1.15	0.02	2003 ± 2	2.77	0.005	2003 ± 1	0.94	0.01	2003 ± 1	1.91
0.015	2003 ± 0	0.98	0.04	2002 ± 2	3.10	0.015	2003 ± 1	0.88	0.02	2002 ± 1	2.31
0.025	2002 ± 0	0.99	0.05	2000 ± 2	3.05	0.025	2002 ± 1	1.04	0.03	1999 ± 1	2.50
0.035	2000 ± 0	0.99	0.06	1999 ± 2	3.50	0.035	2001 ± 1	0.91	0.04	1997 ± 1	2.37
0.045	1997 ± 0	1.21	0.07	1997 ± 2	7.75	0.045	2000 ± 1	0.79	0.05	1994 ± 1	3.07
0.055	1995 ± 1	1.40	0.08	1997 ± 2	2.86	0.055	1998 ± 1	0.87	0.06	1992 ± 1	3.61
0.065	1992 ± 1	1.21	0.09	1996 ± 2	4.21	0.065	1996 ± 1	0.73	0.07	1991 ± 1	2.49
0.075	1989 ± 1	1.14	0.10	1994 ± 2	3.09	0.075	1993 ± 1	0.58	0.08	1988 ± 1	3.51
0.085	1986 ± 1	0.82	0.11	1993 ± 2	5.19	0.085	1988 ± 1	0.69	0.09	1987 ± 2	2.65
0.095	1982 ± 1	0.83	0.12	1992 ± 2	3.30	0.095	1983 ± 1	0.68	0.10	1985 ± 2	3.47
0.11	1977 ± 1	1.59	0.13	1991 ± 2	2.23	0.105	1977 ± 1	0.75	0.11	1983 ± 2	3.74
0.13	1973 ± 1	1.89	0.14	1988 ± 2	4.21	0.115	1971 ± 2	0.87	0.13	1980 ± 2	4.38
0.15	1968 ± 1	1.88	0.16	1986 ± 3	3.37	0.125	1966 ± 2	0.76	0.15	1977 ± 2	3.02
0.17	1963 ± 1	1.64	0.18	1981 ± 3	3.75	0.135	1958 ± 2	0.89	0.17	1970 ± 2	3.13
0.19	1956 ± 1	1.73	0.20	1976 ± 3	2.09	0.15	1951 ± 2	0.67	0.19	1962 ± 2	2.78
0.21	1950 ± 1	1.67	0.22	1965 ± 4	2.40	0.155	1941 ± 3	0.82	0.21	1954 ± 3	2.15
0.23	1944 ± 2	1.67	0.24	1956 ± 5	3.42	0.17	1932 ± 4	0.92	0.23	1942 ± 4	1.87
0.25	1937 ± 2	1.27	0.26	1950 ± 5	4.75	0.19	1920 ± 6	0.85	0.25	1928 ± 5	2.17
0.27	1928 ± 2	1.7	0.28	1946 ± 6	3.54	0.22	1895 ± 11	0.81	0.27	1916 ± 7	1.68
0.29	1921 ± 2	1.36	0.3	1941 ± 6	4.14				0.29	1900 ± 8	1.09
0.31	1912 ± 3	1.66	0.32	1936 ± 7	1.67				0.31	1870 ± 11	0.68
0.33	1905 ± 3	1.02	0.35	1924 ± 9	2.24						
0.35	1892 ± 4	0.67	0.39	1909 ± 12	1.13						
0.38	1870 ± 6	0.52									

8.4 Discussion of Sediment Chronology

Gamma-spectrometric age-dating of undisturbed surface sediment cores taken by scuba divers proved to be a powerful tool to establish a sediment chronology, although not applicable to every core site. Sedimentation rates (assumed as constant) obtained with anthropogenic nuclide ^{137}Cs range between 0.5 and 1.8 kg/(m^2 yr). All ^{137}Cs inventories are higher than 2 kBq/m^2 expected from bomb fallout, which besides the shapes of the depth profiles is a further indication for the presence of Chernobyl fallout in these sediments. Most of the cores contain higher total inventories of $^{210}\mathrm{Pb}_{\mathrm{exc}}$ than inventories of 6 kBq/m^2 known from West European sedimentation studies (Appleby & Oldfield, 1992). The reason for these higher inventories can be either due to the continental effect of $^{210}\mathrm{Pb}_{\mathrm{exc}}$ or due to an additional contribution from maybe higher ^{226}Ra contents in the lake water. The latter hypothesis can only be confirmed by future studies.

Probably the most striking result of the chronological studies performed here is that in the smaller lakes Gradinsko and Kaludjerovac smaller sedimentation rates are obtained for the anthropogenic tracer ^{137}Cs, which integrates over the last two to four decades only, and the natural tracer $^{210}\mathrm{Pb}_{\mathrm{exc}}$ integrating over the last century. In contrast, sedimentation rates in the larger lakes Prošće (PR) and Kozjak (K1) give similar values for ^{137}Cs and ^{210}Pb. This finding could be an indication that sedimentation rates changed in the smaller lakes during the recent decades, whereas, they remained constant in the large lakes.

Sediments from the two large lakes Prošće (PR) and Kozjak (K1) show full agreement between the ^{137}Cs and ^{210}Pb chronologies. On the other hand, in the small lakes Gradinsko (GR) and Kaludjerovac (KA) the ^{137}Cs and ^{210}Pb chronologies do not agree so well. Their sedimentation rate is higher than in PR and K1 and probably also bioturbation plays a role here - ^{137}Cs in Gradinsko Lake is detectable throughout the core and in Kaludjerovac only those samples beyond the dating range of the CF model are free of ^{137}Cs. Bioturbation plays probably a minor role in the cores GR and KA since the sharp boundaries are preserved in the ^{137}Cs record (steep ^{137}Cs gradients in the vicinity of the peaks). But even in the case of the bioturbation in GR and KA, ^{210}Pb dating

would be still reliable since just few sediment mass is moved and below the measurement precision. This fact clearly argue for ^{210}Pb to derive the sediment chronology. The most reliable ^{210}Pb dating model in this study is the CF model, since for this model no contradictions are evident in the present study: with exception of K2, the depth profile of all sediment cores is long enough to observe the complete radioactive decay of $^{210}\mathrm{Pb}_{\mathrm{exc}}$ (the point where the depth profiles ^{214}Pb and ^{210}Pb meet) and any deviation from the exponential decrease of $^{210}\mathrm{Pb}_{\mathrm{exc}}$ with mass depth can be explained as variation of "dilution" of this flux with $^{210}\mathrm{Pb}_{\mathrm{exc}}$-free sediment.

8.5 Chemical Analysis and Chronology of their Input in Lake Sediments

Trace Elements

Trace elements may originate from different anthropogenic sources. Elevated heavy-metal contents (Cd, Cr, Cu, Mn, Ni, Pb, Zn) of recent limnic sediments are often the result of anthropogenic activities like the use of leaded gasoline, or the combustion of other fossil fuels (e.g. Ritson et al., 1994; Suckow & Gäbler, 1997). Elevated phosphorus values may originate from phosphorus based chemicals, e.g. from the production and use of fertilizers. They are also widely used in explosives, pesticides, toothpaste, and detergents.

Analysis of trace elements Al, B, Ba, Cd, Cr, Cu, Mn, Ni, Sr, P, Pb and Zn were performed at the Department of Chemistry, Universitat Autónoma de Barcelona, Spain on five sediment cores from the lakes Prošće (PR), Gradinsko (GR), Kozjak (K1, K2), and Kaludjerovac (KA). Description of measurements methods can be found in Obelić et al. (2005) and Briansó (2006). The heavy metal concentrations that can assumed to be of mainly anthropogenic origin (Cd, Cr, Cu, Ni, Pb, Zn) and therefore indicate some anthropogenic contamination have been compared to environmental quality guidelines with respect to threshold values for metals in sediments - EU directive 786/278/EEC and the Dutch intervention values from the Dutch Ministry of Housing, Spatial Planning and Environment (Table 8.3). The content of heavy metals along the approxi-

mately 40 cm sediment cores from five different locations is much below maximum concentrations permitted for metals in soils in the European Union. There is no significant difference among their concentration in the upper and in the lower segment of the cores. One exception is the Cd value of 3.2 mg/kg in the sediment core Prošće, indicating some anthropogenic contamination, probably from fertilizers, but a natural origin can not be excluded (Obelić et al., 2005, 2006; Horvatinčić et al., 2006).

A comparison of a gamma-spectrometric dating and analysis of **trace elements** have shown an absence of anthropogenic input into lake sediments during the last 130 years: in Prošće Lake (PR) between 1890 and 2003, in Gradinsko Lake (GR) between 1909 and 2003, in Kozjak Lake (K1) between 1895 and 2003, and Kaludjerovac Lake (KA) between 1870 and 2003. Sediments in the core of Kozjak Lake (K2) from the area with the pronounced eutrophication were deposited between 1986 or 1963 and 2003 predominately as the result of a rapid transport of land material into the lake from Rječica River.

Table 8.3: Summary of the statistical results of trace element content from five sediment cores of the Plitvice Lakes compared with maximum allowed concentrations in soils according to the 86/278/EEC directive (C_{EEC}) and Dutch intervention values (C_{DIV}). Analysis of trace elements were performed at the Department of Chemistry, Universitat Autónoma de Barcelona, Spain, Briansó (2006).

Concentration (C) Measured in Sediment					**Directive**	
		$\mathbf{C_{mean}}$	$\mathbf{C_{max}}$	$\mathbf{C_{min}}$	$\mathbf{C_{EEC}}$	$\mathbf{C_{DIV}}$
Al	g/kg	7.6	18.8	0.4		
B	mg/kg	7.7	23.4	0.8		
Ba	mg/kg	37.1	99.9	15.7		
Cd	mg/kg	1.7	3.2	0.4	1–3	12
Cr	mg/kg	11.9	35.2	0.7	100	380
Cu	mg/kg	8.2	23.9	1.8	50-140	190
Mn	mg/kg	106.2	297	5.4		
Ni	mg/kg	30.3	43.8	21.4	30-75	210
Sr	mg/kg	75.2	122	51.4		
P	mg/kg	494	1661	59		
Pb	mg/kg	14.8	39.4	1	50-300	530
Zn	mg/kg	41.2	106	3	150-300	720

Linear Alkylbenzene Sulphonates (LAS)

The distribution of LAS in lake sediments has been proved to be an excellent marker of the input of detergent chemicals via municipal wastewaters and was successfully applied to document usage patterns and wastewater treatment practices in a given area (e.g. Reiser et al., 1997; Ahel & Terzić, 2006). LAS concentrations were measured along the 10 cm long depth profile on the sediment cores of Prošće and Kozjak Lake, the two greatest lakes of the Plitvice Lakes. The measurements were performed at the Center for Marine and Environmental Research at the Rudjer Bošković Institute, Zagreb, Croatia.

The chemical and gamma-spectrometric results indicate an increasing recent anthropogenic contamination by the LAS in Kozjak Lake. The highest LAS concentrations were found in the upper part (4600 ng/g) down to 2-3 cm depth (1800 ng/g). This upper part of the sediment was deposited between 2000 and 2003. Between a depth of 2-3 cm and 10 cm, the LAS concentrations continuously decrease down to around 300 ng/g. This segment of the core was deposited between 1981 and 2000. Similar as in Kozjak Lake, in Prošće Lake an increase of LAS in the upper 3 cm can be observed (from 300 ng/g to 1500 ng/g), which was deposited between 2001 and 2003. Between 2-3 cm and 10 cm the LAS concentration decreases from 300 ng/g to 50 ng/g. This part of the sediment core was deposited between 1980 and 2001.

The maximum LAS concentrations of Kozjak Lake largely exceeds the concentration in Prošće Lake. The elevated concentrations in the upper layers in Kozjak Lake are most probably a result of defects in the sewerage system from tourist accommodations and release of LAS through untreated wastewaters.

Chapter 9

Summary, Conclusion and Outlook

In the present study an integrative approach was applied to investigate karst water and lake sediments on a transboundary aquifer between Croatia and Bosnia-Herzegovina. Isotope-hydrological, geochemical and geochronological methods were applied.

Tracing Precipitation and Groundwater Flow Paths

Deuterium in precipitation and regional wind directions have shown predominantly continental (80%) and less Mediterranean influence (20%) in the Plitvice Lakes area. Stable isotope composition (^{2}H and ^{18}O) in spring and surface waters have shown that groundwater infiltrates in two areas in Croatia and flows towards Una River feeding springs in Bosnia-Herzegovina. The first infiltration area comprises Korana River at the outflow of the Plitvice Lakes, Prijeboj, Krbavsko polje and Koreničko polje. The other infiltration area is situated more in the south around Lapačko polje and the municipality Mazin. Both results were also observed with dye experiments performed between 1973 and 1989. The hydraulic connection between swallow-holes in the Korana River bed and the Bosnian springs Klokot and Privilica near Bihać was suggested after evaluating time series of deuterium. Unfortunately, on this groundwater flow path the abandoned military airport Željava presents a great potential pollution source for the springs, with land mines layed during the last war events in this region (1991-1995).

Water Balance of the Plitvice Lakes

The groundwater flowing from the Korana limestone canyon into the karst aquifer is an important factor in the Plitvice Lakes water balance. In April 2003 after the snow melting, 8.48 Mio. m^3 reached the outflow of the Plitvice Lakes and there was no water loss from the river bed. However, in September 2004, 2.42 Mio. m^3 of 3.71 Mio. m^3 of water coming from the lakes (corresponding to 65%) disappeared in swallow-holes. In the water balance calculations the lake volume, spring and river contributions, precipitation, mixing of lake waters and their tributaries, evaporation, pumping and stratification of lakes were considered. In spring, after the snow melt, the lakes contain 22.95 Mio. m^3 water, whereas after the dry summer months a volume of 22.37 Mio. m^3 was calculated. The Plitvice Lakes are dimictic lakes which undergo stratification in summer and mix in autumn and spring. In September 2004 the thermocline was determined to be at a depth of 10-15 m for Prošće Lake and at 15-18 m in Kozjak Lake. Only the water volume above the thermocline can be involved in the evaporation process. Deuterium enrichment along the lake chain allowed the calculation of evaporation rates for both months: in September 0.159% of water above the thermocline evaporated (39.4 mm). In April the stratification was not developed and less than 0.08% of the whole lake water volume could evaporate (25.9 mm).

Observation of water levels in Kozjak Lake (for the years 2003 and 2004) together with its discharge have shown that increasing pumping rates from 0.06 m^3/s to 0.5 m^3/s would lower the lake water level by less than 10 cm. This means that increasing the pumping rates would not significantly change the hydrological circumstances influencing the tufa growth in the lakes.

Mean Residence Time (MRT) of Water and Karst Storage Capacity

The storage capacity of karst aquifers in the study area was estimated using measured spring discharge data and modeled MRTs for ten springs. To obtain MRTs a multi-tracer lumped parameter modeling approach was applied using the model code "Lumpy". Time series of stable isotopes (^2H and ^{18}O) and tritium (^3H) were used with monthly resolution as well as chlorofluorocarbons (CFCs), sulfur hexafluorid (SF_6) and noble

gases (He, Ne) from samplings campaigns in November 2003 and July 2004. The two campaigns were modeled separately, because they present two different hydrological states: a high discharge state in the rainy autumn and the base flow conditions with low discharge in summer. Using the multi-tracer approach, two components of the groundwater flow could be distinguished: the quick flow in the conduit network with a MRT up to 0.5 years and the slow component in the fissured-porous aquifer with a MRT up to 28 years.

It could be shown that groundwater dating with $^{3}H/^{3}He$ using only the $^{3}He/^{4}He$ ratio and helium and neon concentrations reveals non-unique results owing to fractionation of excess air and possible gas loss. For this reason, in karst studies also the heavy noble gases argon, krypton, xenon should be measured beside the light noble gases helium and neon. Furthermore, it can be concluded that the complexity of the karst system requires a multi-tracer approach, since one environmental trace substance alone leaves too much ambiguity in interpretation. Using the modeled MRTs and measured discharge of each spring, mean storage capacities could be obtained: up to 40 Mio. m^3 in the conduit network and up to 670 Mio. m^3 in the fissured-porous aquifer. However, only for three springs of the Plitvice Lakes (Bijela Rijeka, Crna Rijeka, Plitvica) long time discharge measurements exist, although interrupted during the war events in this area. For other springs there are only a minimum and maximum discharge known for the time before the war events.

Chronology of Anthropogenic Input in Lake Sediments

In the Plitvice Lakes National Park in last decades the process of eutrophication increased in some of the lakes in the last decades. Lake sediments store information about environmental contaminants, such as trace elements (heavy metals) and detergent-derived linear alkylbenzene sulphonates (LAS), which are important anthropogenic factors influencing the process of eutrophication. To establish a history of their input into the undisturbed sediments from the lakes Prošće (PR), Gradinsko (GR), Kozjak (K1, K2) and Kaludjerovac (KA) were obtained by scuba diving and dated with ^{137}Cs and ^{210}Pb method. A gamma-spectrometric age-dating proved to be a powerful tool to

establish a sediment chronology, although not applicable to every core site (K2). The most reliable dating model in this study is the ^{210}Pb CF (constant flux) model. The great lakes (PR, K1) are characterized by slower sedimentation rates than the small lakes (GR, KA). For the lakes PR and K1 the values obtained with anthropogenic nuclide ^{137}Cs ranged between 0.54 and 0.92 kg/(m^2 yr) and for ^{210}Pb 1.3 and 0.8 kg/(m^2 yr), respectively. In the small lakes GR and KA the higher sedimentation rates for both nuclides were obtained: 1.4 and 1.8 kg/(m^2 yr) for ^{137}Cs and 2.6 and 4.4 kg/(m^2 yr) for ^{210}Pb, respectively. Probably the most striking dating result is that in the small lakes Gradinsko and Kaludjerovac Lake a smaller sedimentation rates are obtained for ^{137}Cs than for $^{210}\mathrm{Pb}_{\mathrm{exc}}$. In contrast, sedimentation rates in the larger lakes Prošće and Kozjak (K1) give similar values for both nuclides. This finding could be an indication that sedimentation rates changed in the smaller lakes during the recent decades, whereas they remained constant in the large lakes.

Trace element in sediments mainly from anthropogenic origin (Cd, Cr, Cu, Ni, Pb and Zn) are much below the concentration limits for metals in soil in the European Union. Detergent-derived linear alkylbenzene sulphonates (LAS) in the upper 2-3 cm of Kozjak Lake show strong increasing trend since the year 2000. It could be caused by the defects in the sewerage system from the hotels situated above Kozjak Lake. The occurrence of LAS suggests that waste waters containing those chemical caused by the defects in sewerage system from the hotels situated above Lake Kozjak contribute to eutrophication.

Outlook

This study was able to determine the groundwater flow paths in the aquifer, water balance, mean residence times, aquifer storage capacities as well as the chronology of the anthropogenic input into the lake sediments. It also showed that these settings still pose a challenge in the interpretation of individual findings due to the karst system heterogeneities and the lack of quantitative data. Further research should focus on following issues:

- To quantify heterogeneities and to understand local flow dynamics, more tracer

experiments should be conducted in the study area.

- Long-term monitoring networks are needed to record spring and lake discharge and environmental tracers. This would enable the MRT modeling under unsteady conditions and allow a more realistic volumetric estimation of the freshwater resources.

- To improve the reliability of $^{3}H/^{3}He$ ages also heavy noble gases argon, krypton, xenon should be measured. This allows conclusions about the recharge conditions of infiltrated water including altitude, temperature, excess air, and its fractionation.

- Elevated concentrations of detergent derived chemicals (LAS) in Kozjak Lake are probably caused by defects in the system from the hotels situated above this lake in the last decades. Recently the sewerage system was repaired and new measurements of the uppermost sediment layer should be done in the near future in order to check, if these measures helped to reduce the input of detergent-derived chemicals or if their concentration still increase.

Acknowledgements

The presented work would not exist without the help of many people to whom I would like to express my gratitude.

First, I would like to kindly acknowledge Prof. Hans-Joachim Kümpel for his advice, openness and for strongly supporting me during the project and this thesis. Also thanks to Prof. Barbara Reichert, who largely contributed to the success of this doctoral research. I am indebted to both for their commitment and supervision of this dissertation.

I'm especially grateful to Axel Suckow not only for accompanying the EU project into which my work was embedded but for all "isotopic" conversations, for his strong engagement in spite of the distance between Vienna and Hannover, also to his family, who shared him with me during several weekends... Axel, thank you for your patience, numerous fruitful discussions, inspiring me in an unconventional way of scientific thinking and for invested time and effort to provide detailed comments on this thesis.

I would also like to thank to Prof. Manfred Frechen for his suggestions, an "open door" at any time and for revising the manuscript. Also my colleagues from Geochronology and Isotope Hydrology Section of the GGA-Institut are warmly appreciated for performing laboratory measurements, for encouraging me and for shared pauses at the round table.

Thanks a lot to Thomas Himmelsbach (Section for groundwater protection and groundwater quality of the Federal Institute for Geosciences and Natural Resources in Hannover), to Werner Aeschbach-Hertig (Institut of Environmental Physics, Research Group Groundwater and Paleoclimate of University of Heidelberg), Stephan Weise and Karsten Osenbrück (Isotope Hydrology Department of the Umweltforschungszentrum Leipzig-Halle), Manfred Gröning (Isotope Hydrology Department of IAEA) for their comments and discussions and positive criticism, improving this work. Acknowledgments go also to Jürgen Sültenfuß of the Institute of Environmental Physics, University of Bremen, and Harald Oster, Spurenstofflabor Wachenheim. I hope, discussions will

continue...

My sincere gratitude go to Josip Rubinić (University of Rijeka, Croatia) for his enthusiasm dedicated the challenging questions of the Plitvice Lakes system and exchange of ideas. His work has been an inspiration for me.

I would also like to warmly acknowledge my ANTHROPOL.PROT project colleagues for cooperation and very fruitful and enjoyable work: Bogomil Obelić, Nada Horvatinčić, Ines Krajcar Bronić, Jadranka Barešić, Ahel Terzić, Sanja and Janislav Kapelj. Thanks goes also to Neven Miošić and Hazim Hrvatović, José Luis Briansó, Nejra Džankić, Halid Makić and Asmir Budimlić. My colleague Gordana Zwicker is appreciated for collecting water samples at the Plitvice Lakes and for always being helpful and cordial. Thanks also goes to Halid Merdanić and the staff of the Biotechnical Faculty in Bihać for collecting samples at the Una River area.

This research has profited from the encouragement, advice, support and friendship of Andrei Zschocke, Susanne Stadler, Hanna-Maria Rumpel, Ralf Gelfort, Jan Igel, Robert van Geldern, Gudrun Drewes, Thies Beilecke, Holger Preetz, Sanja Schah-Habdija, Dunja Dragojević-Kersten and Thorsten Fass. Thanks to all of you.

Last, but not least, I express my gratitude to my family for being understanding and supporting me during the most challenging times.

The project was funded by the European Union (INCO: International Scientific Cooperation Projects, contract number ICA2-CT-2002-10009 - ANTHROPOL.PROT).

Bibliography

Aeschbach-Hertig, W., Schlosser, P., Stute, M., Simpson, J., Ludin, A., & Clark, J. F., 1998. A H-3/He-3 study of groundwater flow in a fractured rock aquifer, *Ground Water*, **36**, 661–670.

Aeschbach-Hertig, W., Peeters, F., Beyerle, U., & Kipfer, R., 2000. Palaeotemperature reconstruction from noble gases in ground water taking into account equilibration with entrapped air, *Nature*, **405**, 1040–1044.

Ahel, M. & Terzić, S., 2006. Molecular markers of anthropogenic influence on Plitvice Lakes, Croatia, Book of abstracts of the 11th World Lake Conference, Nairobi, Kenya, Oct. 31 - Nov. 4, 2005, p. 47.

Andrews, J. N., 1991. Noble gases and radioelements in groundwaters, In: Downing, R. A. & Wilkinson, W. B., eds., Applied Groundwater Hydrology, A British Perspective, Clarendon Press, Oxford, pp. 243-265.

ANTHROPOL.PROT, 2006. Final Report: Study of Anthropogenic Pollution after the War and Establishing of Measures for Protection of Plitvice National Park and Bihać Region, Contract No. ICA2-CT-2002-10009-ANTHROPOL.PROT., the 5th framework programme of the European Community for research, technological development and demonstration activities, INCO Copernicus-2, Bruxelles, http://www.irb.hr/en/research/projects/intl/euprojects/ICA2/.

Appleby, P. G. & Oldfield, F., 1992. Application of lead-210 to sedimentation studies, In: Ivanovich, M. & Harmon, R. S., eds., Uranium-series Disequilibrium: Application to Earth, Marine, and Environmental Studies, Clarendon Press, Oxford, pp. 731-783.

Bauer, S., Fulda, C., & Schäfer, W., 2001. A multi-tracer study in a shallow aquifer using age dating tracers ^{3}H, ^{85}Kr, CFC-113 and SF_6 - indication for retarded transport of CFC-113, *Journal of Hydrology*, **248**, 14–34.

Bayer, R., Schlosser, P., Bönisch, G., Rupp, H., Zaucker, F., & Zimmek, G., 1989. Performance and Blank Components of a Mass Spectrometric System for Routine Measurement of Helium Isotopes and Tritium by the ^{3}He Ingrowth Method, In: Sitzungsberichte der Heidelberger Akademie der Wissenschaften, Vol. 5, Springer-Verlag, pp. 241-279.

Beraković, M., 2005. Hidrološka istraživanja - bilanca voda Plitvičkih jezera, *Hrvatska vodoprivreda*, **156 (14)**, 59–63.

Bögli, A., 1980. *Karst hydrology and physical speleology*, Springer, Berlin, Heidelberg, New York, 292 p.

Bonacci, O., 1987. *Karst Hydrology With Special Reference to the Dinaric Karst*, Springer, Berlin, Heidelberg, New York, 184 p.

Božičević, S. & Biondić, B., 1999. The Plitvice Lakes, In: Drew, D. & Hötzl, H., eds., Karst Hydrogeology and Human Activities. Impacts, Consequences and Implications, A. A. Balkema, Rotterdam, pp. 174-178.

Briansó, J. L., 2006. Study of Anthropogenic Pollution after the War and Establishing of Measures for Protection of Plitvice National Park and Bihać Region, In: Final Report of ANTHROPOL.PROT, 2006, Bruxelles.

Bullister, J. L. . & Weiss, R. F., 1988. Determination of CFC_3F and CCl_2F_2 in seawater and air, *Deep Sea Res.*, **35**, 839–854.

Clark, I. D. & Fritz, P., 1997. *Environmental Isotopes in Hydrogeology*, Lewis Publishers, New York, 328 p.

Cook, P. G. & Herczeg, A. L., 2000. *Environmental Tracers in Subsurface Hydrology*, Kluwer Academic Publishers, Boston, 529 p.

Cook, P. G. & Solomon, D. K., 1995. Transport of atmospheric trace gases to the water table; implications for groundwater dating with chlorofluorocarbons and krypton 85, *Water Resources Research*, **31 (2)**, 263–270.

Cook, P. G. & Solomon, D. K., 1997. Recent advances in dating young groundwater: chlorofluorocarbons, $^3H/^3He$ and ^{85}Kr, *Journal of Hydrology*, **191 (1-4)**, 245–265.

Craig, H., 1961. Isotopic variations in natural waters, *Science*, **133 (1702-1703)**.

DHMZ, 1989. *Hidrološka studija sliva Plitvičkih jezera*, Republički hidrometeorološki zavod SR Hrvatske, (Meteorological and Hydrological Service of Croatia).

Doerfliger, N., Jeannin, P. Y., & Zwahlen, F., 1999. Water vulnerability assessment in karst environments: a new method of defining protection areas using a multi-attribute approach and GIS tools (EPIK method), *Environmental Geology*, **39 (2)**, 165–176.

Drew, D., 1999. Introduction, In: Drew, D. & Hötzl, H., eds., Karst Hydrogeology and Human Activities. Impacts, Consequences and Implications, A. A. Balkema, Rotterdam, pp. 3-12.

Džankić, N., Makić, H., & Budimlić, A., 2006. *Prirodni i antropogeni uticaj na kvalitet voda slivnog podrucja rijeke Une (Natural and anthropogenic effect on the quality of the waters in the catchment basin of the Una River)*, Grafičar, Bihać, 174 p.

Ekwurzel, B., Schlosser, P., Smethie, W. J., Plummer, N. L., Busenberg, E., Michel, R. L., Weppernig, R., & Stute, M., 1994. Dating of shallow groundwater: Comparison of the transient tracers $^3H/^3He$, chlorofluorocarbons, and ^{85}Kr, *Water Resources Research*, **30**, 1693–1708.

Ford, D. C. & Williams, P. W., 1989. *Karst geomorphology and hydrology*, Unwin Hyman Ltd., London, 601 p.

Froehlich, K., Gibson, J. J., & Aggarwal, P., 2002. Deuterium excess in precipitation and its climatological significance, In: Study of environmental change using isotope techniques, International Atomic Energy Agency, Vienna, pp. 54-65.

Gäbler, H. E. & Suckow, A., 2003. Chronology of anthropogenic heavy-metal fluxes and Pb isotope ratios derived from radiometrically dated lake sediments in Northern Germany, *Water, Air, and Soil Pollution*, **144**, 243–262.

Gat, J. R. & Gonfiantini, R., 1981. Stable Isotope Hydrology: Deuterium and Oxygen-18 in the Water Cycle, Technical Report Series No. 210, International Atomic Energy Agency, Vienna, 337 p.

Goldberg, E. D., 1963. Geochronology with ^{210}Pb, In: Radioactive dating, International Atomic Energy Agency, Vienna, pp. 121-131.

Gonfiantini, R., 1986. Environmental isotopes in lake studies, In: Fritz, P. & Fontes, J. Ch., eds., Handbook of Environmental Isotope Geochemistry, Vol 2, The Terrestrial Environment, B, Elsevier, Amsterdam, pp. 113-168.

Gunn, J., 2004. *Encyclopedia of caves and karst science*, Fitzroy Dearborn, New York, 902 p.

Heaton, T. H. E. & Vogel, J. C., 1981. Excess air in groundwater, *Journal of Hydrology*, **50**, 201–216.

Holocher, J., Peeters, F., Aeschbach-Hertig, W., Beyerle, U., Hofer, M., Brennwald, M., Kinzelbach, W., & Kipfer, R., 2002. Experimental investigations on the formation of excess air in quasi-saturated porous media, *Geochim Cosmochim Acta*, **66**, 4103–4117.

Horvatinčić, N., Krajcar Bronić, I., Pezdič, J., & Srdoč, D., 1986. The Distribution of Radioactive (^{3}H, ^{14}C) and Stable (^{2}H, ^{18}O) Isotopes in Precipitation, Surface and Groundwaters of NW Yugoslavia, *Nuclear Instruments and Methods in Physics Research*, **B17**, 550–553.

Horvatinčić, N., Ćalić, & Geyh, M. A., 2000. Interglacial Growth of Tufa in Croatia, *Quarternary Research*, **53**, 185–195.

Horvatinčić, N., Briansó, J. L., Obelić, B., Barešić, J., & Krajcar Bronić, I., 2006. Study of Pollution of the Plitvice Lakes by Water and Sediment Analyses, *Water, Air, & Soil Pollution*, **6 (5-6)**, 475–485.

Hötzl, H., 1998. Karst Groundwater, In: Käss, W., ed., Tracing Technique in Geohydrology, A. A. Balkema, Rotterdam, pp. 398-426.

IAEA/WMO, 2006. Global Network of Isotopes in Precipitation (the GNIP Database), http://isohis.iaea.org.

Ivanovich, M., 1992. The Phenomenon of Radioactivity, In: Ivanovich, M. & Harmon, R. S., eds., Uranium-series Disequilibrium: Aplications to Earth, Marine, and Environmental Studies, Clarendon Press, Oxford, pp. 1-33.

Kapelj, J., Kapelj, S., & Singer, D., 2006. Study of Anthropogenic Pollution after the War and Establishing of Measures for Protection of Plitvice National Park and Bihać Region, In: Final Report of ANTHROPOL.PROT, 2006.

Käss, W., Behrens, H., Rossi, P., & Moser, H., 1998. Tracers, In: Käss, W., ed., Tracing Technique in Geohydrology, A. A. Balkema, Rotterdam, pp. 17-315.

Kendall, C. & McDonnell, J. J., 1998. *Isotope Tracers in Catchment Hydrology*, Elsevier, Amsterdam, 839 p.

Kipfer, R., Aeschbach-Hertig, W., Peeters, F., & Stute, M., 2002. Noble Gases in Lakes and Ground Waters, In: Porcelli, D.P., Ballentine, C.J., & Wieler, R. eds., Noble gases in geochemistry and cosmochemistry, Reviews in Mineralogy and Geochemistry 47, pp. 615-700.

Klimchouk, A. B., 2000. The Formation of Epikarst and its Role in Vadose Speleogenesis, In: Klimchouk, A. B., Ford, D. C. Palmer, A. N., & Dreybrodt, W., eds., Speleogenesis. Evolution of Karst Aquifers, National Speleological Society, pp. 91-99.

Kovács, A., 2003. *Geometry and hydraulic parameters of karst aquifers: A hydrodynamic modeling approach*, Ph.D. thesis, Université de Neuchâtel (Suisse).

Krajcar Bronić, I., Vreča, P., Horvatinčić, N., Barešić, J., & Obelić, B., 2006. Distribution of hydrogen, oxygen and carbon isotopes in the atmosphere of Croatia and Slovenia, *Archives of Industrial Hygiene and Toxicology*, **57**, 23–29.

Krishnaswamy, S., Lal, D., Martin, J. M., & Meybeck, M., 1971. Geochronology of lake sediments, *Earth and Planetary Science Letters*, **11**, 407–414.

KWI, 1999. A Lexicon of Cave and Karst Terminology with Special Reference to Environmental Karst Hydrology, The Karst Water Institute, http://www.karstwaters.org/kwidata.htm.

Lucas, L. L. & Unterweger, M. P., 2000. Comprehensive Review and Critical Evaluation of the Half-Life of Tritium, *Journal of Research of the National Institute of Standards and Technology*, **105 (4)**, 541–549.

Maloszewski, P., 2006. Estimation of transport and system parameters in a karst aquifer using artificial and environmental tracer data, *Geophysical Research Abstracts*, **8 (02156)**, European Geosciences Union.

Maloszewski, P. & Zuber, A., 1996. Lumped parameter models for the interpretation of environmental tracer data, Manual on Mathematical Models in Isotope Hydrology. IAEA-TECDOC-910, International Atomic Energy Agency, Vienna, pp. 9-58.

Maloszewski, P., Rauert, W., Stichler, W., & Herrmann, A., 1983. Application of flow models in an alpine catchment area using tritium and deuterium data, *Journal of Hydrology*, **66 (1-4)**, 319–330.

Maloszewski, P., Rauert, W., Trimborn, P., Herrmann, A., & Rau, R., 1992. Isotope hydrological study of mean transit times in an alpine catchment basin (Wimbach, Germany), *Journal of Hydrology*, **140**, 343–360.

Maloszewski, P., Stichler, W., Zuber, A., & Rank, D., 2002. Identifying the flow systems in a karstic-fissured-porous aquifer, the Schneealpe, Austria, by modelling of environmental $^{18}O/^{3}H$ isotopes, *Journal of Hydrology*, **256 (1-2)**, 48–59.

Mangin, A., 1975. Contribution à l'étude hydrodynamique des aquifères karstiques, *Ann. Spéléol*, **29 (3)**, 283–332.

Miošić, N., Hrvatović, H., Brkić, E., & Samardžić, N., 2006. Study of Anthropogenic Pollution after the War and Establishing of Measures for Protection of Plitvice National Park and Bihać Region, In: Final Report of ANTHROPOL.PROT, 2006, Bruxelles.

Mook, W. G., 2001. UNESCO/IAEA Series on Environmental Isotopes in the Hydrological Cycle - Principles and Applications, International Atomic Energy Agency, Vienna, www.iaea.org/programmes/ripc/ih/volumes/volumes.htm.

Nativ, R., Gŭnay, G., Hötzl, H., Reichert, B., Solomon, D. K., & Tezcan, L., 1999. Separation of groundwater-flow components in a karstified aquifer using environmental tracers, *Applied Geochemistry*, **14**, 1001–1014.

NOAA, 2006. Tech. rep., National Oceanic and Atmospheric Administration, Global Monitoring Division, http://www.cmdl.noaa.gov/infodata/.

Obelić, B., Horvatinčić, N., Barešić, J., Briansó, J. L., Babinka, S., & Suckow, A., 2005. Anthropogenic pollution in karst lake sediments (Croatia), In: Özkul, M., Yagiz, S., & Jones, B., eds., Proceedings of the International Travertine Symposium and Technologies Exhibition, Pamukkale University, Denizli (Turkey), Sept. 21-24, 2005, Kozan Ofset Matbaacilik San. ve Tic. Ltd. Sti. Ankara, pp. 188-196.

Obelić, M., Horvatinčić, N., Krajcar Bronić, I., & Barešić, J., 2006. Study of Anthropogenic Pollution after the War and Establishing of Measures for Protection of Plitvice National Park and Bihać Region, In: Final Report of ANTHROPOL.PROT, 2006, Bruxelles.

Oster, H., 1994. *Datierung von Grundwasser mittels FCKW: Voraussetzungen, Möglichkeiten und Grenzen*, Ph.D. thesis, Institut für Umweltphysik, Universität Heidelberg.

Oster, H., Sonntag, C., & Munnich, K. O., 1996. Groundwater age dating with chlorofluorocarbons, *Water Resources Research*, **32**, 2989–3001.

Ozyurt, N. N. & Bayari, C. S., 2005. LUMPED Unsteady: a Visual Basic® code of unsteady-state lumped-parameter models for mean residence time analyses of groundwater systems, *Computers & Geosciences*, **31**, 329–341.

Pennington, W., Cambray, R. S., & Fischer, E. M., 1973. Observations on lake sediments using fallout Cs-137 as a tracer, *Nature*, **242**, 324–326.

Petrik, M., 1958. *Prinosi hidrologiji Plitvica*, Poljoprivredni nakladni zavod, Zagreb, Croatia.

Plummer, L. N. & Busenberg, E., 1999. Chlorofluorocarbons, In: Cook, P. G. & Herczeg, A. L., eds., Environmental Tracers in Subsurface Hydrology, Kluwer Academic Publishers, Boston, pp. 441-478.

Plummer, L. N., Busenberg, E., Böhlke, J. K., Nelms, D. L., Michel, R. L., & Schlosser, P., 2001. Groundwater residence times in Shenandoah National Park, Blue Ridge Mountains, Virginia, USA: a multi-tracer approach, *Chemical Geology*, **179 (1-4)**, 93–111.

Poreda, R. J., Cerling, T. E., & Solomon, D. K., 1988. Tritium and helium isotopes as hydrologic tracers in a shallow unconfined aquifer, *Journal of Hydrology*, **103 (1-9)**.

Rank, D., Völkl, G., Maloszewski, P., & Stichler, W., 1992. Flow dynamics in an Alpine karst masif studies by means of environmental isotopes, In: Isotope Techniques in Water Resources Development, International Atomic Energy Agency, Vienna, pp. 327-343.

Reiser, R., Toljander, H., Albrecht, A., & Giger, W., 1997. Alkylbenzenesulfonates in recent lake sediments as molecular markers for the environmental behavior of detergent-derived chemicals, In: Eganhouse, R. P. ed., Molecular markers in environmental geochemistry, American Chemical Society Symposium Series, Washington DC, 13, pp. 196-212.

Ritson, P. I., Esser, B. K., Niemeyer, S., & Flegal, R. A., 1994. Lead isotopic determination of historical sources of lead to Lake Erie, North America, *Geochimica et Cosmochimica Acta*, **58**, 3297–3305.

Rowland, F. S., 1990. Stratospheric Ozone Depletion by Chlorofluorocarbons, *Ambio*, **19**, 281–292.

Rozanski, K., Araguas Araguas, L., & Gonfiantini, R., 1993. Isotopic patterns in modern global precipitation, In: Swart, P. K., Lohmann, K. C., McKenzie, J.A. & Savin, S., eds., Climate change in continental isotopic records, *AGU Monograph*, **78**, 1–36.

Schell, W. R. & Barnes, R. S., 1986. Environmental isotope and anthropogenic tracers of recent lake sedimentation., In: Fritz, P. & Fontes, J. Ch., eds., Handbook of Environmental Isotope Geochemistry, Vol 2, The Terrestrial Environment, B, Elsevier, Amsterdam, pp. 169-206.

Schlosser, P., Stute, M., Doerr, H., Sonntag, C., & Muennich, K. O., 1988. Tritium/^{3}He dating of shallow groundwater, *Earth and Planetary Science Letters*, **89 (3-4)**, 353–362.

Schmid, S. M., Fügenschuh, B., Matenco, L., Schuster, R., Tischler, M., & Ustaszewski, K., 2006. The Alps-Carpathians-Dinarides-connection: a compilation of tectonic units, Proceedings of the 18th congress of the Carpathian-Balkan Geological Association, Belgrade, serbia, Sept. 03.- 06. 2005, National Committee of Serbia for the International Hydrological Programme of Unesco, Belgrade, pp 535-538.

Solomon, D. K. & Cook, P. G., 1999. ^{3}H and ^{3}He, In: Cook, P. G. & Herczeg, A. L., eds., Environmental Tracers in Subsurface Hydrology, Kluwer Academic Publishers, Boston, pp. 397-424.

Srdoč, D., Horvatinčić, N., Obelić, B., Krajcar, I., & Sliepčević, A., 1985. Calcite deposition processes in karst waters with special emphasis on the Plitvice Lakes, Yugoslavia, *Carsus Iugoslaviae*, **11**, 101–204.

Srdoč, D., Horvatinčić, N., Ahel, M., Giger, W., Schaffner, C., Krajcar Bronić, I., Petricioli, D., Pezdič, J., Marčenko, E., & Plenković-Moraj, A., 1992. Anthropogenic influence on the ^{14}C activity and other constituents of recent lake sediments: a case study, *Radiocarbon*, **34 (3)**, 585–592.

Stute, M., M., F., Frischkorn, H., A., S., F., C. J., Schlosser, P., Broecker, W. S., & Bonani, G., 1995. Cooling of tropical Brazil (5°C) during the Last Glacial Maximum, *Science*, **269**, 379–383.

Suckow, A., 2006. Manual for Labdata: A Database and Laboratory Management System with some Special Features for Isotope Laboratories, Tech. rep., GGA-Institut/IAEA (in preparation).

Suckow, A. & Dumke, I., 2001. A database system for geochemical, isotope hydrological, and geochronological laboratories, *Radiocarbon*, **43 (2)**, 305–317.

Suckow, A. & Gäbler, H. E., 1997. Radiometric dating and heavy metal content of a recent sediment core from Lake Trenntsee in Northeastern Germany, *Isotopes in Environmental and Health Science*, **33 (4)**, 367–376.

Tari, V., 2002. Evolution of the northern and western Dinarides: a tectonostratigraphic approach, In: Berotti, G., Schulmann, K. & Cloetingh, S. A. P. L., eds., Continental collision and the tectono-sedimentary evolution of forelands, EGU Stephan Mueller Special Publication Series 1, pp. 223-236.

Tolstikhin, I. N. & Kamensky, I. L., 1969. Determination of groundwater age by the T-3He method, *Geochem. Int.*, **6**, 810–811.

Volk, C. M., Elkins, J. W., Fahey, D. W., Dutton, G. S., Gilligan, J. M., Loewenstein, M., Podolske, J. R., Chan, K. R., & Gunson, M. R., 1997. Evaluation of source gas lifetimes from stratospheric observations, *Journal of Geophysical Research*, **102 (D21)**, 25543–25564.

Wakeham, S. G., Schaffner, C., & Giger, W., 1980. Polycyclyc aromatic hydrocabons in recent lake sediments, I. Compounds having anthropogenic origins, *Geochimica et Cosmochimica Acta*, **44**, 403–413.

Wakeham, S. G., Schaffner, C., & Giger, W., 1980. Polycyclyc aromatic hydrocabons in recent lake sediments, II. Compounds deriving from biogenic precursors during early diagenesis, *Geochimica et Cosmochimica Acta*, **44**, 415–429.

Walling, D. E. & Quine, T. A., 1992. The use of caesium-137 measurements in soil erosion surveys. Erosion and Sediment Transport Monitoring Programmes in River Basins, *IAHS Publications*, **210 (143-152)**.

Wetzel, R. G. & Likens, G. E., 1991. *Limnological Analysis*, Springer, Berlin, Heidelberg, New York, 429 p.

Zwicker, G. & Rubinić, J., 2005. Water Level Fluctations as an Indicator of Tufa Barrier Growth Dynamics in the Plitvice Lakes, *RMZ - Materials and Geoenvironment*, **51 (1)**, 161–163.

Zwicker, G., Rubinić, J., & Kompar, D., 2006. Hydrology of Plitvice Lakes and the Upper Korana - Corellation and Trends, In: Bruk, S. & Petković, T., eds., Conference abstracts of the XXIII Conference of the Danubian Countries on the Hydrological Forecasting and Hydrological Bases of Water Management, Belgrade, Serbia, Aug. 28-31, 2006, National Committee of Serbia for the International Hydrological Programme of UNESCO, p. 67.

Appendix

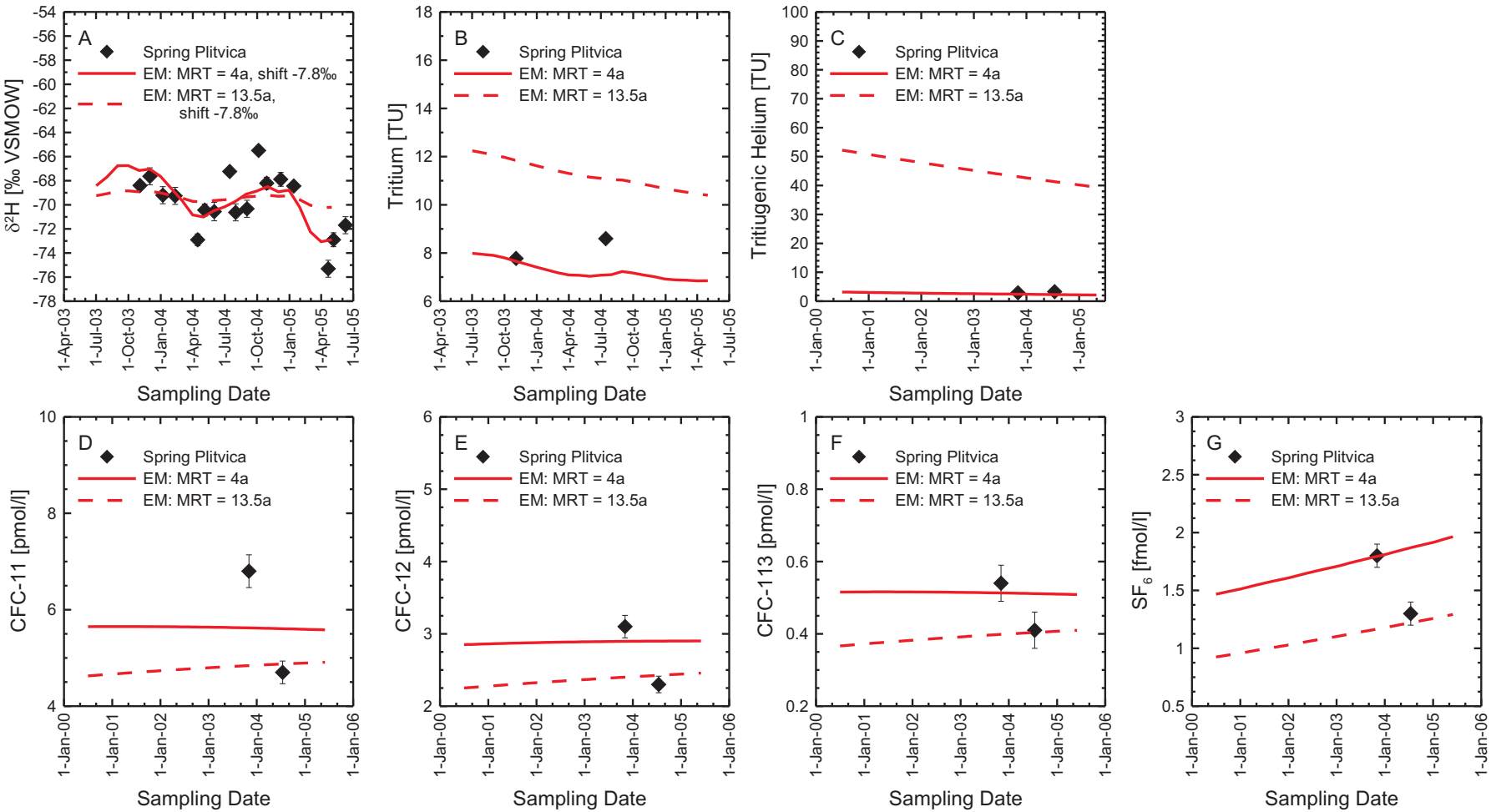

Fig. A.1: Results of lumped parameter models for the spring Plitvica for deuterium (A); tritium (B); noble gases (C); CFC-11 (D); CFC-12 (E); CFC-113 (F); and SF_6 (G).

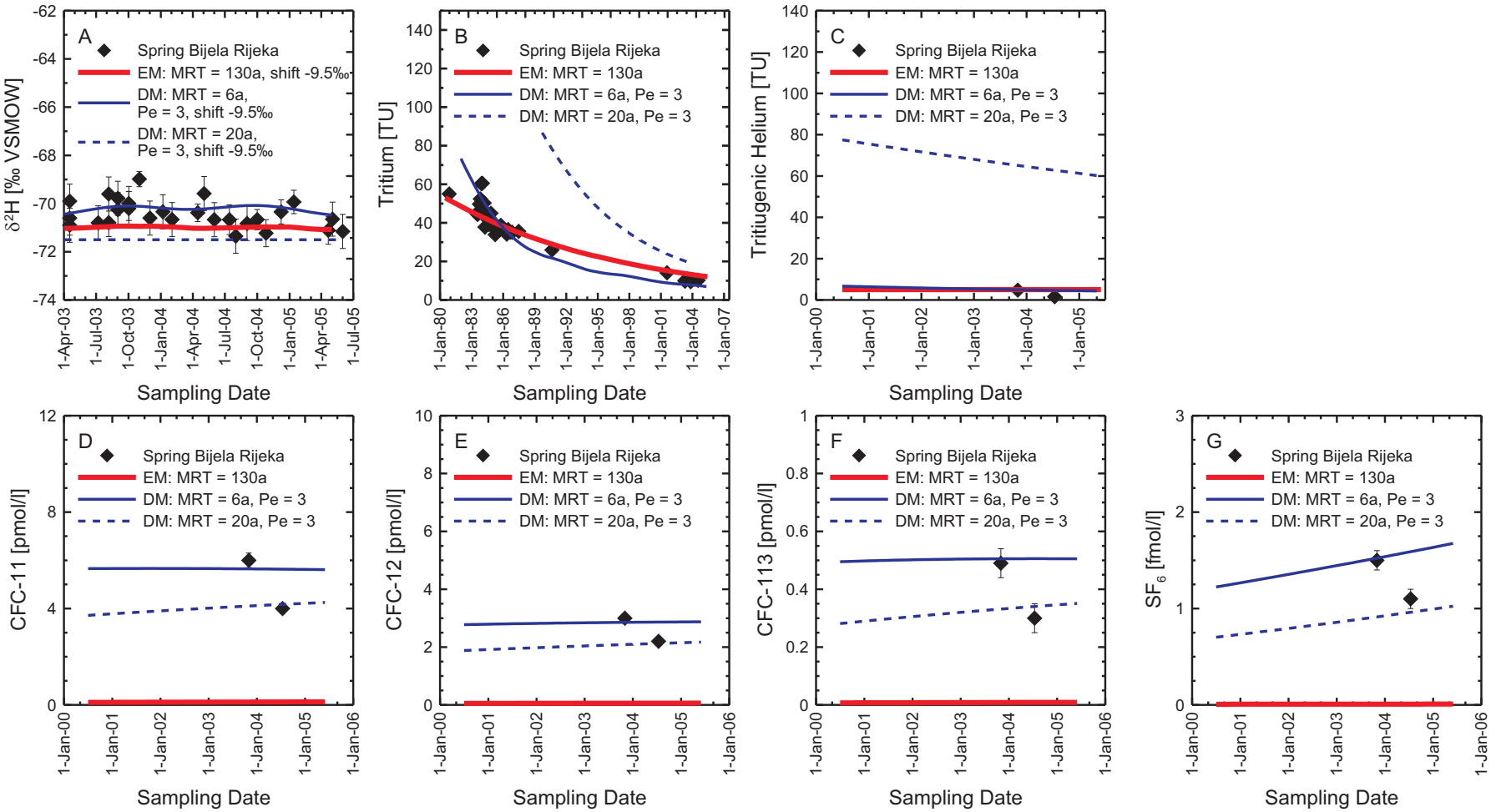

Fig. A.2: Results of lumped parameter modeling models for the spring Bijela Rijeka for deuterium (A); tritium (B); noble gases (C); CFC-11 (D); CFC-12 (E); CFC-113 (F); and SF_6 (G).

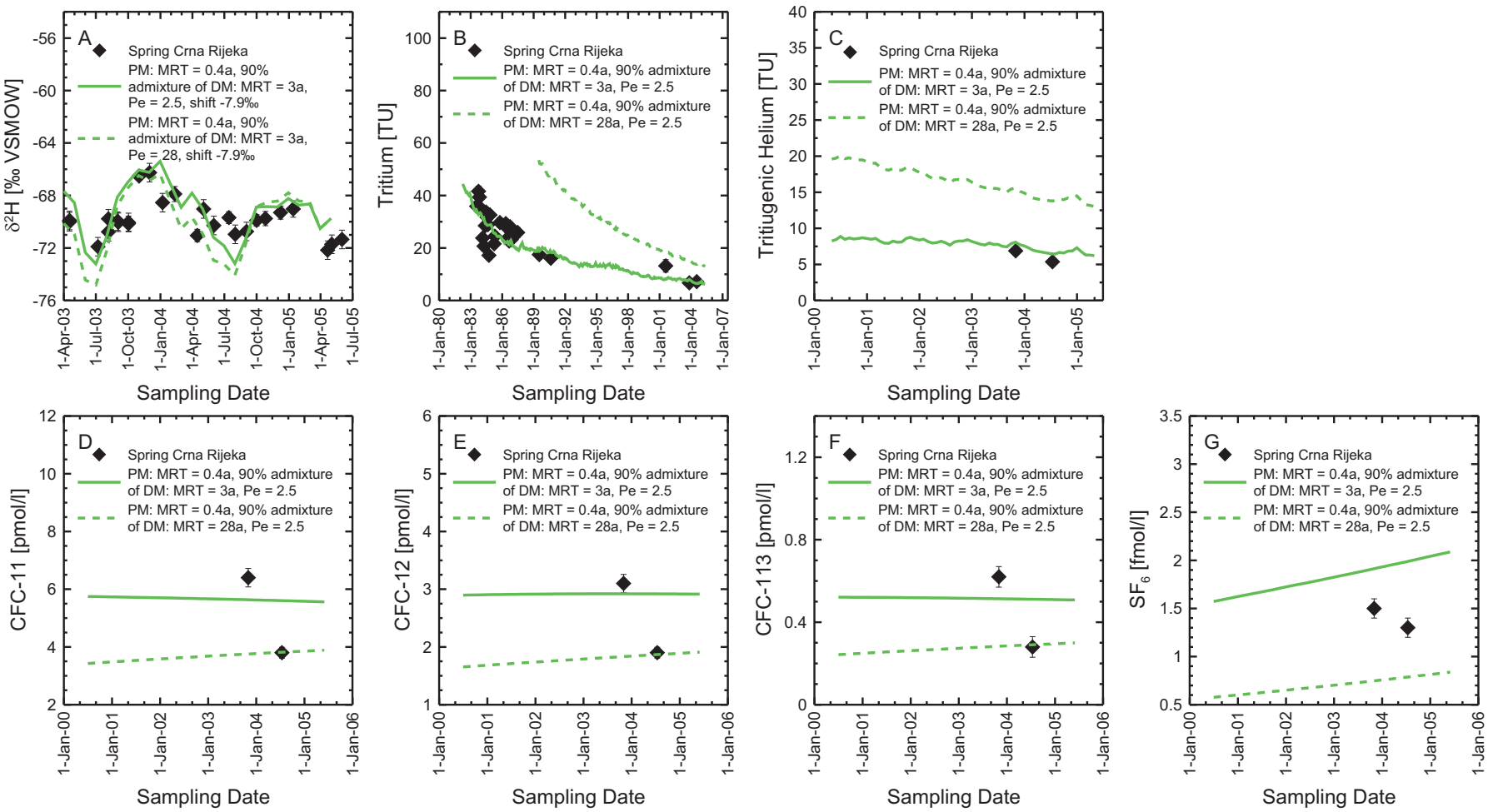

Fig. A.3: Results of lumped parameter models for the spring Crna Rijeka for deuterium (A); tritium (B); noble gases (C); CFC-11 (D); CFC-12 (E); CFC-113 (F); and SF_6 (G).

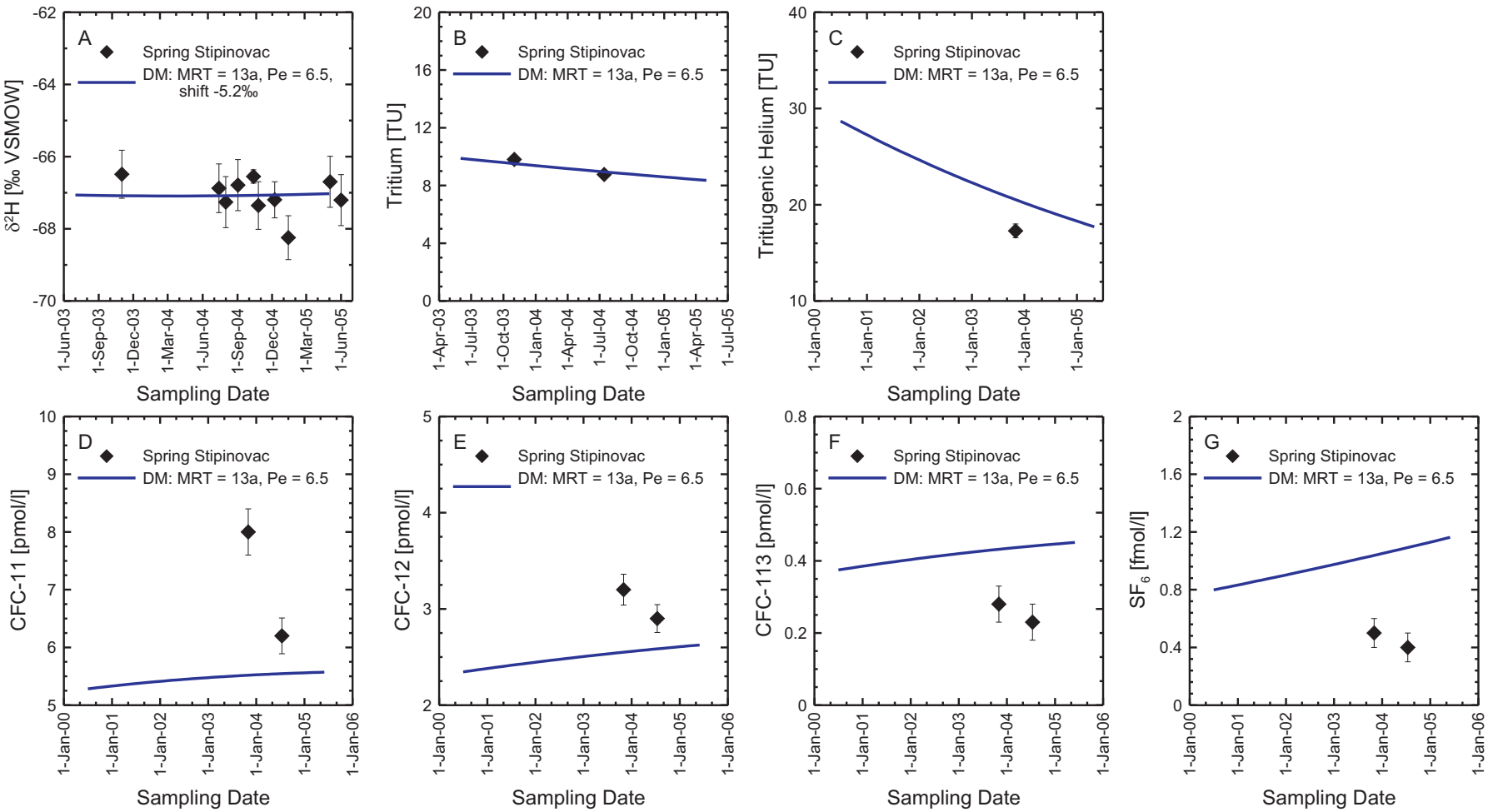

Fig. A.4: Results of lumped parameter models for the spring Stipinovac for deuterium (A); tritium (B); noble gases (C); CFC-11 (D); CFC-12 (E); CFC-113 (F); and SF_6 (G).

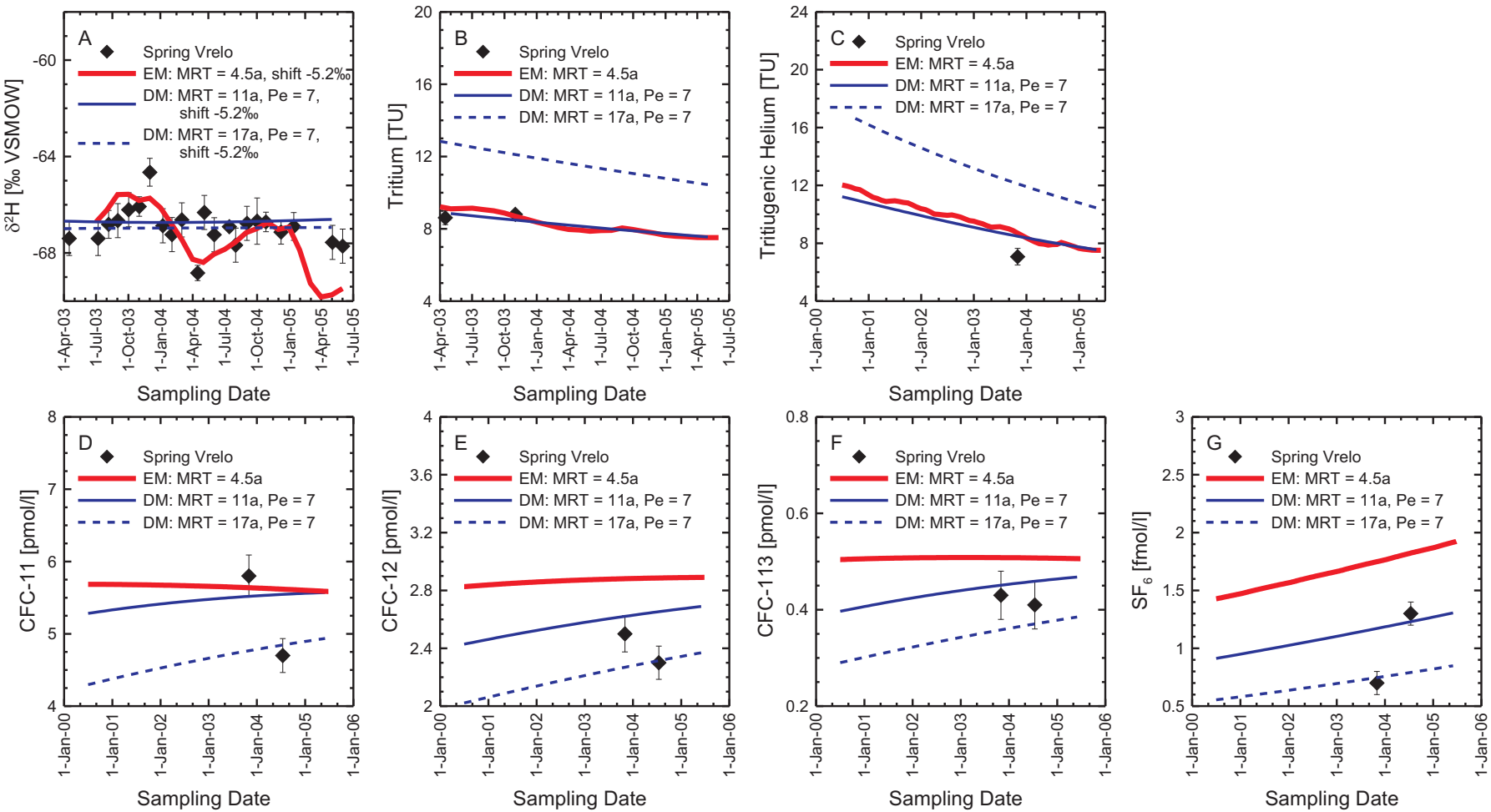

Fig. A.5: Results of lumped parameter modeling for the spring Vrelo for deuterium (A); tritium (B); noble gases (C); CFC-11 (D); CFC-12 (E); CFC-113 (F); and SF_6 (G).

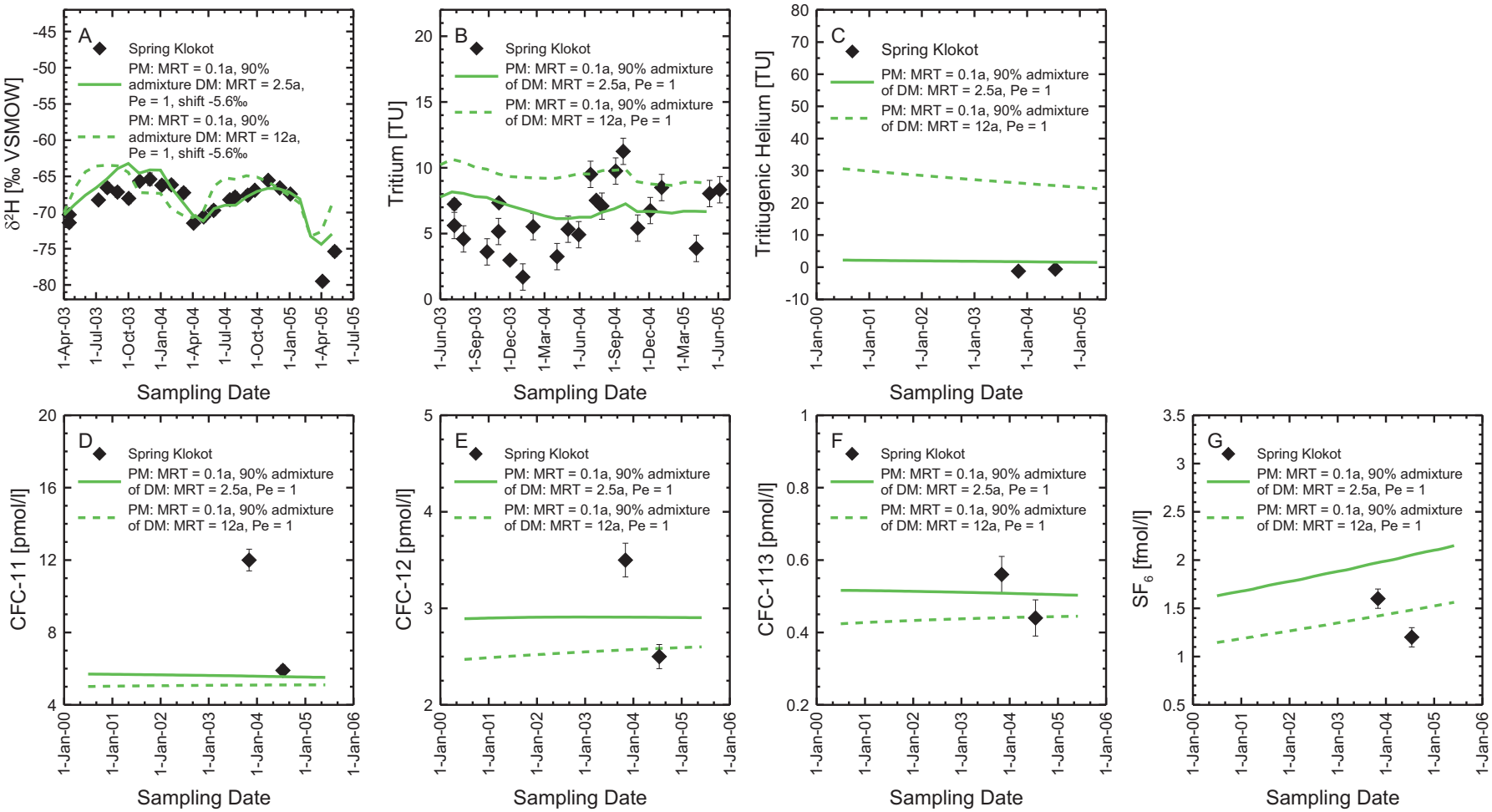

Fig. A.6: Results of lumped parameter models for the spring Klokot for deuterium (A); tritium (B); noble gases (C); CFC-11 (D); CFC-12 (E); CFC-113 (F); and SF_6 (G).

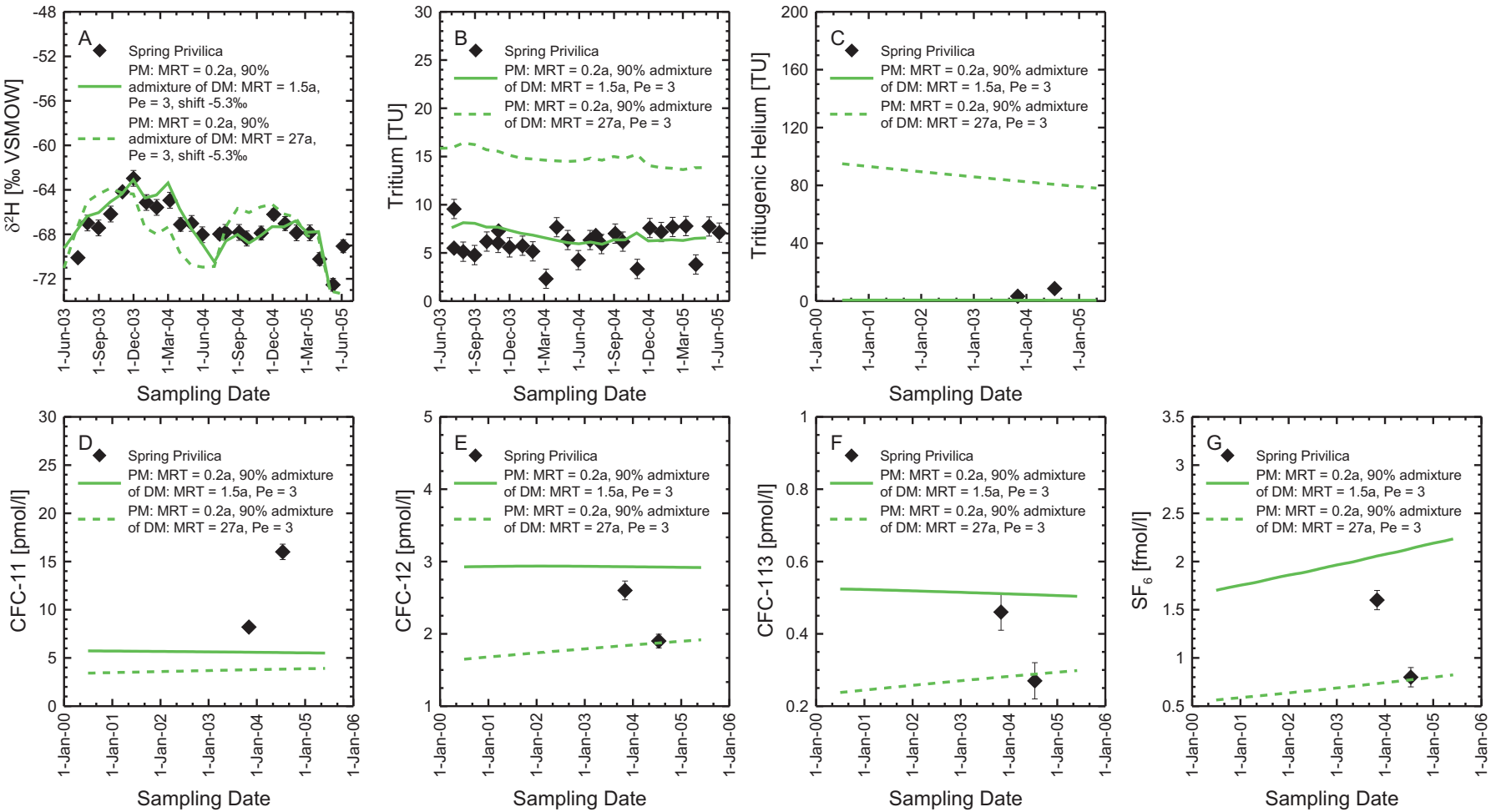

Fig. A.7: Results of lumped parameter models for the spring Privilica for deuterium (A); tritium (B); noble gases (C); CFC-11 (D); CFC-12 (E); CFC-113 (F); and SF_6 (G).

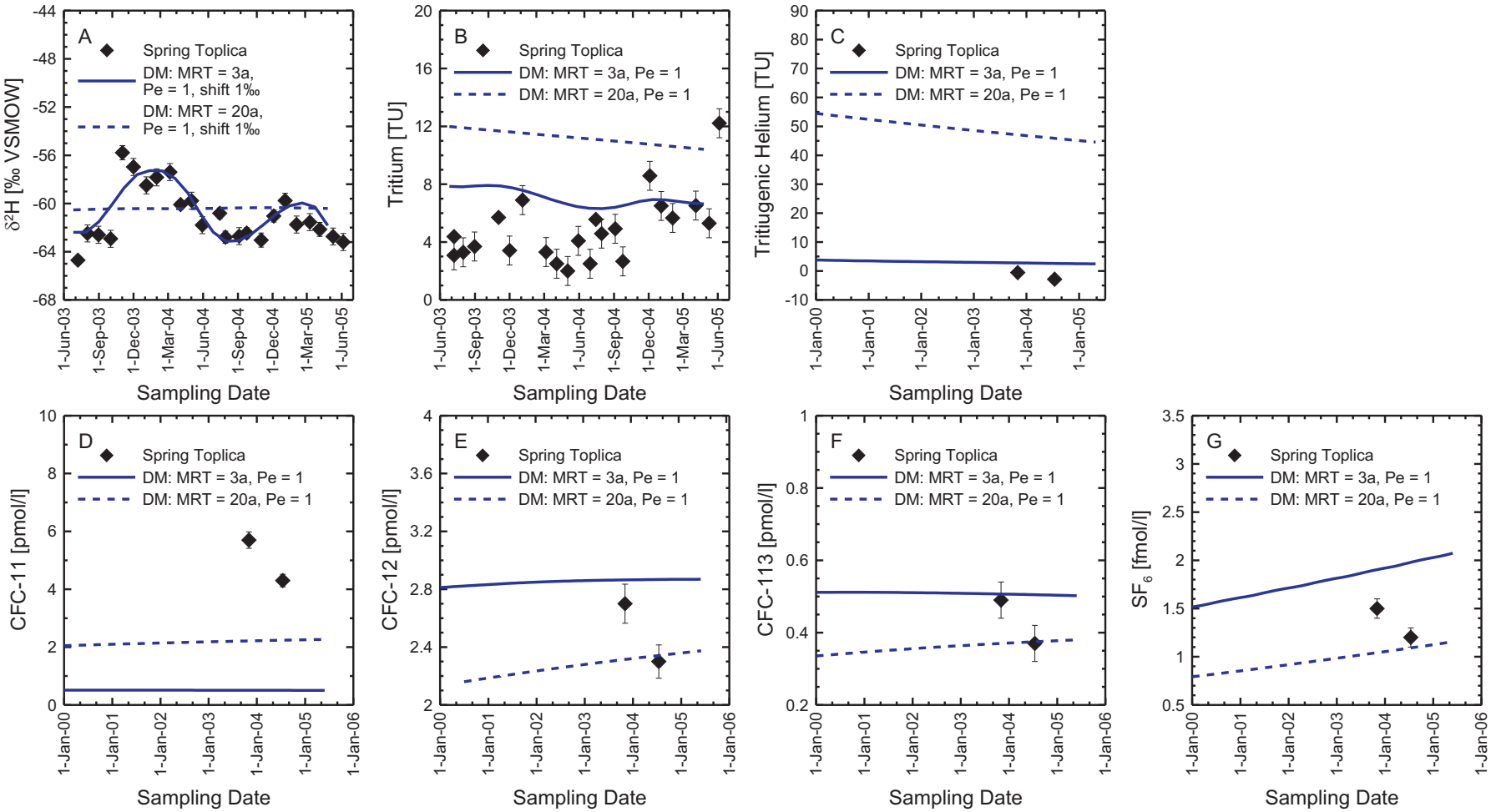

Fig. A.8: Results of lumped parameter models for the spring Toplica for deuterium (A); tritium (B); noble gases (C); CFC-11 (D); CFC-12 (E); CFC-113 (F); and SF_6 (G).

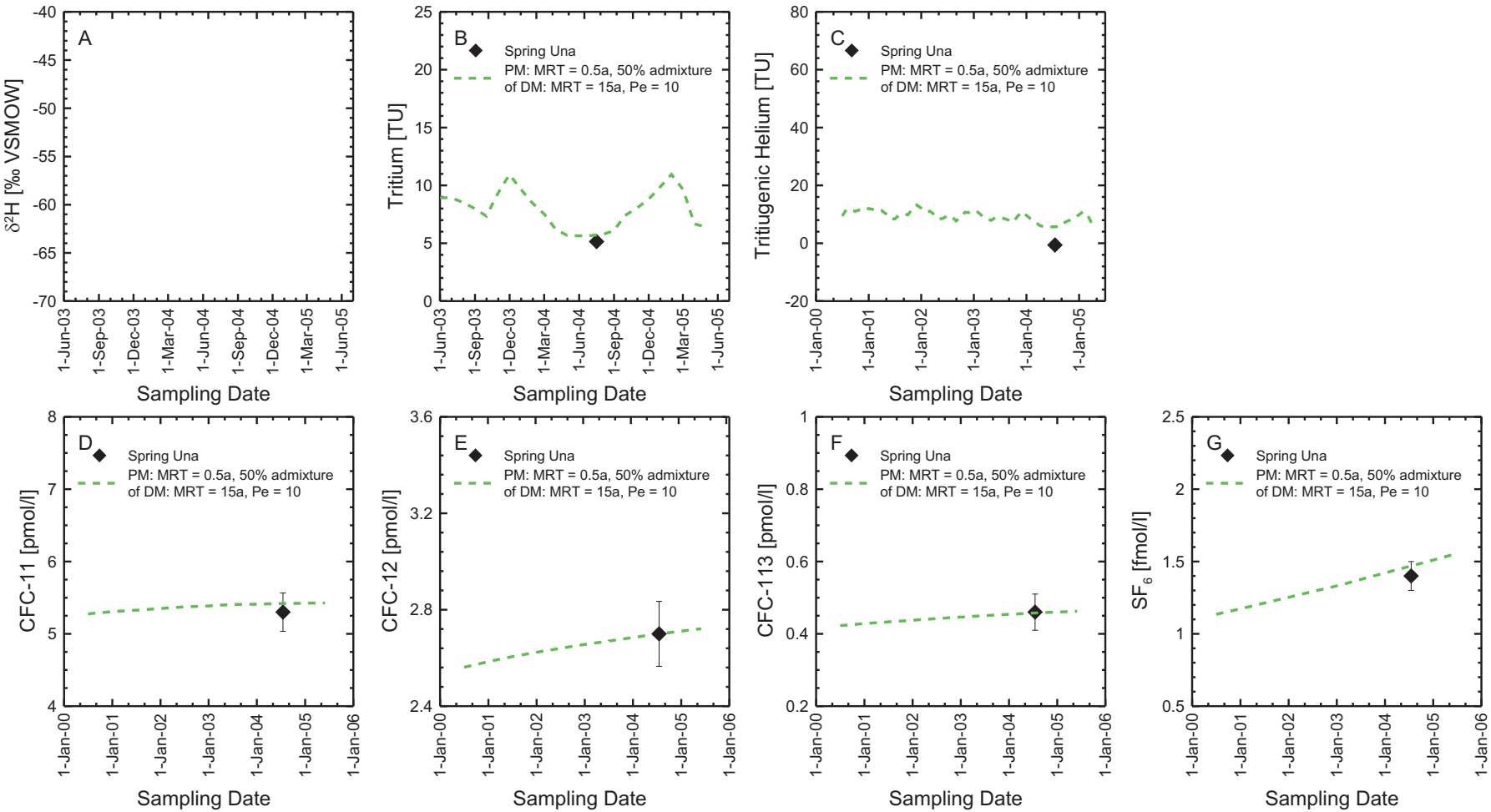

Fig. A.9: Results of lumped parameter models for the spring Una for deuterium (A); tritium (B); noble gases (C); CFC-11 (D); CFC-12 (E); CFC-113 (F); and SF_6 (G).

Table A.1: Stable isotopes (δ^2H and δ^{18}O) and tritium (^{3}H) in spring, river and lake waters of the Plitvice Lakes and Una River. Measurement precision for δ^2H = 0.8‰, δ^{18}O = 0.1‰, ^{3}H = 1 TU (part 1).

SamplingID	**Location**	**Sampling Date**	δ^2H [‰]	δ^{18}**O** [‰]	δ^3**H** [TU]
41630	Prošće Lake	15.04.2003	-69.1	-10.4	
41631	Veliko Jezero Lake	15.04.2003	-69.5	-10.4	
41632	Mali Prstavci Waterfalls	15.04.2003	-68.9	-10.4	
41633	Gradinsko Jezero Lake	15.04.2003	-69.2	-10.3	
41638	Kozjak Lake (bridges)	15.04.2003	-68	-10.3	
41639	Rječica River	15.04.2003	-68.6	-10.5	
41646	Spring Vrelo	16.04.2003	-67.4	-10.2	8.6
41647	Spring Bijela Rijeka	17.04.2003	-70.9	-10.6	9.7
41648	Spring Bijela Rijeka	17.04.2003	-69.9	-10.6	10.1
41649	Spring Crna Rijeka	17.04.2003	-70	-10.4	8.4
41652	Matica	17.04.2003	-69.8	-10.5	
41636	Korana River	15.04.2003	-69.5	-10.3	
41653	Korana River	17.04.2003	-71.1	-10.3	
41634	Veliki Slap Waterfall	15.04.2003	-71.9	-10.7	
41635	Kaludjerovac Lake	15.04.2003	-68.7	-10.4	
41637	Milinovac Lake	15.04.2003	-69.1	-10.3	
41650	Crna Rijeka River	17.04.2003	-69.9	-10.4	
41651	Bijela Rijeka River	17.04.2003	-70.6	-10.6	
41644	Spring Klokot	16.04.2003	-70.3	-10.5	
41645	Spring Klokot	16.04.2003	-71.4	-10.5	
41640	Martin Brod, Una River	16.04.2003	-55.8	-8.8	
41642	Strbacki Buk, Una River	16.04.2003	-60.1	-9.3	
41641	Strbacki Buk1, Una River	16.04.2003	-59.1	-9.3	
41643	Kostelski Buk, Una River	16.04.2003	-61.3	-9.5	
42131	Prošće Lake	07.07.2003	-69.6	-10.3	
42132	Okrugljak Lake	07.07.2003	-68.7	-10.1	
42133	Veliko Jezero Lake	07.07.2003	-66.5	-10.1	
42134	Mali Prstavci Waterfalls	07.07.2003	-67.5	-9.9	
42135	Gradinsko Jezero Lake	07.07.2003	-68.6	-9.9	
42136	Burgetići	07.07.2003	-69.1	-10	
42137	Novakovica Brod Lake	07.07.2003	-67.1	-9.9	
42138	Kozjak Lake (pump station)	07.07.2003	-67.2	-9.9	
42139	Kozjak Lake (bridges)	07.07.2003	-67.5	-9.9	
42140	Rječica River	07.07.2003	-70.9	-10.5	
42141	Spring Vrelo	07.07.2003	-67.4	-10.3	
42142	Spring Bijela Rijeka	07.07.2003	-70.8	-10.6	
42143	Spring Crna Rijeka	07.07.2003	-71.9	-10.6	
42144	Matica	07.07.2003	-71.5	-10.6	
42145	Korana River	07.07.2003	-66.1	-9.7	
42146	Sartuk	07.07.2003	-68.4	-10.1	
42155	Veliki Slap Waterfall	07.07.2003	-70.9	-10.3	
42147	Spring Ostrovica	08.07.2003	-65.7	-9.7	4.5

Table A.2: Stable isotopes (δ^2H and δ^{18}O) and tritium (^{3}H) in spring, river and lake waters of the Plitvice Lakes and Una River. Measurement precision for δ^2H = 0.8‰, δ^{18}O = 0.1‰, ^{3}H = 1 TU (part 2).

SamplingID	**Location**	**Sampling Date**	δ^2H [‰]	δ^{18}**O** [‰]	δ^3**H** [TU]
46665	Spring Ostrovica	08.07.2003			3
42148	Spring Toplica	08.07.2003	-64.7	-9.4	4.4
46674	Spring Toplica	08.07.2003			3.1
42149	Spring Privilica	08.07.2003	-70.1	-10.1	5.5
46683	Spring Privilica	08.07.2003			9.6
42150	Spring Klokot	08.07.2003	-68.3	-10.1	7.2
46692	Spring Klokot	08.07.2003			5.6
42151	Ripač Waterfall	08.07.2003	-63.1	-9.3	
42152	"Sunce"	08.07.2003	-61.5	-9.3	
42153	Bakšaiš	08.07.2003	-61.7	-9.3	
42154	Vrkašić	08.07.2003	-63.1	-9.4	
42280	Prošće Lake	06.08.2003	-67.3		
42281	Veliko Jezero Lake	06.08.2003	-66.8		
42282	Mali Prstavci Waterfalls	06.08.2003	-66.3		
42283	Burgetići	06.08.2003	-66.3		
42284	Kozjak Lake (bridges)	06.08.2003	-65.2		
42285	Rječica River	06.08.2003	-69.3		
42286	Spring Vrelo	06.08.2003	-66.8	-10.2	
42287	Spring Bijela Rijeka	06.08.2003	-70.8	-10.6	
42288	Spring Crna Rijeka	06.08.2003	-70.8	-10.5	
42289	Matica	06.08.2003	-70		
42290	Veliki Slap Waterfall	06.08.2003	-67.4		
42291	Kaludjerovac Lake	06.08.2003	-65		
42292	Milinovac Lake	06.08.2003	-65.4		
42293	Crna Rijeka River	06.08.2003	-69.8	-10.5	
42294	Bijela Rijeka River	06.08.2003	-69.6	-10.5	
42295	Spring Ostrovica	02.08.2003	-63.4	-9.7	
46666	Spring Ostrovica	01.08.2003			3.1
42296	Spring Toplica	02.08.2003	-62.5	-9.5	
46675	Spring Toplica	01.08.2003			3.3
42297	Spring Privilica	02.08.2003	-67	-10	
46684	Spring Privilica	01.08.2003			5.1
42298	Spring Klokot	02.08.2003	-66.6	-10.1	
46693	Spring Klokot	01.08.2003			4.6
42299	Ripač Waterfall	02.08.2003	-59.9		
42300	"Sunce"	02.08.2003	-60.1		
42301	Bakšaiš	02.08.2003	-60.3		
42302	Vrkašić	02.08.2003	-61.3		
42304	Prošće Lake	01.09.2003	-67.4		
42305	Veliko Jezero Lake	01.09.2003	-66.7		
42306	Mali Prstavci Waterfalls	01.09.2003	-65.6		
42307	Burgetići	01.09.2003	-65.7		

Table A.3: Stable isotopes (δ^2H and δ^{18}O) and tritium (^{3}H) in spring, river and lake waters of the Plitvice Lakes and Una River. Measurement precision for δ^2H = 0.8‰, δ^{18}O = 0.1‰, ^{3}H = 1 TU (part 3).

SamplingID	**Location**	**Sampling Date**	δ^2H [‰]	δ^{18}**O** [‰]	δ^3**H** [TU]
42307	Burgetići	01.09.2003	-65.7		
42308	Kozjak Lake (bridges)	03.09.2003	-65.2		
42309	Rječica River	01.09.2003	-69.3		
42310	Spring Vrelo	01.09.2003	-66.7	-10.2	
42311	Spring Bijela Rijeka	01.09.2003	-70.3	-10.5	
42312	Spring Crna Rijeka	01.09.2003	-70	-10.6	
42313	Matica	01.09.2003	-69.8		
42314	Veliki Slap Waterfall	03.09.2003	-68.3		
42315	Kaludjerovac Lake	03.09.2003	-64.6		
42316	Milinovac Lake	03.09.2003	-64.9		
42317	Crna Rijeka River	03.09.2003	-70	-10.5	
42318	Bijela Rijeka River	01.09.2003	-69.8	-10.4	
42319	Spring Ostrovica	31.08.2003	-64.1	-9.7	
46667	Spring Ostrovica	31.08.2003			3.5
42320	Spring Toplica	31.08.2003	-62.6	-9.4	
46676	Spring Toplica	31.08.2003			3.7
42321	Spring Privilica	31.08.2003	-67.4	-9.9	
46685	Spring Privilica	31.08.2003			4.8
42322	Spring Klokot	31.08.2003	-67.2	-10	
46694	Spring Klokot	31.08.2003			2
42323	Ripač Waterfall	31.08.2003	-59.9		
42324	"Sunce"	31.08.2003	-59.7		
42325	Bakšaiš	31.08.2003	-60.2		
42326	Vrkašić	31.08.2003	-61		
42327	Prošće Lake	03.10.2003	-67.5	-10	
42328	Veliko Jezero Lake	03.10.2003	-67.2		
42329	Mali Prstavci Waterfalls	02.10.2003	-66.5		
42330	Burgetići	02.10.2003	-66.3		
42331	Kozjak Lake (bridges)	02.10.2003	-65.2	-9.5	
42332	Rječica River	02.10.2003	-69.2		
42333	Spring Vrelo	02.10.2003	-66.2		
42334	Spring Bijela Rijeka	02.10.2003	-70.2		
42335	Spring Crna Rijeka	02.10.2003	-70.1		
42336	Matica	02.10.2003	-69.8		
42337	Korana River	02.10.2003	-65		
42338	Veliki Slap Waterfall	03.10.2003	-67.9		
42339	Kaludjerovac Lake	02.10.2003	-64.8		
42340	Milinovac Lake	02.10.2003	-65.3		
42341	Crna Rijeka River	02.10.2003	-70.1		
42342	Bijela Rijeka River	02.10.2003	-70		
42343	Spring Ostrovica	02.10.2003	-64.6		
46668	Spring Ostrovica	02.10.2003			6

Table A.4: Stable isotopes (δ^2H and δ^{18}O) and tritium (^{3}H) in spring, river and lake waters of the Plitvice Lakes and Una River. Measurement precision for δ^2H = 0.8‰, δ^{18}O = 0.1‰, ^{3}H = 1 TU (part 4).

SamplingID	**Location**	**Sampling Date**	δ^2H [‰]	δ^{18}**O** [‰]	δ^3**H** [TU]
42344	Spring Toplica	02.10.2003	-62.9		
46677	Spring Toplica	02.10.2003			2
42345	Spring Privilica	02.10.2003	-66.2		
46686	Spring Privilica	02.10.2003			6.2
42346	Spring Klokot	02.10.2003	-68.1		
46695	Spring Klokot	02.10.2003			3.6
42347	Ripač Waterfall	02.10.2003	-60.6		
42348	"Sunce"	02.10.2003	-60.6		
42349	Bakšaiš	02.10.2003	-60.6		
42350	Vrkašić	02.10.2003	-62		
42351	Prošće Lake	01.11.2003	-68.1	-10.3	
42352	Veliko Jezero Lake	01.11.2003	-67.7		
42353	Mali Prstavci Waterfalls	02.11.2003	-67.3		
42354	Burgetići	01.11.2003	-67.2		
42355	Kozjak Lake (bridges)	01.11.2003	-65.5		
42356	Rječica River	01.11.2003	-67.1	-10.2	
42357	Spring Vrelo	01.11.2003	-66.1	-10.1	8.8
42358	Spring Bijela Rijeka	01.11.2003	-69	-10.5	9.5
42359	Spring Crna Rijeka	01.11.2003	-66.5	-10.1	6.7
42360	Matica	01.11.2003	-68.2		
42361	Korana River	01.11.2003	-65.6	-10	
42362	Sartuk	01.11.2003	-65.3	-9.8	
42363	Veliki Slap Waterfall	01.11.2003	-67.4	-10.2	
42364	Kaludjerovac Lake	01.11.2003	-65.9		
42365	Spring Plitvica	03.11.2003	-68.4	-10.4	7.8
42366	Spring Stipinovac	01.11.2003	-66.5	-10	9.8
42367	Spring Ostrovica	02.11.2003	-59	-9.3	6.1
46669	Spring Ostrovica	01.11.2003			4
42368	Spring Toplica	02.11.2003	-55.8	-8.5	5.7
46678	Spring Toplica	01.11.2003			2
42369	Spring Privilica	02.11.2003	-64.2	-9.5	7.3
46687	Spring Privilica	01.11.2003			6
42370	Spring Klokot	02.11.2003	-65.7	-5.1	7.3
46696	Spring Klokot	01.11.2003			5.2
42371	Ripač Waterfall	02.11.2003	-56.5		
42372	"Sunce"	02.11.2003	-56.9		
42373	Bakšaiš	02.11.2003	-56.7		
42374	Vrkašić	02.11.2003	-57.2	-8.8	
42799	Prošće Lake	01.12.2003	-68.3		
42800	Veliko Jezero Lake	01.12.2003	-68		
42801	Mali Prstavci Waterfalls	01.12.2003	-67.4		
42802	Burgetići	01.12.2003	-67.8		

Table A.5: Stable isotopes (δ^2H and δ^{18}O) and tritium (^{3}H) in spring, river and lake waters of the Plitvice Lakes and Una River. Measurement precision for δ^2H = 0.8‰, δ^{18}O = 0.1‰, ^{3}H = 1 TU (part 5).

SamplingID	**Location**	**Sampling Date**	δ^2H [‰]	δ^{18}**O** [‰]	δ^3**H** [TU]
42803	Kozjak Lake (bridges)	01.12.2003	-66.5		
42804	Rječica River	01.12.2003	-68.7		
42805	Spring Vrelo	01.12.2003	-64.7		
42806	Spring Bijela Rijeka	01.12.2003	-70.6		
42807	Spring Crna Rijeka	01.12.2003	-66.3		
42808	Matica	01.12.2003	-66.9		
42809	Korana River	01.12.2003	-66.5		
42810	Sartuk	01.12.2003	-65.2		
42811	Veliki Slap Waterfall	01.12.2003	-67.3		
42812	Kaludjerovac Lake	01.12.2003	-66.4		
42813	Spring Plitvica	01.12.2003	-67.6		
42814	Spring Ostrovica	01.12.2003	-57.4	-8.8	
46670	Spring Ostrovica	01.12.2003			4.1
42815	Spring Toplica	01.12.2003	-57	-8.6	
46679	Spring Toplica	01.12.2003			3.4
42816	Spring Privilica	01.12.2003	-63	-9.3	
46688	Spring Privilica	01.12.2003			5.6
42817	Spring Klokot	01.12.2003	-65.4	-9.9	
46697	Spring Klokot	01.12.2003			3
42818	Ripač Waterfall	01.12.2003	-55.5		
42819	"Sunce"	01.12.2003	-55.9		
42820	Bakšaiš	01.12.2003	-56		
42821	Vrkašić	01.12.2003	-56.9		
42822	Prošće Lake	07.01.2004	-68.4		
42823	Veliko Jezero Lake	07.01.2004	-68.2		
42824	Mali Prstavci Waterfalls	07.01.2004	-68.2		
42825	Burgetići	07.01.2004	-67.9		
42826	Kozjak Lake (bridges)	07.01.2004	-67		
42827	Rječica River	07.01.2004	-69.2		
42828	Spring Vrelo	07.01.2004	-66.9		
42829	Spring Bijela Rijeka	07.01.2004	-70.3		
42830	Spring Crna Rijeka	07.01.2004	-68.5		
42831	Matica	07.01.2004	-68.8		
42832	Korana River	07.01.2004	-67		
42833	Sartuk	07.01.2004	-67.5		
42834	Veliki Slap Waterfall	07.01.2004	-68.5		
42835	Kaludjerovac Lake	07.01.2004	-66.7		
42836	Spring Plitvica	07.01.2004	-69.2		
42837	Spring Ostrovica	04.01.2004	-58.3	-8.9	
46671	Spring Ostrovica	04.01.2004			2
42838	Spring Toplica	04.01.2004	-58.5	-8.8	
46680	Spring Toplica	04.01.2004			6.9

Table A.6: Stable isotopes (δ^2H and δ^{18}O) and tritium (^{3}H) in spring, river and lake waters of the Plitvice Lakes and Una River. Measurement precision for δ^2H = 0.8‰, δ^{18}O = 0.1‰, ^{3}H = 1 TU (part 6).

SamplingID	**Location**	**Sampling Date**	δ^2H [‰]	δ^{18}**O** [‰]	δ^3**H** [TU]
42839	Spring Privilica	04.01.2004	-65.1	-9.7	
46689	Spring Privilica	04.01.2004			5.7
42840	Spring Klokot	04.01.2004	-66.2	-9.9	
46698	Spring Klokot	04.01.2004			2
42841	Ripač Waterfall	04.01.2004	-56.7		
42842	"Sunce"	04.01.2004	-56.5		
42843	Bakšaiš	04.01.2004	-56.8		
42844	Vrkašić	04.01.2004	-57.9		
42845	Prošće Lake	02.02.2004	-69		
42846	Veliko Jezero Lake	02.02.2004	-68.9		
42847	Mali Prstavci Waterfalls	02.02.2004	-68.9		
42848	Burgetići	02.02.2004	-69		
42850	Rječica River	02.02.2004	-69.8		
42851	Spring Vrelo	02.02.2004	-67.2		
42867	Spring Bijela Rijeka	02.02.2004	-70.7		
42852	Spring Crna Rijeka	11.02.2004	-67.9		
42853	Matica	11.02.2004	-68.3		
42854	Korana River	11.02.2004	-68.1		
42855	Sartuk	11.02.2004	-67.2		
42856	Veliki Slap Waterfall	02.02.2004	-68.8		
42857	Kaludjerovac Lake	11.02.2004	-68.1		
42858	Spring Plitvica	11.02.2004	-69.3		
42859	Spring Ostrovica	31.01.2004	-58.2	-8.9	
46672	Spring Ostrovica	31.01.2004			3.4
42860	Spring Toplica	31.01.2004	-57.8	-8.7	
46681	Spring Toplica	31.01.2004			2
42861	Spring Privilica	31.01.2004	-65.6	-9.8	
46690	Spring Privilica	31.01.2004			5.2
42862	Spring Klokot	31.01.2004	-66.2	-9.9	
46699	Spring Klokot	31.01.2004			5.5
42863	Ripač Waterfall	31.01.2004	-56.9		
42864	"Sunce"	31.01.2004	-56.9		
42865	Bakšaiš	31.01.2004	-57.1	-8.8	
42866	Vrkašić	31.01.2004	-57.8	-8.9	
42868	Kozjak Lake (bridges)	01.03.2004	-69	-10.2	
42869	Spring Vrelo	01.03.2004	-66.6	-10.1	
42870	Veliki Slap Waterfall	01.03.2004	-69.5		
42871	Kaludjerovac Lake	01.03.2004	-68.6	-10.1	
42872	Spring Ostrovica	06.03.2004	-58.2	-9	
46673	Spring Ostrovica	06.03.2004			2
42873	Spring Toplica	06.03.2004	-57.4	-8.8	

Table A.7: Stable isotopes (δ^2H and δ^{18}O) and tritium (^{3}H) in spring, river and lake waters of the Plitvice Lakes and Una River. Measurement precision for δ^2H = 0.8‰, δ^{18}O = 0.1‰, ^{3}H = 1 TU (part 7).

SamplingID	**Location**	**Sampling Date**	δ^2H [‰]	δ^{18}**O** [‰]	δ^3**H** [TU]
46682	Spring Toplica	06.03.2004			3.3
42874	Spring Privilica	06.03.2004	-64.9	-9.7	
46691	Spring Privilica	06.03.2004			2.3
42875	Spring Klokot	06.03.2004	-67.3	-10	
46700	Spring Klokot	06.03.2004			2
42876	Ripač Waterfall	06.03.2004	-57.4		
42877	"Sunce"	06.03.2004	-57.4		
42878	Bakšaiš	06.03.2004	-57.5		
42879	Vrkašić	06.03.2004	-58.2		
42880	Prošće Lake	15.04.2004	-69.6	-10.7	
42881	Veliko Jezero Lake	15.04.2004	-69.5		
42882	Mali Prstavci Waterfalls	15.04.2004	-69.3		
42883	Burgetići	15.04.2004	-69.6		
42884	Kozjak Lake (bridges)	15.04.2004	-70.9	-10.5	
42885	Rječica River	15.04.2004	-71.5	-10.5	
42886	Spring Vrelo	15.04.2004	-68.8	-10.2	
42887	Spring Bijela Rijeka	15.04.2004	-70.4	-10.5	
42888	Spring Crna Rijeka	15.04.2004	-71	-10.5	
42889	Matica	15.04.2004	-70.1	-10.5	
42890	Korana River	15.04.2004	-69.6		
42891	Sartuk	15.04.2004	-73.4	-10.6	
42892	Veliki Slap Waterfall	15.04.2004	-74.1	-10.9	
42893	Kaludjerovac Lake	15.04.2004	-69.4		
42894	Spring Plitvica	15.04.2004	-72.9	-10.7	
42895	Spring Ostrovica	03.04.2004	-61.1	-9.4	
47233	Spring Ostrovica	03.04.2004			3.1
42896	Spring Toplica	03.04.2004	-60.1	-9.1	
47248	Spring Toplica	03.04.2004			2.5
42897	Spring Privilica	03.04.2004	-67.1	-10	
47263	Spring Privilica	03.04.2004			7.7
42898	Spring Klokot	03.04.2004	-71.5	-10.6	
47278	Spring Klokot	03.04.2004			3.3
42899	Ripač Waterfall	03.04.2004	-62.3	-9.5	
42900	"Sunce"	03.04.2004	-60.9		
42901	Bakšaiš	03.04.2004	-60.9		
42902	Vrkašić	03.04.2004	-61.5		
42903	Prošće Lake	03.05.2004	-69.9	-10.4	
42904	Veliko Jezero Lake	03.05.2004	-69.8	-10.5	
42905	Mali Prstavci Waterfalls	03.05.2004	-69.7		
42906	Burgetići	03.05.2004	-69.2		
42907	Kozjak Lake (bridges)	03.05.2004	-69	-10.4	

Table A.8: Stable isotopes (δ^2H and δ^{18}O) and tritium (^{3}H) in spring, river and lake waters of the Plitvice Lakes and Una River. Measurement precision for δ^2H = 0.8‰, δ^{18}O = 0.1‰, ^{3}H = 1 TU (part 8).

SamplingID	**Location**	**Sampling Date**	δ^2H [‰]	δ^{18}**O** [‰]	δ^3**H** [TU]
42908	Rječica River	03.05.2004	-69.5	-10.5	
42909	Spring Vrelo	04.05.2004	-66.3	-10.2	
42910	Spring Bijela Rijeka	03.05.2004	-69.6	-10.4	
42911	Spring Crna Rijeka	03.05.2004	-69	-10.4	
42912	Matica	03.05.2004	-69.1	-10.5	
42913	Korana River	05.05.2004	-68.7	-10.3	
42914	Sartuk	05.05.2004	-69.6	-10.3	
42915	Veliki Slap Waterfall	05.05.2004	-70.1		
42916	Kaludjerovac Lake	05.05.2004	-69.3	-10.5	
42917	Spring Plitvica	05.05.2004	-70.4	-10.7	
42918	Spring Ostrovica	02.05.2004	-60.9	-9.4	
47234	Spring Ostrovica	02.05.2004			7.8
42919	Spring Toplica	02.05.2004	-59.8	-9.1	
47249	Spring Toplica	02.05.2004			2
42920	Spring Privilica	02.05.2004	-67	-10.1	
47264	Spring Privilica	02.05.2004			6.3
42921	Spring Klokot	02.05.2004	-70.6	-10.5	
47279	Spring Klokot	02.05.2004			5.3
42922	Ripač Waterfall	02.05.2004	-61.1	-9.4	
42923	"Sunce"	02.05.2004	-60.8		
42924	Bakšaiš	02.05.2004	-61.1		
42925	Vrkašić	02.05.2004	-62.2	-9.7	
42957	Prošće Lake	01.06.2004	-70	-10.3	
42958	Veliko Jezero Lake	01.06.2004	-69.7		
42959	Mali Prstavci Waterfalls	01.06.2004	-69.1		
42960	Burgetići	01.06.2004	-69.1		
42961	Kozjak Lake (bridges)	01.06.2004	-68.9	-10.3	
42962	Rječica River	01.06.2004	-69.8		
42968	Spring Vrelo	01.06.2004	-67.2	-10.2	
42969	Spring Bijela Rijeka	01.06.2004	-70.7	-10.6	
42970	Spring Crna Rijeka	01.06.2004	-70.3	-10.5	
42971	Matica	01.06.2004	-70.3	-10.5	
42972	Korana River	01.06.2004	-68.8	-10.3	
42973	Sartuk	01.06.2004	-69.2	-10	
42974	Veliki Slap Waterfall	01.06.2004	-69.9		
42975	Kaludjerovac Lake	01.06.2004	-68.8	-10	
42976	Spring Plitvica	01.06.2004	-70.6	-10.6	
42978	Spring Ostrovica	30.05.2004	-62.1		
47235	Spring Ostrovica	30.05.2004			6.3
47236	Spring Ostrovica	30.06.2004			3
42979	Spring Toplica	30.05.2004	-61.8		
47250	Spring Toplica	30.05.2004			4.1

Table A.9: Stable isotopes (δ^2H and δ^{18}O) and tritium (^{3}H) in spring, river and lake waters of the Plitvice Lakes and Una River. Measurement precision for δ^2H = 0.8‰, δ^{18}O = 0.1‰, ^{3}H = 1 TU (part 9).

SamplingID	**Location**	**Sampling Date**	δ^2H [‰]	δ^{18}**O** [‰]	δ^3**H** [TU]
42980	Spring Privilica	30.05.2004	-68		
47265	Spring Privilica	30.05.2004			4.3
42981	Spring Klokot	30.05.2004	-69.7		
47280	Spring Klokot	30.05.2004			4.9
42982	Ripač Waterfall	30.05.2004	-61.6		
42983	"Sunce"	30.05.2004	-61.4		
42984	Bakšaiš	30.05.2004	-61.5		
42985	Vrkašić	30.05.2004	-62.5		
42938	Prošće Lake	15.07.2004	-70.3	-10.6	
42945	Veliko Jezero Lake	16.07.2004	-68.8		
42946	Mali Prstavci Waterfalls	16.07.2004	-69		
42948	Burgetići	16.07.2004	-68.9		
42950	Kozjak Lake (bridges)	16.07.2004	-68.7	-10.3	
42951	Rječica River	16.07.2004	-70.1	-10.4	
42942	Spring Vrelo	14.07.2004	-66.9	-10.3	
42929	Spring Bijela Rijeka	14.07.2004	-70.7	-10.7	10.2
42930	Spring Crna Rijeka	14.07.2004	-69.7	-10.6	7.2
42952	Matica	14.07.2004	-70.9		
42953	Korana River	14.07.2004	-68		
42954	Sartuk	14.07.2004	-69.3	-10.5	
42964	Veliki Slap Waterfall	01.07.2004	-69.6		
42965	Kaludjerovac Lake	01.07.2004	-68.4		
42935	Spring Plitvica	15.07.2004	-67.2	-10.3	8.6
42936	Spring Stipinovac	14.07.2004	-66.9	-10.2	8.8
42937	Spring of Una River	17.07.2004			5.1
42931	Spring Ostrovica	15.07.2004	-61.4	-9.6	6.2
42932	Spring Toplica	15.07.2004	-60.8	-8.8	5.6
47251	Spring Toplica	30.06.2004			2.5
42933	Spring Privilica	15.07.2004	-68	-10	6.8
47266	Spring Privilica	30.06.2004			6.3
42934	Spring Klokot	15.07.2004	-68.2	-10.2	7.5
47281	Spring Klokot	30.06.2004			9.5
42966	Ripač Waterfall	30.06.2004	-61.9		
42943	"Sunce"	15.07.2004	-61.1		
42944	Bakšaiš	15.07.2004	-61.2		
42956	Vrkašić	14.07.2004	-62.4	-9.3	
43129	Prošće Lake	01.08.2004	-68.8	-10.3	
43130	Veliko Jezero Lake	01.08.2004	-68.8		
43131	Mali Prstavci Waterfalls	01.08.2004	-68.5	-10.2	
43132	Burgetići	01.08.2004	-68.5	-10.1	
43133	Kozjak Lake (bridges)	01.08.2004	-67.6	-10	
43134	Rječica River	01.08.2004	-70.2	-10.3	

Table A.10: Stable isotopes (δ^2H and δ^{18}O) and tritium (^{3}H) in spring, river and lake waters of the Plitvice Lakes and Una River. Measurement precision for δ^2H = 0.8‰, δ^{18}O = 0.1‰, ^{3}H = 1 TU (part 10).

SamplingID	**Location**	**Sampling Date**	δ^2**H** [‰]	δ^{18}**O** [‰]	δ^3**H** [TU]
43135	Spring Vrelo	01.08.2004	-67.7	-10.2	
43136	Spring Bijela Rijeka	01.08.2004	-71.4	-10.5	
43137	Spring Crna Rijeka	01.08.2004	-71	-10.6	
43138	Matica	01.08.2004	-71	-10.5	
43139	Korana River	01.08.2004	-67.5	-10	
43140	Sartuk	01.08.2004	-66.8	-9.9	
43141	Veliki Slap Waterfall	01.08.2004	-69		
43142	Kaludjerovac Lake	01.08.2004	-67.6		
43143	Spring Plitvica	01.08.2004	-70.6		
43144	Spring Stipinovac	01.08.2004	-67.3	-10.1	
43145	Spring Ostrovica	30.07.2004	-64.2	-9.7	
47237	Spring Ostrovica	30.07.2004			4
43146	Spring Toplica	30.07.2004	-62.8	-9.3	
47252	Spring Toplica	30.07.2004			4.6
43147	Spring Privilica	30.07.2004	-67.8	-10	
47267	Spring Privilica	30.07.2004			5.9
43148	Spring Klokot	30.07.2004	-67.9	-10	
47282	Spring Klokot	30.07.2004			7.1
43149	Ripač Waterfall	30.07.2004	-62	-9.4	
43150	"Sunce"	30.07.2004	-61.8	-9.3	
43151	Bakšaiš	30.07.2004	-62		
43152	Vrkašić	30.07.2004	-62.8	-9.5	
43153	Prošće Lake	01.09.2004	-68.9	-10.2	
43154	Veliko Jezero Lake	02.09.2004	-68.4	-10.1	
43155	Mali Prstavci Waterfalls	02.09.2004	-67.5		
43156	Burgetići	02.09.2004	-67.5		
43157	Kozjak Lake (bridges)	02.09.2004	-67.2	-9.9	
43158	Rječica River	02.09.2004	-69.5	-10.4	
43159	Spring Vrelo	02.09.2004	-66.8	-10.1	
43160	Spring Bijela Rijeka	02.09.2004	-70.8	-10.6	
43161	Spring Crna Rijeka	02.09.2004	-70.7	-10.6	
43162	Matica	02.09.2004	-70.5		
43164	Sartuk	02.09.2004	-68	-10.1	
43165	Veliki Slap Waterfall	02.09.2004	-68.9		
43166	Kaludjerovac Lake	02.09.2004	-67		
43167	Spring Plitvica	02.09.2004	-70.3	-10.5	
43168	Spring Stipinovac	02.09.2004	-66.8	-10.1	
43169	Spring Ostrovica	04.09.2004	-63.8	-9.7	
47238	Spring Ostrovica	04.09.2004			4.2
43170	Spring Toplica	04.09.2004	-62.7	-9.4	
47253	Spring Toplica	04.09.2004			4.9
43171	Spring Privilica	04.09.2004	-67.8	-10	

Table A.11: Stable isotopes (δ^2H and δ^{18}O) and tritium (^{3}H) in spring, river and lake waters of the Plitvice Lakes and Una River. Measurement precision for δ^2H = 0.8‰, δ^{18}O = 0.1‰, ^{3}H = 1 TU (part 11).

SamplingID	**Location**	**Sampling Date**	δ^2**H** [‰]	δ^{18}**O** [‰]	δ^3**H** [TU]
47268	Spring Privilica	04.09.2004			7
43172	Spring Klokot	04.09.2004	-67.6	-10.1	
47283	Spring Klokot	04.09.2004			9.8
43173	Ripač Waterfall	04.09.2004	-61.4		
43174	"Sunce"	04.09.2004	-61.4	-9.3	
43175	Bakšaiš	04.09.2004	-61.3		
43176	Vrkašić	04.09.2004	-62.4		
46735	Prošće Lake	04.10.2004	-68.5	-10.3	
46736	Veliko Jezero Lake	04.10.2004	-68.5		
46737	Mali Prstavci Waterfalls	04.10.2004	-68.1		
46738	Burgetići	04.10.2004	-67.9		
46739	Kozjak Lake (bridges)	04.10.2004	-66.1	-10.1	
46740	Rječica River	01.10.2004	-69.7		
46741	Spring Vrelo	01.10.2004	-66.7	-10.2	
46742	Spring Bijela Rijeka	01.10.2004	-70.7	-10.6	
46742	Spring Bijela Rijeka	01.10.2004	-70.7	-10.6	
46743	Spring Crna Rijeka	01.10.2004	-69.9	-10.6	
46744	Matica	01.10.2004	-70.3		
46745	Korana River	01.10.2004	-66.7		
46746	Sartuk	01.10.2004	-66.2	-10	
46747	Veliki Slap Waterfall	01.10.2004	-65	-10	
46748	Kaludjerovac Lake	05.10.2004	-67		
46749	Spring Plitvica	05.10.2004	-65.5	-9.8	
46750	Spring Stipinovac	13.10.2004	-66.5	-10.3	
43177	Spring Ostrovica	24.09.2004	-64.2	-9.8	
47239	Spring Ostrovica	24.09.2004			5
43178	Spring Toplica	24.09.2004	-62.5	-9.5	
47254	Spring Toplica	24.09.2004			2.7
43179	Spring Privilica	24.09.2004	-68.4	-10.1	
47269	Spring Privilica	24.09.2004			6.2
43180	Spring Klokot	24.09.2004	-66.9	-10	
47284	Spring Klokot	24.09.2004			11.3
43181	Ripač Waterfall	24.09.2004	-61.5		
43182	"Sunce"	24.09.2004	-61		
43183	Bakšaiš	24.09.2004	-60.9		
43184	Vrkašić	24.09.2004	-62.6		
46751	Prošće Lake	26.10.2004	-68.8		
46752	Veliko Jezero Lake	26.10.2004	-68.7		
46753	Mali Prstavci Waterfalls	26.10.2004	-68.5		
46754	Burgetići	26.10.2004	-68.6		
46755	Kozjak Lake (bridges)	05.11.2004	-67.1	-10	
46756	Rječica River	17.11.2004	-69.1		

Table A.12: Stable isotopes (δ^2H and δ^{18}O) and tritium (^{3}H) in spring, river and lake waters of the Plitvice Lakes and Una River. Measurement precision for δ^2H = 0.8‰, δ^{18}O = 0.1‰, ^{3}H = 1 TU (part 12).

SamplingID	**Location**	**Sampling Date**	δ^2**H** [‰]	δ^{18}**O** [‰]	δ^3**H** [TU]
46757	Spring Vrelo	26.10.2004	-66.7	-10.3	
46758	Spring Bijela Rijeka	26.10.2004	-71.2	-10.5	
46759	Spring Crna Rijeka	26.10.2004	-69.8	-10.5	
46760	Matica	26.10.2004	-69.8		
46761	Korana River	17.11.2004	-66.8	-10.1	
46762	Sartuk	28.10.2004	-66	-9.9	
46763	Veliki Slap Waterfall	05.11.2004	-68.8		
46764	Kaludjerovac Lake	05.11.2004	-66.8		
46765	Spring Plitvica	28.10.2004	-68.2	-10.1	
46766	Spring Stipinovac	26.10.2004	-67.4	-10.3	
46767	Spring Ostrovica	01.11.2004	-61.9	-9.3	
47240	Spring Ostrovica	01.11.2004			4.3
46768	Spring Toplica	01.11.2004	-63	-9.4	
47255	Spring Toplica	01.11.2004			2
46769	Spring Privilica	01.11.2004	-67.9	-10.1	
47270	Spring Privilica	01.11.2004			3.3
46770	Spring Klokot	01.11.2004	-65.6	-9.9	
47285	Spring Klokot	01.11.2004			5.4
46771	Ripač Waterfall	01.11.2004	-60.9		
46772	"Sunce"	01.11.2004	-61.2		
46773	Bakšaiš	01.11.2004	-61.3		
46774	Vrkašić	01.11.2004	-61.4	-9.4	
46775	Prošće Lake	21.12.2004	-68.9	-10.3	
46776	Veliko Jezero Lake	21.12.2004	-69.3	-10.4	
46777	Mali Prstavci Waterfalls	21.12.2004	-69.1		
46778	Burgetići	21.12.2004	-69		
46779	Kozjak Lake (bridges)	21.12.2004	-68.6	-10.2	
46780	Rječica River	08.12.2004	-69.2		
46781	Spring Vrelo	08.12.2004	-67.1	-10.1	
46782	Spring Bijela Rijeka	08.12.2004	-70.3	-10.4	
46783	Spring Crna Rijeka	08.12.2004	-69.3	-10.3	
46784	Matica	08.12.2004	-69.5	-10.3	
46785	Korana River	17.12.2004	-68.4	-10.2	
46786	Sartuk	07.12.2004	-66	-9.7	
46789	Spring Plitvica	07.12.2004	-67.9	-10.2	
46790	Spring Stipinovac	08.12.2004	-67.2	-10.1	
46791	Spring Ostrovica	04.12.2004	-61	-9.3	
47241	Spring Ostrovica	04.12.2004			3.8
46792	Spring Toplica	04.12.2004	-61	-9.2	
47256	Spring Toplica	04.12.2004			8.6
46793	Spring Privilica	04.12.2004	-66.2	-9.9	
47271	Spring Privilica	04.12.2004			7.6

Table A.13: Stable isotopes (δ^2H and δ^{18}O) and tritium (^{3}H) in spring, river and lake waters of the Plitvice Lakes and Una River. Measurement precision for δ^2H = 0.8‰, δ^{18}O = 0.1‰, ^{3}H = 1 TU (part 13).

SamplingID	**Location**	**Sampling Date**	δ^2**H** [‰]	δ^{18}**O** [‰]	δ^3**H** [TU]
46794	Spring Klokot	04.12.2004	-66.6	-10.3	
47286	Spring Klokot	04.12.2004			6.8
46795	Ripač Waterfall	04.12.2004	-58.5		
46796	"Sunce"	04.12.2004	-58.3		
46797	Bakšaiš	04.12.2004	-58.4	-9.1	
46798	Vrkašić	04.12.2004	-58.8	-9.1	
46799	Prošće Lake	13.01.2005	-68.9	-10	
46800	Veliko Jezero Lake	13.01.2005	-69.5		
46801	Mali Prstavci Waterfalls	13.01.2005	-68.7	-10.4	
46802	Burgetići	13.01.2005	-69.5		
46804	Rječica River	13.01.2005	-69.4	-10.3	
46805	Spring Vrelo	13.01.2005	-66.9	-10.3	
46806	Spring Bijela Rijeka	13.01.2005	-69.9	-10.6	
46807	Spring Crna Rijeka	13.01.2005	-69	-10.5	
46808	Matica	13.01.2005	-68.7		
46809	Korana River	13.01.2005	-68.2	-10.2	
46810	Sartuk	13.01.2005	-67	-10	
46811	Veliki Slap Waterfall	13.01.2005	-68.8		
46812	Kaludjerovac Lake	14.01.2005	-68.8		
46813	Spring Plitvica	13.01.2005	-68.4	-10.3	
46814	Spring Stipinovac	13.01.2005	-68.2	-10	
46815	Spring Ostrovica	03.01.2005	-59.5	-9.3	
47242	Spring Ostrovica	03.01.2005			5.3
46816	Spring Toplica	03.01.2005	-59.8	-9	
47257	Spring Toplica	03.01.2005			6.5
46817	Spring Privilica	03.01.2005	-67	-9.9	
47272	Spring Privilica	03.01.2005			7.2
46818	Spring Klokot	03.01.2005	-67.5	-10.1	
47287	Spring Klokot	03.01.2005			8.5
46819	Ripač Waterfall	03.01.2005	-59.2	-9.3	
46820	"Sunce"	03.01.2005	-59.8		
46821	Bakšaiš	03.01.2005	-59.9		
46822	Vrkašić	03.01.2005	-60.5		
46827	Kozjak Lake (bridges)	02.02.2005	-70	-10.3	
46839	Spring Ostrovica	02.02.2005	-62.9	-9.4	
46843	Ripač Waterfall	02.02.2005	-60.9	-9.2	
46844	"Sunce"	02.02.2005	-61.1	-9.3	
46845	Bakšaiš	02.02.2005	-61.1		
46846	Vrkašić	02.02.2005	-61.9	-9.4	
46983	Spring Ostrovica	09.03.2005	-62.8	-9.6	
46984	Spring Toplica	09.03.2005	-61.5	-9.2	
46985	Spring Privilica	09.03.2005	-67.9	-10	

Table A.14: Stable isotopes (δ^2H and δ^{18}O) and tritium (^{3}H) in spring, river and lake waters of the Plitvice Lakes and Una River. Measurement precision for δ^2H = 0.8‰, δ^{18}O = 0.1‰, ^{3}H = 1 TU (part 14).

SamplingID	**Location**	**Sampling Date**	δ^2**H** [‰]	δ^{18}**O** [‰]	δ^3**H** [TU]
46986	Ripač Waterfall	09.03.2005	-61		
46987	"Sunce"	09.03.2005	-61	-9.3	
46988	Bakšaiš	09.03.2005	-61.6		
46989	Vrkašić	09.03.2005	-63	-9.5	
47095	Prošće Lake	26.04.2005	-72.1		
47096	Veliko Jezero Lake	26.04.2005	-72.5		
47097	Mali Prstavci Waterfalls	26.04.2005	-72.4		
47098	Burgetići	26.04.2005	-72.5		
47099	Kozjak Lake (bridges)	30.03.2005	-73.6		
47100	Rječica River	30.03.2005	-76.4		
47101	Spring Bijela Rijeka	21.04.2005	-71.1		
47102	Spring Crna Rijeka	21.04.2005	-72.2		
47103	Veliki Slap Waterfall	30.03.2005	-81.8		
47104	Kaludjerovac Lake	30.03.2005	-72.4		
47105	Spring Plitvica	21.04.2005	-75.3		
46990	Spring Ostrovica	04.04.2005	-65.2	-9.9	
47245	Spring Ostrovica	04.04.2005			7.5
46991	Spring Toplica	04.04.2005	-62.1	-9.3	
47260	Spring Toplica	04.04.2005			6.5
46992	Spring Privilica	04.04.2005	-70.2	-10.4	
47275	Spring Privilica	04.04.2005			3.8
46997	Spring Klokot	04.04.2005	-79.5	-11.7	
47290	Spring Klokot	04.04.2005			3.9
46993	Ripač Waterfall	04.04.2005	-66		
46994	"Sunce"	04.04.2005	-66.1	-10	
46995	Bakšaiš	04.04.2005	-66.2	-10	
46996	Vrkašić	04.04.2005	-67.1		
47106	Prošće Lake	17.05.2005	-71.2		
47107	Veliko Jezero Lake	17.05.2005	-71.6		
47108	Mali Prstavci Waterfalls	17.05.2005	-71.5		
47109	Burgetići	17.05.2005	-71.5		
47110	Kozjak Lake (bridges)	28.04.2005	-72.5		
47111	Rječica River	03.05.2005	-71.3		
47158	Spring Vrelo	03.05.2005	-67.6		
47112	Spring Bijela Rijeka	03.05.2005	-70.6		
47113	Spring Crna Rijeka	03.05.2005	-71.7		
47114	Matica	03.05.2005	-71.4		
47115	Korana River	06.05.2005	-72.3		
47116	Sartuk	06.05.2005	-72.5		
47117	Veliki Slap Waterfall	28.04.2005	-73.6		
47118	Kaludjerovac Lake	28.04.2005	-72.4		
47119	Spring Plitvica	06.05.2005	-72.9		

Table A.15: Stable isotopes (δ^2H and δ^{18}O) and tritium (^{3}H) in spring, river and lake waters of the Plitvice Lakes and Una River. Measurement precision for δ^2H = 0.8‰, δ^{18}O = 0.1‰, ^{3}H = 1 TU (part 15).

SamplingID	**Location**	**Sampling Date**	δ^2**H** [‰]	δ^{18}**O** [‰]	δ^3**H** [TU]
47120	Spring Stipinovac	03.05.2005	-66.7		
47121	Spring Ostrovica	09.05.2005	-63.7		
47246	Spring Ostrovica	09.05.2005			6.4
47122	Spring Toplica	09.05.2005	-62.7		
47261	Spring Toplica	09.05.2005			5.3
47123	Spring Privilica	09.05.2005	-72.5		
47276	Spring Privilica	09.05.2005			7.7
47124	Spring Klokot	09.05.2005	-75.4		
47291	Spring Klokot	09.05.2005			8
47125	Ripač Waterfall	09.05.2005	-65.6		
47126	"Sunce"	09.05.2005	-65.7		
47127	Bakšaiš	09.05.2005	-65.8		
47128	Vrkašić	09.05.2005	-66.6		
47129	Prošće Lake	02.06.2005	-71		
47130	Veliko Jezero Lake	02.06.2005	-71		
47131	Mali Prstavci Waterfalls	02.06.2005	-70.9		
47132	Burgetići	02.06.2005	-70.8		
47133	Kozjak Lake (bridges)	07.06.2005	-70.7		
47134	Rječica River	01.06.2005	-70.6		
47135	Spring Vrelo	01.06.2005	-67.7		
47136	Spring Bijela Rijeka	01.06.2005	-71.2		
47137	Spring Crna Rijeka	01.06.2005	-71.3		
47138	Matica	01.06.2005	-71.4		
47139	Korana River	09.06.2005	-70.8		
47140	Sartuk	09.06.2005	-71.1		
47141	Veliki Slap Waterfall	07.06.2005	-71.6		
47142	Kaludjerovac Lake	07.06.2005	-70.8		
47143	Spring Plitvica	09.06.2005	-71.7		
47144	Spring Stipinovac	01.06.2005	-67.2		
47145	Spring Ostrovica	05.06.2005	-65.7		
47247	Spring Ostrovica	05.06.2005			4.5
47146	Spring Toplica	05.06.2005	-63.2		
47262	Spring Toplica	05.06.2005			12.2
47147	Spring Privilica	05.06.2005	-69.1		
47277	Spring Privilica	05.06.2005			7.1
47292	Spring Klokot	05.06.2005			8.3
47150	"Sunce"	05.06.2005	-64.3		
47151	Bakšaiš	05.06.2005	-64.3		
47152	Vrkašić	05.06.2005	-65.5		

Table A.16: Results of CFC/SF_6 in spring, river and lake waters of the Plitvice Lakes and Una River.

SamplingID	Location	Sampling Date	CFC-11 [pmol/l]	CFC-11 Error	CFC-12 [pmol/l]	CFC-12 Error	CFC-113 [pmol/l]	CFC-113 Error	SF_6 [fmol/l]	SF_6 Error
42375	Kozjak Lake	01.11.03	5.7	0.3	2.8	0.1	0.5	0.1	1.7	0.1
42357	Spring Vrelo	01.11.03	5.8	0.3	2.5	0.1	0.4	0.1	0.7	0.1
42358	Spring Bijela Rijeka	01.11.03	6.0	0.3	3.0	0.2	0.5	0.1	1.5	0.1
42359	Spring Crna Rijeka	01.11.03	6.4	0.3	3.1	0.2	0.6	0.1	1.5	0.1
42365	Spring Plitvica	03.11.03	6.8	0.3	3.1	0.2	0.5	0.1	1.8	0.1
42366	Spring Stipinovac	01.11.03	8.0	0.4	3.2	0.2	0.3	0.1	0.5	0.1
42367	Spring Ostrovica	02.11.03	6.3	0.3	2.9	0.1	0.5	0.1	1.5	0.1
42368	Spring Toplica	02.11.03	5.7	0.3	2.7	0.1	0.5	0.1	1.5	0.1
42369	Spring Privilica	02.11.03	8.2	0.4	2.6	0.1	0.5	0.1	1.6	0.1
42370	Spring Klokot	02.11.03	12.0	0.6	3.5	0.2	0.6	0.1	1.6	0.1
42372	"Sunce"	02.11.03	7	0.4	3.5	0.2	0.6	0.1	1.8	0.1
42374	Vrkašić	02.11.03	8.7	0.4	3.4	0.2	0.5	0.1	1.9	0.1
42374	Vrkašić	02.11.03	8.7	0.4	3.4	0.2	0.5	0.1	1.9	0.1
42938	Prošće Lake	15.07.04	4.6	0.2	2.3	0.1	0.4	0.1	1.6	0.1
42939	Kozjak Lake	16.07.04	3.5	0.2	2.0	0.1	0.3	0.1	1.4	0.1
42942	Spring Vrelo	14.07.04	4.7	0.2	1.9	0.1	0.3	0.1	0.4	0.1
42929	Spring Bijela Rijeka	14.07.04	4.0	0.2	2.2	0.1	0.3	0.1	1.1	0.1
42930	Spring Crna Rijeka	14.07.04	3.8	0.2	1.9	0.1	0.3	0.1	1.3	0.1
42935	Spring Plitvica	15.07.04	4.7	0.2	2.3	0.1	0.4	0.1	1.3	0.1
42936	Spring Stipinovac	14.07.04	6.2	0.3	2.9	0.1	0.2	0.1	0.4	0.1
42937	Spring of Una River	17.07.04	5.3	0.3	2.7	0.1	0.5	0.1	1.4	0.1
42931	Spring Ostrovica	15.07.04	5.0	0.3	2.3	0.1	0.4	0.1	1.0	0.1
42932	Spring Toplica	15.07.04	4.3	0.2	2.3	0.1	0.4	0.1	1.2	0.1
42933	Spring Privilica	15.07.04	16.0	0.8	1.9	0.1	0.3	0.1	0.8	0.1
42934	Spring Klokot	15.07.04	5.9	0.3	2.5	0.1	0.4	0.1	1.2	0.1
42943	"Sunce"	15.07.04	5.6	0.3	2.6	0.1	0.5	0.1	1.2	0.1

Table A.17: Results of noble gases (He, Ne) in spring, river and lake waters of the Plitvice Lakes and Una River.

SamplingID	Location	Sampling Date	^{3}H [TU]	^{3}H Error	He [Nml/g]	He Error	Ne [Nml/g]	Ne Error	^{3}He/^{4}He	^{3}He/^{4}He Error
42357	Spring Vrelo	01.11.2003	8.8	0.1	7.02E-08	4.97E-10	2.99E-07	2.11E-09	1.72E-06	1.22E-08
42358	Spring Bijela Rijeka	01.11.2003	9.5	0.1	5.38E-08	3.11E-10	2.30E-07	1.33E-09	1.63E-06	9.39E-09
42359	Spring Crna Rijeka	01.11.2003	6.7	0.1	4.83E-08	3.42E-10	2.06E-07	1.46E-09	0.00000173	1.22E-08
42365	Spring Plitvica	03.11.2003	7.8	0.1	5.23E-08	3.74E-10	2.20E-07	1.56E-09	1.50E-06	1.06E-08
42366	Spring Stipinovac	01.11.2003	9.8	0.1	7.82E-08	5.53E-10	3.31E-07	2.34E-09	2.03E-06	1.44E-08
42367	Spring Ostrovica	02.11.2003	6.1	0.1	5.81E-08	5.81E-10	2.36E-07	2.36E-09	0.00000141	1.41E-08
42368	Spring Toplica	02.11.2003	5.7	0.1	6.34E-08	4.48E-10	2.63E-07	1.86E-09	1.38E-06	9.76E-09
42369	Spring Privilica	02.11.2003	7.3	0.1	5.07E-08	5.07E-10	2.06E-07	2.06E-09	0.00000147	1.47E-08
42370	Spring Klokot	02.11.2003	7.3	0.1	5.25E-08	3.72E-10	2.23E-07	1.57E-09	1.32E-06	9.37E-09
42929	Spring Bijela Rijeka	14.07.2004	10.2	0.2	4.90E-08	4.90E-10	2.29E-07	2.29E-09	1.61E-06	1.61E-08
42930	Spring Crna Rijeka	14.07.2004	7.2	0.2	4.80E-08	4.80E-10	2.26E-07	2.26E-09	1.82E-06	1.82E-08
42936	Spring Stipinovac	14.07.2004	8.8	0.1						
42935	Spring Plitvica	15.07.2004	8.6	0.2	4.67E-08	4.67E-10	2.13E-07	2.13E-09	1.65E-06	1.65E-08
42931	Spring Ostrovica	15.07.2004	6.2	0.1	6.30E-08	3.64E-10	2.62E-07	1.51E-09	1.51E-06	8.70E-09
42932	Spring Toplica	15.07.2004	5.6	0.1	6.28E-08	6.28E-10	2.71E-07	2.71E-09	1.35E-06	1.35E-08
42933	Spring Privilica	15.07.2004	6.8	0.1	6.11E-08	6.11E-10	2.54E-07	2.54E-09	1.74E-06	1.74E-08
42934	Spring Klokot	15.07.2004	7.5	0.2	6.06E-08	3.50E-10	2.36E-07	1.36E-09	1.27E-06	7.31E-09
42937	Spring of Una River	17.07.2004	5.1	0.1	9.82E-08	5.67E-10	2.18E-07	1.26E-09	7.07E-07	4.08E-09

Table A.18: Results of gamma-spectrometric measurements for caesium and lead radioisotopes [in Bq/kg] on the core of Prošće Lake (PR).

SamplingID	Location	Upper Depth [m]	Lower Depth [m]	Water Content [%]	Cs-137 [Bq/kg]	Cs-137 Error	Pb-214 [Bq/kg]	Pb-214 Error	Bi-214 [Bq/kg]	Bi-214 Error	Pb-210 [Bq/kg]	Pb-210 Error
42426	Prošće Lake (PR)	0	0.01	1	100.4	1	49.3	1.7	45.5	1.9	599.5	8.1
42427	Prošće Lake (PR)	0.01	0.02	0.9	101	1.3	39.8	1.7	30.6	1.9	683.2	9.1
42428	Prošće Lake (PR)	0.02	0.03	0.8	103.1	1.7	35.9	1	37.8	1.8	648.7	8.6
42429	Prošće Lake (PR)	0.03	0.04	0.8	112.9	1.5	34.3	1.4	37.7	1.8	614.8	8.6
42430	Prošće Lake (PR)	0.04	0.05	0.7	118	1.3	41.4	1.4	39.2	1.6	479.8	6.9
42431	Prošće Lake (PR)	0.05	0.06	0.7	142.7	1.2	43.2	1	43.7	1.8	394.2	6.8
42432	Prošće Lake (PR)	0.06	0.07	0.7	139.9	1.1	42.8	1.4	41.4	1.6	420	6.3
42433	Prošće Lake (PR)	0.07	0.08	0.7	166.6	1	40.7	0.8	42.9	1.5	404.8	6.3
42434	Prošće Lake (PR)	0.08	0.09	0.7	225.7	1.4	36.9	1.6	38.1	1.8	498.1	7.5
42435	Prošće Lake (PR)	0.09	0.1	0.7	208.3	1.3	41.7	1.4	39.7	1.5	438.6	5.8
42436	Prošće Lake (PR)	0.1	0.12	0.7	59.9	0.8	31.5	0.9	31	1.7	210.3	5.7
42437	Prošće Lake (PR)	0.12	0.14	0.6	23.4	0.5	31.9	0.9	29.1	1.8	164.6	5.3
42438	Prošće Lake (PR)	0.14	0.16	0.6	7.6	0.4	37.2	0.9	35.7	1.8	151.8	5.2
42439	Prošće Lake (PR)	0.16	0.18	0.6	8.6	0.7	32.8	0.8	32.2	1.4	142.7	4.5
42440	Prošće Lake (PR)	0.18	0.2	0.6	3.7	0.3	34.4	0.9	33.2	1.7	120.5	5.3
42441	Prošće Lake (PR)	0.2	0.22	0.6	0.7		42.2	1.3	38.9	1.5	115	3.9
42442	Prošće Lake (PR)	0.22	0.24	0.6	1.5	0.3	50.4	1.5	52.6	1.8	110.5	5.3
42443	Prošće Lake (PR)	0.24	0.26	0.6	0.7		47.4	1.5	46.3	1.8	110.9	5.6
42444	Prošće Lake (PR)	0.26	0.28	0.6	0.8		57.6	1.6	55.2	2	93.3	5.5
42445	Prošće Lake (PR)	0.28	0.3	0.6	1.9	0.4	56.1	1.4	53	1.6	92.5	4.5
42446	Prošće Lake (PR)	0.3	0.32	0.6	0.7		48.7	0.8	48.9	1.6	71.2	3.7
42447	Prošće Lake (PR)	0.32	0.34	0.6	0.7		51.7	1.6	49.9	1.9	80.9	5
42448	Prošće Lake (PR)	0.34	0.36	0.6	0.8		36	0.9	30	1.7	66.1	5.3
42449	Prošće Lake (PR)	0.36	0.4	0.6	0.7		31.6	0.7	29.9	1.4	50.8	3.7
42450	Prošće Lake (PR)	0.4	0.44	0.7	1.6	0.4	45.1	1.6	42.7	1.9	34.5	5.9

Table A.19: Results of gamma-spectrometric measurements for caesium and lead radioisotopes [in Bq/kg] on the core of Gradinsko Lake (GR).

SamplingID	Location	Upper Depth [m]	Lower Depth [m]	Water Content [%]	Cs-137 [Bq/kg]	Cs-137 Error	Pb-214 [Bq/kg]	Pb-214 Error	Bi-214 [Bq/kg]	Bi-214 Error	Pb-210 [Bq/kg]	Pb-210 Error
42495	Gradinsko Lake (GR)	0	0.03	0.8	11.8	0.8	16	1.2	14.6	1.4	79	8.9
42496	Gradinsko Lake (GR)	0.03	0.04	0.7	15.2	1.1	11.4	0.9	11.5	1.2	65.6	3.7
42497	Gradinsko Lake (GR)	0.04	0.05	0.7	18.4	0.8	11.5	1	6.1	1.4	63.2	4.4
42498	Gradinsko Lake (GR)	0.05	0.06	0.7	22.6	0.4	8.3	0.6	7.5	1.1	51.7	3.5
42499	Gradinsko Lake (GR)	0.06	0.07	0.7	81.3	1.4	9.7	0.7	9.7	1.4	28.6	3.7
42500	Gradinsko Lake (GR)	0.07	0.08	0.7	74.2	1.8	8.1	1	8.1	1.4	58.7	3.8
42501	Gradinsko Lake (GR)	0.08	0.09	0.7	35.2	0.4	10.1	0.5	10.1	0.8	42.9	2.5
42502	Gradinsko Lake (GR)	0.09	0.1	0.6	12	0.4	10.2	0.9	10	1.2	53.5	3.4
42503	Gradinsko Lake (GR)	0.1	0.11	0.6	6.8	0.3	12.7	0.9	12.1	1.2	37.3	4.3
42504	Gradinsko Lake (GR)	0.11	0.12	0.6	9.2	0.8	14.2	1.2	12.3	1.1	51.9	4.1
42505	Gradinsko Lake (GR)	0.12	0.13	0.6	6.8	0.3	8.2	0.6	8.5	1.1	61.4	3.1
42506	Gradinsko Lake (GR)	0.13	0.15	0.5	19.1	0.4	10.1	0.5	10.4	1	36.4	2.8
42507	Gradinsko Lake (GR)	0.15	0.17	0.5	11.5	0.4	9.4	0.8	9.6	1.2	40	4.8
42508	Gradinsko Lake (GR)	0.17	0.19	0.4	9.5	0.7	9.4	0.6	9.7	1.2	32.7	3.7
42509	Gradinsko Lake (GR)	0.19	0.21	0.4	7.8	0.5	9.8	0.6	12.6	1.2	45.5	3.6
42510	Gradinsko Lake (GR)	0.21	0.23	0.4	8.7	0.8	12.3	0.9	11.9	1	35	2.9
42511	Gradinsko Lake (GR)	0.23	0.25	0.4	7.3	0.8	10.2	1	8.7	1.2	22.2	3.2
42512	Gradinsko Lake (GR)	0.25	0.27	0.4	3.8	0.3	7.2	0.9	9.1	1.2	14.3	2.9
42513	Gradinsko Lake (GR)	0.27	0.29	0.4	3.3	0.3	8.3	0.4	9	0.8	16.7	2.6
42514	Gradinsko Lake (GR)	0.29	0.31	0.4	2.8	0.2	9	0.7	7.6	1	15	2.6
42515	Gradinsko Lake (GR)	0.31	0.33	0.4	2.2	0.2	9.4	0.5	8.3	1	22.4	3
42516	Gradinsko Lake (GR)	0.33	0.37	0.4	3.6	1	11.9	1	8.4	1.2	18.5	2.7
42517	Gradinsko Lake (GR)	0.37	0.41	0.4	2.4	0.5	7.4	0.6	6.5	1.1	15.7	3

Table A.20: Results of gamma-spectrometric measurements for caesium and lead radioisotopes [in Bq/kg] on the core of Kozjak Lake (K1).

SamplingID	Location	Upper Depth [m]	Lower Depth [m]	Water Content [%]	Cs-137 [Bq/kg]	Cs-137 Error	Pb-214 [Bq/kg]	Pb-214 Error	Bi-214 [Bq/kg]	Bi-214 Error	Pb-210 [Bq/kg]	Pb-210 Error
42451	Kozjak Lake (K1)	0	0.01	0.9	108.1	1.1	26.9	0.9	25.1	1.8	340.7	7.1
42452	Kozjak Lake (K1)	0.01	0.02	0.9	109.1	1.7	23.4	1	22.7	1.8	355.8	7.4
42453	Kozjak Lake (K1)	0.02	0.03	0.9	116.7	1.5	28.5	1.7	24.2	1.7	303.7	8.9
42454	Kozjak Lake (K1)	0.03	0.04	0.9	101.2	1.2	23.4	0.9	20.5	1.6	332.3	6.7
42455	Kozjak Lake (K1)	0.04	0.05	0.9	106.1	0.9	27.1	0.7	27.3	1.4	365.9	5.6
42456	Kozjak Lake (K1)	0.05	0.06	0.8	102	1	32.1	1.5	26.2	1.8	321.8	6.7
42457	Kozjak Lake (K1)	0.06	0.07	0.8	104.4	1	32.2	1.5	34.8	1.7	356	6.7
42458	Kozjak Lake (K1)	0.07	0.08	0.8	114.7	1	27.8	1.4	26.6	1.6	397	6.5
42459	Kozjak Lake (K1)	0.08	0.09	0.7	97.8	1.5	31.9	1.2	28.7	1.6	301.9	6.5
42460	Kozjak Lake (K1)	0.09	0.1	0.7	100.2	0.9	34.6	0.8	36.2	1.5	273.2	5.4
42461	Kozjak Lake (K1)	0.1	0.11	0.7	74.4	1.3	45.3	1.7	41.6	2	224.5	6.5
42462	Kozjak Lake (K1)	0.11	0.12	0.6	53.8	0.6	32.4	0.8	32.9	1.4	160.2	4.6
42463	Kozjak Lake (K1)	0.12	0.13	0.6	26.2	1.2	33.5	1.4	31.5	1.6	156.4	11.4
42464	Kozjak Lake (K1)	0.13	0.14	0.6	15.2	0.4	27.2	1.3	24.2	1.5	110.9	4.9
42465	Kozjak Lake (K1)	0.14	0.15	0.6	6.1	0.4	17.6	1.3	18.2	1.5	105.5	4.4
42466	Kozjak Lake (K1)	0.15	0.16	0.5	0.7		23.6	0.7	22.1	1.4	76.4	4.1
42467	Kozjak Lake (K1)	0.16	0.18	0.5	0.7		27.1	0.7	27.1	1.3	63	3.9
42468	Kozjak Lake (K1)	0.18	0.2	0.5	0.7		22.8	0.8	21.3	1.5	48.9	4.2
42469	Kozjak Lake (K1)	0.2	0.25	0.5	0.7		22.4	0.7	25.7	1.5	35.2	4.3
42470	Kozjak Lake (K1)	0.25	0.29	0.5	0.5		17	0.9	16.2	1.2	22.1	3

Table A.21: Results of gamma-spectrometric measurements for caesium and lead radioisotopes [in Bq/kg] on the core of Kozjak Lake (K2).

SamplingID	Location	Upper Depth [m]	Lower Depth [m]	Water Content [%]	Cs-137 [Bq/kg]	Cs-137 Error	Pb-214 [Bq/kg]	Pb-214 Error	Bi-214 [Bq/kg]	Bi-214 Error	Pb-210 [Bq/kg]	Pb-210 Error
42471	Kozjak Lake (K2)	0	0.04	0.9	148.3	1.3	33.9	1	25	2.2	282	7.6
42472	Kozjak Lake (K2)	0.04	0.05	0.8	179.1	1.2	40.6	1	39.2	1.9	290.8	6.6
42473	Kozjak Lake (K2)	0.05	0.06	0.8	186.6	1.8	50.7	1.3	47.1	2.2	313.8	7.7
42474	Kozjak Lake (K2)	0.06	0.07	0.7	215.8	1.5	48.8	1.2	50.6	2.2	272.7	8.2
42475	Kozjak Lake (K2)	0.07	0.08	0.8	187.2	1.4	39.9	0.9	38.1	1.7	273.7	6.7
42476	Kozjak Lake (K2)	0.08	0.09	0.8	167.8	1.4	56.9	2	56.7	2.3	307.9	7.3
42477	Kozjak Lake (K2)	0.09	0.1	0.8	136.8	1.2	51.2	1.4	58.9	2.2	257.4	6.9
42478	Kozjak Lake (K2)	0.1	0.11	0.8	110.6	0.9	56.4	1	56.9	1.8	264.1	6.2
42479	Kozjak Lake (K2)	0.11	0.12	0.8	98.4	1.1	50.6	1.2	51.1	2.2	191.2	7.8
42480	Kozjak Lake (K2)	0.12	0.13	0.7	77.8	1.3	38.1	1	36.7	1.9	178.1	7.5
42481	Kozjak Lake (K2)	0.13	0.14	0.7	76.5	0.8	46	0.9	46.1	1.7	215	5.4
42482	Kozjak Lake (K2)	0.14	0.16	0.8	65.9	0.7	45.2	0.9	47.8	1.8	204.8	5.7
42483	Kozjak Lake (K2)	0.16	0.18	0.8	42.2	0.5	28.3	1.1	25.2	1.3	155.4	3.8
42484	Kozjak Lake (K2)	0.18	0.2	0.7	36.6	0.9	21.8	0.7	22.7	1.4	97.8	3.8
42485	Kozjak Lake (K2)	0.2	0.22	0.7	49	0.6	30.3	0.8	30.6	1.4	99.4	4.4
42486	Kozjak Lake (K2)	0.22	0.24	0.7	69.5	1.4	34.6	1	32.2	1.8	79.8	4.7
42487	Kozjak Lake (K2)	0.24	0.26	0.7	114.7	1.1	59.6	1.1	60.7	2.1	135.5	5.8
42488	Kozjak Lake (K2)	0.26	0.28	0.7	59.8	1.3	111.1	1.9	112.4	2.2	177.1	5.6
42489	Kozjak Lake (K2)	0.28	0.3	0.7	39.3	1.1	128.4	2.3	121.7	2.8	195.8	7.8
42490	Kozjak Lake (K2)	0.3	0.32	0.8	41.4	1.9	106.4	1.3	106.2	2.5	205.9	6.2
42491	Kozjak Lake (K2)	0.32	0.34	0.8	34	0.6	80.8	1.1	73.1	2.2	215	6.6
42492	Kozjak Lake (K2)	0.34	0.36	0.8	12.5	1.4	88.1	2.3	74.6	2.6	221.3	7.8
42493	Kozjak Lake (K2)	0.36	0.39	0.8	7.2	0.4	72.6	1.2	72.6	1.8	189.9	5.9
42494	Kozjak Lake (K2)	0.39	0.42	0.8	18	0.7	61.4	1.4	62.1	2.6	216.6	9.4

Table A.22: Results of gamma-spectrometric measurements for caesium and lead radioisotopes [in Bq/kg] on the core of Kaludjerovac Lake (KA).

SamplingID	Location	Upper Depth [m]	Lower Depth [m]	Water Content [%]	Cs-137 [Bq/kg]	Cs-137 Error	Pb-214 [Bq/kg]	Pb-214 Error	Bi-214 [Bq/kg]	Bi-214 Error	Pb-210 [Bq/kg]	Pb-210 Error
42518	Kaludjerovac Lake (KA)	0	0.01	0.6	11.9	0.7	14.1	1	9	1.2	139.7	4.1
42519	Kaludjerovac Lake (KA)	0.01	0.02	0.6	12.3	0.3	8.3	0.5	9.4	0.9	108.6	3.4
42520	Kaludjerovac Lake (KA)	0.02	0.03	0.6	13.2	0.3	7.5	0.5	8	1	93.2	3.5
42521	Kaludjerovac Lake (KA)	0.03	0.04	0.6	22.1	1.2	11.6	0.9	10.5	1.1	95.2	4
42522	Kaludjerovac Lake (KA)	0.04	0.05	0.6	54.4	1	6.5	0.5	7.2	1	66.1	3.2
42523	Kaludjerovac Lake (KA)	0.05	0.06	0.6	119.1	0.9	7.9	0.4	8.6	0.9	55.8	2.7
42524	Kaludjerovac Lake (KA)	0.06	0.07	0.6	78.9	1.2	12	1.1	9.9	1.1	78	4.1
42525	Kaludjerovac Lake (KA)	0.07	0.08	0.6	26.8	0.4	12	0.9	8.7	1	55.6	3.4
42526	Kaludjerovac Lake (KA)	0.08	0.09	0.6	9.5	0.3	8.9	0.5	10.1	1.1	63.7	3.3
42527	Kaludjerovac Lake (KA)	0.09	0.1	0.6	8.1	0.3	10.1	0.8	11	1	49.2	3.4
42528	Kaludjerovac Lake (KA)	0.1	0.12	0.5	8.7	0.5	10.6	0.8	9.6	1	44.9	3
42529	Kaludjerovac Lake (KA)	0.12	0.14	0.5	25.3	0.6	9.4	0.6	10.4	1	36.5	3.5
42530	Kaludjerovac Lake (KA)	0.14	0.16	0.4	24	0.6	9.7	0.6	10.1	1	44.7	3.1
42531	Kaludjerovac Lake (KA)	0.16	0.18	0.4	16	0.3	9.5	0.4	9.5	0.7	36.6	2.1
42532	Kaludjerovac Lake (KA)	0.18	0.2	0.4	14.4	0.7	9.9	0.5	12.8	1	34.2	3.1
42533	Kaludjerovac Lake (KA)	0.2	0.22	0.3	11.9	0.3	9.4	0.4	9.7	1	33.6	2.9
42534	Kaludjerovac Lake (KA)	0.22	0.24	0.3	9.7	0.2	10	0.6	7.9	0.7	29.3	2
42535	Kaludjerovac Lake (KA)	0.24	0.26	0.3	7.9	0.3	9.8	0.5	10	1.1	20.5	2.7
42536	Kaludjerovac Lake (KA)	0.26	0.28	0.3	8.2	0.6	10.6	1	10.2	1.2	20.1	3
42537	Kaludjerovac Lake (KA)	0.28	0.3	0.3	8.4	0.8	9.6	0.6	10.3	1.1	18.5	3.2
42538	Kaludjerovac Lake (KA)	0.3	0.32	0.3	4.8	0.2	10.3	0.5	7.7	0.7	16	1.8
42539	Kaludjerovac Lake (KA)	0.32	0.34	0.3	3.8	0.2	10.1	0.5	10.5	0.8	14.4	2.2
42540	Kaludjerovac Lake (KA)	0.34	0.36	0.3	0.7		10	0.8	10.7	1.2	14.7	2.8
42541	Kaludjerovac Lake (KA)	0.36	0.39	0.3	1.8	0.3	8.8	0.6	8.5	1	10	
42542	Kaludjerovac Lake (KA)	0.39	0.42	0.3	1.9	0.2	12.2	0.9	11.2	1	10	